Effect of Various Saturation Levels, Leaching Solution pH, and Leaching Cycle on Electrical Conductivity from Coal Mine Spoil Leachate

John Martin Parker

Thesis submitted to the faculty of the Virginia Polytechnic Institute and State University in partial fulfillment of the requirements for the degree of

Master of Science

In

Crop and Soil Environmental Sciences

Matt Eick, Chair

W. Lee Daniels, Co-Chair

Stephen Schoenholtz

Carl Zipper

July 26, 2013

Blacksburg, VA

Keywords: leaching columns, overburden, total dissolved solids, selenium

The Effect of Various Saturation Levels, Leaching Solution pH, and Leaching Cycle on Electrical Conductivity from Coal Mine Spoil Leachate

John M. Parker

ABSTRACT

Historically, environmental research associated with Appalachian coal surface mines focused on acid mine drainage and reclamation. Recent studies suggest that electrical conductivity (EC) levels above 500 μS cm^{-1} can impair Appalachian streams, shifting the focus towards limiting release of total dissolved solids (TDS) and associated elements of concern. Previous column studies utilized an unsaturated bi-weekly leaching design to evaluate the behavior of overburden with respect to TDS, pH, and trace metals. The objective of this study was to determine the effects of column saturation, leaching solution chemistry, and leaching cycle on the release of TDS and associated elements from an unweathered sandstone. Treatments evaluating potential saturation, leaching solution pH, and leaching cycle included saturated, standard method, vacuum, and standpipe fitted columns; simulated acid rain, de-ionized water, and $CaCO_3$ leaching solutions; and 2x $week^{-1}$, 1x $week^{-1}$, 2x $month^{-1}$, and 1x day^{-1} leaching cycles. Saturation level in the column significantly impacted leachate pH, EC level, and the release of sulfate, bicarbonate, and associated cations by potentially affecting trace sulfide oxidation and carbonate dissolution reactions. Little evidence of saturation was noted with the standard method. Leaching solution bulk chemistry did not alter leachate chemistry. Longer times between dosing cycles corresponded to higher EC, bicarbonate, and associated cation levels, especially over time. Sulfate, Ca, and Se exhibited the greatest percent release based on total mass losses during peak elution. For managing TDS, time between precipitation events and saturation level can strongly affect short and long-term EC level, its major contributors, and elements of concern.

DEDICATION

To Mom and Dad, without you I wouldn't be where I am today. Thank you for everything.

ACKNOWLEDGEMENTS

I would like to thank Dr. Lee Daniels and Dr. Matt Eick for the opportunity to continue my education. Their guidance, encouragement, and expertise was invaluable throughout this process. I'd also like to thank ARIES for funding this project and the Powell River Project for supplying the mine spoil used in this study. Committee members Dr. Carl Zipper and Dr. Stephen Schoenholtz should be recognized for their support and insight. Additionally, without Julie Burger and Dr. Zenah Orndorff guiding me in the lab, none of this would have been possible. A special thanks to Steve Nagle, Dan Johnson, and Katie Haering for their help with column construction, spoil preparation, and leaching. A big thank you to Dr. Mike Beck for his assistance with the statistical analyses. And lastly, thanks to Kelly Phillips for continued moral support and occasional "off the books" assistance.

TABLE OF CONTENTS

ABSTRACT ii
DEDICATION iii
ACKNOWLEDGEMENTS iv
TABLE OF CONTENTS v
LIST OF TABLES viii
LIST OF FIGURES x
CHAPTER 1. INTRODUCTION AND LITERATURE REVIEW 1
INTRODUCTION 1
LITERATURE REVIEW 3
TDS Compliance and Environmental Impact 3
Column Leaching Studies 4
Leachate pH 6
Total Dissolved Solids and EC 7
Trace Metals and Elements of Interest 8
Column Leaching Techniques 10
Column Design 10
Dosing Cycle 13
Leaching Solution pH 14
CHAPTER 2. MATERIALS AND METHODS 16
Geology 16
Spoil Preparation 16
Spoil Characterization Methods 16
Column Construction and Packing 17
Objective 1: Effects of Possible Zone of Saturation on Leachate Chemistry and EC 20
Objective 2: Influence of Leaching Solution pH on Leachate Chemistry and EC 23
Objective 3: Effects of Leaching Cycle on Leachate Chemistry and EC 24
Sample Analysis 24
Statistical Analysis 25
CHAPTER 3. SPOIL CHARACTERIZATION AND EFFECTS OF VARIOUS SATURATION LEVELS 27
SPOIL CHARACTERIZATION 27
EFFECT OF VARIOUS LEVELS OF SATURATION 29
Potential Saturation Zone 29
Electrical Conductivity (EC) 30

Leachate pH 33
Sulfate 35
Bicarbonate 37
Arsenic (As) and Selenium (Se) 40
Calcium (Ca), Iron (Fe), Magnesium (Mg), and Manganese (Mn) 42
Cadmium (Cd), Copper (Cu), Nickel (Ni), Lead (Pb), and Zinc (Zn) 52
Aluminum (Al) Chloride (Cl), Potassium (K), and Sodium (Na) 60
Charge and Mass Distribution 66

CHAPTER 4. EFFECTS OF LEACHING SOLUTION pH 72
Electrical Conductivity 72
Leachate pH 74
Sulfate 74
Bicarbonate 77
Arsenic (As) and Selenium (Se) 77
Calcium (Ca), Iron (Fe), Magnesium (Mg), and Manganese (Mn) 79
Aluminum (Al), Chloride (Cl), Potassium (K), and Sodium (Na) 87
Charge and Mass Distribution 94

CHAPTER 5. EFFECTS OF LEACHING CYCLE 99
Electrical Conductivity 99
Leachate pH 101
Sulfate 104
Bicarbonate 104
Arsenic (As) and Selenium (Se) 108
Calcium (Ca), Iron (Fe), Magnesium (Mg), and Manganese (Mn) 108
Cadmium (Cd), Copper (Cu), Nickel (Ni), Lead (Pb), and Zinc (Zn) 117
Aluminum (Al), Chloride (Cl), Potassium (K), and Sodium (Na) 118
Charge and Mass Distribution 122

CHAPTER 6. PEAK ELUTION TOTAL MASS LOSSES 127
Effect of Saturation and Vacuum 127
Leaching Solution pH 132
Dosing Cycle 134

CHAPTER 7. SUMMARY AND CONCLUSIONS 137

SUMMARY 137
Effect of Saturation and Vacuum 139
Effect of Leaching Solution pH 142
Effect of Leaching Cycle 143
Charge and Mass Distribution 145
Peak Elution Mass Losses 145
Sulfate 145
Bicarbonate 146
Arsenic (As) and Selenium (Se) 146
Calcium (Ca), Iron (Fe), Magnesium (Mg), and Manganese (Mn) 147
Cadmium (Cd), Copper (Cu), Nickel (Ni), Lead (Pb), and Zinc (Zn) 147
Aluminum (Al), Chloride (Cl), Potassium (K), and Sodium (Na) 148

CONCLUSIONS 149

REFERENCES 151

APPENDICES 157
Appendix A: Leaching and analysis schedules 157
Table A-1. Leaching and analysis schedule for treatments 1-7 157
Table A-2. Leaching and analysis schedule for treatment 8 158
Table A-3. Leaching and analysis schedule for treatment 9 158
Table A-4. Leaching and analysis schedule for treatment 10 159
Appendix B. Correlation matrices 160
Table B-1. Treatment four correlation matrix over leaches zero to nine 160
Table B-2. Treatment four correlation matrix over leaches thirteen to thirty-nine 166
Appendix C. Effects of saturation figures 171
Figure C-1. Leachate Ni from standpipe, saturated, vacuum and standard method columns 171
Figure C-2. Leachate Cl from standpipe, saturated, vacuum and standard method columns 172
Appendix D. Leaching solution pH figures 173
Figure D-1. Leachate Ca from columns leached with simulated acid rain, DI water and CaCO3 173
Figure D-2. Leachate Mg from columns leached with simulated acid rain, DI water and CaCO3. 174
Figure D-3. Leachate Mn from columns leached with simulated acid rain, DI water and CaCO3. 175
Figure D-4. Leachate Cd from columns leached with simulated acid rain, DI water and CaCO3. 176
Figure D-5. Leachate Cu from columns leached with simulated acid rain, DI water and CaCO3. 177
Figure D-6. Leachate Ni from columns leached with simulated acid rain, DI water and CaCO3. 178
Figure D-7. Leachate Ni from columns leached with simulated acid rain, DI water and CaCO3. 179
Appendix E. Effect of leaching cycle figures 180
Figure E-1. Leachate Fe from columns dosed 2x $week^{-1}$, 1x $week^{-1}$, 2x $month^{-1}$, and 1x day^{-1} 180
Figure E-2. Leachate Cd from columns dosed 2x $week^{-1}$, 1x $week^{-1}$, 2x $month^{-1}$, and 1x day^{-1}. 181
Figure E-3. Leachate Cu from columns dosed 2x $week^{-1}$, 1x $week^{-1}$, 2x $month^{-1}$, and 1x day^{-1} 182
Figure E-4. Leachate Ni from columns dosed 2x $week^{-1}$, 1x $week^{-1}$, 2x $month^{-1}$, and 1x day^{-1} 183
Figure E-5. Leachate Pb from columns dosed 2x $week^{-1}$, 1x $week^{-1}$, 2x $month^{-1}$, and 1x day^{-1} 184
Figure E-6. Leachate Zn from columns dosed 2x $week^{-1}$, 1x $week^{-1}$, 2x $month^{-1}$, and 1x day^{-1} 185
Figure E-7. Leachate Al from columns dosed 2x $week^{-1}$, 1x $week^{-1}$, 2x $month^{-1}$, and 1x day^{-1} 186
Figure E-8. Leachate Na from columns dosed 2x $week^{-1}$, 1x $week^{-1}$, 2x $month^{-1}$, and 1x day^{-1} 187

LIST OF TABLES

Table 1. Summary of all treatments across all three objectives. Treatments across all objectives were labeled sequentially to minimize sampling error, but each objective was treated as an individual study..... 19

Table 2. Selected chemical properties of the mine spoil used in the column leaching study. 28

Table 3. Total mass (mg) of Ca, K, Mg, and Na per kg of mine spoil used in the column leaching study..... 29

Table 4. Total mass (mg) of Al, As, Cd, Cu, Fe, Mn, Ni, Pb, Se, and Zn per kg of mine spoil used in the column leaching study. Selenium levels were below detection and the total Se content was calculated using the detection limit. 29

Table 5. Summary of repeated measures statistical analysis at various saturation levels. 30

Table 6. Filtered vs. unfiltered leachate Al, As, Cd, Cu, Fe, Mn, Na, Ni, Pb, Se, and Zn at leach one from the standpipe (T1), saturated (T2), vacuum (T3), and standard method (T4) columns..... 47

Table 7. Summary of repeated measures statistical analysis for leaching solution pH 72

Table 8. Filtered vs. unfiltered leachate Al, As, Cd, Cu, Fe, Mn, Na, Ni, Pb, Se, and Zn at leach one for columns leached with simulated acid rain via standard method (T4), DI (T5), and $CaCO_3$ (T6) leaching solutions. 84

Table 9. Summary of repeated measures statistical analysis on various leaching cycles. 99

Table 10. Filtered vs. unfiltered leachate for selected elements at leach one from columns leached 2x $week^{-1}$ (T7), 1x $week^{-1}$ (T8), 2x $month^{-1}$ (T9), and 1x day^{-1} (T10). 113

Table 11. Total original mass (mg) of sulfate, Ca, K, Mg, and Na per leaching column (1.5 kg spoil)..... 127

Table 12. Total mass (µg) of As, Cd, Cu, Ni, Pb, Se, and Zn per leaching column (1.5 kg spoil)..... 127

Table 13. Total mass (mg) of sulfate, bicarbonate, Ca, Cl, K, Mg, and Na leached from the standpipe (T1), saturated (T2), vacuum (T3), and standard columns (T4) during the first five leaching cycles..... 128

Table 14. Total mass (μg) of Al, As, Cd, Cu, Fe, Mn, Ni, Pb, Se, and Zn leached from the standpipe (T1), saturated (T2), vacuum (T3), and standard columns (T4) during the first five leaching cycles. 128

Table 15. Percent release of sulfate, Ca, K, Mg, and Na from the standpipe (T1), saturated (T2), vacuum (T3), and standard columns (T4) during the first five leaching cycles. 129

Table 16. Percent release of Al, As, Cd, Cu, Fe, Mn, Ni, Pb, Se, and Zn from the standpipe (T1), saturated (T2), vacuum (T3), and standard columns (T4) during the first five leaching cycles. 129

Table 17. Total mass of sulfate, bicarbonate, Ca, Cl, K, Mg, and Na released from the columns leached with simulated acid rain (T4), DI water (T5), and $CaCO_3$ (T6) during the first five leaching cycles. 133

Table 18. Total mass (μg) of Al, As, Cd, Cu, Fe, Mn, Ni, Pb, Se, and Zn released from columns leached with the simulated acid rain (T4), DI water (T5), and $CaCO_3$ (T6) leaching during the first five leaching cycles. 133

Table 19. Percent release of sulfate, Ca, K, Mg, and Na from the columns leached with simulated acid rain (T4), DI water (T5), and $CaCO_3$ (T6) during the first five leaching cycles. 133

Table 20. Percent release of Al, As, Cd, Cu, Fe, Mn, Ni, Pb, Se, and Zn released from columns leached with simulated acid rain (T4), DI water (T5), and $CaCO_3$ (T6) during the first five leaching cycles. 134

Table 21. Total mass (mg) of sulfate, bicarbonate, Ca, Cl, K, Mg, and Na released from the columns leached 2x $week^{-1}$ (T7), 1x $week^{-1}$ (T8), 2x $month^{-1}$ (T9), and 1x day^{-1} (T10) during the first five leaching cycles. 134

Table 22. Total mass (μg) of Al, As, Cd, Cu, Fe, Mn, Ni, Pb, Se, and Zn released from columns leached 2x $week^{-1}$ (T7), 1x $week^{-1}$ (T8), 2x $month^{-1}$ (T9), and 1x day^{-1} (T10) during the first five leaching cycles. 135

Table 23. Percent release of sulfate, Ca, K, Mg, and Na from the columns leached 2x $week^{-1}$ (T7), 1x $week^{-1}$ (T8), 2x $month^{-1}$ (T9), and 1x day^{-1} (T10) during the first five leaching cycles. 135

Table 24. Percent release of Al, As, Cd, Cu, Fe, Mn, Ni, Pb, Se, and Zn released from columns leached 2x $week^{-1}$ (T7), 1x $week^{-1}$ (T8), 2x $month^{-1}$ (T9), and 1x day^{-1} (T10) during the first five leaching cycles. 135

LIST OF FIGURES

Figure 1. Image of column set-up for treatments 1, 2 and 4-10. 21

Figure 2. Image of vacuum column design used on treatment three columns…….. 22

Figure 3. Visual confirmation of perching. 30

Figure 4. Leachate electrical conductivity (EC) from standpipe, saturated, vacuum and standard method columns. 32

Figure 5. Leachate pH from standpipe, saturated, vacuum and standard method columns.. 34

Figure 6. Leachate sulfate (SO_4) from standpipe, saturated, vacuum and standard method columns. 36

Figure 7. Leachate bicarbonate from standpipe, saturated, vacuum and standard method columns.. 38

Figure 8. Leachate As from standpipe, saturated, vacuum and standard method columns.. 41

Figure 9. Leachate Se from standpipe, saturated, vacuum and standard method columns… 43

Figure 10. Leachate Ca from standpipe, saturated, vacuum and standard method columns. 44

Figure 11. Leachate Fe from standpipe, saturated, vacuum and standard method columns.. 46

Figure 12. Leachate Mg from standpipe, saturated, vacuum and standard method columns.. 49

Figure 13. Leachate Mn from standpipe, saturated, vacuum and standard method columns.. 51

Figure 14. Leachate Cd from standpipe, saturated, vacuum and standard method columns.. 53

Figure 15. Leachate Cu from standpipe, saturated, vacuum and standard method columns.. 55

Figure 16. Leachate Pb from standpipe, saturated, vacuum and standard method columns.. 57

Figure 17. Leachate Zn from standpipe, saturated, vacuum and standard method columns.. 59

Figure 18. Leachate Al from standpipe, saturated, vacuum and standard method columns.. 61

Figure 19. Leachate K from standpipe, saturated, vacuum and standard method columns... 64

Figure 20. Leachate Na from standpipe, saturated, vacuum and standard method columns.. 65

Figure 21. Charge distribution of dominant cations and anions at leach one from standpipe (T1), saturated (T2), vacuum (T3), and standard method (T4) columns……. 67

Figure 22. Charge distribution of dominant cations and anions at leach thirty-nine from standpipe (T1), saturated (T2), vacuum (T3), and standard method (T4) columns……. 68

Figure 23. Mass distribution of dominant cations and anions at leach one from standpipe (T1), saturated (T2), vacuum (T3), and standard method (T4) columns…….. 69

Figure 24. Mass distribution of dominant cations and anions at leach thirty-nine from standpipe (T1), saturated (T2), vacuum (T3), and standard method (T4) columns……. 70

Figure 25. Leachate electrical conductivity (EC) from columns leached with simulated acid rain, DI water and $CaCO_3$.. 73

Figure 26. Leachate pH from columns leached with simulated acid rain, DI water and $CaCO_3$.....75

Figure 27. Leachate sulfate (SO_4) from columns leached with simulated acid rain, DI water and $CaCO_3$.. 76

Figure 28. Leachate bicarbonate from columns leached with simulated acid rain, DI water and $CaCO_3$. 78

Figure 29. Leachate As from columns leached with simulated acid rain, DI water and $CaCO_3$.....80

Figure 30. Leachate Se from columns leached with simulated acid rain, DI water and $CaCO_3$.....81

Figure 31. Leachate Fe from columns leached with simulated acid rain, DI water and $CaCO_3$.....83

Figure 32. Leachate Pb from columns leached with simulated acid rain, DI water and $CaCO_3$.....86

Figure 33. Leachate Al from columns leached with simulated acid rain, DI water and $CaCO_3$.....88

Figure 34. Leachate Cl from columns leached with simulated acid rain, DI water and $CaCO_3$.....90

Figure 35. Leachate K from columns leached with simulated acid rain, DI water and $CaCO_3$.....92

Figure 36. Leachate Na from columns leached with simulated acid rain, DI water and $CaCO_3$.....93

Figure 37. Charge distribution of dominant cations and anions at leach one from columns leached with simulated acid rain (T4, pH 4.6), DI (T5, pH 6), and $CaCO_3$ (T6, pH 8.0).....95

Figure 38. Charge distribution of dominant cations and anions at leach thirty-nine from columns leached with simulated acid rain (T4, pH 4.6), DI (T5, pH 6), and $CaCO_3$ (T6, pH 8.0).....96

Figure 39. Mass distribution of dominant cations and anions at leach one from columns leached with simulated acid rain (T4, pH 4.6), DI (T5, pH 6), and $CaCO_3$ (T6, pH 8.0).....97

Figure 40. Mass distribution of dominant cations and anions at leach thirty-nine from columns leached with simulated acid rain (T4, pH 4.6), DI (T5, pH 6), and $CaCO_3$ (T6, pH 8.0).....98

Figure 41. Leachate electrical conductivity (EC) from columns dosed 2x $week^{-1}$, 1x $week^{-1}$, 2x $month^{-1}$, and 1x day^{-1}.....100

Figure 42. Leachate pH from columns dosed 2x $week^{-1}$, 1x $week^{-1}$, 2x $month^{-1}$, and 1x day^{-1}.....102

Figure 43. Leachate sulfate (SO_4) from columns dosed 2x $week^{-1}$, 1x $week^{-1}$, 2x $month^{-1}$, and 1x day^{-1}.....105

Figure 44. Leachate sulfate (SO_4) from columns dosed 2x $week^{-1}$, 1x $week^{-1}$, 2x $month^{-1}$, and 1x day^{-1}.....106

Figure 45. Leachate As from columns dosed 2x week^{-1}, 1x week^{-1}, 2x month^{-1}, and 1x day^{-1}.....109

Figure 46. Leachate Se from columns dosed 2x week^{-1}, 1x week^{-1}, 2x month^{-1}, and 1x day^{-1}.....110

Figure 47. Leachate Ca from columns dosed 2x week^{-1}, 1x week^{-1}, 2x month^{-1}, and 1x day^{-1}.....111

Figure 48. Leachate Mg from columns dosed 2x week^{-1}, 1x week^{-1}, 2x month^{-1}, and 1x day^{-1}.....114

Figure 49. Leachate Mn from columns dosed 2x week^{-1}, 1x week^{-1}, 2x month^{-1}, and 1x day^{-1}.....116

Figure 50. Leachate Cl from columns dosed 2x week^{-1}, 1x week^{-1}, 2x month^{-1}, and 1x day^{-1}.....119

Figure 51. Leachate K from columns dosed 2x week^{-1}, 1x week^{-1}, 2x month^{-1}, and 1x day^{-1}.....121

Figure 52. Charge distribution of dominant cations and anions at leach one from columns leached 2x week^{-1} (T7), 1x week^{-1} (T8), 2x month^{-1} (T9), and 1x day^{-1} (T10).....123

Figure 53. Charge distribution of dominant cations and anions at leach nine from columns leached 2x week^{-1} (T7), 1x week^{-1} (T8), 2x month^{-1} (T9), and 1x day^{-1} (T10).....124

Figure 54. Mass distribution of dominant cations and anions at leach one from columns leached 2x week^{-1} (T7), 1x week^{-1} (T8), 2x month^{-1} (T9), and 1x day^{-1} (T10).....125

Figure 55. Mass distribution of dominant cations and anions at leach nine from columns leached 2x week^{-1} (T7), 1x week^{-1} (T8), 2x month^{-1} (T9), and 1x day^{-1} (T10).....126

CHAPTER 1. INTRODUCTION AND LITERATURE REVIEW

INTRODUCTION

Over the past few years, total dissolved solids (TDS) have been implicated as a major stressor of benthic fauna in streams receiving drainage from Appalachian coal mining operations (Bernhardt et al., 2012; Chapman et al., 2000; Green et al., 2000; Pond et al. 2008; Pond, 2010; Weber-Scannell and Duffy, 2007). Total dissolved solids is generally defined as the quantity or mass of non-volatile inorganic and organic substances contained in solution. The majority of these substances in leachate from coal mine spoils are inorganic ions, mainly HCO_3^-, SO_4^{2-}, Cl^-, Ca^{2+}, K^+, Mg^{2+}, and Na^+ (Bryant et al., 2002; Lindberg et al., 2011). These ions are naturally found over a wide range of concentrations in water bodies; however, elevated concentrations are found as a result of anthropogenic activities such as mining operations (Abdalla, 2009). The nature of the various TDS solutes impacting surface water bodies is important as certain ions may be more toxic to aquatic life compared to others (Goodfellow et al, 2000; Mount et al., 1997). However, TDS or electrical conductivity (EC) measurements, which measure the conductivity of salts dissolved in water, do not speciate specific ions. Due to labor and precision constraints, TDS is generally not directly measured, but rather estimated by EC, which has a linear relationship with TDS (Daniels et al., 2009; Hood and Oertel, 1984) that will vary somewhat depending on the ionic composition of the leachate.

The Safe Drinking Water Act lists TDS under secondary contaminants with a maximum contaminant level (sMCL) of 500 mg L^{-1} (USEPA, 2009). Toxicity to aquatic organisms is caused by increased salinity, changes in ionic composition, and toxicity to specific ions in the receiving bodies of water (Weber-Scannell and Duffy, 2007). Recently, research has

demonstrated that TDS released from coal mining may be adversely affecting streams in southern Appalachia (Bodkin et al., 2007). Shifts in aquatic communities, lowered biodiversity, and loss of salt intolerant species were seen when the salinity levels increased (Weber-Scannell and Duffy, 2007). Previously, the main concerns with mining effluent were low pH, and high concentrations of iron (Fe) and manganese (Mn; Orndorff et al., 2010).

Freshwater streams in the Appalachian Region (VA, WV, TN, and Ky) are home to many sensitive macroinvertibrates and there are growing concerns that TDS released from mining operations are threatening the health of these streams (Bodkin et al., 2007). Levels of TDS in streams between 300 $\mu S\ cm^{-1}$ and 500 $\mu S\ cm^{-1}$ show negative impacts, while TDS levels greater than 500 $\mu S\ cm^{-1}$ are considered by many as impaired (Silva and Giles, 2010). With these findings, the EPA issued new guidance and delayed or reversed mining permits if TDS discharge levels were predicted to be too high downstream of mining operations (Silva and Giles, 2010). However, a recent court ruling (National Mining Association, 2011) found no fault behind the science of the guidance, but stated that the EPA overstepped its authority under the Clean Water Act (CWA) and Surface Mining Control and Reclamation Act and could not enforce the new guidance as law, stating that it is up to individual states (or the EPA) to come up with defined numerical water quality standards.

Many of the previous studies concerning TDS release from mine spoils utilized a similar (or "standard") column leaching method to evaluate the spoil. This method has been used over the years and utilizes a bi-weekly leaching cycle with simulated acid rain (Daniels et al., 2009; Halvorson and Gentry, 1990; Hood and Oertel, 1984; Orndorff et al., 2010). However, questions have been raised about the potential for saturation in presumptively unsaturated columns as well as the effects of varying leaching solution pH and leaching cycle on the predicted TDS release

from mine spoils. The purpose of this three-part study was to observe the effects of zones of saturation (if present), leaching solution pH, and leaching cycle on the release of TDS and elements of concern over extended periods of time.

LITERATURE REVIEW

TDS Compliance and Environmental Impact

Mountaintop mining with associated valley fills located above headwater streams is an increasingly common type of surface mining used to mine coal in Kentucky, West Virginia, and Southwest Virginia (Palmer et al., 2010). This type of surface mining consists of the removal of vegetation and topsoil, coupled with blasting of bedrock to gain access to the underlying coal. The large volume of bedrock, or overburden, removed during the mining process is replaced into the mine pit with the excess placed into adjacent valleys, often burying ephemeral, intermittent and perennial streams in the process (Palmer et al., 2010; USEPA, 2011). Leachate from valley fills in the central Appalachians often contains elevated pH, electrical conductivity (EC) and TDS due to increased concentrations of sulfate, bicarbonate, Ca, Mg, Fe, Mn, Se, alkalinity, and K (Bryant et al., 2002; Hartman et al., 2005; Lindberg et al., 2011). Green et al. (2000) found that increases in EC correlated with decreases in overall biologic condition in streams associated with mountaintop mining and valley fills. In addition, both Green et al. (2000) and Pond et al. (2008) showed that healthy Appalachian streams, unaffected by mining activities, had EC values less than 500 $\mu S\ cm^{-1}$. When streams in the Appalachian region receive alkaline mine drainage, EC values often exceed 500 $\mu S\ cm^{-1}$. Pond et al. (2008) found significantly fewer taxa and less proportional abundance of insects belonging to the orders *Ephemoptera, Plecoptera*, and *Trichoptera* in West Virginia streams affected by mountaintop mining as indicated by EC values over 500 $\mu S\ cm^{-1}$. Shifts in aquatic communities, lowered biodiversity, and loss of salt intolerant

species were seen when the salinity levels increased (Weber-Scannell and Duffy, 2007). Chapman et al., (2000) found that > 1000 mg TDS L^{-1} affected chironomid larvae. Using general additive models, Bernhardt et al. (2012) established that biological impairment of streams occurs when ionic strength exceeded 308 μS cm^{-1} or sulfate concentrations exceed 50 mg L^{-1}, however, these values had high variance. Thus it is clear that there are strong correlations between elevated TDS levels in streams associated with mining activities and the negative impacts on benthic fauna.

The 300 μS cm^{-1} and 500 μS cm^{-1} levels have been widely cited as benchmarks above which, adverse effects on benthic fauna are observed in Appalachian streams (Bernhardt et al., 2012; Palmer et al., 2010; Pond et al., 2008). The EPA issued new guidance using 300 μS cm^{-1} as the cutoff for current and future permit issuance in the Appalachian region and 500 μS cm^{-1} as a level for field non-compliance (Cormier et al., 2013; US EPA 2011b). A recent court decision (National Mining Association, 2011), ruled against the EPA, stating that the EPA had overstepped its bounds in trying to use its new guidance to regulate EC using the CWA and SMCRA. It could not use the CWA and SMCRA to promote its final guidance as "*de facto*" law without going through all the proper procedures used to develop and gain public approval of current surface water quality standards. The ruling stated that it was up to the states (or the EPA) to develop numerical water quality standards pertaining to effluent from coalmines in the Appalachian region.

Column Leaching Studies

Carrucio et al. (1993) performed an overburden analysis and leachate prediction techniques comparing acid-base accounting, humidity weathering cells, column tests (large and

small), and Soxhlet reactors for the purpose of predicting field leaching conditions. They concluded that the leaching columns provided the best approximations of field weathering conditions. Historically, column leaching studies have primarily focused on pH/acidity generation via pyrite oxidation, TDS release from mine spoil, and the kinetics of trace metal leaching (Carrucio et al., 1993; Daniels et al., 2009; Halverson and Gentry 1990; Hood and Oertel 1984; Orndorff et al., 2010). Many of the unweathered rocks encountered in coal and metal mining environments contain acid forming materials such as pyrite (FeS_2) and other sulfide minerals (Doepker and O'Connor, 1991; Doye and Duchesne, 2005). When pyrite is oxidized, both metals and acidity are released (Kleinmann et al., 1981) and then interact with the balance of the mineral matrix of the mine spoil, refuse or tailings. The primary mechanism of pyrite oxidation is shown below (Singer and Stumm, 1970).

$FeS_2 + 7/2O_2 + H_2O \rightarrow Fe^{2+} + 2SO_4^{2-} + 2H^+$

$Fe^{2+} + 7/H_2O + 1/4O_2 \rightarrow Fe(OH)_3(s) + 2H^+$

$Fe^{2+} + 1/2O_2 + H^+ \rightarrow Fe^{3+} + 1/2H_2O$

$FeS_2 + 14Fe^{3+} + 8H_2O \rightarrow 15Fe^{2+} + 2SO_4^{2-} + 16H^+$

Pyrite oxidation is often coupled with carbonate mineral dissolution and subsequent neutralization reactions in mine spoils and wastes. The mechanism of the dissolution of carbonates is presented below (Berner and Morse, 1974).

$CaCO_3 \rightarrow Ca^{2+} + CO_3^{2-}$

$H^+ + CaCO_3 \rightarrow Ca^{2+} + HCO_3^-$

$2H^+ + CaCO_3 \rightarrow Ca^{2+} + H_2CO_3$

$H_2CO_3 + CaCO_3 \rightarrow Ca^{2+} + 2HCO_3^-$

Sulfate, bicarbonate, Ca, and Fe are the common end products of the acid-base neutralization reactions associated with pyrite oxidation and carbonate mineral dissolution in coal mine spoil. In work that preceded this study and framed my objectives, Orndorff et al. (2010) evaluated the leaching potential of predominantly non-acid forming spoils from southwestern Appalachian coal mines using a column leaching procedure based on earlier work by Stewart et al. (1997) and Daniels et al. (1999).

Leachate pH

The pH of overburden in southwestern Virginia largely depends on the quantities of carbonates and reactive pyrite (sulfur) present in the rock as well as the weathering environment. The relatively high pH (> 7.0) of many overburden strata from this region is due to secondary carbonate rock cements which can range up to > 2.5% of original rock mass (Howard et al., 1988). Due to these compounds, the pH of weathered and partially oxidized mine spoils and unweathered spoils generally ranges from 4.5 to 6.0 and 6.5 to 8.0, respectively (Roberts et al., 1988). This relationship was seen in the column leaching study by Orndorff et al. (2010), where pH values of unweathered overburden samples were between 7.0 and 8.0 and pH for weathered samples ranged from 4.0 to 7.0. Overburden from coal mines in Indiana showed a similar trend with the majority of the spoils having an alkaline pH with a smaller percentage of acid-forming spoils (Hood and Oertel, 1984). Agouridis et al. (2012) examined the leachate from weathered (brown) and unweathered (gray) sandstones using 0.4 ha cells at the Bent Mountain surface mine in Kentucky and also saw moderately alkaline pH values for both types of spoil.

Various researchers have reported on the apparent interactions between the acid-base chemistry of the spoils packed into columns vs. the nature of the leaching solutions employed. In

the column leaching study by Halverson and Gentry (1990), leachate pH was not affected by the pH of the influent solutions. However, the spoil used in their column study was acid forming and the buffering capacity of the system may have negated any pH effects (Halverson and Gentry, 1990). In another study, column leachates generated from the same spoil material had a higher pH when run under unsaturated conditions as compared to saturated conditions (Daniels et al., 2009). Siderite ($FeCO_3$) dissolution reactions in the columns and the effects of CO_2 partial pressure on carbonate cement dissolution were suggested as two possible explanations (Daniels et al., 2009).

Total Dissolved Solids and EC

Total dissolved solids refers to the mass/quantity of non-volatile inorganic and organic substances dissolved in solution. In leachate from coal mine spoils, the majority of these substances are inorganic ions, mainly HCO_3^-, SO_4^{2-}, Cl^-, Ca^{2+}, K^+, Mg^{2+}, and Na^+ (Agouridis et al., 2012; Hartman et al., 2005; Orndorff et al., 2010). Total dissolved solids is only rarely measured directly due to it being very labor intensive and is generally estimated via electrical conductivity (EC) or specific conductance (SC; EC corrected to 25^o C). Studies show correlation coefficients greater than 0.95 when plotting TDS and EC, thus making EC a very effective measure for TDS in solutions with similar ion balances but differing TDS concentrations (Daniels et al., 2009; Hood and Oertel, 1984). Leachate EC (proxy for TDS) is typically higher in leachates from unweathered mine spoil than from weathered materials from roughly the same geology, and this observed difference is most profound in finer textured mudstones (Agouridis et al., 2012; Orndorff et al., 2010). Regardless of leachate pH, samples with high concentrations of sulfides released large quantities of TDS for the duration of one study by Daniels et al. (2009).

On a mass basis, TDS eluted by fresh mine spoils is dominated by sulfates under unsaturated flow conditions and by a mix of sulfates and bicarbonate under saturated flow conditions (Orndorff et al., 2010). In non-sulfidic materials, leachate EC/TDS values peak within the first few leaching cycles and then drop quickly and eventually level off after 10 to 20 leaching events (Halverson and Gentry, 1990; Hood and Oertel, 1984; Orndorff et al. 2010). In the previously mentioned study by Agouridis et al (2012), EC levels from the unweathered gray sandstone approached the 500 $\mu S\ cm^{-1}$ benchmark within two years. For non-sulfidic materials, the degree of saturation in the columns in one study by Daniels et al. (2009) did not appear to have significant effects on leachate EC since both the saturated and unsaturated columns did not show treatment effects (Daniels et al., 2009). However, an earlier study (Daniels et al., 2006) with strongly acid-forming refuse materials showed that saturated conditions inhibited pyrite oxidation and led to lower EC generation over time.

Trace Metals and Elements of Interest

The primary elements of interest commonly analyzed for in mine spoil leachates are Al, As, Ca, Cr, Cu, Fe, K, Mg, Mn, Na, Ni, S (as SO_4^{2-}), Se, Zn, and C (as HCO_3^-) (Agouridis et al., 2012; Halverson and Gentry, 1990; Orndorff et al., 2010). However, as mentioned earlier, bulk TDS tends to be dominated by Ca, HCO_3, K, Mg, and SO_4 in terms of total mass and charge (moles). Using sequential extraction techniques vs. column leachate data, Daniels et al. (2009) found that As, Cr, Cu, Ni, Zn, and Se were found in the recalcitrant (residual) portion of the overburden, but that very low levels (at or below levels of detection) were released under moderate pH conditions via carbonate dissolution. However, even though Se was present in the spoils in low concentrations and in the recalcitrant mineral fraction, initial leachates contained

significant concentrations of Se relative to the MCL for drinking water (0.050 mg/L; Daniels et al., 2009).

Thus it appears that Ca, Fe, HCO_3, Mn, and SO_4 concentration in leachate from the moderate pH spoils from central Appalachia are controlled by acid-base reactions which in turn are governed by trace pyrite oxidation, carbonate reactions and relative water saturation and associated oxidation potentials. Sulfate release is a function of the acid-base reactions mentioned above and the initial amount and size of sulfide-S present in the spoil. The majority of sulfate released from low-sulfur spoil occurs during the first leaching events and sulfate then rapidly decreases and levels off over time (Daniels et al., 2009). Leachate from unweathered spoils contained a higher concentration of Ca compared to the weathered spoil, which was not true for other base cations such as Mg^{2+}, and $K^{+.}$ Calcium release patterns are similar to the pattern seen with SO_4^{2-} leaching. While Agouridis et al., (2012) used 0.4 ha test cells constructed on a surface mine and not leaching columns, they observed that levels of sulfate, Cl, and Ca decreased over the course of the two year study.

Iron elution in column studies is generally reported to be more variable and often does not follow the same pattern seen with sulfate leaching, presumably due internal oxide precipitation reactions in the columns. Due to the high pH of the leachate (>7.0) most of the Fe precipitates out into insoluble oxy-hydroxide forms via hydrolysis reactions (Orndorff et al., 2010). In spite of the fact that Mn and Fe are both redox sensitive and show similar patterns of release, leachates contained higher concentrations of Mn than Fe due to its increased solubility at higher pH values (7-8; Daniels et al., 2009).

In contrast to sulfate, bicarbonate release is more variable with time and often increases over the course of a column leaching study because it is governed by the dissolution of

carbonates present in the mine spoil. Saturation level of the spoil also plays a large role in HCO_3^- release. Saturated mine spoil leaches significantly more bicarbonate than unsaturated spoil of similar geology for acid-forming materials, but this may or may not hold true for non acid-forming spoils. Acid neutralization reactions in low S materials were thought to account for the lower levels in unsaturated spoil leaching columns (Orndorff et al., 2010). Halverson and Gentry (1990) ran a factorial analysis on the leachates from their column study and saw that Mn, Mg, Fe, Zn, Ca, and SO_4^{2-} all showed a similar release pattern which correlated with the number of leaching cycles. This grouping of elements and associated pattern of release was roughly consistent with the results of the column studies by Orndorff et al. (2010) showing that the acid-base reactions of pyrite oxidation and carbonate dissolution were directly controlling the leachate chemistry. Differences in mine spoil pH could account for the variations in trace metal release since moderate-to-high pH materials were used by Orndorff et al. (2010) and an acid-forming material was used by Halverson and Gentry (1990).

Column Leaching Techniques

Current column leaching techniques are primarily geared toward the study of acidity and the metals released in the leachate from mine spoils (Orndorff et al., 2010). Little is known about how traditional leaching procedures affect TDS release from mine spoils, because until recently, bulk TDS elution was not always a major concern.

Column Design

Leaching columns are commonly constructed out of PVC pipe or smooth bore ABS plastic drainpipe (Beck et al., 2007; Daniels et al., 2009; Jackson et al., 1993; Orndorff et al.,

2010; Stewart et al., 2001). Plexiglas has also been used to construct columns (Zysset and Berggren, 2002). Column sizes range from approximately 3 cm to 20 cm in diameter (Beck et al., 2007; Forsberg et al., 2008; Orndorff et al., 2010; Stewart et al., 1997; Zysset and Berggren, 2002). Reported column lengths vary from 14 cm to 120 cm; thus, there is no standard column length (Doepker and O'Connor, 1993; Halverson and Gentry, 1990; Li and Wong, 2010; Stewart et al., 1997). However, the majority of mine spoil/waste columns reported to date have been around 40 cm long (Daniels et al., 2009; Orndorff et al., 2010; Stewart et al., 1997).

Unsaturated column leaching procedures more closely mimic natural mine fill systems (Bradham and Carrucio, 1990) than do saturated columns or harsher bench top oxidation procedures, such as Soxhlet reactors (via heating and reflux). All reported column protocols use a type of filter pack material (sand or glass beads) coupled with filter paper and nylon mesh to promote uniform drainage of the influent through the treatment/reaction zone and to ensure that unsaturated conditions exist in the columns. Simulated precipitation or other influent solutions is added to the columns either drop-wise (Doepker and O'Connor, 1991), continuously via peristaltic pump, (Zysset and Berggren et al., 2001), or via a single dose of 2.5 cm given weekly or bi-weekly (Daniels et al., 1999; Halversen and Gentry, 1990; Orndorff et al., 2010). The amount of influent solution is often based on annual rainfall data, but many studies intentionally add solution more frequently to accelerate weathering reactions. In the single and bi-weekly dosing used in our laboratories at Virginia Tech, a perforated cup is used to uniformly distribute the precipitation to prevent channelization and preferential flow (Orndorff et al., 2010).

Acid-washed sand and glass beads along with filter paper and nylon mesh are used as the filter pack material to aid in drainage in many studies. The filter paper and nylon mesh prevent fine particulate migration and blocking of the leachate collection device. Acid-washed sand in

the bottom of the columns acts as a reservoir to prevent the bottom of the treatment zone in the columns from becoming saturated (Daniels et al., 2009; Jackson et al., 1993; Orndorff et al., 2010; Stewart et al., 1997). Sand packs and filter paper are not the only options: glass filter discs, glass–fiber filters, and 0.2 um filters are also used to prevent fine particulate losses and blockage of the drainage holes (Forsberg et al., 2008; Zysset and Berggren, 2001). According to Orndorff et al. (2010), a thin layer of saturation in the sand and in the bottom of the treatment zone may develop after each dosing cycle due to "perching" of a thin saturated zone at the sand-open-air interface at the bottom of the column. It is unclear if this possible saturated layer has any effects on the leachate kinetics or chemistry, but Orndorff et al. (2010) have routinely observed Fe-oxides, jarosite and other oxidized mineral phases at the bottom of their columns, which would tend to discount the possibility of a significant prolonged period of saturation and low electropotential (Eh) at the bottom of their columns.

Zysset and Berggren (2001) designed a column set-up that would ensure persisting unsaturated flow conditions. The design utilizes a vacuum pump and pressure sensor with a vacuum of 10 kPa to ensure that the system remains unsaturated (Zysset and Berggren, 2001). Forsberg et al. (2008) also used the set-up designed by Zysset and Berggren (2001) to promote unsaturated flow conditions in their column study on leaching of metals from mine tailings.

The size (diameter) of the column and the degree of sorting in the sample is critical to the amount of that leachate that will drain from the columns and the ease with which it will drain through the set-up (Caruccio et al., 1993). They recommended that particle size for the columns should range between 2 and 4 mm; smaller particles coupled with capillarity may hold leachate from draining and cause saturated conditions (Caruccio et al., 1993). In the larger diameter (approximately 20 cm) column studies by Beck et al. (2007), Jackson et al. (1993), and Stewart

et al. (2001) the coal refuse samples were sieved to $\leq$2.5 cm and were always < 15% of column diameter. In smaller column studies (approximately 7-10 cm in diameter) the samples of mine spoil and coal refuse were sieved through a 2 mm sieve to discard the coarse fragments (Halverson and Gentry, 1990). However, Orndorff et al. (2010) also used coarse fragments in their column study that passed through a 1cm sieve. In most column studies, once the samples are sieved, they are then mixed well to promote uniformity and eliminate preferential flow (Halverson and Gentry, 1990; Jackson et al., 1993; Orndorff et al., 2010; Stewart et al., 2001) and carefully placed in thin lifts within the columns to avoid sorting.

Leachate is generally collected by a plastic funnel or concave PVC cap with attached nipple connected to the bottom of the column. Stewart et al. (1997; 2001) and Jackson et al. (1993) used a plastic funnel filled with glass wool in order to wick the leachate from the bottom of the column. The funnels were sealed with silicon to prevent gas exchange and an attached plastic tube with an HDPE stopper was then used to drain the leachate from the funnel or PVC nipple (Jackson et al., 1993; Orndorff et al., 2010; Stewart et al., 1997; 2001). These studies also kept sufficient leachate in the tubing or funnel at the bottom of the column to form an air block and prevent excessive oxygen from diffusing up into the bottom of the columns.

Dosing Cycle

The dosing cycle for mine spoil/waste column studies varies considerably. Unsaturated columns have been dosed weekly (Daniels et al., 1999; Halverson and Gentry, 1990; Stewart et al., 2001), bi-weekly (Beck et al., 2007; Daniels et al., 2009; Orndorff et al., 2010; Stewart et al., 1997) and continuously (Forsberg et al., 2008; Zysset and Berggren, 2001). Studies that examined the leaching of mine spoils with regards to TDS are Halverson and Gentry (1990) and

Orndorff et al. (2010) and they used weekly and bi-weekly dosing cycles, respectively. In saturated mine spoil columns, leaching solution is added, as needed, to offset evaporative loss and ensure that the columns remain saturated above the acid-washed sand (Orndorff et al., 2010) between dosing cycles. At the start of each column run, the leaching cycles may be accelerated to hydrate the unsaturated columns and bring them to field capacity in order to allow for an approximately equal volume of leachate to drain after each simulated rain event (Orndorff et al., 2010; Stewart et al. 2001).

The only literature on the effects of various leaching cycles on coal mine spoil leachate is a preliminary experiment done by Hood and Oertel (1984). In this study, de-ionized water was used as the leaching solution. Reported aeration times in between leaching events were one day, two days, four days, one week, two weeks, and four weeks. They reported that the different leaching cycles had little to no effect on leachate conductivity (EC). A once per week leaching cycle was chosen for their full column leaching experiment in order to maximize the aeration time between leaching events and still complete the study in a reasonable length of time (Hood and Oertel 1984).

Leaching Solution pH

Column leaching studies evaluating leachate chemistry from coal mine spoils have primarily used either simulated acid rain or de-ionized water as the leaching solution (Daniels et al., 2009; Halverson and Gentry, 1990; Hood and Oertel, 1984; Orndorff et al., 2010). Halverson and Gentry (1990) performed a study on the long-term leaching of mine spoil from Kentucky with simulated precipitation of varying pH. Six treatments with pH values of 3.8, 4.2, 4.6, 5.6 and a DI water control of pH 6.4 were applied to the columns and all leaching solutions

with pH values 5.6 and below had similar leachate chemistry (Halverson and Gentry, 1990). There was no mention of how the ionic strength varied. The leachates from the column using a pH 6.4 leaching solution were not run in triplicate like the acid rain treatments and did not show a statistically significant difference in leaching contaminants of concern compared to the other treatments (Halverson and Gentry, 1990). Leachate pH was not affected by the pH of the simulated acid rain or the DI water control and as mentioned earlier, the spoil was strongly acid forming. Many subsequent studies have used the simulated acid rain as prepared in Halverson and Gentry (1990) as the leaching solution for column studies (Daniels et al., 2009; Orndorff et al., 2010). There is no literature on the effects of an alkaline pH (>7.0) leaching solution, representing carbonate rich leachate, on leachate chemistry from the coal mine spoils of central Appalachia.

CHAPTER 2. MATERIALS AND METHODS

Geology

Mine spoil from the Harlan Formation located at the Powell River Project site in Southwest Virginia was used for the duration of this project. This spoil was chosen because of its relatively uniform TDS elution curve (relative to other spoils sampled recently studied by our group), with high (> 800 us cm^{-1}EC) initial spike and subsequent rapid decrease in TDS that is seen with many other non-sulfidic mine spoils. The Harlan Formation is predominantly comprised of sandstone (up to 48%) with siltstone, shale, and coal present as well (USGS, 1993). The spoil for this experiment was from an unweathered, medium gray sandstone portion of this formation. Particle size analysis of the bulk spoil showed that approximately 44% was > 2mm and 56% < 2mm (Burt, 2004). Particle size analysis of the < 2 mm fraction by the Virginia Tech Soils Laboratory showed that the spoil was 84% sand, 10% silt, and 6% clay.

Spoil Preparation

The spoil was air dried and crushed to pass through a 1.25 cm (1/2 in) diameter sieve and then back-blended in order to maintain the entire mass of spoils of the pre-crushed spoil. The cone and quarter method was used to divide the spoil into 1200 cm^3 (approximately 1500 g) subsamples and to uniformly distribute the coarse and fine materials.

Spoil Characterization Methods

All parameters were performed in triplicate unless noted otherwise. Saturated paste extracts were used to determine electrical conductivity (EC) and pH (Rhoades, 1996). The spoil samples were crushed to pass through a 2 mm sieve mixed with deionized (DI) water forming a

paste-like consistency, equilibrated for approximately 1.5 hours, then filtered and analyzed. Calcium carbonate equivalence (CCE) was conducted in duplicate and determined by AOAC method 955.01 (AOAC International, 2002). Samples for total S were powder ground and run in duplicate on a Leco S632 sulfur analyzer. To calculate the concentrations (mg kg^{-1}) of Al, As, Cd, Ca, Cu, Fe, K, Mg, Mn, Na, Ni, Pb, Se, and Zn, a 0.5 g spoil sample was acid digested using EPA Method 3051A, Revision 1 (USEPA, 2007). The acid digested samples were then analyzed for the elements of interest via Thermo Electron Corporation ICP-MS, X-Series USEPA method SW 846 6020A, revision 1 (USEPA 2007).

Column Construction and Packing

Columns were constructed out of PVC pipe with an inner diameter of 7.4 cm, length of 40 cm, and a concave PVC end cap with attached plastic nipple and tygon tubing. Further information on this column design can be found in Orndorff et al. (2010). A perforated circular plastic disk was placed in the bottom of the columns to support the filter paper, mesh, and spoil. Nylon mesh with a diameter of 0.1 mm and Whatman #1 filter paper were placed on top of the plastic disk to prevent both fine and coarse particulates from both leaching out of the columns and blocking the drainage tube. A 2.5 cm layer of acid-washed sand was placed on top of the filter paper, which helped promote uniform leachate drainage and act as a leachate reservoir to insure the bottom of the spoil samples remained unsaturated. Based on the column study by Orndorff et al. (2010), 1200 cm^3 of spoil, was added to each column in small lifts to avoid coarse and fine particulate stratification. Finally, 2.5 cm of coarse acid washed sand was placed on top of the spoil to promote uniform infiltration of the leaching solution. All columns for this experiment were constructed and packed following this method and specific details for several

treatments are discussed in the following sections. All treatments were run in triplicate and Table 1 presents a summary of all treatments.

Table 1. Summary of all treatments across all three objectives. Treatments across all objectives were labeled sequentially to minimize sampling error, but each objective was treated as an individual study.

Research Objective	Treatment #	Experiment	Saturation	Leaching Cycle (Frequency)	Solution	Comment
Objective 1	**1**	Saturation Effects	Standard Unsat. (w Standpipe)	2x $week^{-1}$	pH 4.6 acid rain	Standpipe at spoil bottom – sand interface
	2	Saturation Effects	Saturated	2x $week^{-1}$	pH 4.6 acid rain	Drainage tubes clamped to keep columns saturated
	3	Saturation Effects	Vacuum	2x $week^{-1}$	pH 4.6 acid rain	Vacuum
	4	Saturation Effects	Standard Unsat.	2x $week^{-1}$	pH 4.6 acid rain	
Objective 2	**4**	Leaching Solution pH	Standard Unsat.	2x $week^{-1}$	pH 4.6 acid rain	pH 4.6 simulated acid rain
	5	Leaching Solution pH	Standard Unsat.	2x $week^{-1}$	DI pH 6	DI water (pH 6)
	6	Leaching Solution pH	Standard Unsat.	2x $week^{-1}$	$CaCO_3$ pH 8	$CaCO_3$ (pH 8)
Objective 3	**7**	Leaching cycle	Standard Unsat.	2x $week^{-1}$	pH 4.6 acid rain	
	8	Leaching cycle	Standard Unsat.	1x $week^{-1}$	pH 4.6 acid rain	
	9	Leaching cycle	Standard Unsat.	2x $month^{-1}$	pH 4.6 acid rain	
	10	Leaching cycle	Standard Unsat	1x day	pH 4.6 acid rain	

Objective 1 – Effects of Possible Zone of Saturation on Leachate Chemistry and EC

According to Orndorff et al. (2010) the sand pack and bottom of the treatment zone (spoil sample) may remain saturated for a period of time following column leaching, due to "perching" from linear strong textural differences between the spoil and coarse sand as well as the open atmospheric interface below. Four treatments were used to see if this zone of saturation exists and if it has any effects on leachate chemistry and TDS release from the mine spoil. Treatment one used a standpipe to detect saturation, treatment two was run completely saturated, and treatment three was run unsaturated with a vacuum of -20 kpa (-0.2 bars) applied for a period of time to ensure completely unsaturated conditions. Treatment four consisted of the standard column design that has been used in previous column leaching experiments by Orndorff et al. (2010).

Treatment one consisted of a standpipe located at the interface between the sand pack and the bottom of the spoil treatment zone in the column. A hole was drilled into the side of the column and a plastic nipple was inserted right at the interface so that the bottom of the nipple was right on top of the sand pack. The nipple remained flush with the inside of the column and did not protrude into the sand and spoil. Tygon tubing was attached to the nipple and held vertical so that any saturated water that was backing up at that level would be visible in the tubing. The standpipes were inspected for evidence of perching during column leaching, approximately 30 minutes after leaching, and again prior to sample collection. Any instances of perching were noted and photographed. The basic column set up for all treatments, excluding treatment three, is shown in Figure 1.

Figure 1. Image of column set-up for treatments 1, 2 and 4 -10.

Overall, the columns were run under unsaturated conditions with simulated rainfall with pH 4.8 as prepared by Halverson and Gentry (1990) used as the leaching solution. The columns were dosed bi-weekly with 2.54 cm (125 ml) of the simulated rainfall with leachate samples collected the following day, following the column procedure used by Orndorff et al. (2010). The drainage tubes were clamped shut once the samples were collected to minimize oxygen movement up into the columns. Simulated precipitation was gently poured into a perforated plastic cup to insure uniform drainage onto the sand and eliminate preferential flow. Initial leaching was accelerated to bring the columns to approximate field capacity and subsequently generate a piston flow response thereafter so that after each leaching approximately the same volume would drain out. This was accomplished by adding 125 ml aliquots of leaching solution to the columns until approximately 125 ml of leachate filled the sample bottles, thus bringing the columns to field capacity and generating the desired volume of leachate.

Columns for treatment two were run under saturated conditions. Leaching solution was added until the columns were saturated at the surface of the acid-washed sand. Each column was covered with Saran Wrap and acid rain was added when needed to offset evaporative losses. The

drainage tubes were clamped shut to keep the columns saturated and prevent gas exchange in the bottom of the columns. Columns were leached according to the same methods as in treatment one except the leachate was drained the day of sample collection so that oxidation of leachate would not occur. For the first leaching event, leaching solution was added until the columns were saturated above the sand pack.

The vacuum manifold and column design is shown below in Figure 2. Treatment three columns were leached under a vacuum of approximately -20 kpa. A vacuum manifold was constructed to fit around the three columns and had an attached gauge to insure the pressure was kept at -20 kpa. The vacuum was turned on prior to leaching to adjust the pressure and then left on until approximately 125 ml of leachate drained out and no drips were present. Once the columns stopped dripping, the vacuum was shut off in order to keep the columns at field capacity and prevent excessive oxidation of the spoil. Prior to leachate collection, the vacuum was turned back on for five minutes to drain any leachate that may have collected overnight. Initial leaching was performed as described in treatment one.

Figure 2. Image of vacuum column design used on treatment three columns. Pressure gauge used to insure vacuum set to -20 kpa (-0.2 bars).

Columns for treatment four followed the standard column design detailed above. The columns were leached in the same methods described for treatment one, as the only difference between the two is the standpipe, which may have slightly increased airflow into the columns. This treatment was also used in the effects of leaching solution pH aspect of this study.

Objective 2: Influence of Leaching Solution pH on Leachate Chemistry and EC

Three different leaching solutions were used to observe the effects of leaching solution pH on leachate chemistry and quantity of TDS eluted from mine spoil. Treatment four consisted of simulated rainfall (pH 4.6 prepared according to Halverson and Gentry 1990), and treatment five used deionized water (pH 6.5). Treatment six columns were leached with approximately pH 8.0 water representing leachate from carbonate rich mine spoil (high pH water). The pH 8.0 leaching solution consisted of 3-4 mg of calcium carbonate ($CaCO_3$), 3 mg of calcium chloride ($CaCl_2$) and 1 L of de-ionized water. Calcium carbonate brought the pH up to around 8.0 and the $CaCl_2$ raised the EC to approximately 17 $\mu S\ cm^{-1}$, so that it would have similar EC levels to that of the simulated rainfall. Fresh pH 8.0 leaching solution was made up before each leaching event to offset acidification caused by CO_2 carbonation reactions.

Each leaching solution was randomly assigned to a set of columns and dosed bi-weekly with 2.5 cm (125 ml) of the respective leaching solution with leachate samples collected the following day, following the column procedure used by Orndorff et al. (2010). Leaching solutions were poured into a perforated plastic cup to insure uniform drainage onto the sand and eliminate preferential flow. Initial leaching was accelerated to bring the columns to an approximate field capacity as described in treatment one.

Objective 3: Effects of Leaching Cycle on Leachate Chemistry and EC

Four different leaching cycles were applied to four sets of columns to see if leaching cycle had any effects on leachate chemistry and TDS release from the mine spoil samples. The four leaching cycles used for the duration of the experiment were: bi-weekly, once weekly, bi-monthly, and once daily. Treatment seven columns were given the standard bi-weekly dosing schedule used by Daniels et al. (2009) and Orndorff et al. (2010). Columns were leached on Monday and Thursday of each week. Columns for treatment eight were leached according to the once weekly schedule. These columns were leached on Thursday of each week for the duration of the study. Treatment nine columns received the bi-monthly leaching schedule. Columns were leached on the first and third Thursday of each month. Treatment ten columns received the once daily leaching cycle. Columns were leached early each morning and leachate was collected and analyzed prior to the next leaching event. Columns were leached under unsaturated conditions with simulated acid rain as described in detail in treatment one.

Sample Analysis

Samples for all treatments were collected within 24 hours after leaching and weighed and analyzed for: pH, EC, sulfate, bicarbonate (IC), Al, As, Ca, Cd, Cl, Cu, Fe, K, Mg, Mn, Na, Ni, Pb, Se, and Zn. Weight, pH, and EC were collected after each leaching cycle whereas sulfate, IC, and the metals were analyzed based on their respective sampling schedule, found in Appendix A, Tables A-1 through A-4. After weighing, samples were decanted into sterile 15 mL test tubes for metal analysis via Thermo Electron Corporation ICP-MS, X-Series USEPA method SW 846 6020A, revision 1 (USEPA 2007). A 0.45 μm filter was used to filter certain samples at leach one. Three drops of 8 N nitric acid were added to the test tubes to acid preserve the

samples prior to analysis. To analyze for inorganic carbon (bicarbonate) leachate samples were decanted into 60 mL amber vials and filled completely insuring no head space and run on a Shimadzu Carbon Analyzer. The values were numerically converted from total inorganic carbon to bicarbonate (HCO_3) by multiplying the inorganic carbon value by 5. Samples for sulfur analysis were decanted into 25 mL bottles and determined via USEPA method SW 846 6010B, revision 2 (USEPA, 2001), using a Spectro ARCOS ICP Model FHS16 with CETAC Autosampler Type: ASX-520. Sulfur values were numerically converted to sulfate by multiplying the sulfur value by three. Column leachate along with three drops of 8 N HNO_3 were added to sixty mL bottles in order to acid preserve the samples in accordance with the sampling schedule. Electrical conductivity and pH were run on a standard EC and pH meter and samples were placed in glass test tubes for analysis. Electrical conductivity was reported as straight EC, without temperature correction to 25°C.

Statistical Analysis

The experimental design consisted of a three-part study with ten total treatments run in triplicate. Each study (objective) was treated as a separate experiment, however, treatments were labeled sequentially (1-10) to easily identify each treatment. Overall treatment effects on leachate concentrations for all parameters of interest were analyzed using a one-way repeated measures analysis of variance (ANOVA). The repeated measures ANOVA was carried out separately on each research objective. Mean separations using the LSmeans Student's t were used to perform treatment contrasts at specific leaching cycles. The repeated measures analysis was carried out on all leaching cycles for research objectives one and two. However, due to different total numbers of leaching cycles in objective three, only data from the first ten leaching

cycles were used in the analysis. In addition, one-way ANOVAs with associated mean separations (via t-tests) were used to detect differences for specific leach contrasts for objective three. Treatment effects on the total mass of elements of interest were also analyzed via one-way ANOVAs and mean separations. SAS JMP was used to conduct all of the aforementioned statistical tests. The Pearson product-moment correlation was used to construct correlation matrices on all measured parameters for the treatments. Two correlation matrices were constructed for each treatment (leaches 0 – 9 and 13 – 39), representing both the initial release and continued leaching of parameters of interest over time. Correlation matrices were constructed using Statplus: Mac. Sigmaplot^{tm} v. 11.0 was used to construct all figures.

CHAPTER 3. SPOIL CHARACTERIZATION AND EFFECTS OF VARIOUS SATURATION LEVELS

SPOIL CHARACTERIZATION

Selected chemical and physical properties of the spoil are presented in Table 2. Analysis of the bulk spoil showed that it was approximately 44% rock fragments (> 2mm) and 56% fines (< 2mm). The pH of the raw spoil using saturated paste extract was slightly alkaline (pH 7.32). This is fairly common for fresh, unweathered, non-sulfidic mine spoils from this region resulting from hydrolysis of freshly abraded primary mineral grains, carbonate dissolution, and rapid trace pyrite oxidation (Orndorff et al., 2010). The saturated paste pH (7.32) was greater than the leachate pH (4 – 7) from all treatments during the initial leaching cycle. However, after the initial dosing cycle, all treatments maintained significantly higher leachate pH (7.8 – 8.3) than the saturated paste extract.

The soluble salt content of the saturated paste extract, as represented by EC, was 744 μS cm^{-1}. Similar to pH, trace pyrite oxidation and hydrolysis of broken primary mineral grains likely contributed to the majority of EC (Orndorff et al., 2010). Leachate EC from all treatments (1200 – 1800 μS cm^{-1}) was higher than the saturated paste EC (744 μS cm-1) over the first few leaching events, suggesting that the saturated paste was not a good indicator of the initial flush of TDS. In addition, long-term EC from all treatments (200 – 300 μS cm^{-1}) was significantly lower than the saturated paste (744 μS cm^{-1}) also suggesting that the method did not give an accurate representation of the longer-term leachate EC.

Table 2. Selected chemical properties of the mine spoil used in the column leaching study. Values expressed as mean and (standard deviation).

Material	Saturated Paste		CCE	Total S	Particle Size Analysis					
	pH	EC µS cm^{-1}	%	%	% Coarse >2mm	% Fines <2mm	% Sand	% Silt	% Clay	Textural Class
Harlan Formation	7.32 (0.12)	744 (26)	3.53 (0.74)	0.02 (0.0001)	44	56	84	10	6	Loamy Sand

The total S content of the spoil (0.02%) is well below the threshold level of 0.2%, above which spoil has the potential to be acid-forming in the absence of significant carbonates (Orndorff, 2001). Low S content is to be expected since many unweathered spoils in Southwest Virginia are non acid-forming and contain trace amounts of pyrite (Schatzel and Stewart, 2012). Further discussion of sulfate leaching can be found in the section on total mass during peak elution. The spoil had a relatively high neutralization capacity (3.53% CCE), which is consistent with the bicarbonate elution seen with the leaching column trials discussed below. In addition, the alkaline pH values seen with the saturated paste and column leachate reflect the high CCE of the spoil.

The total elemental analysis for selected parameters of interest is presented in Tables 3 and 4. Levels of Al, Ca, Fe, K, Mg, and Na are characteristic of carbonate and feldspar rich overburden from the central Appalachian region (Schatzel and Stewart, 2012). The trace metal content of the spoil ranged from below detection to 20 mg kg^{-1}. However, the Zn content is much higher than the other trace metals. This could be due to the presence of siderite ($FeCO_3$), as Zn is a common substitute (Shikazono, 1977). The Se level in the spoil was below detection using the acid digestion and the detection limit was used to report the potential maximum amount of Se that could be in the spoil samples.

Table 3. Total mass (mg) of Ca, K, Mg, and Na per kg of mine spoil used in the column leaching study. Values expressed as mean and (standard deviation).

Sample ID	Ca mg kg^{-1}	K mg kg^{-1}	Mg mg kg^{-1}	Na mg kg^{-1}
Harlan VA-16	32,401 (427)	7115 (488)	3770 (21)	1036 (72)

Table 4. Total mass (mg) of Al, As, Cd, Cu, Fe, Mn, Ni, Pb, Se, and Zn per kg of mine spoil used in the column leaching study. Values expressed as mean and (standard deviation). Selenium levels were below detection and the total Se content was calculated using the detection limit.

Sample ID	Al mg kg^{-1}	As mg kg^{-1}	Cd mg kg^{-1}	Cu mg kg^{-1}	Fe mg kg^{-1}	Mn mg kg^{-1}	Ni mg kg^{-1}	Pb mg kg^{-1}	Se mg kg^{-1}	Zn mg kg^{-1}
Harlan VA-16	26,119 (2131)	3 (0.1)	0.04 (0.01)	14 (0.4)	19,886 (639)	505 (15)	16 (0.4)	9 (0.2)	0.1 (0)	40 (5)

EFFECT OF VARIOUS LEVELS OF SATURATION

Potential Saturation Zone

Perching at the sand-spoil interface in the bottom of the treatment zone was visually confirmed on only one occasion, after the second leaching event. As shown in Figure 3, there was a small amount of leachate present in the standpipe indicating perching at the interface. The image was taken approximately five minutes after the columns were dosed and perched leachate disappeared within approximately fifteen minutes. Slight staining of the tubing and faint precipitates were evident in all three standpipes. This indicated that perching likely occurred more than once. However, it is unlikely that these brief and transient perching events had any effect on leachate chemistry. As discussed below, the standard column method is significantly different from the saturated and vacuum columns for the majority of parameters of interest. This further suggests that the columns were truly unsaturated and not confounded by transient perching events. However, the increased airflow from the vacuum could have altered the leachate chemistry due to increased oxidation and weathering of the spoil.

Figure 3. Visual confirmation of perching. This was the only occurrence of perching, as noted by the presence of leachate in the standpipe.

Overall treatment effects for the effects of the saturation study are presented in Table 5.

Table 5. Summary of repeated measures statistical analysis at various saturation levels.

Source	pH	EC	HCO_3	SO_4	Al	As	Ca	Cd	Cl	Cu	Fe	K	Mg	Mn	Na	Ni	Pb	Se	Zn
TRT	***	*	**	*	NS	**	NS	NS	NS	*	*	*	*	***	NS	NS	**	NS	*
Leach#	***	***	***	***	***	***	***	***	***	***	NS	***	***	***	***	***	*	***	***
TRT*Leach	***	***	***	***	*	***	***	***	***	**	NS	***	***	***	***	NS	**	***	**

TRT, Treatment; NS, Not significant; * $P < 0.05$, ** $P < 0.01$, and *** $P < 0.001$

Electrical Conductivity (EC)

The level of saturation in the columns had a significant overall treatment effect ($p = 0.0434$) on leachate EC. The standard method and standpipe fitted columns eluted greater EC values than the vacuum columns, while the saturated columns were not significantly different from the other treatments. Initial EC values ranged from 1200 $\mu S\ cm^{-1}$ to 1650 $\mu S\ cm^{-1}$ and rapidly declined below the presumed regulatory threshold of 500 $\mu S\ cm^{-1}$ after the fourth leaching cycle. Treatment two (saturated), did show a small spike in EC values on the fourth leaching event and afterwards continued to decline. Electrical conductivity values for each

treatment leveled off between roughly between 200 $\mu S\ cm^{-1}$ and 300 $\mu S\ cm^{-1}$ for the remainder of the study.

Significant differences in EC release patterns were seen over the first ten and four of the last five leaching cycles. These effects are presented in Figure 4. Initially, the saturated, standard, and standpipe fitted columns eluted the highest levels of EC compared to the vacuum columns ($p = 0.0333$). These high EC values were presumably due to rapid trace pyrite oxidation as well as flushing off salts and other hydrated reaction products from the edges of mineral grains via exchange and rapid hydrolysis (Orndorff et al., 2010). However, the standard, vacuum, and standpipe fitted columns maintained higher EC levels than the saturated columns ($p = 0.0014$, $p = 0.0195$) over the next two leaching events. Continued saturation likely suppressed the pyrite oxidation during this span and thus lower EC levels seen with the saturated columns.

Even though the overall treatment effect did not show any significant differences between the saturated columns and the other three treatments, saturated columns eluted higher EC values ($p < 0.01$) than all other treatments between leaches three and eight. In addition, the EC values from the standard and standpipe columns were greater than the vacuum columns ($p < 0.01$) over this span. This could reflect changes in redox chemistry and possible siderite and other carbonate mineral dissolution under saturated conditions. The spike and overall higher EC values seen over this span was observed for bicarbonate, Ca, Mg, and Mn as well.

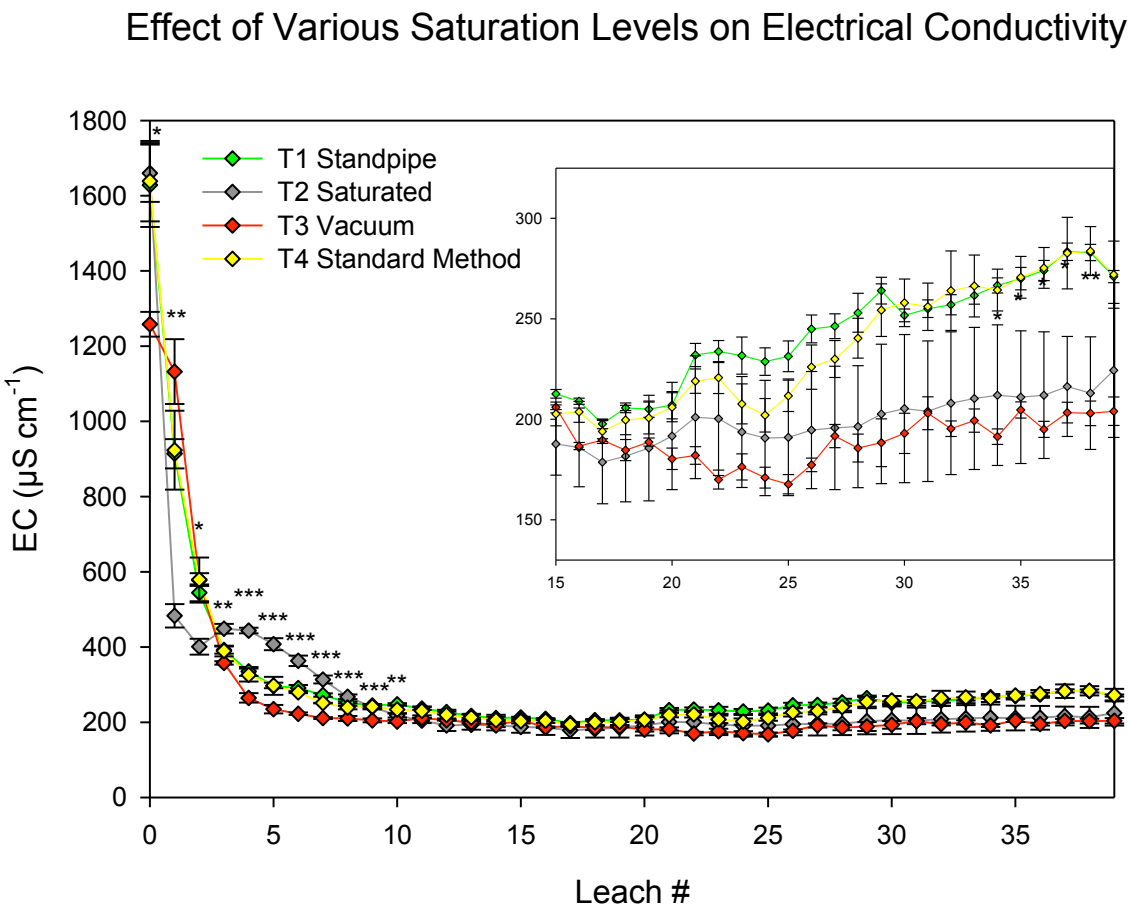

Figure 4. Leachate electrical conductivity (EC) from standpipe, saturated, vacuum and standard method columns. The 40 leaching cycles occurred over 20 weeks. Three leaching cycles corresponds to one pore volume. Error bars represent one standard error above and below the mean. Where indicated, treatment means by date were significantly different * $P < 0.05$, ** $P < 0.01$, and *** $P < 0.001$.

However, the standard and standpipe fitted columns eluted greater EC values than either the saturated or vacuum columns for the remainder of the experiment. The observed significant differences over that time were at leaches thirty-five through thirty- eight where the standard and standpipe columns were higher than both the vacuum and saturated columns ($p < 0.05$).Once again, the longer-term pattern of EC release is driven by the dissolution of carbonates. Further detail on the effects of varying CO_2 partial pressures from the various treatments is discussed below. Overall, EC release did seem to respond to differences in in oxygen supply, (via standard atmospheric diffusion in the standard method, through the standpipe, application of vacuum, and slowed diffusion via saturation) in the columns. This possibly controlled initial pyrite oxidation and possible siderite weathering and carbonate dissolution over longer periods of time.

Leachate pH

The relative saturation of the columns strongly affected leachate pH ($p = 0.0002$). Overall, the leachate from the unsaturated vacuum, standard, and standpipe columns yielded significantly greater pH values compared to the columns leached under saturated conditions. These significant differences between unsaturated and saturated conditions were apparent across the majority of leaching cycles, as seen in Figure 5. Initial leachate pH for both the standpipe and vacuum columns was approximately 7.0 and increased over the initial leaching cycles, eventually reaching steady state after leach three with pH values of 8.1 - 8.3. Treatment two (saturated) started at approximately pH 6.5 and rapidly increased to pH 7.3 after the second leaching event. Then, after the sixth leaching cycle, leachate pH leveled off around 7.8 where it remained. Initial moderate pH (5 -7) values for the vacuum and standpipe columns

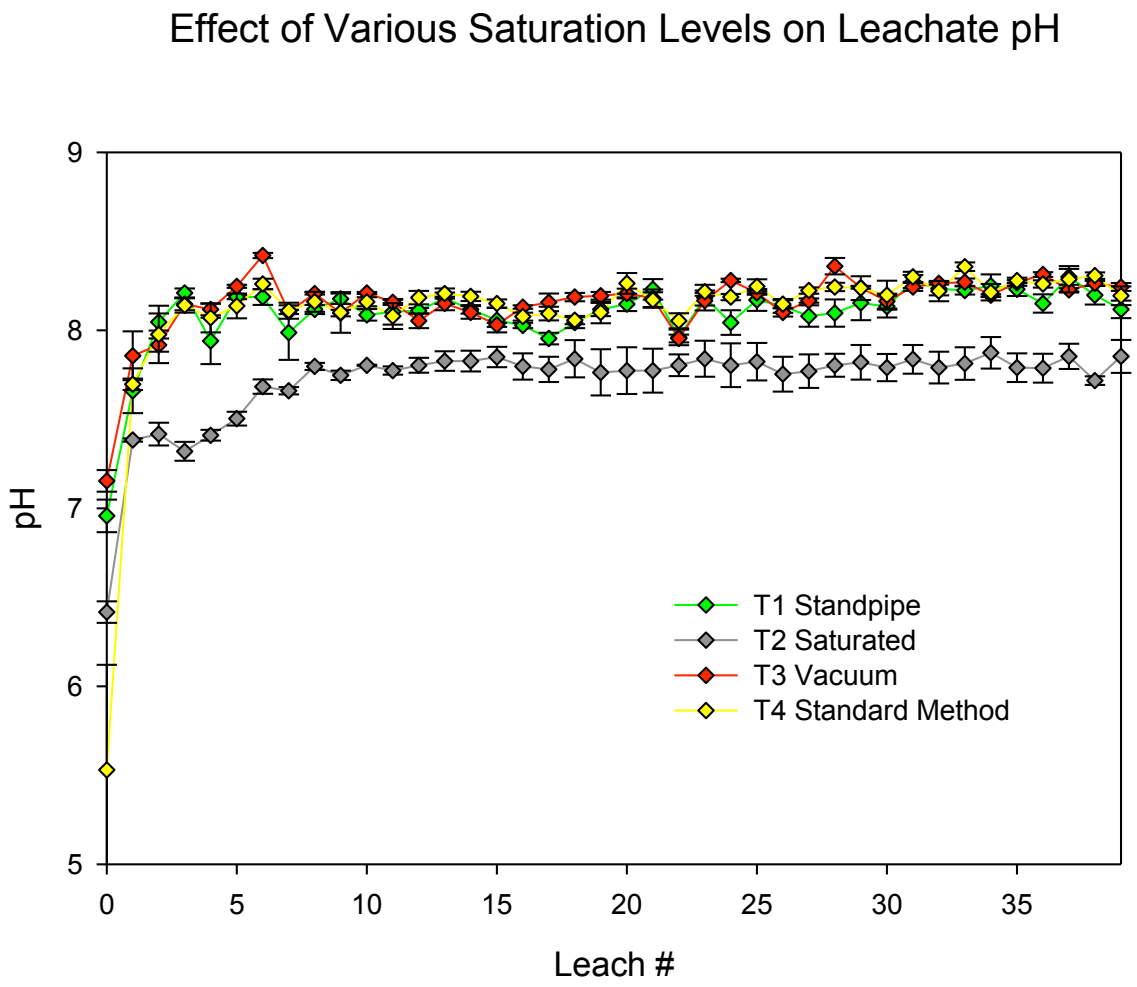

Figure 5. Leachate pH from standpipe, saturated, vacuum and standard method columns. The 40 leaching cycles occurred over 20 weeks. Three leaching cycles corresponds to one pore volume. Error bars represent one standard error above and below the mean. Due to spatial limitations, the level of significance associated with treatment differences is not given, but in general, the values shown by leach # can be considered significantly different when greater than two standard errors apart.

potentially reflect the acid base neutralization reactions associated with pyrite oxidation and carbonate dissolution.

Leachate from the standard method was moderately acidic (pH 5) reflecting rapid trace pyrite oxidation coupled with minimal carbonate dissolution. As shown in Appendix B, Table B-1, the subsequent rise in pH is strongly correlated with the increase in bicarbonate concentration ($p = 0.00395$). Previous research has shown that elevated CO_2 partial pressures in soils can increase the rate of mineral weathering (Berg and Banwart, 2000; Karberg et al., 2005). Therefore its possible that increased CO_2 partial pressures in the unsaturated treatments likely caused a decrease in internal column pH, which increased the dissolution of carbonate minerals, ultimately yielding higher leachate pH values than that of the saturated columns. An increase in rapid trace pyrite oxidation could be the cause of the lower pH values seen in the saturated columns over leaches one through four.

Sulfate

The saturation level in the columns had a strong overall treatment effect on sulfate release ($p = 0.0358$). Standpipe and standard columns released greater levels of sulfate than the saturated columns, while the vacuum columns were not significantly different from the other two treatments. Initial concentrations of sulfate for the standard, standpipe, and saturated columns were around 750 mg L^{-1}, while treatment three (vacuum columns) was approximately 550 mg L^{-1}. Sulfate concentrations quickly declined and leveled off around 10 mg L^{-1} after leach nine. Noteworthy differences in sulfate release were seen over leaches one and four through thirty, represented in Figure 6. Presumably initial sulfate release was driven by rapid trace pyrite

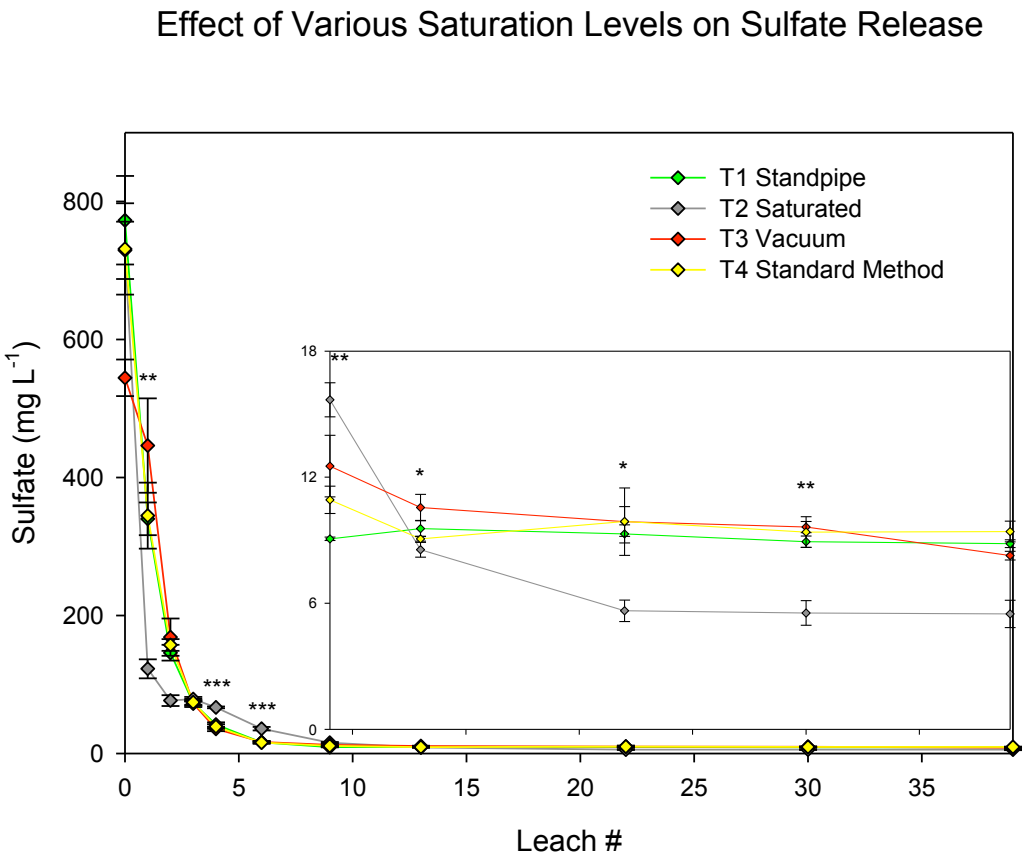

Figure 6. Leachate sulfate (SO_4) from standpipe, saturated, vacuum and standard method columns. The 40 leaching cycles occurred over 20 weeks. Three leaching cycles corresponds to one pore volume. Error bars represent one standard error above and below the mean. Where indicated, treatment means by date were significantly different * $P < 0.05$, ** $P < 0.01$, and *** $P < 0.001$. Detection limit = 0.12 mg L^{-1} and values below the detection limit were reported as 0.12 mg L^{-1}.

oxidation, as earlier work by Orndorff et al. (2010) suggested this as a probable mechanism of sulfate release. The standard, standpipe, and vacuum columns eluted higher sulfate levels than the saturated columns ($p = 0.0050$) over leaches two and three. Saturation likely suppressed the pyrite oxidation during leaches one and two, which explained the lower sulfate concentrations seen with treatment two. Sulfate concentrations from the saturated columns were significantly greater than both the standpipe and vacuum columns between leaches four and six ($p = 0.0002$, $p < 0.0001$). This slight increase in sulfate over these leaching cycles also corresponded with higher levels of Ca, Mg, and Mn. Over time, the sulfate levels in the saturated columns decreased below the levels seen with the standard, standpipe, and vacuum columns with significant differences on leach thirty ($p = 0.0014$). This suggested that saturation may have suppressed long-term pyrite oxidation.

Bicarbonate

The release of bicarbonate was significantly affected by saturated and unsaturated conditions ($p = 0.0024$). Overall, the saturated columns leached higher concentrations of bicarbonate than the standard and vacuum columns. In addition, standard and standpipe columns leached greater concentrations of bicarbonate than the vacuum columns. The treatment effects were most apparent over the first ten leaching cycles as the saturated columns were significantly greater than all three of the unsaturated treatments ($p < 0.01$); see Figure 7. In addition, bicarbonate concentrations from the standard and standpipe columns were significantly greater than the vacuum columns ($p < 0.001$) during the fist ten leaching cycles.

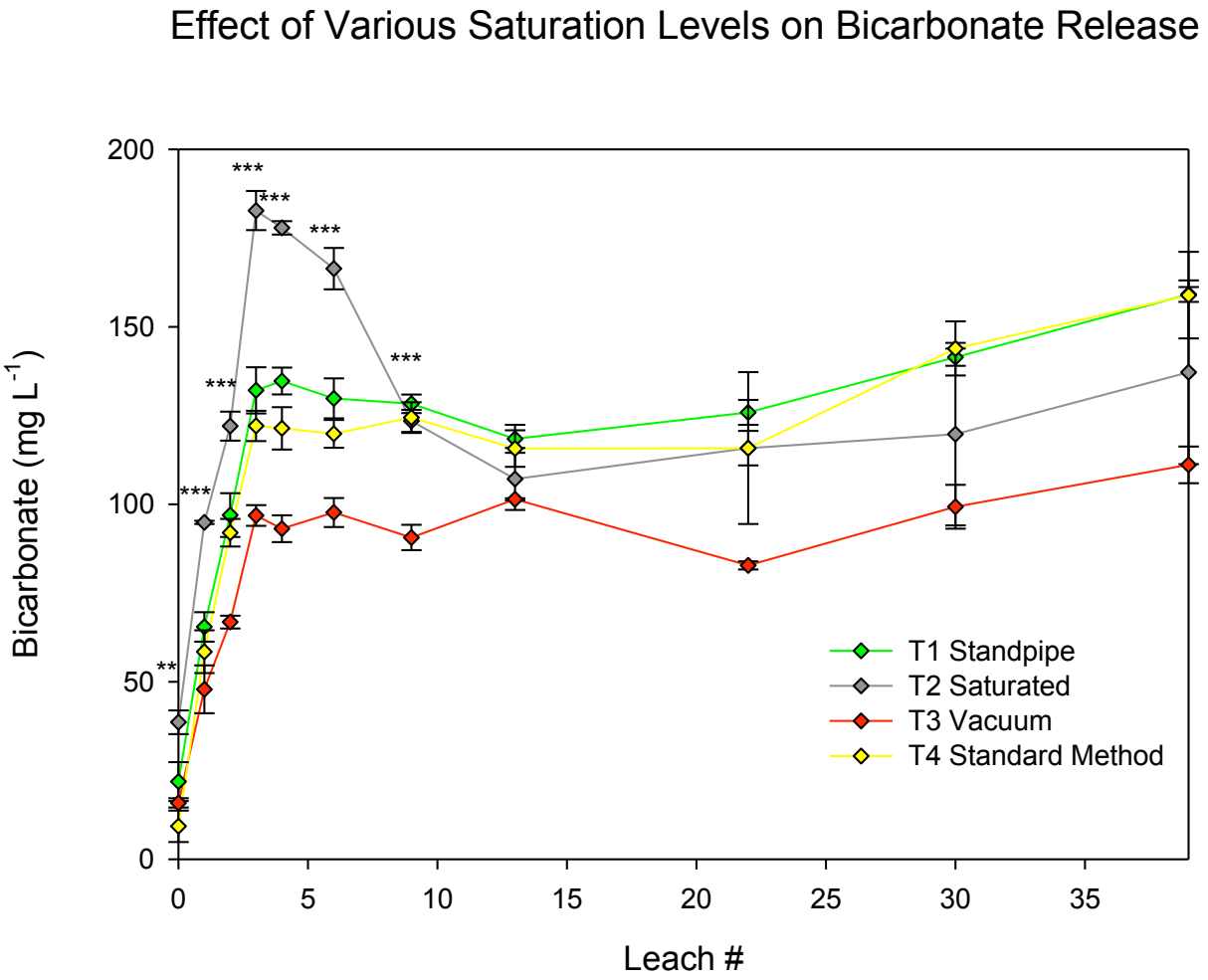

Figure 7. Leachate bicarbonate from standpipe, saturated, vacuum and standard method columns. The 40 leaching cycles occurred over 20 weeks. Three leaching cycles corresponds to one pore volume. Error bars represent one standard error above and below the mean. Where indicated, treatment means by date were significantly different * $P < 0.05$, ** $P < 0.01$, and *** $P < 0.001$.

Initial bicarbonate release from the standard method, standpipe, and vacuum columns ranged between 10 mg $L^{-1}$to 20 mg L^{-1}, while the saturated columns released approximately 40 mg L^{-1}. Bicarbonate concentrations increased rapidly over the next four leaching cycles, peaking between leaches three and four with treatments one (standpipe), two (saturated), three (vacuum), and four (standard method) eluting approximately 175 mg L^{-1}, 130 mg L^{-1}, 100 mg L^{-1}, and 122 mg L^{-1}, respectively. Then, concentrations from both the standpipe and vacuum columns began to steadily increase for the rest of the experiment. Bicarbonate levels in the saturated columns declined sharply to 110 mg L^{-1}, leveled out and then steadily increased again over time. No statistically significant differences were seen among treatments after leach thirteen.

Bicarbonate release strongly reflects the relative level of saturation in the columns. The lower levels of bicarbonate seen in the standard, standpipe, and vacuum columns compared to the saturated columns possibly reflected acid neutralization reactions, even though low levels of sulfate were present in the leachate (Orndorff et al., 2010). Secondary sulfates were potentially retained in the columns. The neutralization reactions likely consumed any acidity that was present. In addition, the higher levels of bicarbonate observed under saturated conditions were potentially due to greater contact time between the spoil and the leaching solution in the columns. However, it did not appear that the level of saturation had any effect on bicarbonate release over extended periods of time as no significant differences between treatments were noted over the final fifteen leaching cycles.

Arsenic (As) and Selenium (Se)

Overall, the release of As from the mine spoil was strongly affected by the level of saturation within the column ($p = 0.0018$). The vacuum columns eluted the highest As levels. In addition, the standpipe fitted columns leached higher amounts of As than the saturated columns as seen in Figure 8. The standard method was not significantly different from either the standpipe or saturated columns. Initial As release was between 4.5 $\mu g\ L^{-1}$ to 7.0 $\mu g\ L^{-1}$, and with the exception of the spike in As in the vacuum columns in leach one, concentrations rapidly declined, falling below the detection limit of 0.30 $\mu g\ L^{-1}$ after leach nine. The minor spike at leach thirteen may have been due to instrument error from the ICP-MS. The pattern of As release closely mirrored that of sulfate, which is consistent with its chalcophilic nature (McBride, 1994). In addition, greater As concentrations in leachate from unsaturated treatments suggested that the As may have been present in a pyritic form and released during oxidation as As is commonly found in pyrite (Huffman et al., 1994). The higher levels of As from the vacuum and standpipe columns compared to the saturated columns reflect this, since the vacuum and standpipe allowed for greater aeration of the spoil and thus greater potential for pyrite oxidation compared to the saturated columns.

The level of saturation in the columns did not have an overall treatment effect on Se release from the mine spoil. Initial Se release from the four treatments ranged from 40-50 $\mu g\ L^{-1}$, which is roughly twice the criteria maximum concentration (CMC) of 20 $\mu g\ L^{-1}$. Leachate concentrations steadily declined, but remained above the CMC for the first three leaching cycles and then dropped below the CCC to levels below the detection limit of 0.8 $\mu g\ L^{-1}$ between leaching cycles six and nine. Even though there was not an overall treatment effect,

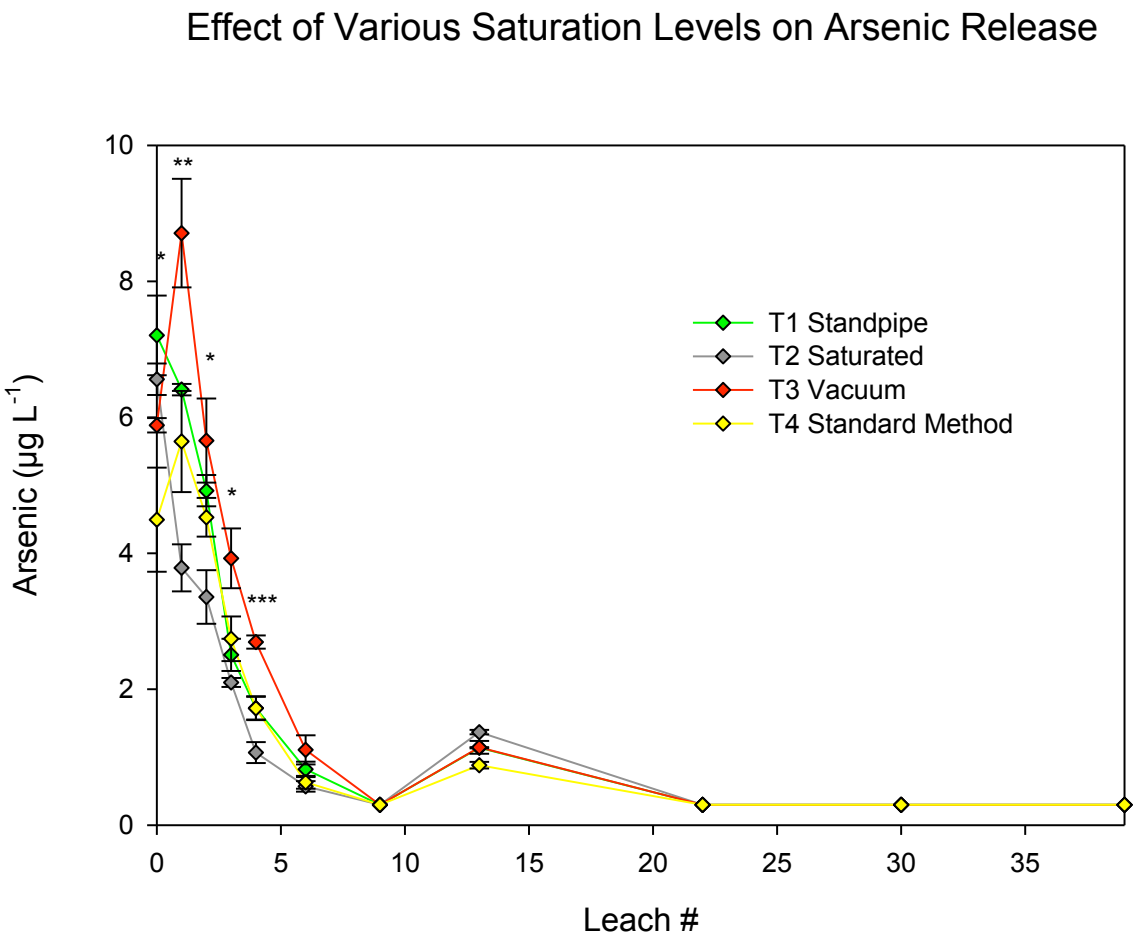

Figure 8. Leachate As from standpipe, saturated, vacuum and standard method columns. The 40 leaching cycles occurred over 20 weeks. Three leaching cycles corresponds to one pore volume. Error bars represent one standard error above and below the mean. Where indicated, treatment means by date were significantly different * $P < 0.05$, ** $P < 0.01$, and *** $P < 0.001$. Detection limit = 0.3 µg L^{-1} and values below the detection limit were reported as 0.3 µg L^{-1}.

leaches one, two, and four showed significant differences for leach specific contrasts. Selenium levels eluted from the standard, vacuum, and standpipe columns were significantly greater than the saturated columns over leaches one and two ($p = 0.0020$, $p = 0.0121$) as seen in Figure 9. However, Se leaching from the saturated columns was greater than the unsaturated treatments at leach four ($p = 0.0099$). The release pattern of Se and associated treatment effects closely matched that of sulfate and As. This suggested that the Se was present in the spoil in pyritic forms, as a metal sulfide, or possibly as PbSe (J. Unrine, personal communication), and subsequently released via rapid trace sulfide oxidation.

Calcium (Ca), Iron (Fe), Magnesium (Mg), and Manganese (Mn)

Overall, the level of saturation in the columns did not have a treatment effect on Ca release from the mine spoil. However, over the first nine leaching cycles, the pattern of Ca release was affected by the level of saturation as shown in Figure 10. With the exception of the initial leaching cycle, the unsaturated treatments had greater Ca levels over the first three leaching cycles ($p < 0.05$). However, the saturated columns were significantly greater than the standard method, standpipe, and vacuum columns over leaches three through nine ($p < 0.001$). The general release pattern of Ca closely matched that of sulfate. Initial concentrations from all treatments ranged from 175 mg L^{-1} to 230 mg L^{-1}, quickly declined to 25 mg L^{-1}, and then slowly increased over the remaining leaching cycles. The only deviation from this pattern was seen in treatment two, where Ca concentrations increased over the third and fourth leaching cycle. This increase was observed for bicarbonate as well, which suggested that carbonate dissolution drove

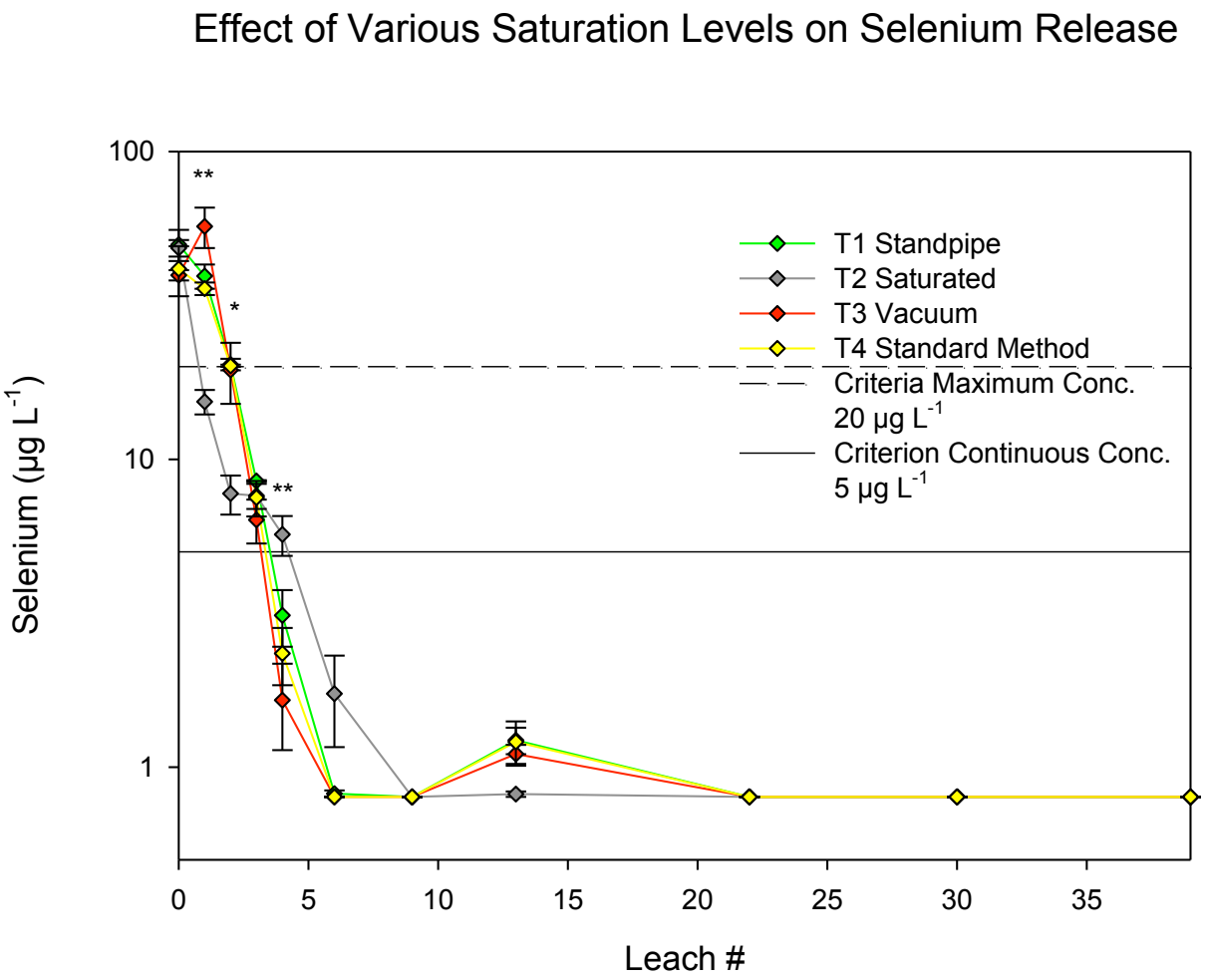

Figure 9. Leachate Se from standpipe, saturated, vacuum and standard method columns. The 40 leaching cycles occurred over 20 weeks. Three leaching cycles corresponds to one pore volume. Error bars represent one standard error above and below the mean. Where indicated, treatment means by date were significantly different * $P < 0.05$, ** $P < 0.01$, and *** $P < 0.001$. Detection limit = 0.8 µg L^{-1} and values below the detection limit were reported as 0.8 µg L^{-1}.

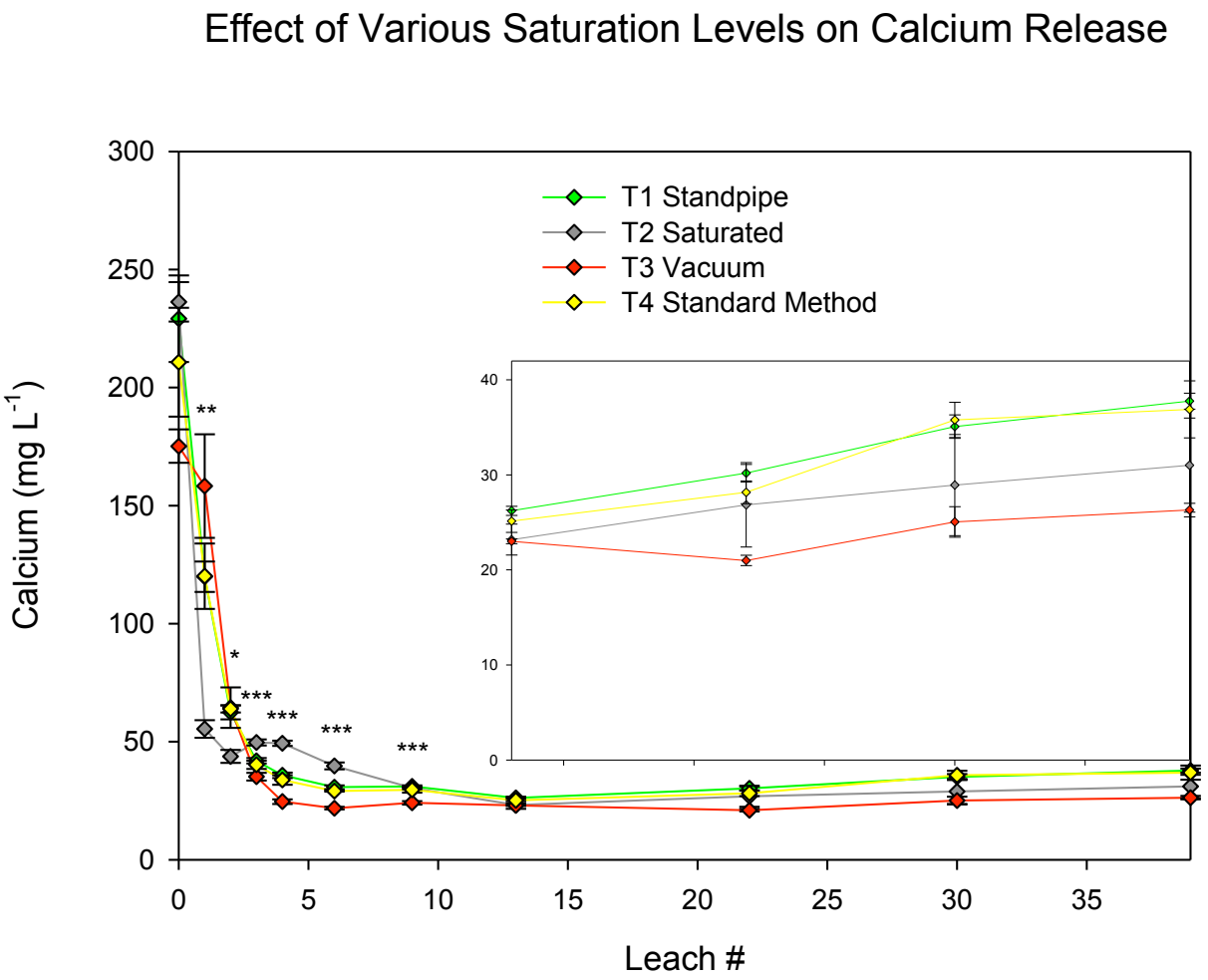

Figure 10. Leachate Ca from standpipe, saturated, vacuum and standard method columns. The 40 leaching cycles occurred over 20 weeks. Three leaching cycles corresponds to one pore volume. Error bars represent one standard error above and below the mean. Where indicated, treatment means by date were significantly different * $P < 0.05$, ** $P < 0.01$, and *** $P < 0.001$. Detection limit = 0.01 mg L^{-1} and values below the detection limit were reported as 0.01 mg L^{-1}.

the release of Ca from the spoil. The steady increase seen in concentrations over the final leaching cycles was strongly correlated with increases in EC and bicarbonate, as shown in Appendix B, Table B-2. In both the saturated and unsaturated columns, initial Ca release was likely the result of the acid base reactions associated with pyrite oxidation, carbonate dissolution, and Ca-feldspar weathering. The dissolution of siderite, which can contain Ca impurities, in the saturated columns may also have been responsible for the spike in Ca concentrations seen over leaches three and four (Anthony et al., 2005).

Overall, the degree of saturation in the columns had a strong treatment effect on the release of iron from the mine spoil ($p = 0.0334$). The vacuum columns leached greater concentrations of Fe compared to the saturated, standard, and standpipe columns. Leaches four and thirteen best exhibited the overall treatment effect ($p = 0.0401$, $p = 0.0068$) as shown in Figure 11. With the exception of the initial leaching event, the standard and standpipe columns eluted levels of Fe that fluctuated around the detection limit of 5.0 $\mu g\ L^{-1}$ for the duration of the leaching study. Initially, the saturated columns released around 500 $\mu g\ L^{-1}$, but rapidly declined and eventually leveled off around 75 $\mu g\ L^{-1}$. The three replicates in treatment three varied considerably, as indicated by the large error bars over leaches three, four, and thirty in Figure 11. Initial Fe release was approximately 300 $\mu g\ L^{-1}$and with the exception of the leaches mentioned above, oscillating between 125 $\mu g\ L^{-1}$ and 180 $\mu g\ L^{-1}$ for the majority of leaching cycles. Iron did not follow the same pattern of release seen by sulfate or other products of pyrite oxidation. In the standpipe and standard columns, iron likely precipitated and remained in the column as insoluble oxy-hydroxide precipitates as Moricz et al. (2012) suggests that above pH 4 Fe will hydrolyze and precipitate as Fe-hydrite. The slightly higher levels of Fe from the

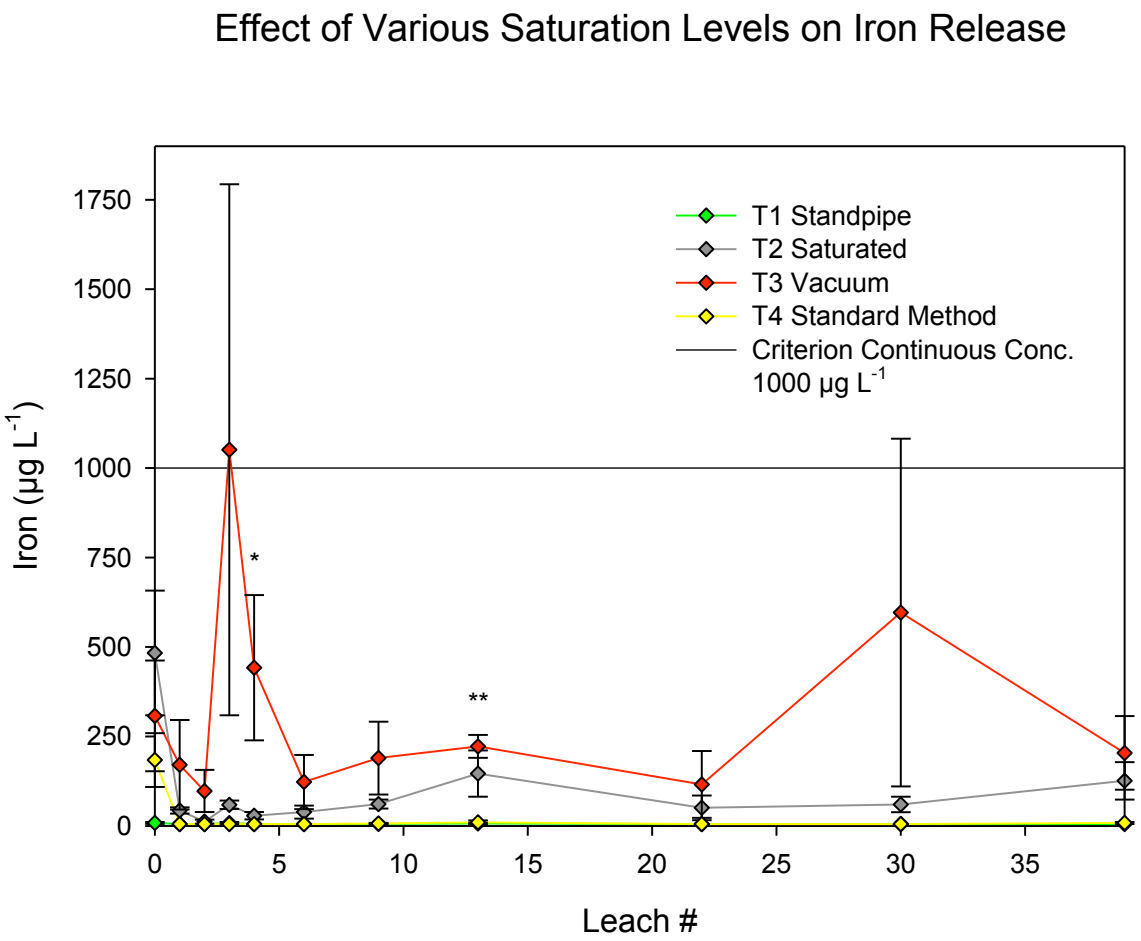

Figure 11. Leachate Fe from standpipe, saturated, vacuum and standard method columns. The 40 leaching cycles occurred over 20 weeks. Three leaching cycles corresponds to one pore volume. Error bars represent one standard error above and below the mean. Where indicated, treatment means by date were significantly different * $P < 0.05$, ** $P < 0.01$, and *** $P < 0.001$. Detection limit = 5.0 µg L^{-1} and values below the detection limit were reported as 5.0 µg L^{-1}.

saturated columns were likely due to the partial reduction of insoluble Fe^{3+} to water soluble Fe^{2+}. The initial high Fe release from the vacuum columns was likely due to fine colloidal material being pulled through the filter materials in the bottom of the columns. As shown in Table 6, leachate filtered through a 0.45 μm filter contained Fe levels below detection, while unfiltered leachate contained 171 μg $L^{-1}$of Fe. However, the higher concentrations of Fe may have been also due to the increased aeration of the vacuum causing the oxidation of Fe^{2+} in siderite ($FeCO_3$) to Fe^{3+}, decreasing its stability and enhancing the release of Fe.

Table 6. Filtered vs. unfiltered leachate Al, As, Cd, Cu, Fe, Mn, Na, Ni, Pb, Se, and Zn at leach one from the standpipe (T1), saturated (T2), vacuum (T3), and standard method (T4) columns.

Leach 1		Al	As	Cd	Cu	Fe	Mn	Na	Ni	Pb	Se
		μg L^{-1}									
T1	**Filtered**	20 (7)	6 (1)	0.1 (0)	5 (1)	5 (0)	389 (69)	3266 (114)	1 (2)	0.5 (0)	39 (5)
	Unfiltered	24 (7)	6 (0)	0.1 (0)	5 (1)	5 (0)	394 (66)	3286 (80)	3 (5)	0.5 (0)	39 (6)
T2	**Filtered**	11 (4)	3 (0)	0.1 (0)	1 (0)	5 (0)	278 (14)	1497 (263)	2 (2)	0.5 (0)	15 (2)
	Unfiltered	55 (4)	4 (1)	0.1 (0)	1 (0)	43 (15)	282 (14)	1504 (251)	0.3 (0)	0.5 (0)	15 (2)
T3	**Filtered**	23 (14)	9 (2)	7 (6)	4 (1)	5 (0)	410 (31)	4197 (640)	0.3 (0)	0.5 (0)	53 (13)
	Unfiltered	130 (14)	9 (1)	7 (6)	5 (1)	171 (216)	417 (32)	4208 (637)	0.3 (0)	0.5 (0)	57 (15)
T4	**Filtered**	49 (37)	5 (1)	0.1 (0)	2 (1)	5 (0)	381 (224)	3134 (522)	1 (2)	0.5 (0)	39 (7)
	Unfiltered	107 (37)	6 (1)	0.1 (0)	2 (0)	5 (0)	3723 (210)	3068 (482)	2 (3)	0.5 (0)	36 (3)

Detection limit for Cd = 0.1 μg L^{-1}, Fe = 5 μg L^{-1}, Ni = 0.3 μg L^{-1}, and Pb = 0.5 μg L^{-1}. Values expressed as mean and (standard deviation).

The level of saturation in the columns had a significant overall treatment effect on Mg release from the spoil samples ($p = 0.0426$) as seen in Figure 12. Magnesium release from the standpipe columns was significantly greater than both the columns under vacuum and completely saturated. In addition the standard columns yielded higher levels of Mg than those under vacuum, but were not significantly different from the saturated or standpipe columns. The general release pattern of Mg was similar for each treatment across all leaching cycles and closely matched that of sulfate and calcium. Initial concentrations ranged from 30 mg L^{-1} to 45 mg L^{-1}, quickly declined to 5 mg L^{-1}, and then over time increased up to 6 mg L^{-1}. The saturated columns slightly deviated from this release pattern, as Mg concentrations increased over the third and fourth leaching cycles.

However, the first ten leaching cycles show a slightly different trend, as seen in Figure 14. Initially the saturated, standard, and standpipe columns eluted higher Mg concentrations than the columns under vacuum ($p = 0.0468$). Over the second and third leaching cycles, treatments one (standpipe), two, (saturated), and four (standard method) leached greater levels of Mg than treatment three (vacuum) ($p = 0.0041$). With the exception of leach zero, the greatest release of Mg appeared to occur under unsaturated conditions during the first three leaching events. In contrast, over leaches three to six, the saturated columns eluted greater concentrations of Mg than the unsaturated treatments ($p < 0.001$). The standard and standpipe fitted columns also released significantly higher amounts of Mg than the vacuum columns over this span.

The observed treatment effects over the first three leaching cycles were likely the result of the acid base reactions associated with pyrite oxidation and carbonate dissolution

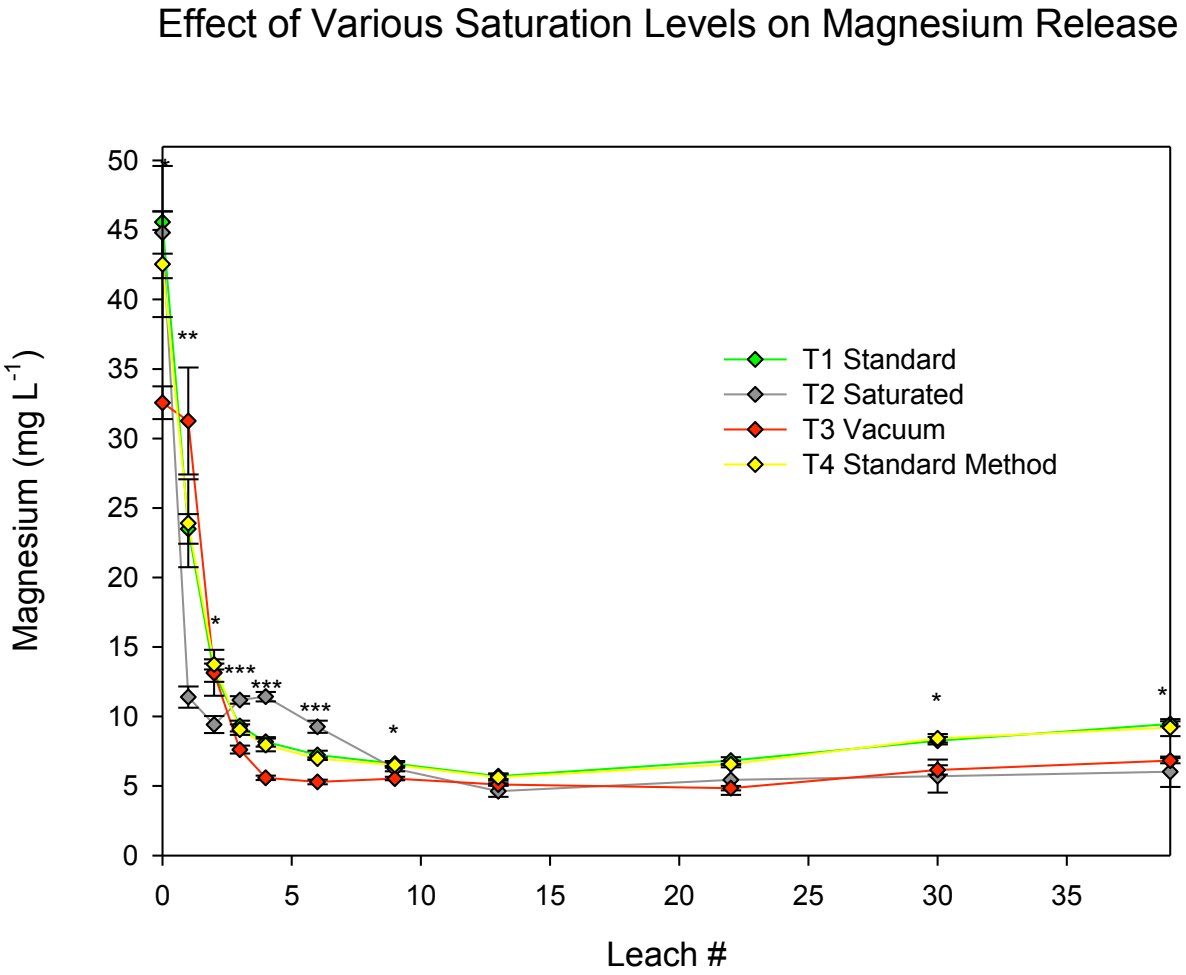

Figure 12. Leachate Mg from standpipe, saturated, vacuum and standard method columns. The 40 leaching cycles occurred over 20 weeks. Three leaching cycles corresponds to one pore volume. Error bars represent one standard error above and below the mean. Where indicated, treatment means by date were significantly different * $P < 0.05$, ** $P < 0.01$, and *** $P < 0.001$. Detection limit = 0.005 mg L^{-1} and values below the detection limit were reported as 0.005 mg L^{-1}.

described above (Orndorff et al., 2010). Increased carbonate dissolution and possible siderite ($FeCO_3$) dissolution in the saturated columns may also have been responsible for the spike in Mg concentrations seen over leaches three and four, as Mg is a common impurity in siderite (Anthony et al., 2005). Spikes in several parameters of interest (Ca, bicarbonate, sulfate) were also observed over this span. Increased contact time between the leaching solution and the spoil may have increased the dissolution of carbonates potentially causing the observed increases. The steady increase seen in concentrations over the final leaching cycles was strongly correlated with increases in EC, bicarbonate, and Ca, suggesting that carbonate dissolution over time may have driven Mg leaching, as shown in Appendix B, Table B-2.

Manganese release was significantly affected by the saturation level in the columns ($p = 0.0005$). Overall, the saturated columns eluted considerably more Mn than the standpipe, standard, and vacuum columns. In addition, the standard columns leached significantly higher levels on Mn than the vacuum columns. The standpipe did not appear to affect the release of Mn as no treatment effect was observed between the standpipe and standard columns.

With the exception of leach one, where the unsaturated columns were higher in Mn, the saturated columns were significantly higher in Mn than the other treatments for the majority of leaching cycles ($p < 0.05$). The pattern of release for the standpipe and vacuum columns mirror those seen with Ca, Mg, and sulfate. Initial Mn release from treatments one (standpipe), two (saturated), three (vacuum), and four (standard) was between 730 $\mu g\ L^{-1}$ and 1200 $\mu g\ L^{-1}$, shown in Figure 13. After thirty leaching cycles, the standard, standpipe columns, and vacuum columns leveled off around 1 $\mu g\ L^{-1}$, 1.4 $\mu g\ L^{-1}$ and 20 $\mu g\ L^{-1}$, respectively. Under saturated conditions

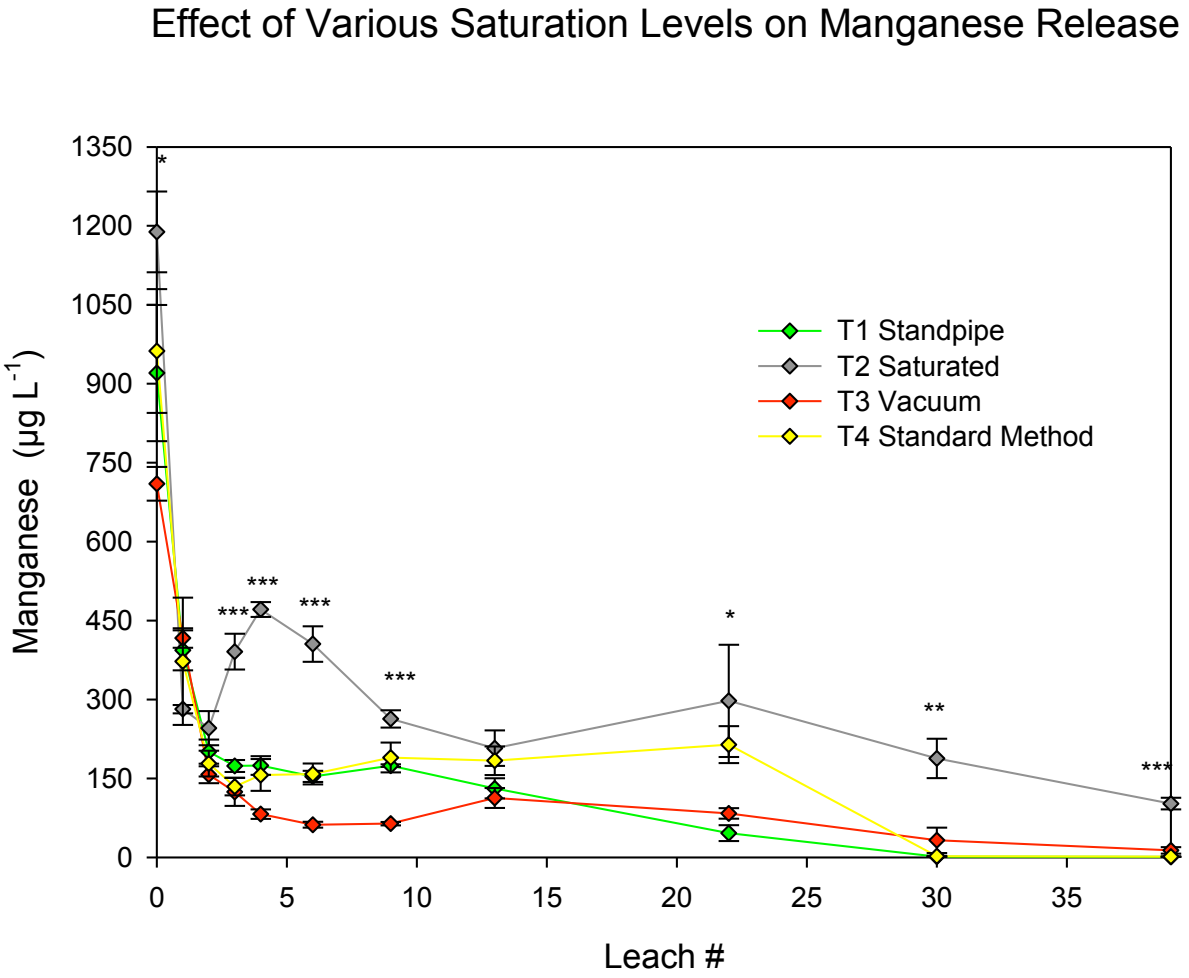

Figure 13. Leachate Mn from standpipe, saturated, vacuum and standard method columns. The 40 leaching cycles occurred over 20 weeks. Three leaching cycles corresponds to one pore volume. Error bars represent one standard error above and below the mean. Where indicated, treatment means by date were significantly different * $P < 0.05$, ** $P < 0.01$, and *** $P < 0.001$. Detection limit = 0.5 µg L^{-1} and values below the detection limit were reported as 0.5 µg L^{-1}.

Mn concentrations were around 100 μg L^{-1}after forty leaching cycles. Manganese did not increase over the final leaching cycles like Mg and Ca. However, under saturated conditions Mn showed a similar spike in concentrations over leaches three and four like bicarbonate, Ca, and Mg. The large spike in Mn concentrations seen under saturated conditions was potentially due to the dissolution of siderite, as Mn commonly substitutes for Fe. However, previous research has shown that amorphous Mn can act as an oxidizing agent in low oxygen sulfide oxidation environments (like present in the saturated and unsaturated columns), generating large quantities of soluble Mn (Evangelou, 1995). The Mn forms a redox couple with Fe and as the Fe is oxidized the Mn becomes water-soluble. The increased solubility of Mn under moderate redox conditions compared to Fe may reflect this relationship.

Cadmium (Cd), Copper (Cu), Nickel (Ni), Lead (Pb), and Zinc (Zn)

Saturation level had a moderate treatment effect on Cd release from the mine spoil ($p = 0.0507$). Cadmium concentrations from the vacuum columns were slightly greater than the standard, standpipe, and saturated columns as shown in Figure 14. The standard method, standpipe, and saturated columns eluted values near the CCC of 0.25 μg L^{-1} during the first leaching event and then remained below the detection limit of 0.10 μg L^{-1} for all subsequent leaching cycles. Initial release of Cd from the vacuum columns was approximately 13 μg L^{-1} and remained above the CMC of 2 μg L^{-1} for the first five leaching cycles and above the CCC for all leaching cycles. The higher/sustained release of Cd under the vacuum was likely due to increased carbonate dissolution via greater pyrite oxidation compared to the other treatments as Cd can be carbonate bound (Swaine, 1990). In addition, Cd is chalcophilic and the increased

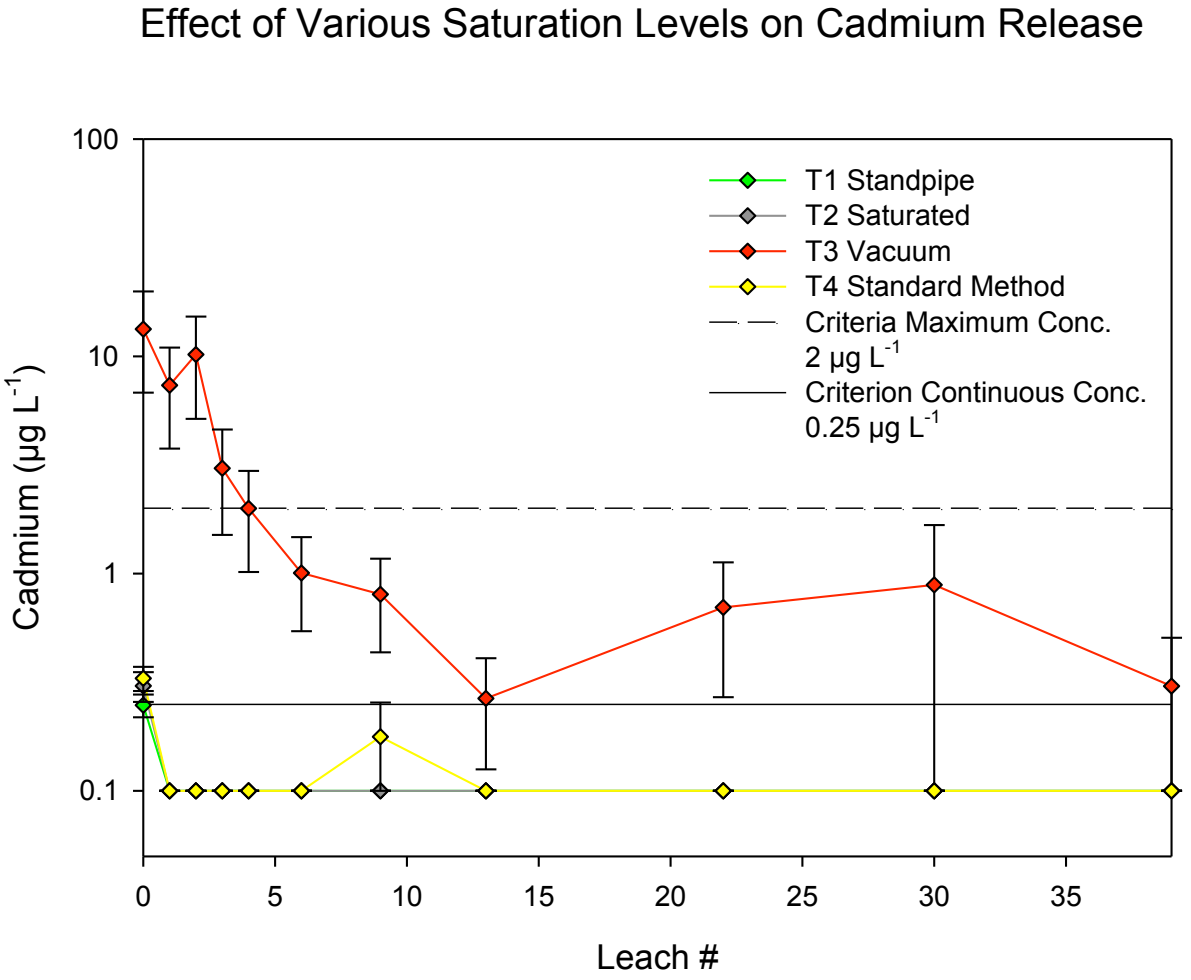

Figure 14. Leachate Cd from standpipe, saturated, vacuum and standard method columns. The 40 leaching cycles occurred over 20 weeks. Three leaching cycles corresponds to one pore volume. Error bars represent one standard error above and below the mean. Detection limit = 0.1 µg L^{-1} and values below the detection limit were reported as 0.1 µg L^{-1}.

pyrite oxidation potentially caused by the vacuum likely contributed to the prolonged release of Cd (McBride, 1994).

Copper release from the mine spoil was strongly affected by the level of saturation in the columns ($p = 0.0037$). Overall, the standpipe and vacuum columns eluted significantly higher levels of Cu than the standard and saturated columns as shown in Figure 15 with the most apparent differences in the second leaching cycle ($p = 0.0009$). Initial Cu concentrations ranged from 5 μg L^{-1} to 8 μg L^{-1} and after leach six, remained at or below the detection limit of 0.60 μg L^{-1}. Copper release patterns closely followed the release of sulfate, As and Se. This was expected as Cu is a chalcophile and the higher levels of Cu under unsaturated conditions reflect increased rapid trace pyrite oxidation. The increased airflow from the standpipe and vacuum likely increased pyrite oxidation and subsequent higher levels of Cu compared to the standard columns. Lower levels from the saturated columns were likely the result of suppressed pyrite oxidation in the low oxygen environment. Lower redox conditions in the saturated columns likely suppressed pyrite and metals sulfide oxidation, which resulted in the low levels of Cu in the leachate.

Nickel release from the mine spoil was not affected by the level of saturation in the columns. The CCC of 20 μg L^{-1} was exceeded over the initial leaching cycles as concentrations ranged from 27 μg L^{-1} to 40 μg L^{-1} for the four treatments. Concentrations dropped over the first seven leaching cycles, leveling off around 1 μg L^{-1} as seen in Appendix C, Figure C-1. While there was not a significant treatment effect and considerable variability within treatments, it appeared that the unsaturated treatments eluted slightly higher levels of Ni over the first fourteen leaching cycles. Specific leach contrasts on leaches six and thirteen reflect his as the standpipe

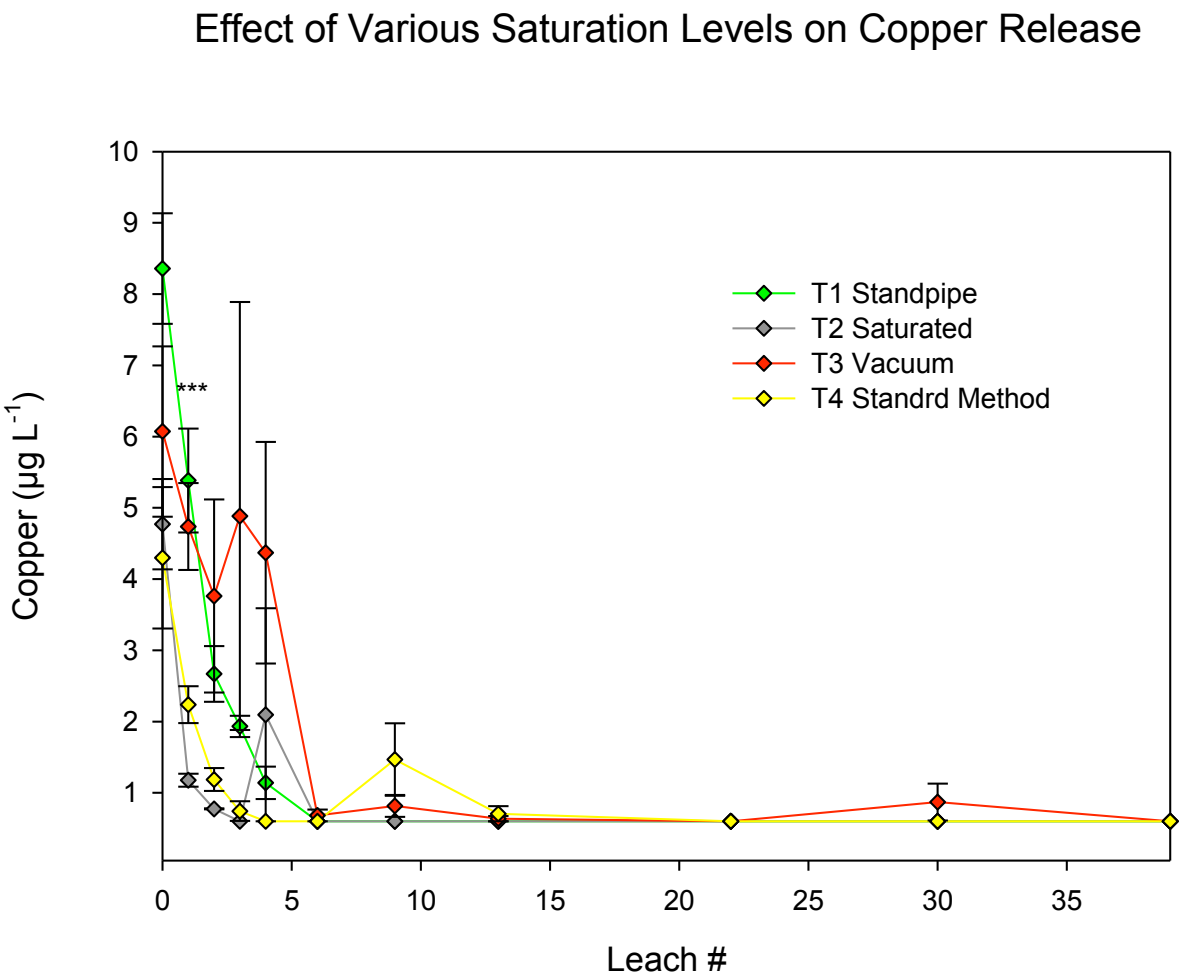

Figure 15. Leachate Cu from standpipe, saturated, vacuum and standard method columns. The 40 leaching cycles occurred over 20 weeks. Three leaching cycles corresponds to one pore volume. Error bars represent one standard error above and below the mean. Where indicated, treatment means by date were significantly different * $P < 0.05$, ** $P < 0.01$, and *** $P < 0.001$. Detection limit = 0.6 µg L^{-1} and values below the detection limit were reported as 0.6 µg L^{-1}.

and vacuum columns eluted higher levels at leach six and vacuum yielded the highest concentrations at leach thirteen. Over time, Ni release did not appear to be affected by any of the treatments and is consistent with the overall repeated measures analysis. Nickel is also chalcophilic and was likely present in the spoil as a copper sulfide substituted within pyrite. The slightly higher levels seen in vacuum and standpipe columns were likely due to increased pyrite oxidation via increased airflow, while under saturated conditions, the pyrite oxidation was suppressed. Overall, the levels of Ni are very low and were not a significant component of TDS or leachate chemistry.

The level of saturation in the columns had a significant treatment effect ($p = 0.0047$) on Pb release from the mine spoil. Leachate from the vacuum columns was significantly higher in Pb concentration than the standard, standpipe, and saturated columns. Based on specific leach contrasts, leach four reflected the overall treatment effect ($p = 0.0038$), as seen in Figure 16. Between 0.75 $\mu g\ L^{-1}$ and 2.2 $\mu g\ L^{-1}$ of Pb eluted from the columns during the initial leaching cycle. After the first leaching, the standard, saturated, and standpipe columns remained at or below the detection limit of 0.50 $\mu g\ L^{-1}$ for the remainder of the study. With the exception of spikes around 3 $\mu g\ L^{-1}$, 4 $\mu g\ L^{-1}$, and 2 $\mu g\ L^{-1}$ seen over leaches three, four, and thirty, the vacuum columns fluctuated just above the detection limit. The pattern of Pb release seen in the vacuum columns closely follows that seen with Al, Cu, Fe, and Ni. Lead is a chalcophile and commonly found associated with pyrite. However, as mentioned earlier, PbSe has also been

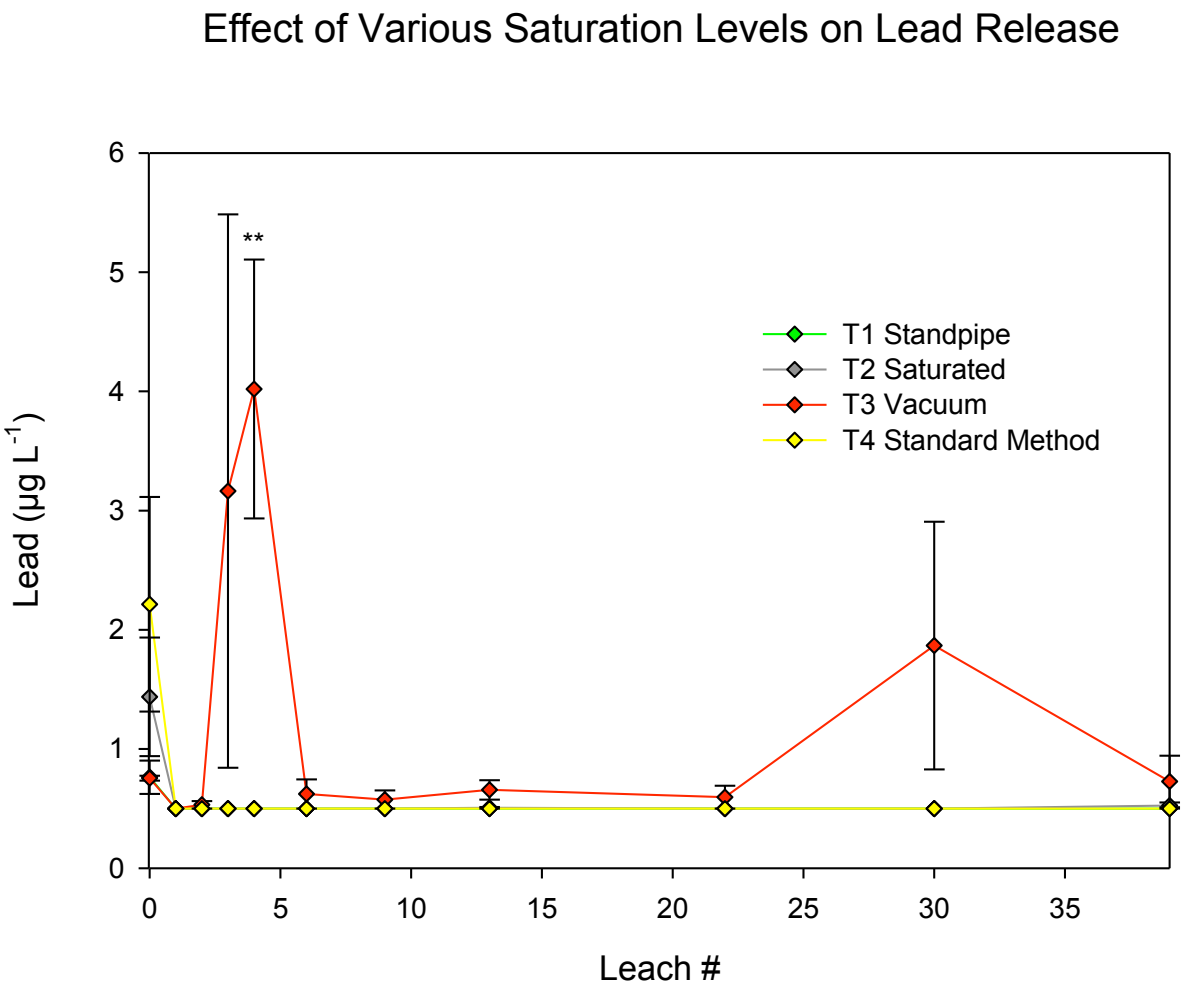

Figure 16. Leachate Pb from standpipe, saturated, vacuum and standard method columns. The 40 leaching cycles occurred over 20 weeks. Three leaching cycles corresponds to one pore volume. Error bars represent one standard error above and below the mean. Where indicated, treatment means by date were significantly different * $P < 0.05$, ** $P < 0.01$, and *** $P < 0.001$. Detection limit = 0.5 µg L^{-1} and values below the detection limit were reported as 0.5 µg L^{-1}.

identified as a significant "weatherable phase" in similar strata from eastern Kentucky (J. Unrine, personal communication). Regardless, this suggests that increased oxidation in the vacuum columns likely accelerated the weathering of pyrite and associated metal sulfides.

Zinc release from the mine spoil was strongly affected by the level of saturation present in the columns ($p = 0.0187$). Columns leached under vacuum eluted considerably higher concentrations of Zn than the standard, standpipe or the saturated columns. These treatment effects were the strongest at leaches zero through nine, and leach thirty, as shown in Figure 17 ($p < 0.05$). Initial Zn concentrations for the all the treatments were above the regulatory standard of 120 μg L^{-1}, with concentrations of 173 μg L^{-1}, 139 μg L^{-1}, and 333 μg L^{-1}, respectively. After the initial spike, Zn release from both the standpipe, standard, and saturated columns decreased rapidly and eventually leveled off around 1 μg L^{-1}after thirty-one leaching cycles. In contrast, Zn concentrations from the vacuum columns fluctuated between 175 μg L^{-1} and 250 μg L^{-1} over the first five leaching cycles and then eventually leveled off around 20 μg L^{-1}. Zinc can be found in pyritic and multiple carbonate forms including siderite and its mechanisms of release are similar to the trace metals mentioned above. Greater oxidation of the spoil under vacuum likely caused increased pyrite oxidation and potentially some parallel siderite dissolution, which resulted in the higher observed Zn levels.

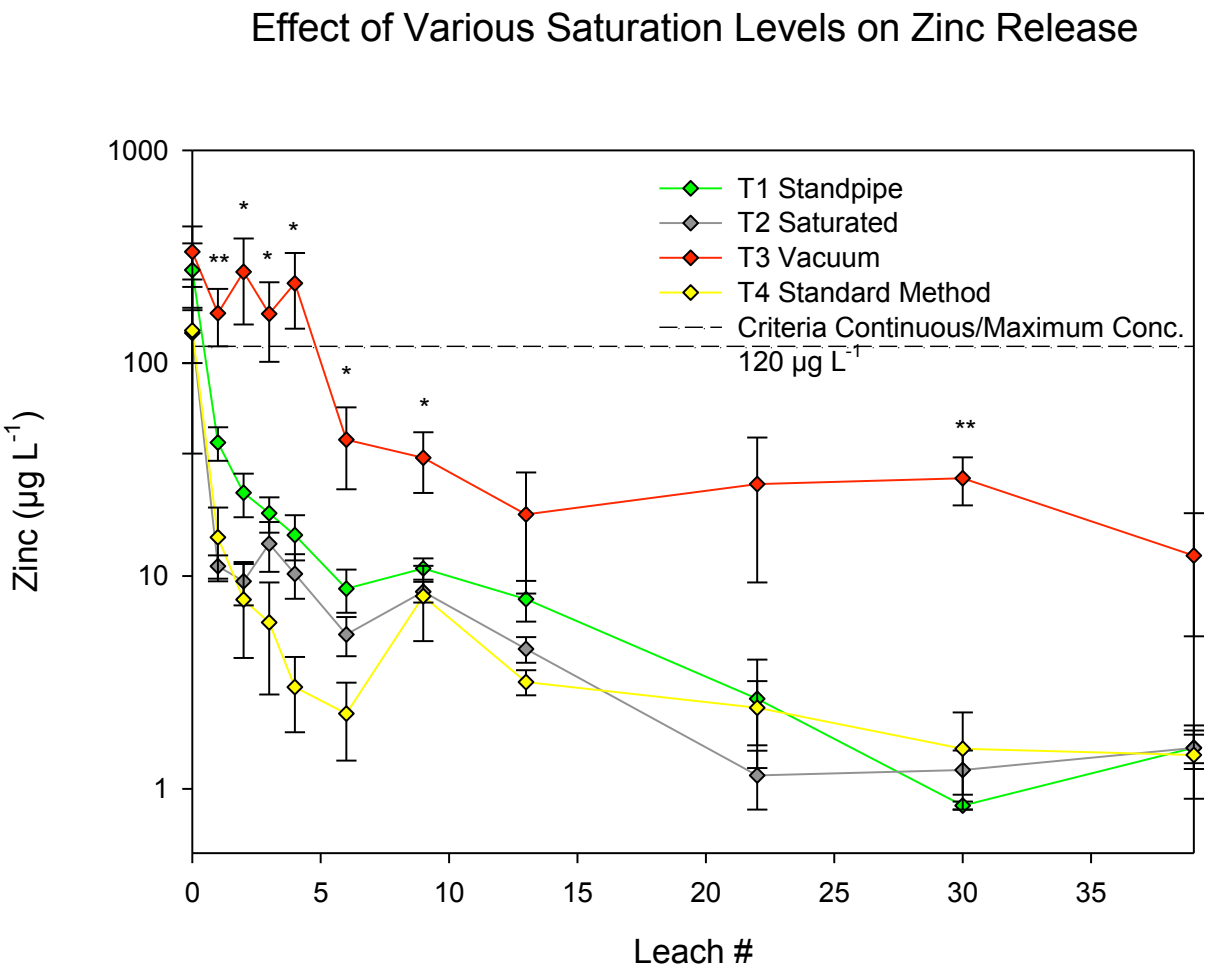

Figure 17. Leachate Zn from standpipe, saturated, vacuum and standard method columns. The 40 leaching cycles occurred over 20 weeks. Three leaching cycles corresponds to one pore volume. Error bars represent one standard error above and below the mean. Where indicated, treatment means by date were significantly different * $P < 0.05$, ** $P < 0.01$, and *** $P < 0.001$. Detection limit = 0.8 µg L^{-1} and values below the detection limit were reported as 0.8 µg L^{-1}.

Aluminum (Al) Chloride (Cl), Potassium (K), and Sodium (Na)

The level of saturation did not appear to influence the release of Al from the mine spoil. All treatments eluted high initial levels of Al, and based on the filtered data presented below this was presumably due to stripping of colloidal aluminosilicates from the freshly abraded spoils surfaces. Initial Al release varied considerably as treatments one (standpipe), two (saturated), three (vacuum), and four (standard method) eluted approximately 180 μg L^{-1}, 500 μg L^{-1}, 280 μg L^{-1}, and 1378 μg L^{-1}, as shown in Figure 18. Aluminum concentrations from both the standard, standpipe, and saturated columns dropped rapidly and reached steady state after the second leaching cycle, stabilizing at approximately 20 μg L^{-1}, 15 μg L^{-1}, 50 μg L^{-1}, and 20 μg/L respectively. With the exception of leaches three and thirty, where Al release spiked over 400 μg $L^{-1}$and 275 μg L^{-1}, Al release from the vacuum columns fluctuated around 120 μg L^{-1}. Aluminum concentrations from the vacuum columns remained at or above the CCC of 87 μg L^{-1} for the duration of the experiment. Even though an overall treatment effect was not observed, specific leach contrasts on leaches four, thirteen, and thirty-nine, showed that the vacuum columns leached higher levels of Al than the saturated, standpipe, and standard method columns ($p = 0.0299$, $p = 0.0040$, $p = 0.004$).

Overall, Al release was likely driven first by colloid release followed by hydrolysis of Al on the edges of mineral grains, as Al is a dominant cation on the spoil. As shown in Table 6, Al levels were much lower in the filtered (0.45 *u*m filter) leachate than in the unfiltered at leach one, further suggesting that fine colloids contributed to the initial release of Al. Higher Al levels from the vacuum columns compared to that of the standard method were likely due to the increased weathering and subsequent hydrolysis of Al due to increased oxygenation of the spoil under

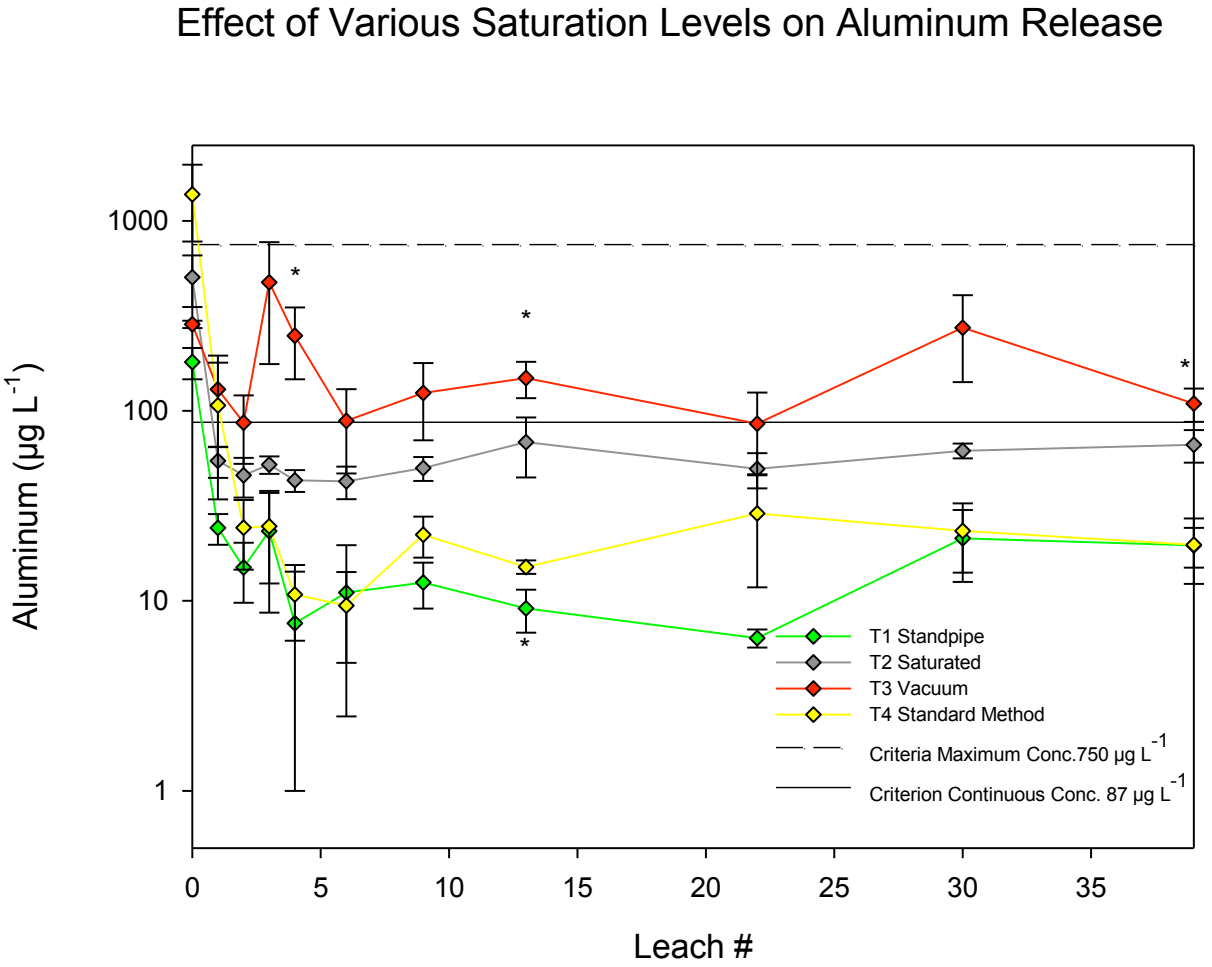

Figure 18. Leachate Al from standpipe, saturated, vacuum and standard method columns. The 40 leaching cycles occurred over 20 weeks. Three leaching cycles corresponds to one pore volume. Error bars represent one standard error above and below the mean. Where indicated, treatment means by date were significantly different * $P < 0.05$, ** $P < 0.01$, and *** $P < 0.001$. Detection limit = 1.0 µg L^{-1} and values below the detection limit were reported as 1.0 µg L^{-1}.

vacuum. The spikes in leachate Al from the vacuum columns were also possibly due to colloids being pulled through the filter materials.

The level of saturation in the columns did not have an overall effect on Cl release from the spoil. Treatment two (saturated) eluted higher concentrations of Cl than treatments one (standpipe) and three (vacuum) during the first leaching cycle ($p = 0.0120$). In addition, Cl levels from the standard columns were higher than the standpipe fitted columns (see Appendix C, Figure C-2). The standpipe and vacuum columns released 15 mg L^{-1} and 25 mg L^{-1}, respectively, of Cl over the initial leaching cycle, while the saturated and standard columns eluted approximately 50 mg L^{-1} and 40 mg L^{-1}. Chloride concentrations from the standard, saturated, and standpipe concentrations rapidly dropped and fell below the detection limit of 5.0 mg L^{-1} after two to three leaching events. The vacuum columns declined slightly slower and fell below the detection limit after the fourth leaching cycle.

The pattern of Cl release was similar to that of sulfate and many of the base cations described above. Chloride release was likely a function of water movement in the columns coupled with simple dissolution of highly trace Cl in the spoils since higher concentrations were released under saturated conditions. The initial concentrations of Cl in this spoil were very low and elution values were also low compared to sulfate and bicarbonate and were well below the CCC standard of 230 mg L^{-1} and CMC of 800 mg L^{-1}.

Potassium release from the spoil was strongly affected by the level of saturation in the columns ($p = 0.0426$). Overall, the standard and standpipe columns leached greater amounts of K than the saturated columns, while leachate from the vacuum columns was not statistically

different from the other three treatments. As shown in Figure 19, the treatment effects were strongly evident over leaches one, two, twenty-two, and thirty-nine ($p < 0.05$). Initial K release ranged from 27 mg L^{-1} to 32 mg L^{-1}. Potassium concentrations quickly declined to approximately 10 mg L^{-1} over the first six to seven leaching cycles before eventually leveling off around 3 mg L^{-1}.

Higher levels of K released from standard and standpipe fitted columns over two of the first three leaching cycles possibly reflected the rapid hydrolysis weathering of feldspars and micas present in the spoil as K-feldspars are widely found in the Appalachian region (Bogner and Sobek, 1979). The overall high initial levels could also have been due to initial flushing of mobile colloids. Saturated conditions potentially accelerated the initial release via exchange reactions, but likely suppressed it over time by slowing the indirect effects of sulfide oxidation (less protons driving hydrolysis of feldspars and K release from edges of mica) and overall chemical weathering of the spoil.

The saturation level in the columns had a marginally significant effect on Na release from the mine spoil ($p = 0.0651$) as seen in Figure 20. Overall, the standpipe and vacuum columns eluted more Na than the saturated columns. The standard columns were not significantly different from the other three treatments. As shown in Figure 20, the overall treatment effect was most evident over the second and third leaching cycles. However, the saturated columns eluted significantly higher levels of Na than the standpipe and standard columns at leaches zero, six, thirteen, and twenty-two ($p < 0.05$). Initial Na release ranged between 4000 μg L^{-1} in treatment three, to 5500 μg L^{-1} for treatments one (standpipe), two (saturated), and four (standard

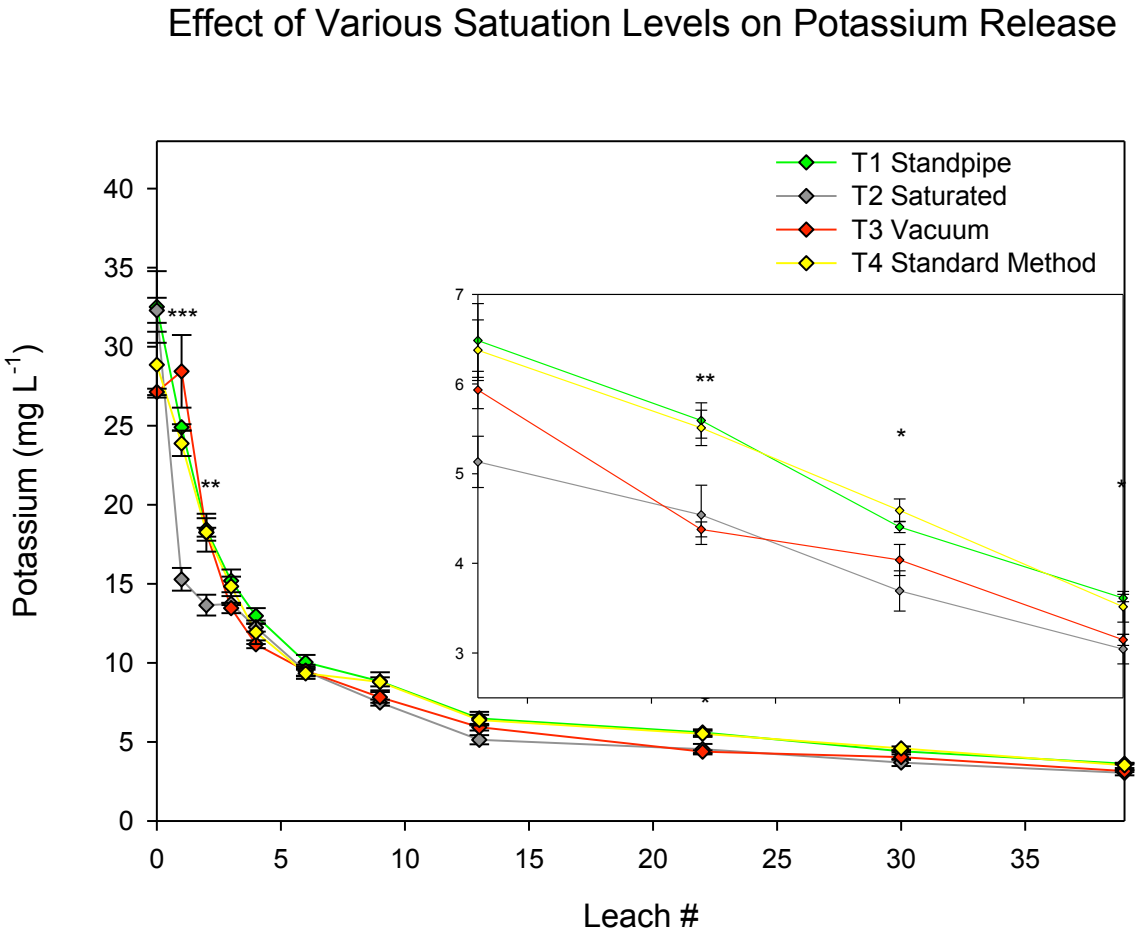

Figure 19. Leachate K from standpipe, saturated, vacuum and standard method columns. The 40 leaching cycles occurred over 20 weeks. Three leaching cycles corresponds to one pore volume. Error bars represent one standard error above and below the mean. Where indicated, treatment means by date were significantly different * $P < 0.05$, ** $P < 0.01$, and *** $P < 0.001$. Detection limit = 0.005 mg L^{-1} and values below the detection limit were reported as 0.005 mg L^{-1}.

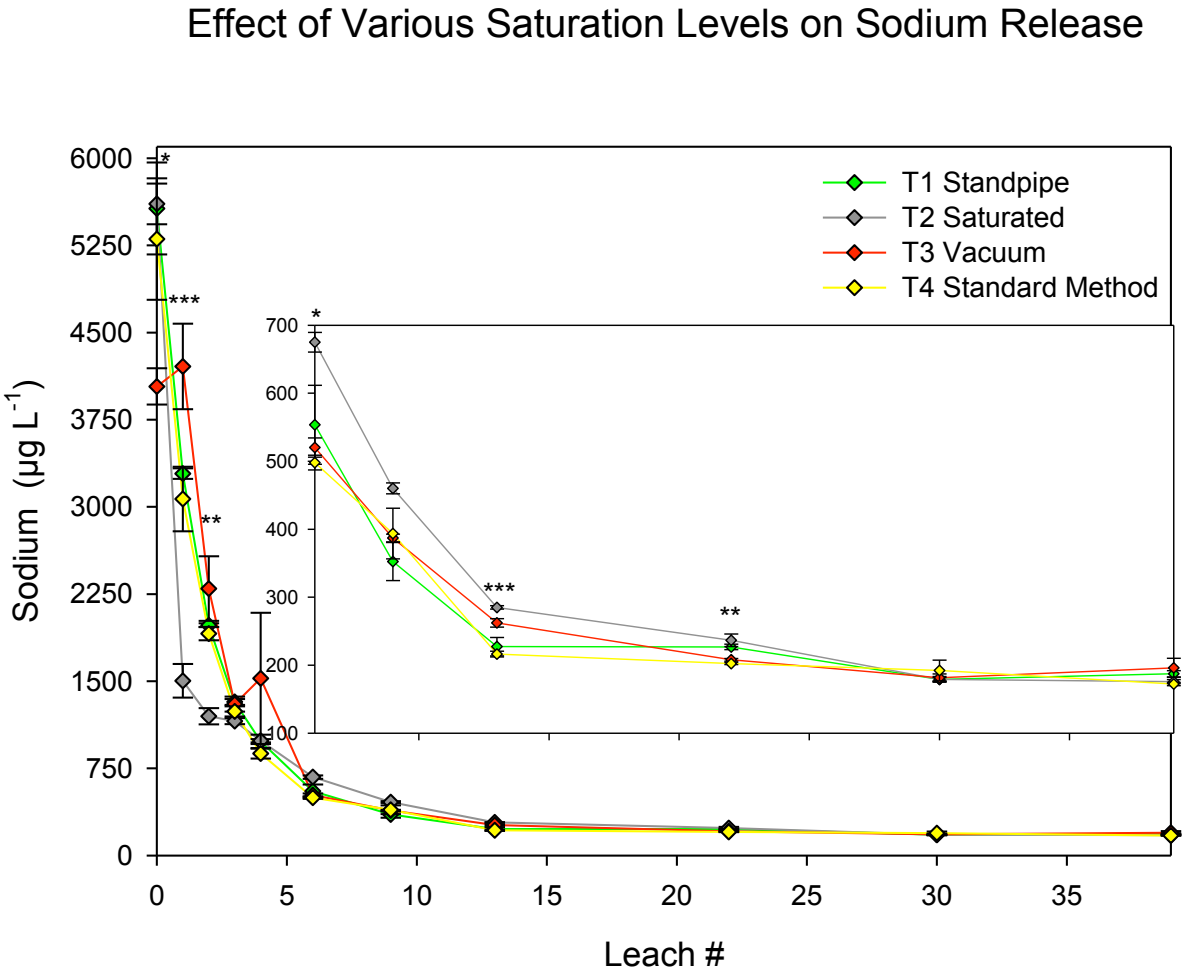

Figure 20. Leachate Na from standpipe, saturated, vacuum and standard method columns. The 40 leaching cycles occurred over 20 weeks. Three leaching cycles corresponds to one pore volume. Error bars represent one standard error above and below the mean. Where indicated, treatment means by date were significantly different * $P < 0.05$, ** $P < 0.01$, and *** $P < 0.001$. Detection limit = 5.0 µg L^{-1} and values below the detection limit were reported as 5.0 µg L^{-1}.

method). Sodium concentrations quickly dropped and leveled off between 175 μg L^{-1} and 200 μg L^{-1} after leach thirteen. Both the mechanisms and patterns of Na release were very similar to that of K (described above), as the weathering of feldspars presumably also drove the Na release.

Charge and Mass Distribution

Saturation level in the columns appeared to have a minor effect on the total distribution of cations and anions in the leachate, and seemed to influence the total $mmol_c$ in the leachate. As shown in Figures 21 and 22, all treatments showed an approximate 50:50 split between cations and anions both during peak elution (L1) and over time (L39). Columns leached under saturated conditions released lower $mmol_c$ compared to the unsaturated treatments, 8 $mmol_c$ vs. 17-23 $mmol_c$. Calcium was the major cation contributing to the total $mmol_c$. During peak elution (L1) sulfate was the dominant anion contributing to the charge under unsaturated conditions, while sulfate and bicarbonate contributed to the total charge under saturated conditions. Across all treatments, bicarbonate was the dominant anion, while Ca and to a lesser extent Mg were the major cations contributing to the total $mmol_c$ by the end of the experiment.

Mass distribution of the leachate was affected by the saturation level in the columns. As shown in Figures 23 and 24, the mass distribution of the leachate during peak elution (L1) was dominated by sulfate under unsaturated conditions and by sulfate and bicarbonate under saturated conditions. Calcium was also a significant contributor to the total TDS during leach one, with higher levels of Ca from the standpipe fitted columns. While the saturation level seemed to affect the mass distribution during the peak elution, by leach thirty-nine, all four treatments showed a similar composition. Bicarbonate became the major contributor

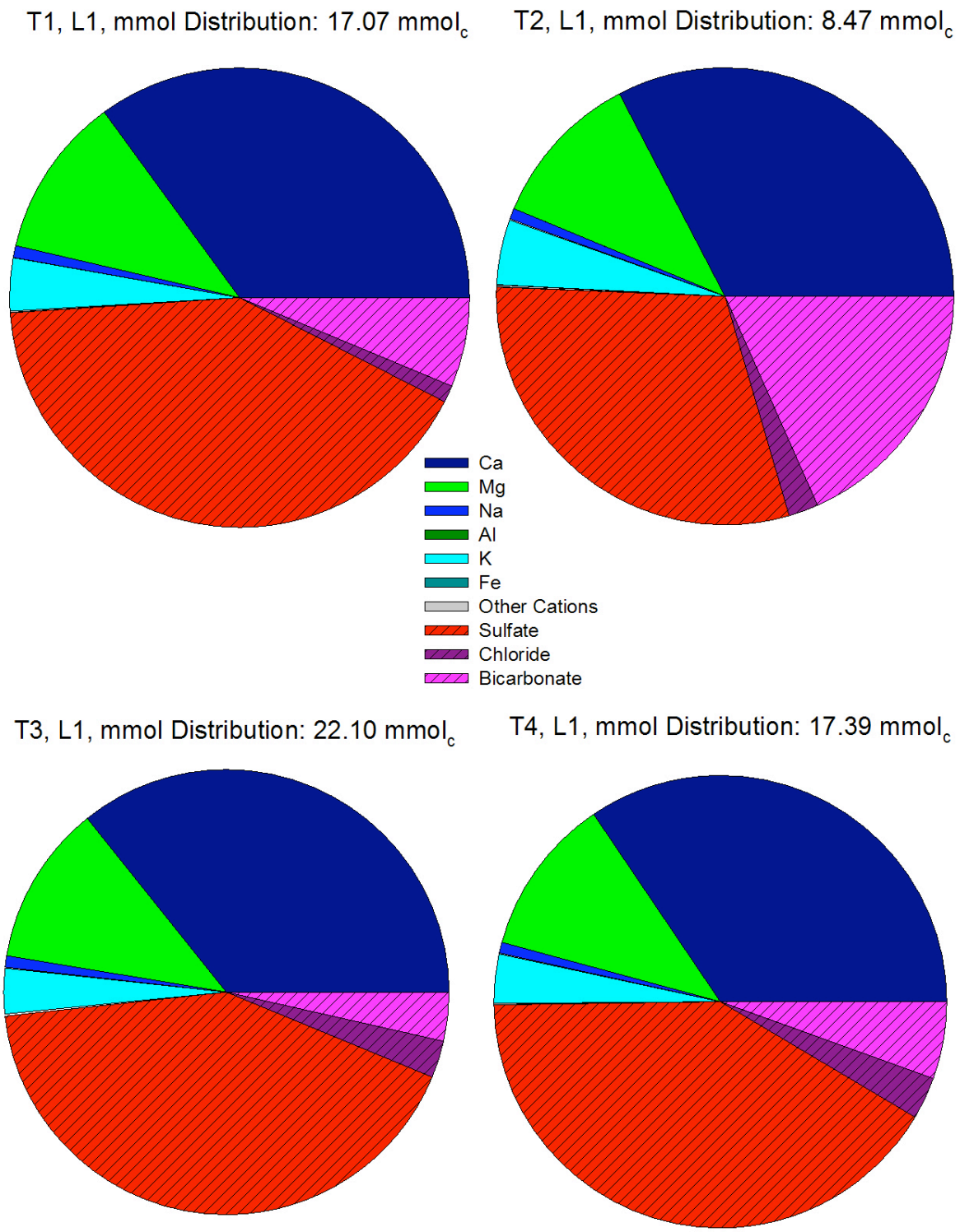

Figure 21. Charge distribution of dominant cations and anions at leach one from standpipe (T1), saturated (T2), vacuum (T3), and standard method (T4) columns. L = Leach #.

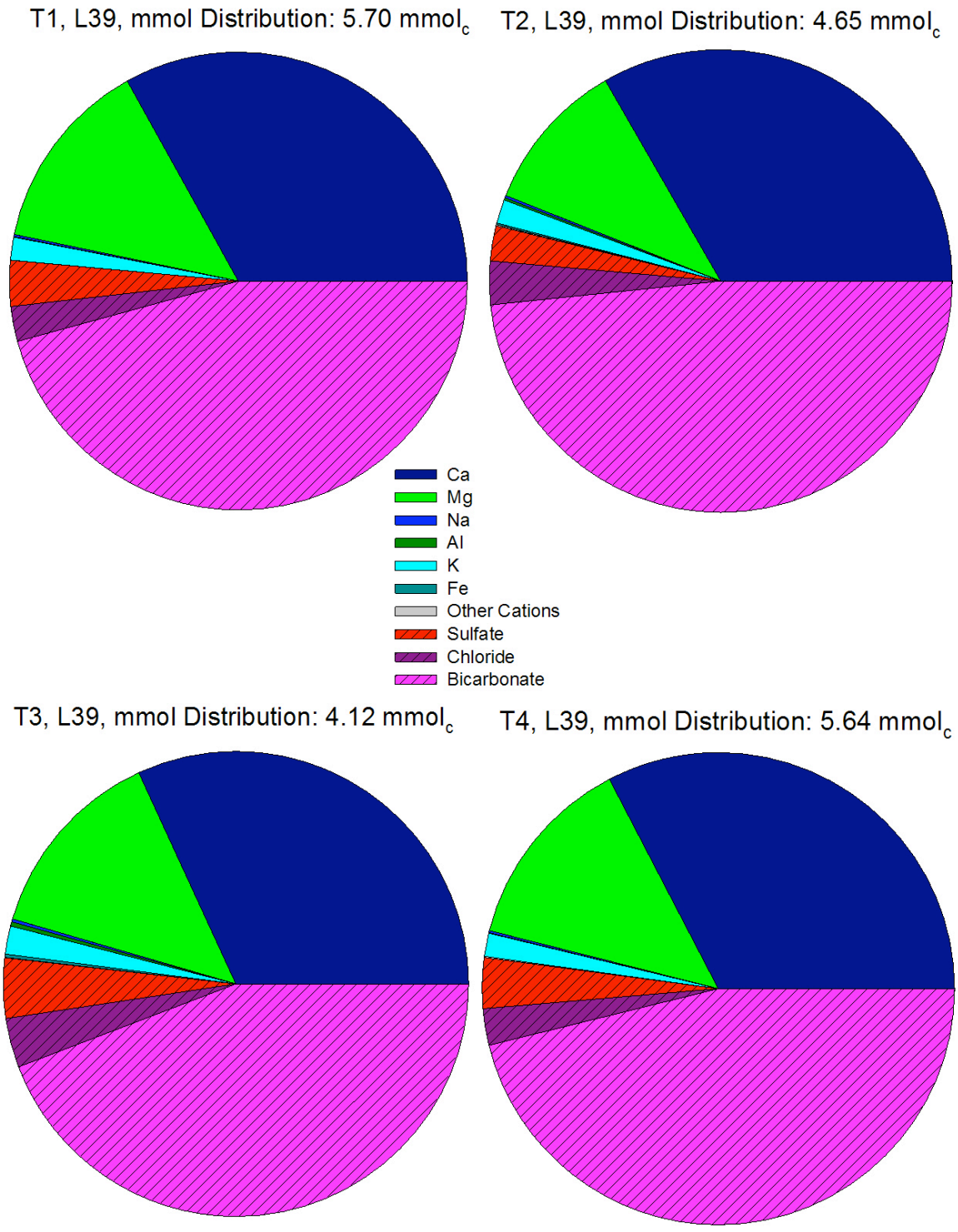

Figure 22. Charge distribution of dominant cations and anions at leach thirty-nine from standpipe (T1), saturated (T2), vacuum (T3), and standard method (T4) columns. L = Leach #.

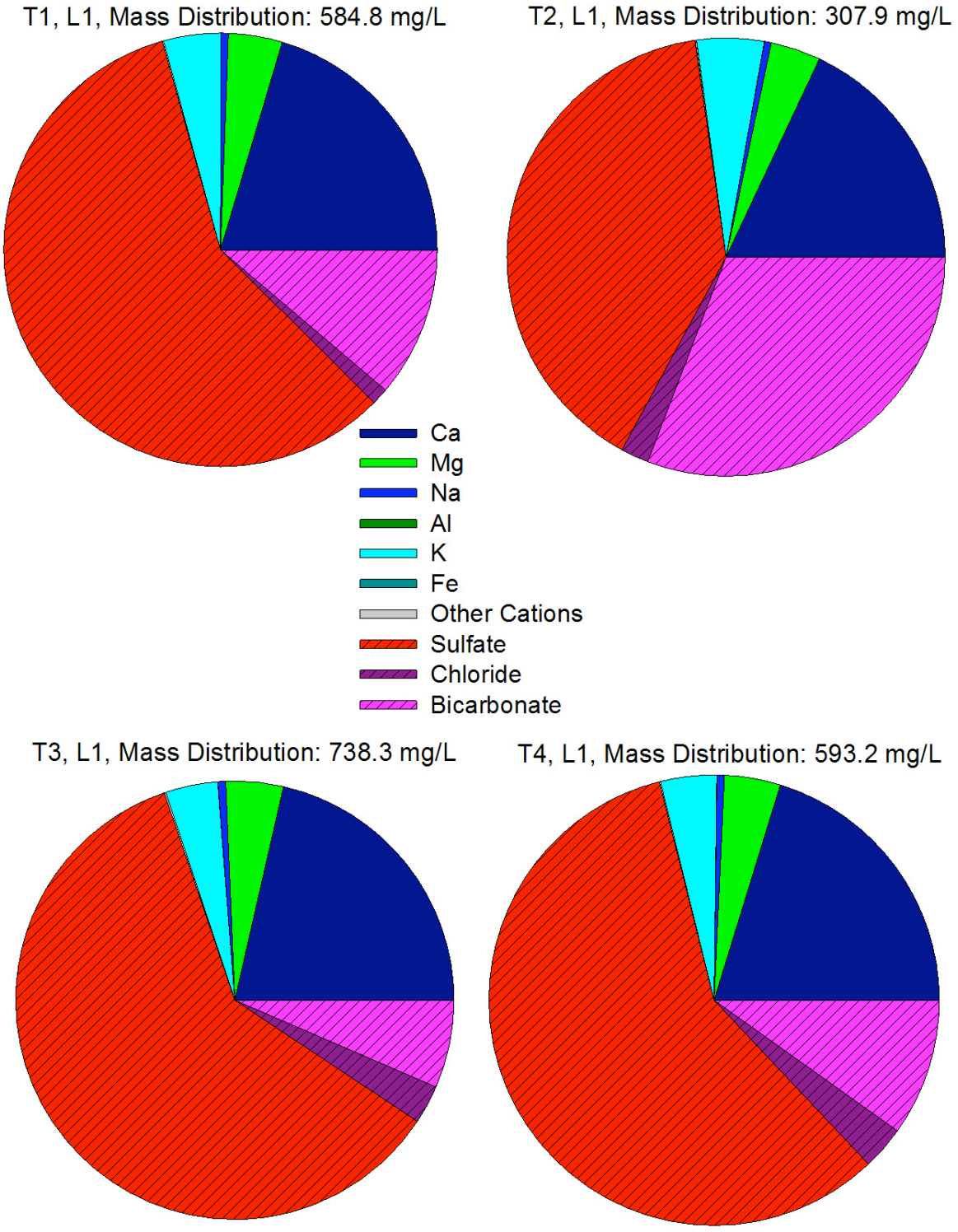

Figure 23. Mass distribution of dominant cations and anions at leach one from standpipe (T1), saturated (T2), vacuum (T3), and standard method (T4) columns. L = Leach #.

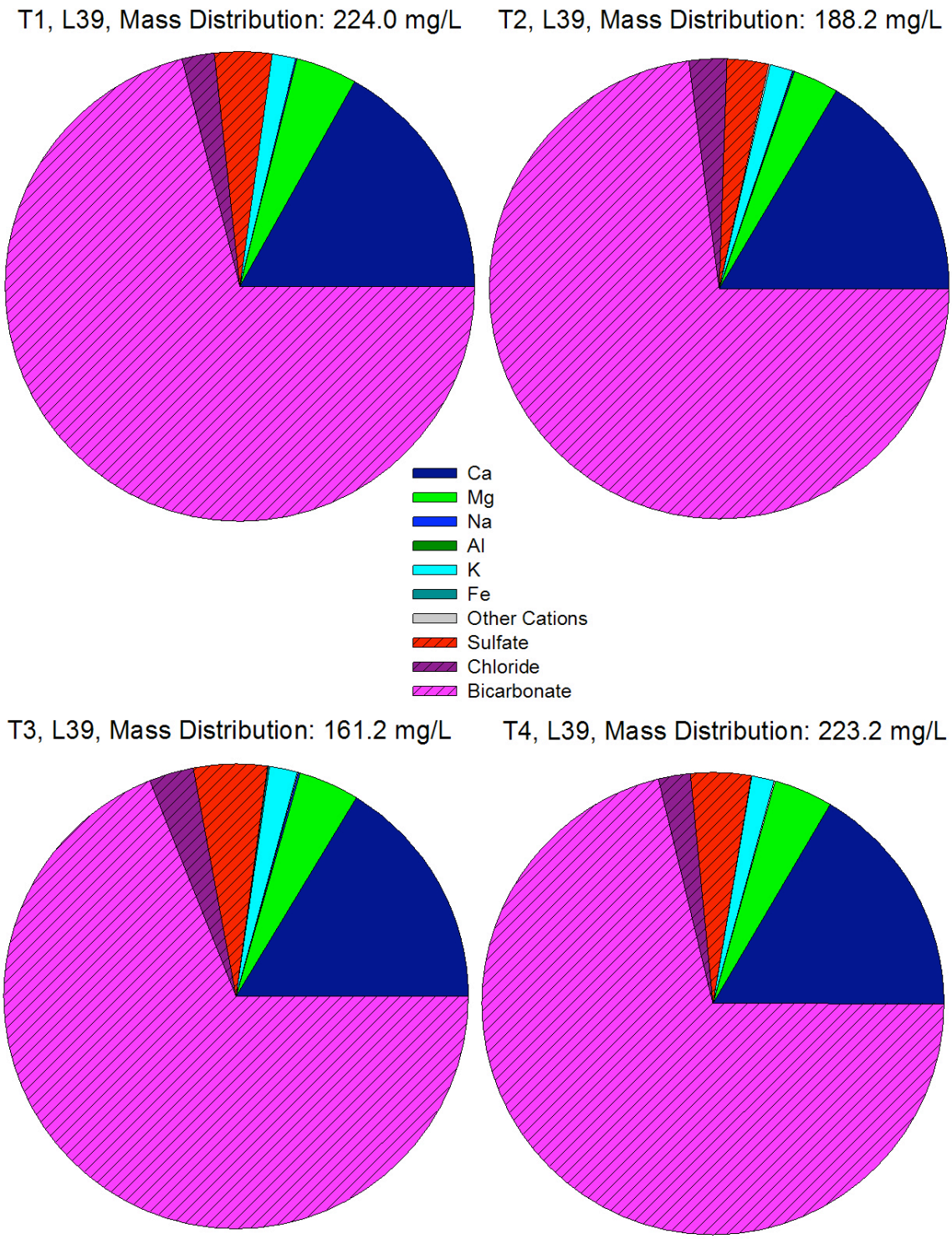

Figure 24. Mass distribution of dominant cations and anions at leach thirty-nine from standpipe (T1), saturated (T2), vacuum (T3), and standard method (T4) columns. L = Leach #.

of TDS comprising approximately 70% of the total mass eluted at leach thirty-nine. The relative contribution of Ca at leach thirty-nine was similar to its contribution during the peak elution (L1).

The change from a sulfate to bicarbonate system was a likely the function of increased carbonate dissolution over time coupled with decreasing pyrite oxidation due to low total S in the spoil (< 0.02%). This trend was also observed in the column study by Orndorff et al. (2010). Rapid hydrolysis of freshly broken mineral grains during peak elution as discussed above coupled with increased carbonate dissolution over time likely drove the relatively steady cation release patterns observed across all treatments.

CHAPTER 4. EFFECTS OF LEACHING SOLUTION pH

Overall treatment effects for the leaching solution pH study are presented in Table 7.

Table 7. Summary of repeated measures statistical analysis for leaching solution pH

Source	pH	EC	HCO_3	SO_4	Al	As	Ca	Cd	Cl	Cu	Fe	K	Mg	Mn	Na	Ni	Pb	Se	Zn
TRT	NS	NS	*	NS	*	NS	NS	NS	NS	NS	*	*	NS	NS	NS	NS	**	NS	NS
Leach#	***	***	***	***	***	***	***	***	***	***	***	***	***	***	***	***	***	***	***
TRT* Leach#	***	*	**	*	***	*	NS	***	**	***	***	NS	NS	NS	NS	NS	***	NS	NS

TRT, Treatment; NS, Not significant; * $P < 0.05$, ** $P < 0.01$, and *** $P < 0.001$

Electrical Conductivity

Leaching solution pH had a moderate overall treatment effect ($p = 0.0519$) on the EC of the leachate from the mine spoil. Even though the overall treatment effect was not strongly significant, leachate EC from treatment five (DI) was significantly higher than treatment six ($CaCO_3$) ($p < 0.05$) across four of the last five leaching cycles, as shown in Figure 25. Treatment four (simulated acid rain) was not significantly different from either of the other treatments for these selected leaching cycles. Initial leachate EC for all three treatments ranged from 1400 to 1600 μS cm^{-1}, as shown in Figure 25, and within the first three leaching cycles, dropped below 500 μS cm^{-1}, down to approximately 200 μS cm^{-1}, where it leveled off until leach twenty.

Initial leachate EC was presumably due to rapid trace pyrite oxidation as well as flushing of salts and other hydrate reaction products from the edges of mineral grains via exchange and rapid hydrolysis (Orndorff et al., 2010). Subsequently, EC values began to slowly increase, and the final leachate EC values for the acid rain, DI, and $CaCO_3$ columns ended at approximately 240 μS cm^{-1}, 300 μS cm^{-1}, and 275 μS cm^{-1}, respectively. The slow increases in EC over time likely followed heightened carbonate dissolution described below.

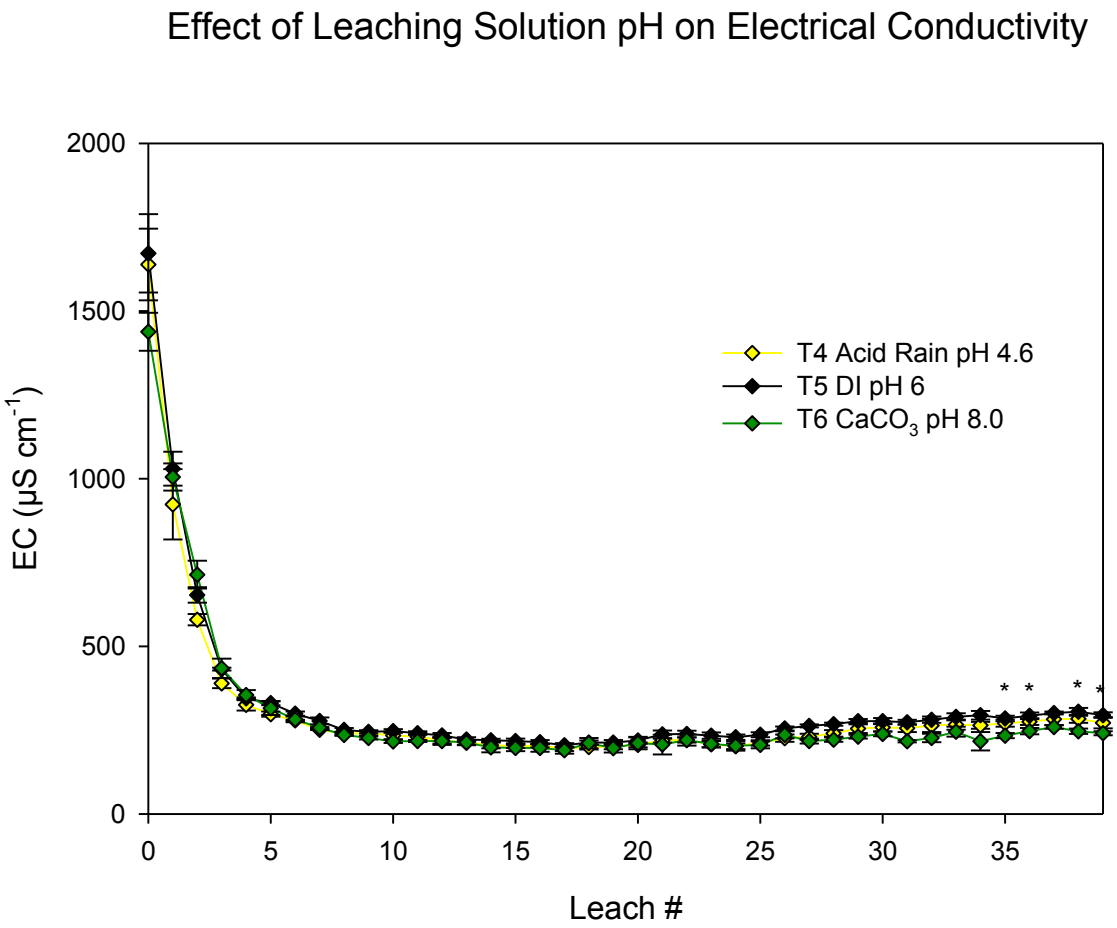

Figure 25. Leachate electrical conductivity (EC) from columns leached with simulated acid rain, DI water and $CaCO_3$. The 40 leaching cycles occurred over 20 weeks. Three leaching cycles correspond to one pore volume. Error bars represent one standard error above and below the mean.

Leachate pH

Leaching solution pH also had a modest overall treatment effect on the pH of the leachate ($p = 0.0632$). Initial pH values ranged between 4.5-6.5, but increased over subsequent leaching cycles, reaching steady state after leach three with leachate pH values between 8.1-8.3, shown in Figure 26. The saturated paste pH was considerably higher than leachate pH for the first leaching event. In contrast, leachate pH surpassed the saturated paste pH value after the initial leaching cycle and maintained substantially higher levels for the entire duration of the experiment. Initially, acidic pH values observed with the $CaCO_3$ solution possibly reflect rapid trace pyrite oxidation coupled with low initial production of bicarbonate via dissolution. The subsequent rise in pH was strongly correlated with increases in bicarbonate concentrations ($p = 0.00395$), suggesting that carbonate dissolution controls the pH over time (See Appendix B, Table B-2).

Sulfate

Sulfate release was unaffected by leaching solution pH across all leaching cycles. Initial sulfate release ranged between 600-800 mg L^{-1}, and rapidly decreased below 10 mg L^{-1} by leach ten before leveling off between 7-9 mg L^{-1} for the remainder of the study, seen in Figure 27. The initial spike in sulfate release likely reflects rapid and trace oxidation of pyrite in the spoil. In addition, the low levels of sulfate released from the spoil over time were consistent with the total S content in the spoil (0.02%).

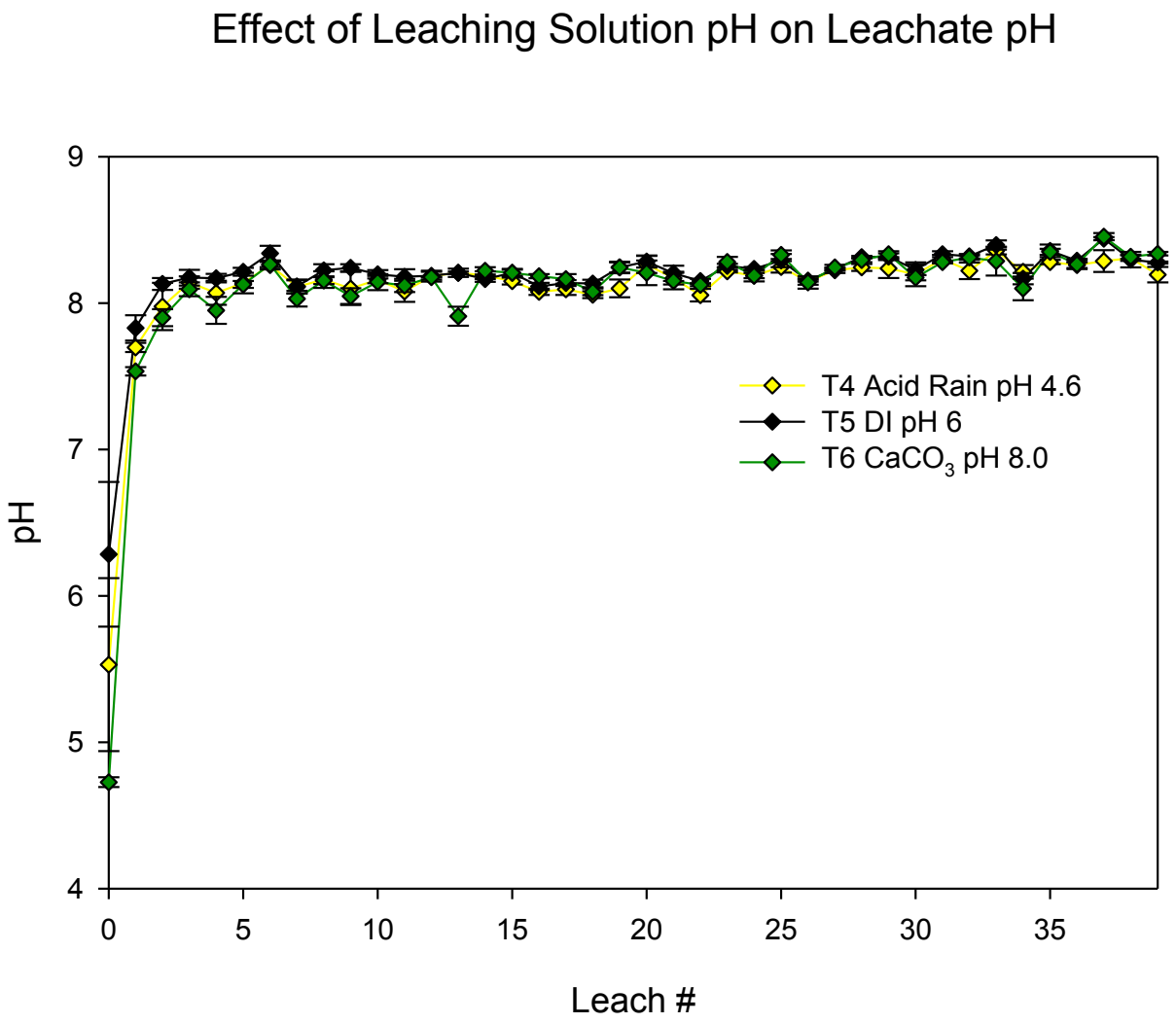

Figure 26. Leachate pH from columns leached with simulated acid rain, DI water and $CaCO_3$. The 40 leaching cycles occurred over 20 weeks. Three leaching cycles correspond to one pore volume. Error bars represent one standard error above and below the mean.

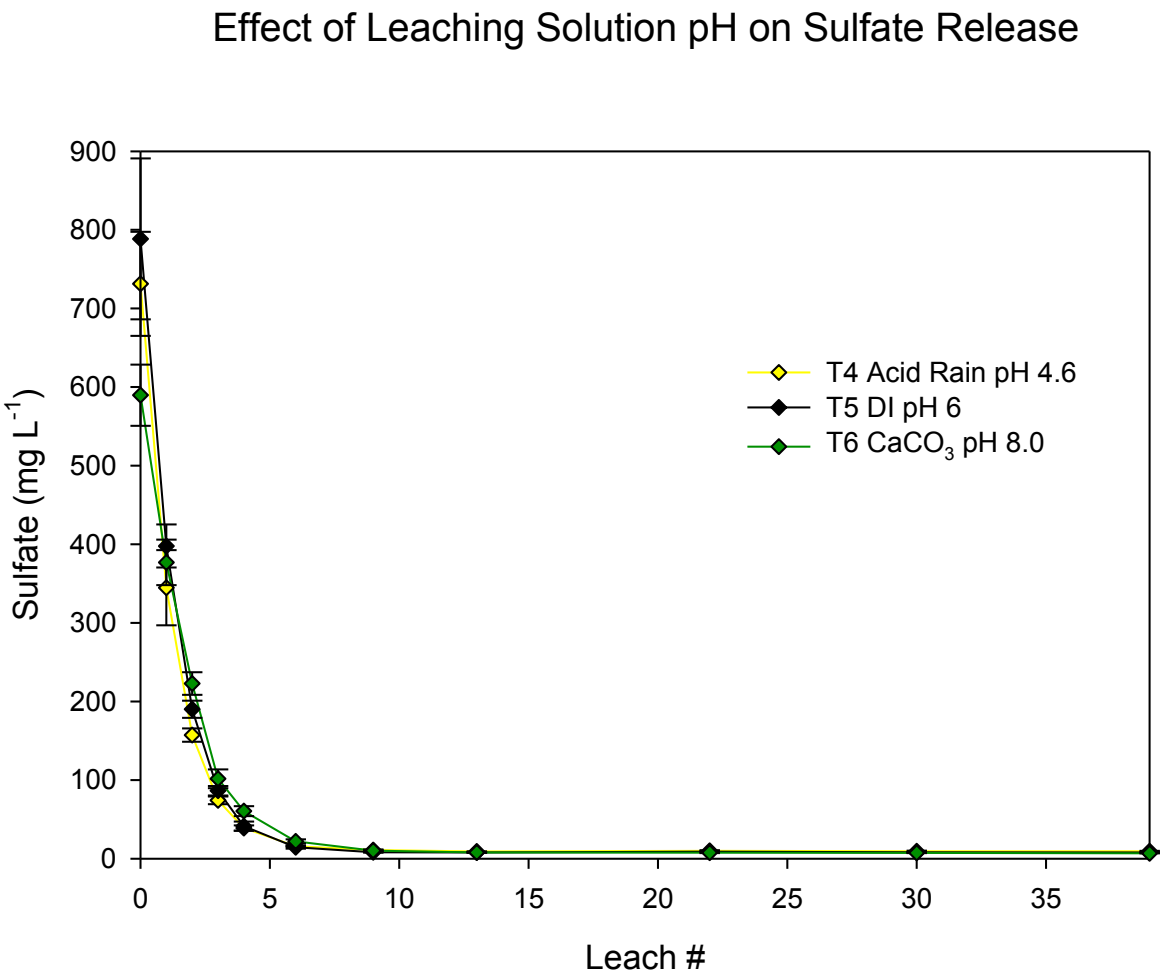

Figure 27. Leachate sulfate (SO_4) from columns leached with simulated acid rain, DI water and $CaCO_3$. The 40 leaching cycles occurred over 20 weeks. Three leaching cycles correspond to one pore volume. Error bars represent one standard error above and below the mean. Detection limit = 0.12 mg L^{-1} and values below the detection limit were reported as 0.12 mg L^{-1}.

Bicarbonate

Leaching solution pH had a significant overall effect ($p = 0.0297$) on bicarbonate release from the spoil samples. Overall, columns leached with DI water leached significantly more bicarbonate than the columns leached with the $CaCO_3$ solution. However, the simulated acid rain was not significantly different than either the DI water or $CaCO_3$ solutions. Bicarbonate release increased sharply over the first four leaching cycles and leveled off around 120 mg L^{-1} after leach four as shown in Figure 28. Values then began to steadily increase over the last three leaching cycles, ending between 140-180 mg L^{-1}. The strongest overall treatment effect can be seen in leaches three through nine and thirty and thirty-nine where treatment five (DI) was significantly greater than treatment six ($CaCO_3$) ($p < 0.05$). Treatment four (acid rain) was significantly greater than treatment six ($CaCO_3$) over leaches four through nine, but did not show an overall treatment effect as mentioned above. The observed treatment effects were likely caused by differences in internal column pH. Bicarbonate leaching from the lower pH simulated acid rain and DI water likely increased the dissolution of carbonates via acid-base neutralization reactions resulting from a decrease in internal column pH. In contrast, the higher pH $CaCO_3$ solution possibly had a higher internal column pH and therefore less carbonate dissolution.

Arsenic (As) and Selenium (Se)

The release of As from the mine spoil was unaffected by leaching solution pH. Initial As release was fairly low, ranging between 4-6 μg L^{-1}, which is significantly lower than the criterion continuous concentration (CCC) of 150 μg L^{-1} for Virginia surface waters. Arsenic concentrations dropped rapidly across all treatments and within nine leaching cycles were

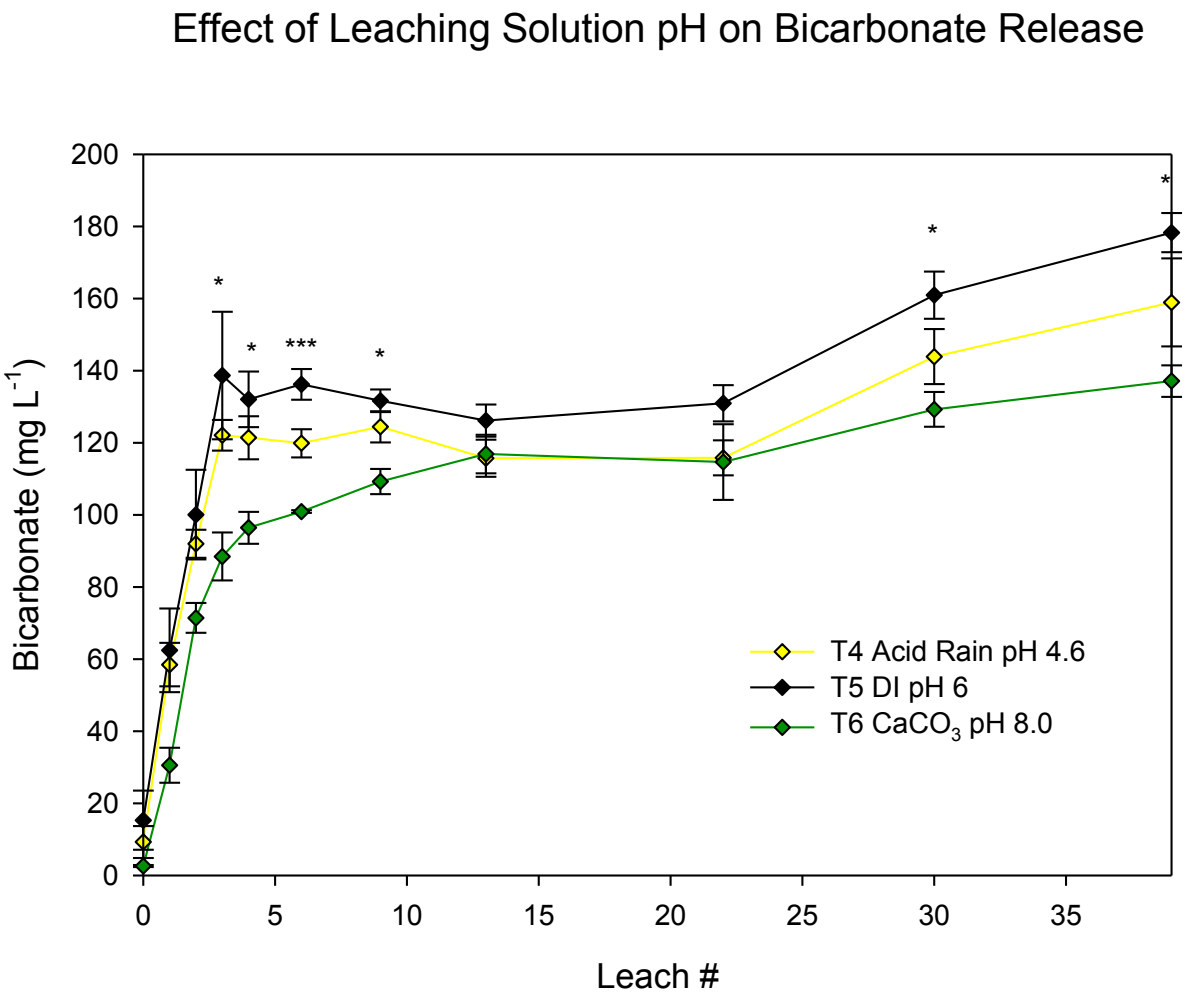

Figure 28. Leachate bicarbonate from columns leached with simulated acid rain, DI water and $CaCO_3$. The 40 leaching cycles occurred over 20 weeks. Three leaching cycles correspond to one pore volume. Error bars represent one standard error above and below the mean. Where indicated, treatment means by date were significantly different * $P < 0.05$, ** $P < 0.01$, and *** at $P < 0.001$.

below the detection limit of 0.30 μg L^{-1} where they remained for the duration of the study as seen in Figure 29. The minor spike at leach thirteen was present for Se as well, but may have been due to instrument error from the ICPMS and not an actual spike in concentrations. The pattern of As release closely mirrors that of sulfate, which is consistent with its chalcophilic nature (McBride, 1994).

Leaching solution pH did not have an overall effect on the release of Se from the mine spoil. Initial release of Se ranged from 40-50 μg L^{-1}, which is roughly twice the criteria maximum concentration (CMC) of 20 μg L^{-1}. Leachate concentrations steadily declined, but remained above the CMC for the first three leaching cycles and then dropped below the Criterion Continuous Concentration (CCC) to levels below the detection limit of 0.8 μg L^{-1} between leaching cycles six and nine, shown in Figure 30. The pattern of Se release, like As, closely resembles that of sulfate, which is consistent with the chalcophilic nature of Se. Therefore, likely as the rapid trace pyrite oxidation slowed, so did the release of Se. While leaching solution pH did not have a treatment effect on Se release, the Se levels were above the Virginia surface water quality standards for four to six leaching cycles.

Calcium (Ca), Iron (Fe), Magnesium (Mg), and Manganese (Mn)

Calcium release from the mine spoil was unaffected by leaching solution pH. Initial Ca release ranged from 200 mg L^{-1} -250 mg L^{-1} and rapidly declined below 50 mg L^{-1} where it leveled off for the rest of the study. As seen in Appendix C, Figure C-1, the initial pattern of Ca release closely follows that of sulfate, which was consistent with the strong correlation coefficient ($r = 0.99875$, $p < 0.0001$) seen between the two over the first nine leaching cycles.

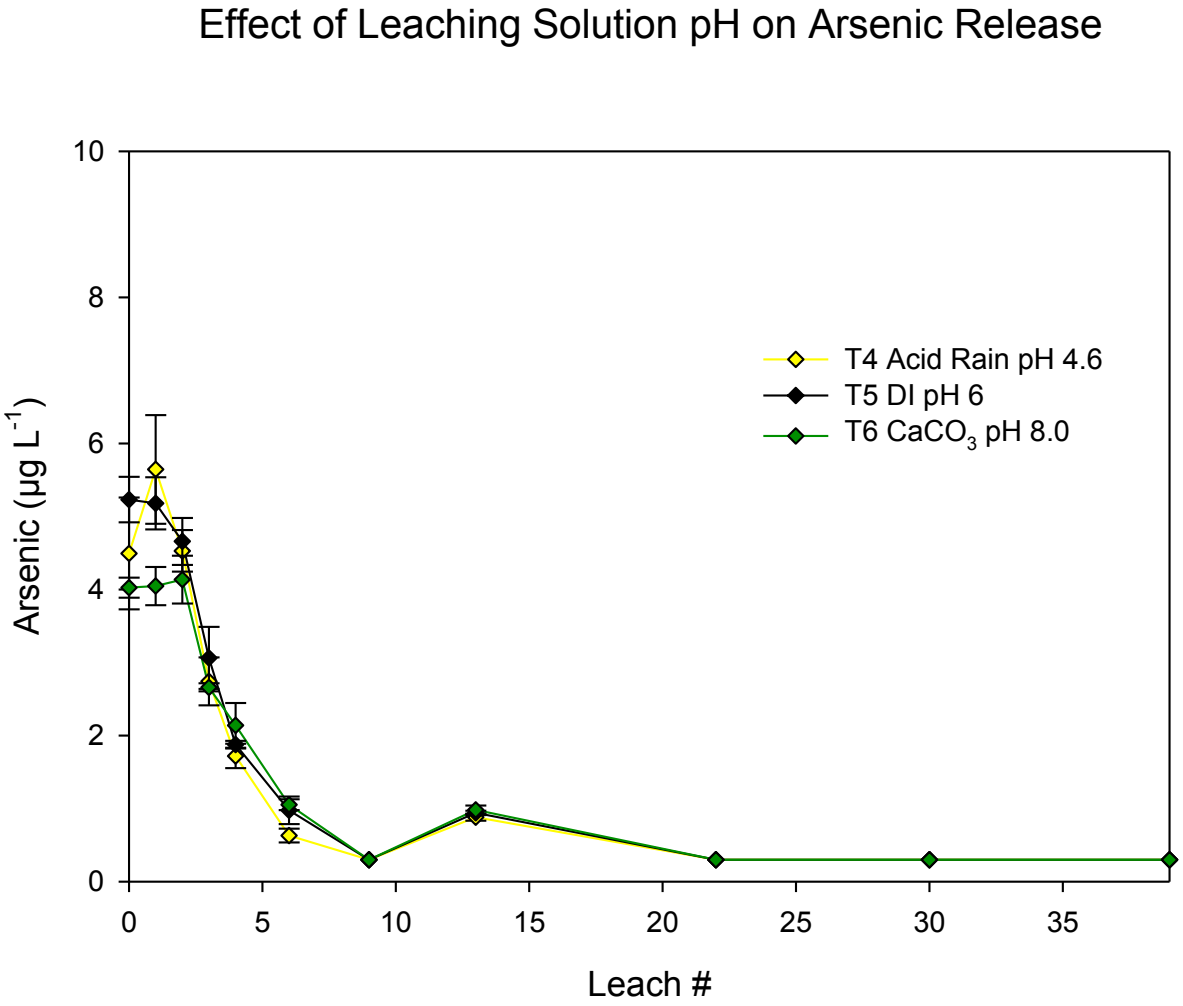

Figure 29. Leachate As from columns leached with simulated acid rain, DI water and $CaCO_3$. The 40 leaching cycles occurred over 20 weeks. Three leaching cycles correspond to one pore volume. Error bars represent one standard error above and below the mean. Detection limit = 0.3 µg $L^{-1}$and values below the detection limit were reported as 0.3 µg L^{-1}.

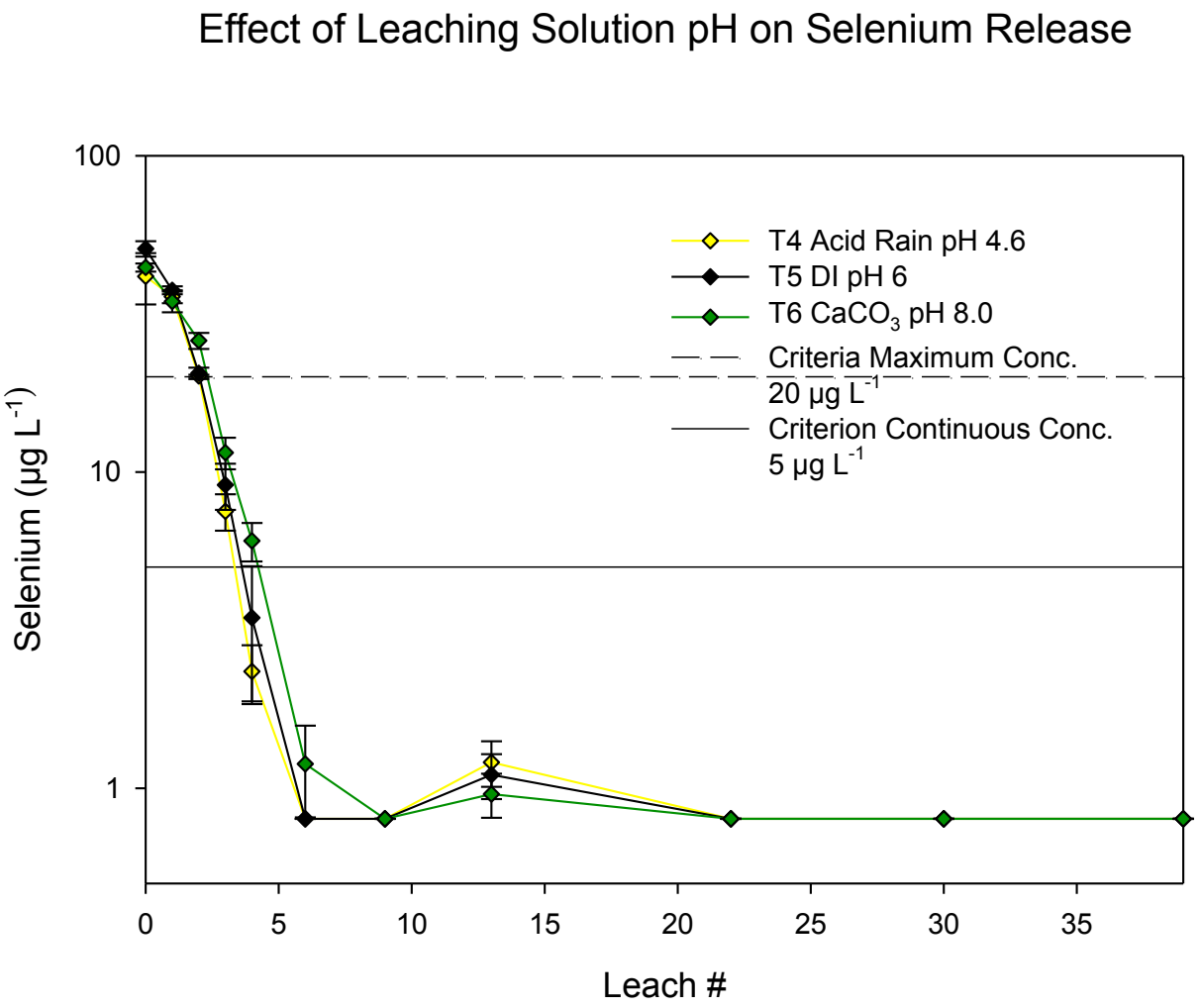

Figure 30. Leachate Se from columns leached with simulated acid rain, DI water and $CaCO_3$. The 40 leaching cycles occurred over 20 weeks. Three leaching cycles correspond to one pore volume. Error bars represent one standard error above and below the mean. Detection limit = 0.8 µg L^{-1} and values below the detection limit were reported as 0.8 µg L^{-1}.

However, Ca concentrations began to slowly increase near the end of the study and were strongly correlated with the increase in bicarbonate seen over extended time ($r = 0.9556$, $p = 0.0433$). This suggests that the initial Ca release is associated with carbonates interacting with pyrite oxidation as well as exchange reactions occurring at the surfaces of fractured feldspars, while carbonate dissolution drove the more sustained release over time.

Leaching solution pH had a significant overall effect ($p = 0.0290$) on the release of iron (Fe) from the mine spoil. Treatment six ($CaCO_3$) leached greater concentrations of Fe than both the simulated acid rain and the DI water. The most pronounced difference between treatments was in the initial leaching event, where both treatments four (acid rain) and five (DI) yielded concentrations between 120 $\mu g\ L^{-1}$ and 180 $\mu g\ L^{-1}$ and treatment six ($CaCO_3$) leached around 400 $\mu g\ L^{-1}$ of Fe (Figure 31). After the initial leaching cycles, Fe concentrations rapidly dropped below the detection limit of 5 $\mu g\ L^{-1}$ where they remained for the majority of leaching cycles. Spikes in Fe concentrations were observed at leaches nine, thirteen, and thirty-nine for treatments four and six, while treatment five (DI) remained below the detection limit. However, no significant differences between treatments were seen in any of these leaching events. Bruno et al. (1992) showed that bicarbonate can enhance the dissolution of hematite, which may help explain greater leachate Fe from columns dosed with the $CaCO_3$ leaching solution. As shown in Table 8, the Fe concentration in the leachate from treatment six ($CaCO_3$) filtered post collection was below detection, while the unfiltered leachate was approximately 14 $\mu g\ L^{-1}$. Therefore, the initial high levels of Fe observed in the leachate were likely due to fine colloids passing through the filter media in the columns.

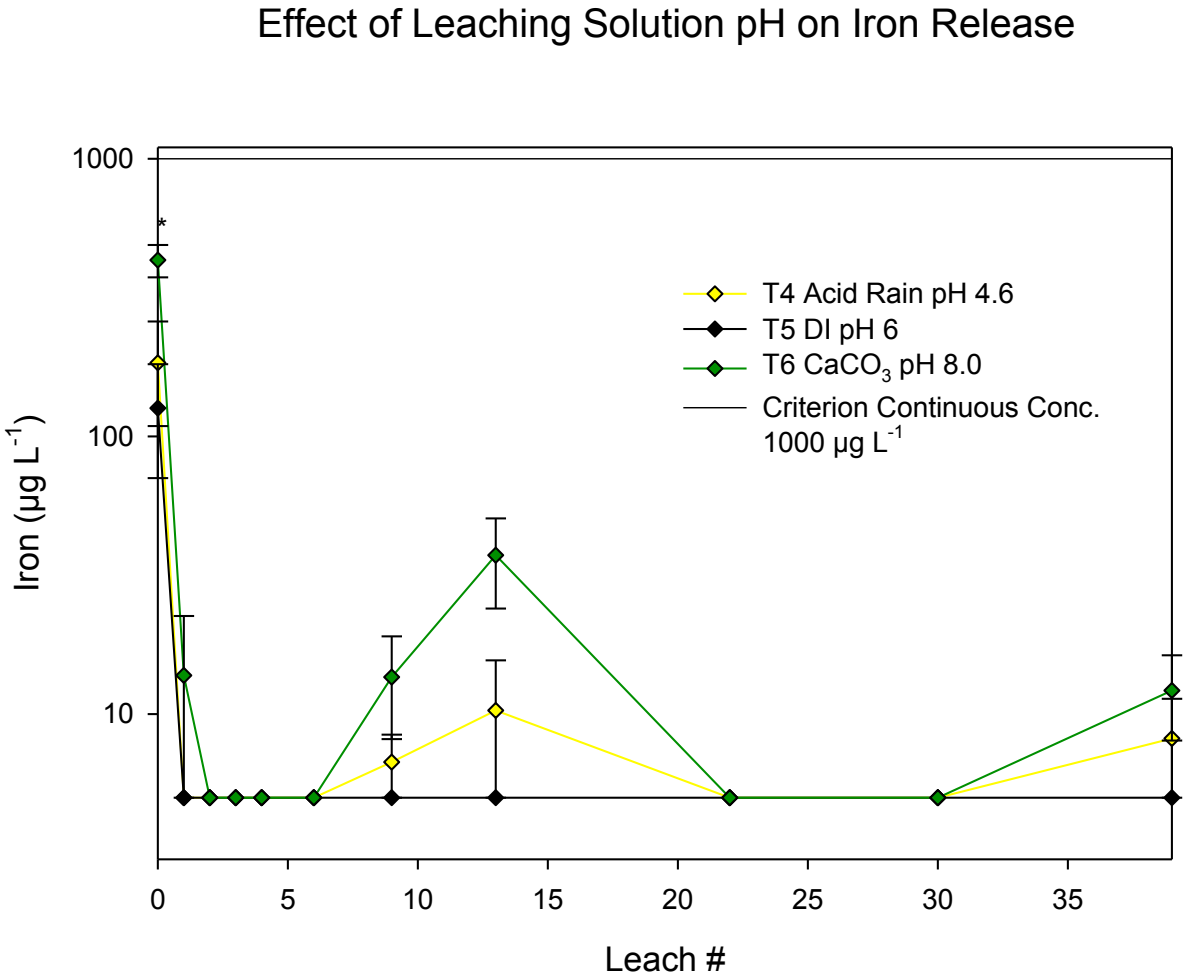

Figure 31. Leachate Fe from columns leached with simulated acid rain, DI water and $CaCO_3$. The 40 leaching cycles occurred over 20 weeks. Three leaching cycles correspond to one pore volume. Error bars represent one standard error above and below the mean. Where indicated, treatment means by date were significantly different * $P < 0.05$, ** $P < 0.01$, and *** at $P < 0.001$. Detection limit = 5.0 µg L^{-1} and values below the detection limit were reported as 5.0 µg L^{-1}.

Table 8. Filtered vs. unfiltered leachate Al, As, Cd, Cu, Fe, Mn, Na, Ni, Pb, Se, and Zn at leach one for columns leached with simulated acid rain via standard method (T4), DI (T5), and $CaCO_3$ (T6) leaching solutions.

Leach 1		Al	As	Cd	Cu	Fe	Mn	Na	Ni	Pb	Se
		μg L^{-1}									
T4	Filtered	49 (37)	5 (1)	0.1 (0)	2 (1)	5 (0)	381 (224)	3134 (522)	1 (2)	0.5 (0)	39 (7)
	Unfiltered	107 (37)	6 (1)	0.1 (0)	2 (0)	5 (0)	373 (210)	3068 (482)	2 (3)	0.5 (0)	36 (3)
T5	Filtered	46 (35)	5 (1)	0.1 (0)	2 (0)	5 (0)	587 (22)	3129 (564)	3 (2)	0.5 (0)	37 (3)
	Unfiltered	54 (35)	5 (1)	0.1 (0)	2 (0)	5 (0)	586 (23)	3126 (532)	2 (2)	0.5 (0)	38 (2)
T6	Filtered	46 (15)	4 (1)	0.1 (0)	2 (0.2)	5 (0)	481 (99)	3062 (183)	1 (2)	0.5 (0)	35 (5)
	Unfiltered	62 (15)	4 (0)	0.1 (0)	2 (0)	14 (15)	478 (95)	3038 (201)	0.4 (0)	0.5 (0)	35 (5)

Note detection limit for Cd = 0.1 μg L^{-1}, Fe = 5.0 μg L^{-1}, Ni = 0.4 μg L^{-1}, and Pb = 0.5 μg L^{-1}. Values expressed as mean and (standard deviation).

Leaching solution pH did not have an effect on Mg release from the mine spoil. The release patterns of Mg mirrored the release of sulfate and Ca. Initial concentrations ranged from 37 mg L^{-1} to 47 mg L^{-1} and rapidly declined to approximately 5 mg L^{-1} around leach thirteen, as shown in Appendix C, Figure C-2. Magnesium concentrations then began to slowly increase slowly in the same pattern as seen with Ca, possibly reflecting increased long term dissolution of carbonates.

Leaching solution pH did not affect manganese (Mn) release from the spoil samples. Manganese concentrations began around 1000 μg L^{-1}, rapidly decreased, and then leveled off at around 200 μg L^{-1} after four leaching cycles, shown in Appendix C, Figure C-3. Much later, after leach twenty-two, Mn concentrations dropped from roughly 200 μg L^{-1} to 1-2 μg L^{-1} where they remained. No other parameters of interest showed this unusual terraced pattern of release. Manganese is redox sensitive and presumably soluble over the range of pH values exhibited by the columns. It should be noted that the sharp decrease in Mn concentrations near the end of the experiment coincided with the slight increases seen with EC, bicarbonate, Ca, and Mg. Manganese solubility declines above pH 6.5 the unusual pattern of release could be a function of decreasing solubility over time as leachate pH and carbonate concentrations increased.

Cadmium (Cd), Copper (Cu), Nickel (Ni), Lead (Pb), and Zinc (Zn)

Cadmium, Cu, Ni, and Zn were unaffected by leaching solution pH across all leaching cycles. In contrast, Pb leaching was strongly influenced by leaching solution pH. Copper, Cd, and Ni were present in very low concentrations and exhibited similar patterns of release. As seen in Figures C-4 – C-7 presented in Appendix C, the release of these metals is characterized by an initial spike and subsequent rapid decrease in concentration near or below the detection limit of each parameter. The release patterns of these trace metals were similar to that of sulfate, albeit at much lower concentrations. However, this supports the fact that these metals were present in sulfide forms due to their chalcophilic nature and were released during the initial and rapid trace pyrite oxidation reactions mentioned above. It should be noted that the CCC was exceeded only on the initial leaching cycle and concentrations declined below the threshold in following leaching events.

Lead release was significantly affected by leaching solution pH ($p = 0.0057$). The $CaCO_3$ leaching solution eluted greater concentrations of Pb than the DI water, while the simulated acid rain was not significantly different from either treatment five (DI) or six ($CaCO_3$). As shown in Figure 32, after the first leaching cycle, lead concentrations ranged from 0.8 $\mu g\ L^{-1}$ to 4 $\mu g\ L^{-1}$ and then fell below the detection limit of 0.5 $\mu g\ L^{-1}$ for all remaining leaching cycles. Lead solubility appeared to be a function of initial leachate pH; the more acidic initial leachate pH values from columns leached with the $CaCO_3$ and acid rain yielded greater Pb concentrations than the less acidic leachate from the DI water. Lead is also found in pyritic materials (as a PbS)

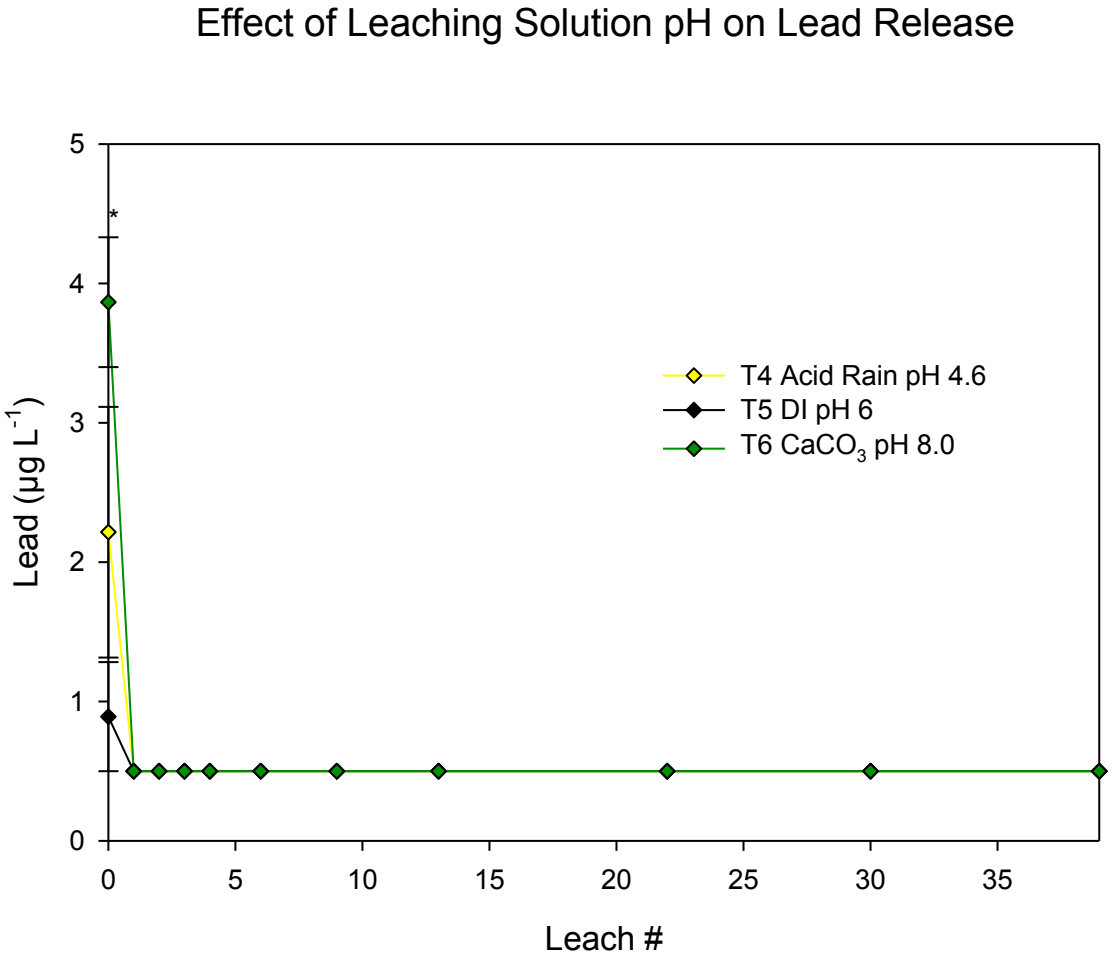

Figure 32. Leachate Pb from columns leached with simulated acid rain, DI water and $CaCO_3$. The 40 leaching cycles occurred over 20 weeks. Three leaching cycles correspond to one pore volume. Error bars represent one standard error above and below the mean. Where indicated, treatment means by date were significantly different * $P < 0.05$, ** $P < 0.01$, and *** at $P < 0.001$. Detection limit = 0.5 µg L^{-1} and values below the detection limit were reported as 0.5 µg L^{-1}.

and the initial spike possibly reflected the rapid oxidation of the trace amounts of lead sulfides present in the pyrite.

Zinc was also unaffected by leaching solution pH. It showed roughly the same pattern of release outlined above, except for a spike in concentrations seen across all treatments between leaches six and thirteen. Following that small spike, concentrations began to decline, nearing the detection limit of 0.80 μg L^{-1}. The initial pattern of Zn release follows closely with sulfate, which is consistent with the presumed chalcophilic nature of Zn. However, the spike seen after leach six suggests that there may be an additional source of Zn in the spoil. Based on some preliminary thin section data, siderite ($FeCO_3$) dissolution was a potential source for the Zn release over time since Zn can substitute for the Fe.

Aluminum (Al), Chloride (Cl), Potassium (K), and Sodium (Na)

Aluminum release was strongly affected by leaching solution pH ($p = 0.0159$). The $CaCO_3$ leaching solution eluted significantly more Al compared to the DI leaching solution ($p = 0.0136$), while the simulated acid rain was not significantly different from either of the other two treatments. As shown in Figure 33, this difference was most apparent in the initial leaching cycle, where approximately 3500 μg L^{-1} of Al were released by treatment six ($CaCO_3$) and treatments four (acid rain) and five (DI) eluted 1400 μg L^{-1} and 600 μg L^{-1}, respectively. No other leaching cycle showed any significant differences among treatments, however, the $CaCO_3$ leaching solution leached consistently higher values of total Al for the duration of the study. After two leaching cycles, Al concentrations dropped below both the CMC and CCC for Virginia and remained relatively constant (10 μg L^{-1} - 40 μg L^{-1}) for the remainder of leaching events.

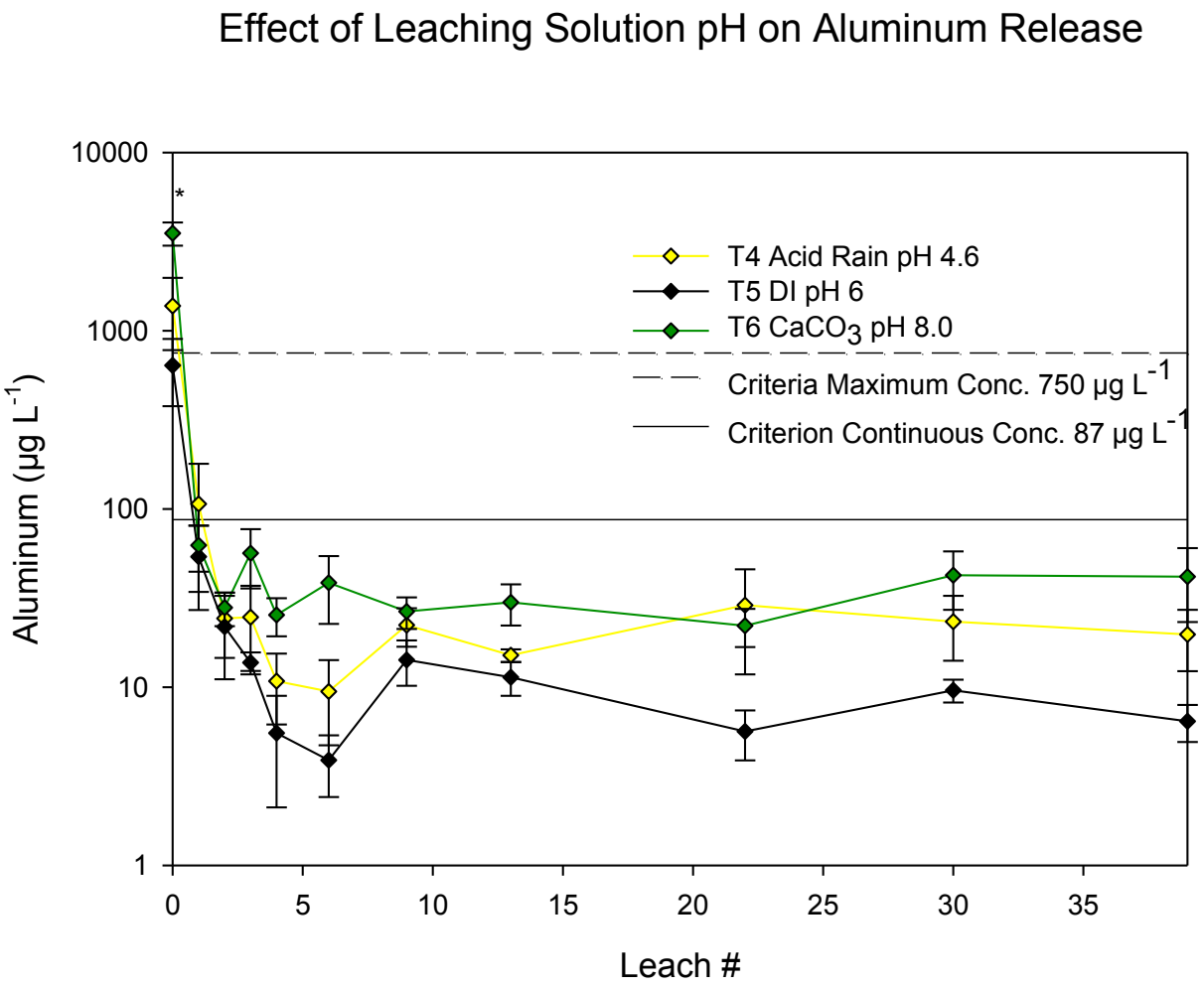

Figure 33. Leachate Al from columns leached with simulated acid rain, DI water and $CaCO_3$. The 40 leaching cycles occurred over 20 weeks. Three leaching cycles correspond to one pore volume. Error bars represent one standard error above and below the mean. Where indicated, treatment means by date were significantly different * $P < 0.05$, ** $P < 0.01$, and *** at $P < 0.001$. Detection limit = 1.0 µg L^{-1} and values below the detection limit were reported as 1.0 µg L^{-1}.

Aluminum release was the result of initial colloids passing through the filter media in the columns followed by rapid hydrolysis of Al on the edges of mineral grains, and its solubility versus pH relationship. As shown in Table 8, Al concentrations in leachate filtered post collection were much lower than the unfiltered leachate. This suggested that the bulk of Al was in a colloidal form and passed through the filter media in the columns. Aluminum elution over the first ten leaching cycles (where the rapid drop is seen) was based on its inherent solubility relationship with pH, where Al solubility increases in moderately acidic ($pH < 5.5$) and moderately alkaline ($pH > 9$) environments. In addition, the sharp drop could have also been due to the decrease in mobile colloids. The trend over the first ten leaching cycles was supported by the strong inverse correlation between Al and pH ($r = -0.992$, $p < 0.0001$) and bicarbonate ($r = -0.867$, $p = 0.0115$), seen in Appendix B, Table B-1. This could possibly explain the observed treatment effect for the initial leaching cycle. Since the simulated acid rain (pH 4.6) and the $CaCO_3$ (pH 8.0) leached somewhat higher concentrations of Al compared to the DI (pH 6).

Leaching solution pH also had a modest overall treatment effect on Cl release from mine spoil ($p = 0.0778$). This treatment effect was most pronounced in leaches two, three, and four, where the Cl concentrations in the leachate from the $CaCO_3$ leaching solution were significantly greater than both the simulated acid rain and DI water ($p = 0.0220$, $p < 0.0001$, and $p = 0.0003$, respectively). These differences are displayed in Figure 34. Chloride release followed the same pattern as sulfate, with high initial concentrations and subsequent rapid decrease. After six leaching cycles, Cl concentrations were below the detection limit of 5.0 mg L^{-1} where they remained for the duration of the study. The higher Cl levels observed in leachate from treatment six ($CaCO_3$) were possibly from bicarbonate exchanging with Cl on the edges of Al/Fe-oxides. It is unlikely that the greater leachate Cl concentrations from columns dosed with the $CaCO_3$

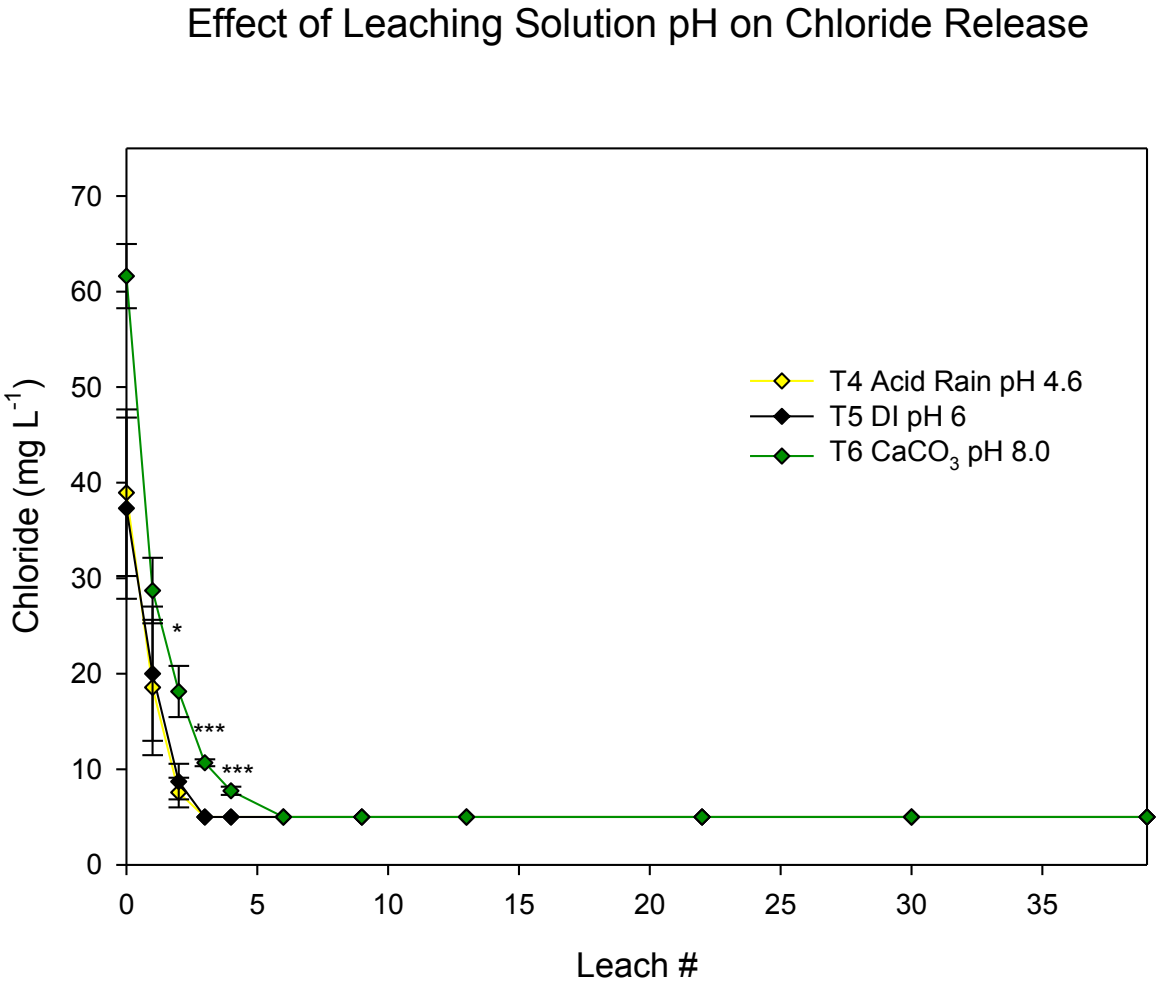

Figure 34. Leachate Cl from columns leached with simulated acid rain, DI water and $CaCO_3$. The 40 leaching cycles occurred over 20 weeks. Three leaching cycles correspond to one pore volume. Error bars represent one standard error above and below the mean. Where indicated, treatment means by date were significantly different * $P < 0.05$, ** $P < 0.01$, and *** at $P < 0.001$. Detection limit = 5.0 mg L^{-1} and values below the detection limit were reported as 5.0 mg L^{-1}.

leaching solution were due to the $CaCl_2$ used in the recipe because only 3 mg of $CaCl_2$ were used in a liter of leaching solution and the differences between treatments was at least 10 mg L^{-1}.

Potassium release was strongly affected by leaching solution pH ($p = 0.0388$). Overall, treatment five (DI) leached significantly greater concentrations of K compared to treatments four (simulated acid rain) and six ($CaCO_3$). However, no individual leaching cycle showed any significant treatment effects. As seen in Figure 35, initial K release ranged between 25 mg L^{-1} - 35 mg L^{-1} and steadily decreased to approximately 4 mg L^{-1} following the same release patterns as calcium and sulfate. It is unclear as to what may have caused the observed treatment effects, as the internal column leaching environment is a complex system.

Leaching solution pH did not have an overall treatment effect on sodium (Na) release from the mine spoil. However, leaches nine though thirty-nine all showed significant differences ($p < 0.01$ among treatments). Across these leaching cycles the simulated acid rain eluted the greatest amount of Na compared to the DI water and $CaCO_3$ leaching solutions. These individual treatment differences are presented in Figure 36. Sodium is used in making the simulated acid rain and the higher levels seen in the leachate from columns leached with the acid rain compared to the other treatments reflects the Na in the recipe. Additionally, exchange and direct hydrolysis of feldspars also likely drove the release of Na from the mine spoil.

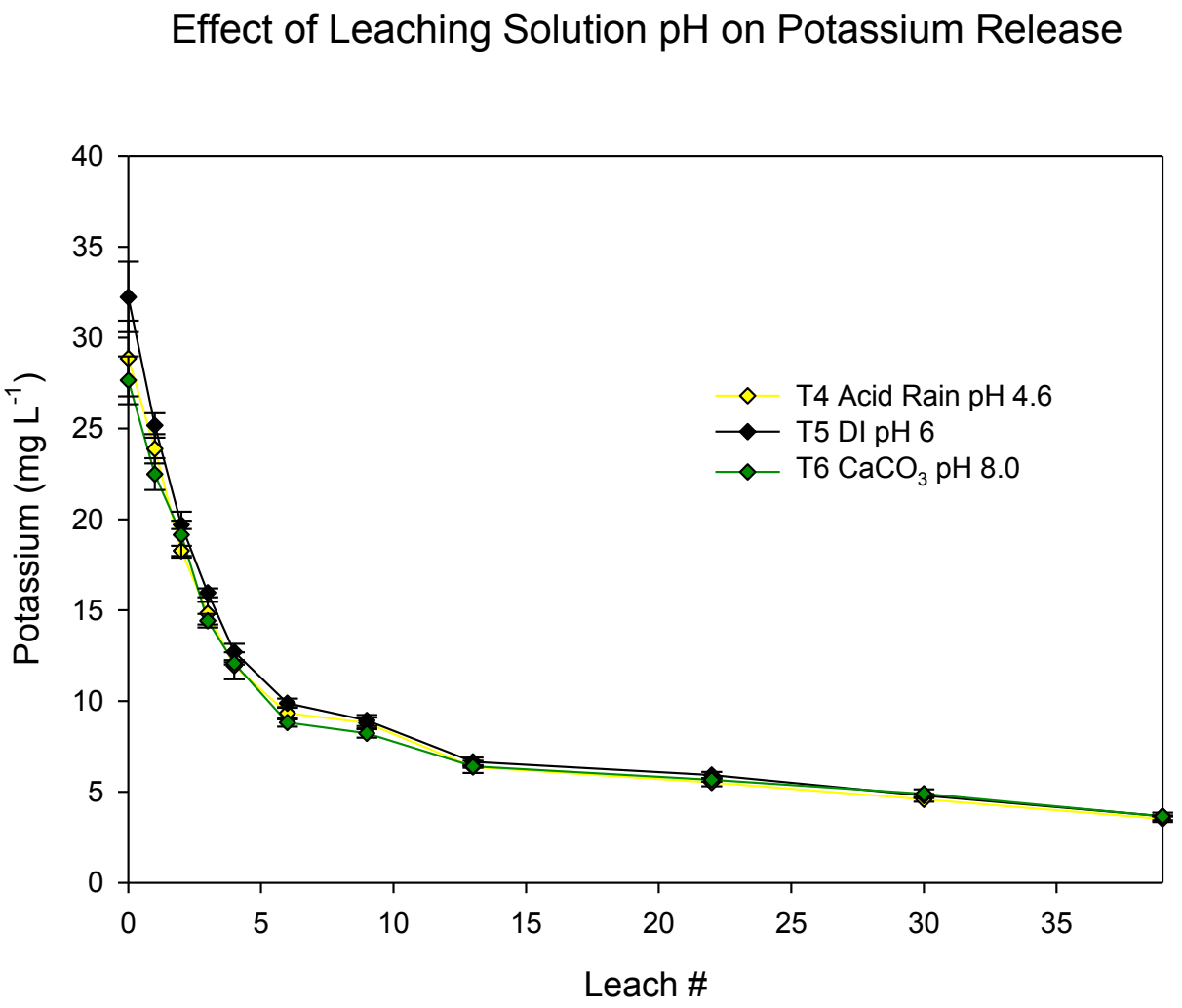

Figure 35. Leachate K from columns leached with simulated acid rain, DI water and $CaCO_3$. The 40 leaching cycles occurred over 20 weeks. Three leaching cycles correspond to one pore volume. Error bars represent one standard error above and below the mean. Detection limit = 0.005 mg L^{-1} and values below the detection limit were reported as 0.005 mg L^{-1}.

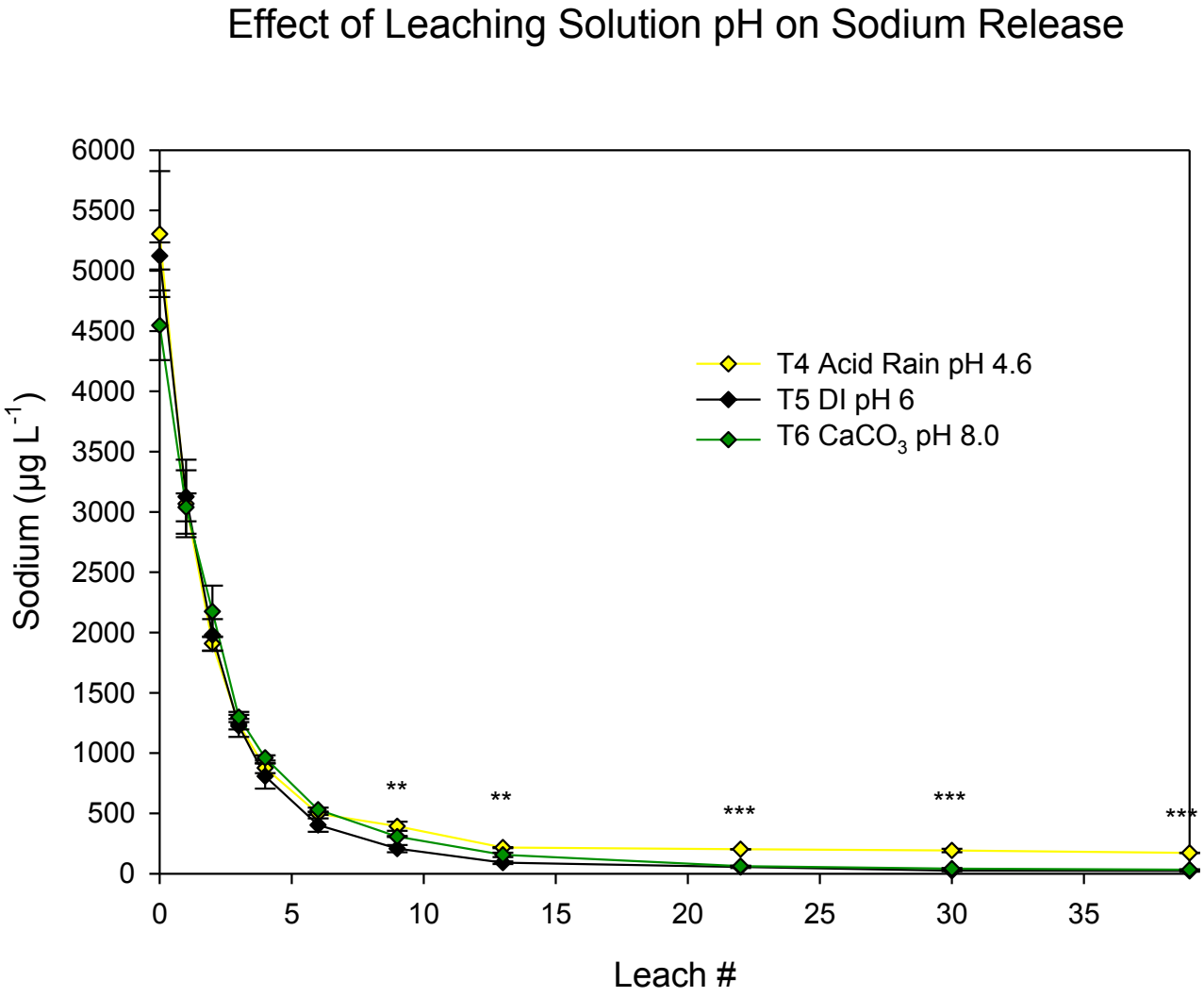

Figure 36. Leachate Na from columns leached with simulated acid rain, DI water and $CaCO_3$. The 40 leaching cycles occurred over 20 weeks. Three leaching cycles correspond to one pore volume. Error bars represent one standard error above and below the mean. Where indicated, treatment means by date were significantly different * $P < 0.05$, ** $P < 0.01$, and *** at $P < 0.001$. Detection limit = 5.0 µg L^{-1} and values below the detection limit were reported as 5.0 µg $L^{-1.}$

Charge and Mass Distribution

Leaching solution pH did not seem to affect the distribution of cations and anions in the leachate. As shown in Figures 37-38, the charge distribution for each treatment was split evenly between the cations and anions during peak elution (L1) and over time (L39). The dominant cations contributing to the total charge consisted of Ca, Mg, and to a lesser extent K. Interestingly, the relative contributions of $mmol_c$ from Ca, Mg, and K changed very little if at all from leach one to leach thirty-nine. In contrast, the distribution of $mmol_c$ from anions changed throughout the experiment. Sulfate was the dominant anion during peak elution (L1), while bicarbonate was the major contributor over time (L39). The transition from sulfate to a bicarbonate dominated system was a likely a function of increased carbonate dissolution over time coupled with decreasing pyrite oxidation due to low total S in the spoil (< 0.02%).

The mass distribution of the parameters of interest did not appear to be affected by leaching solution pH, as shown in Figures 39 - 40. Sulfate dominated the TDS release during peak elution (L1), but by the end of the experiment (L39) bicarbonate is the main contributor to TDS. Dominant cations, Ca, Mg, and K, maintained their relative contributions to TDS seen in leach one through the end of the experiment (L39). As discussed above, decreasing pyrite oxidation coupled with increased carbonate dissolution likely resulted in the observed trends.

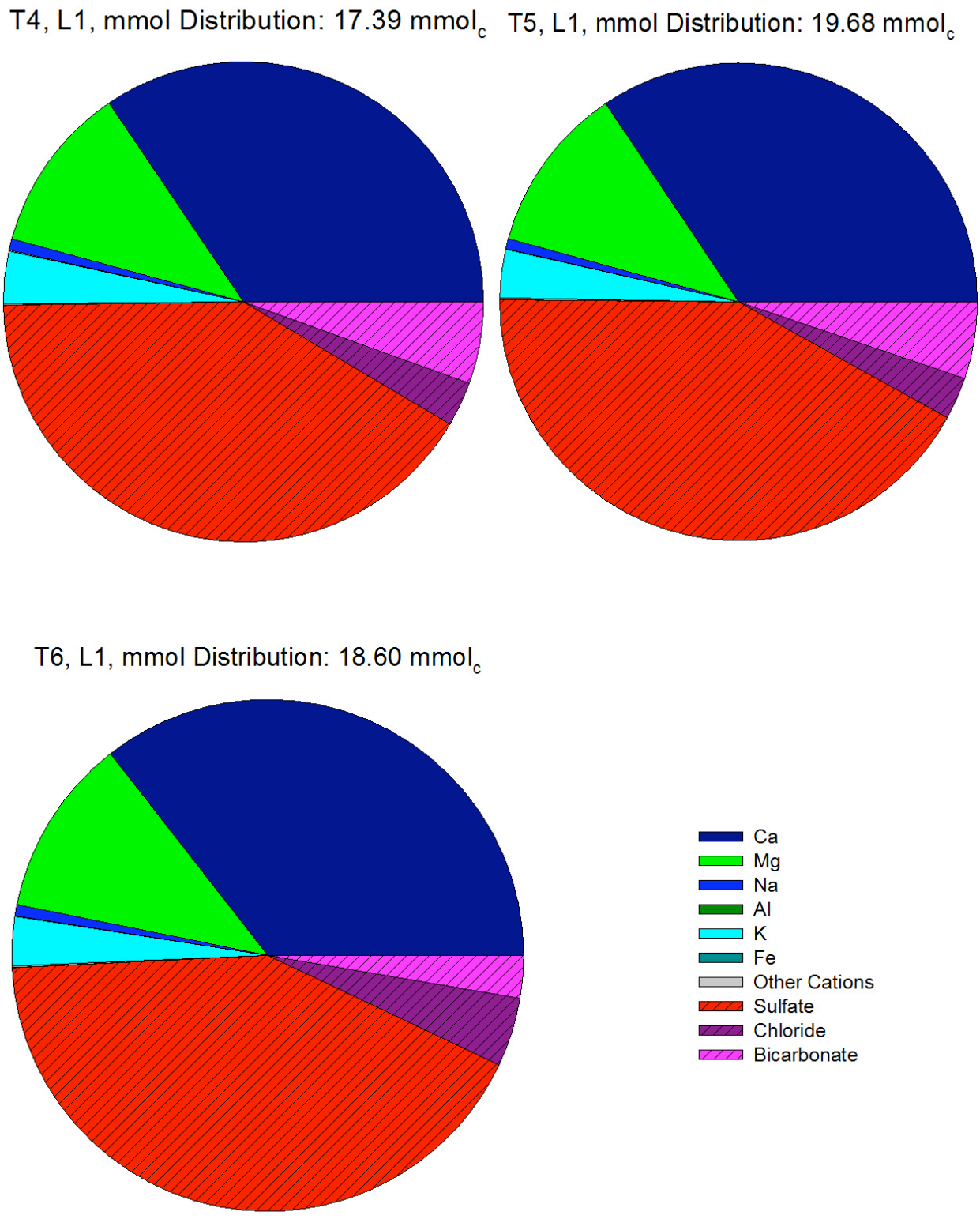

Figure 37. Charge distribution of dominant cations and anions at leach one from columns leached with simulated acid rain (T4, pH 4.6), DI (T5, pH 6), and $CaCO_3$ (T6, pH 8.0). L = Leach #.

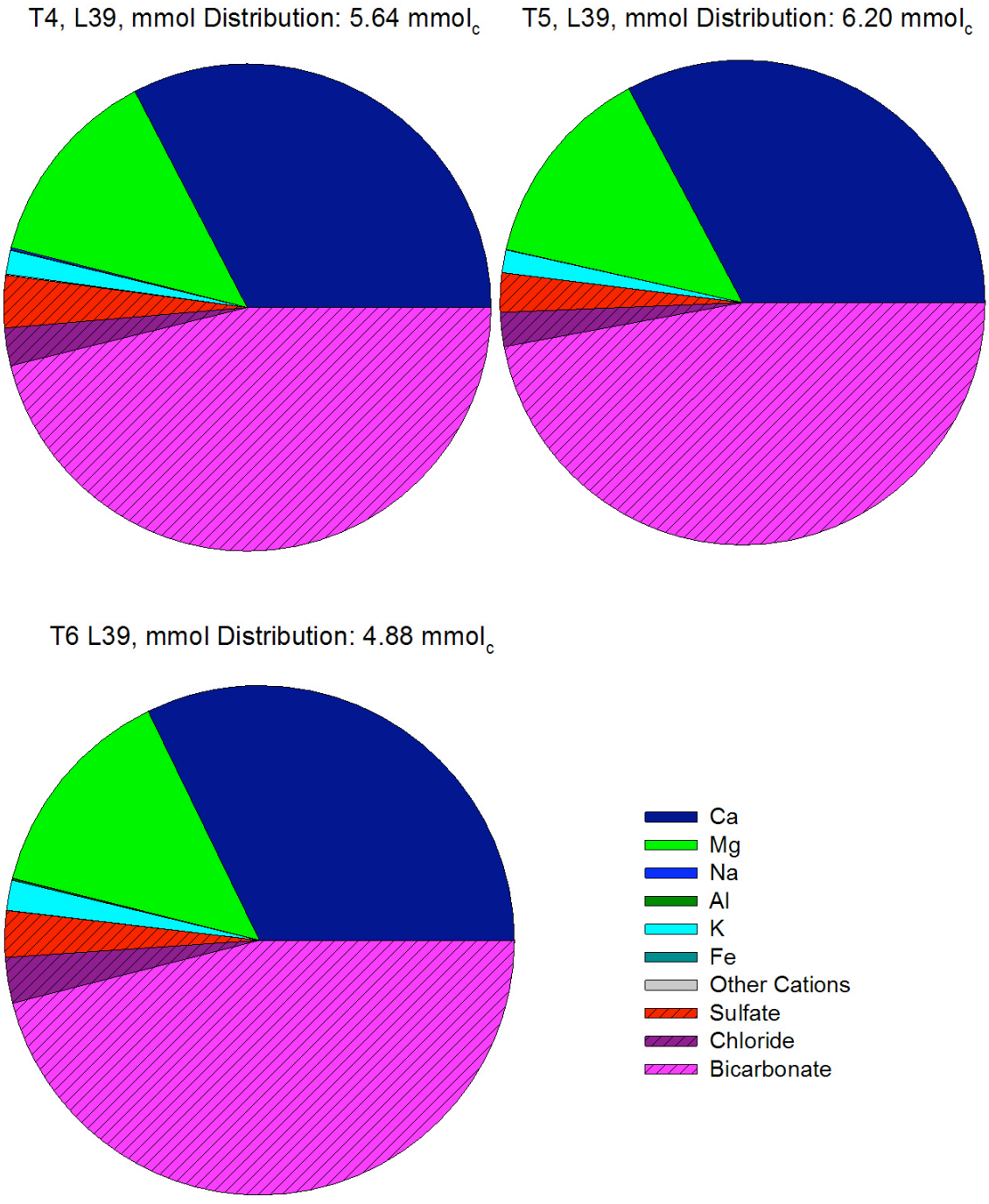

Figure 38. Charge distribution of dominant cations and anions at leach thirty-nine from columns leached with simulated acid rain (T4, pH 4.6), DI (T5, pH 6), and $CaCO_3$ (T6, pH 8.0). L = Leach #.

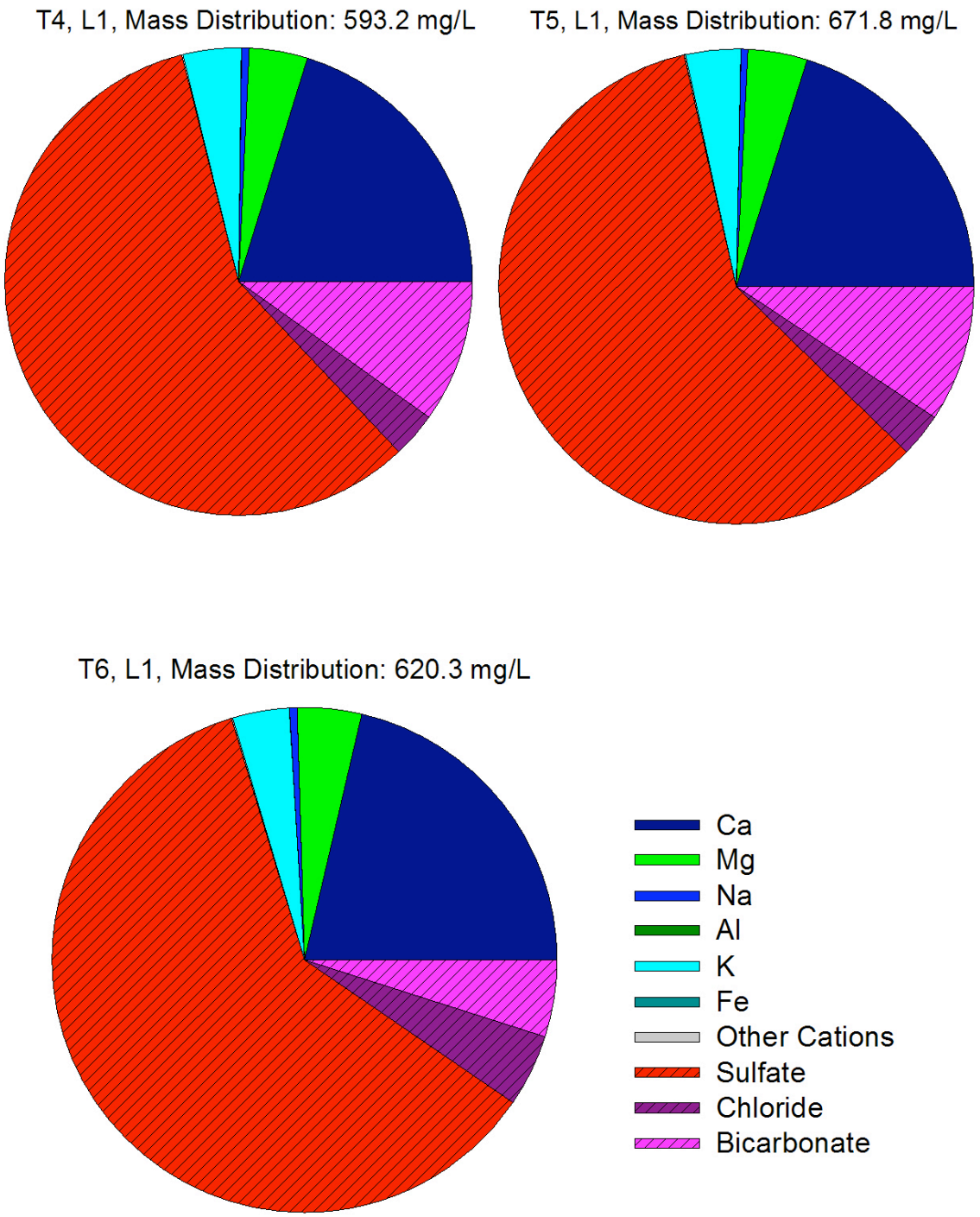

Figure 39. Mass distribution of dominant cations and anions at leach one from columns leached with simulated acid rain (T4, pH 4.6), DI (T5, pH 6), and $CaCO_3$ (T6, pH 8.0). L = Leach #.

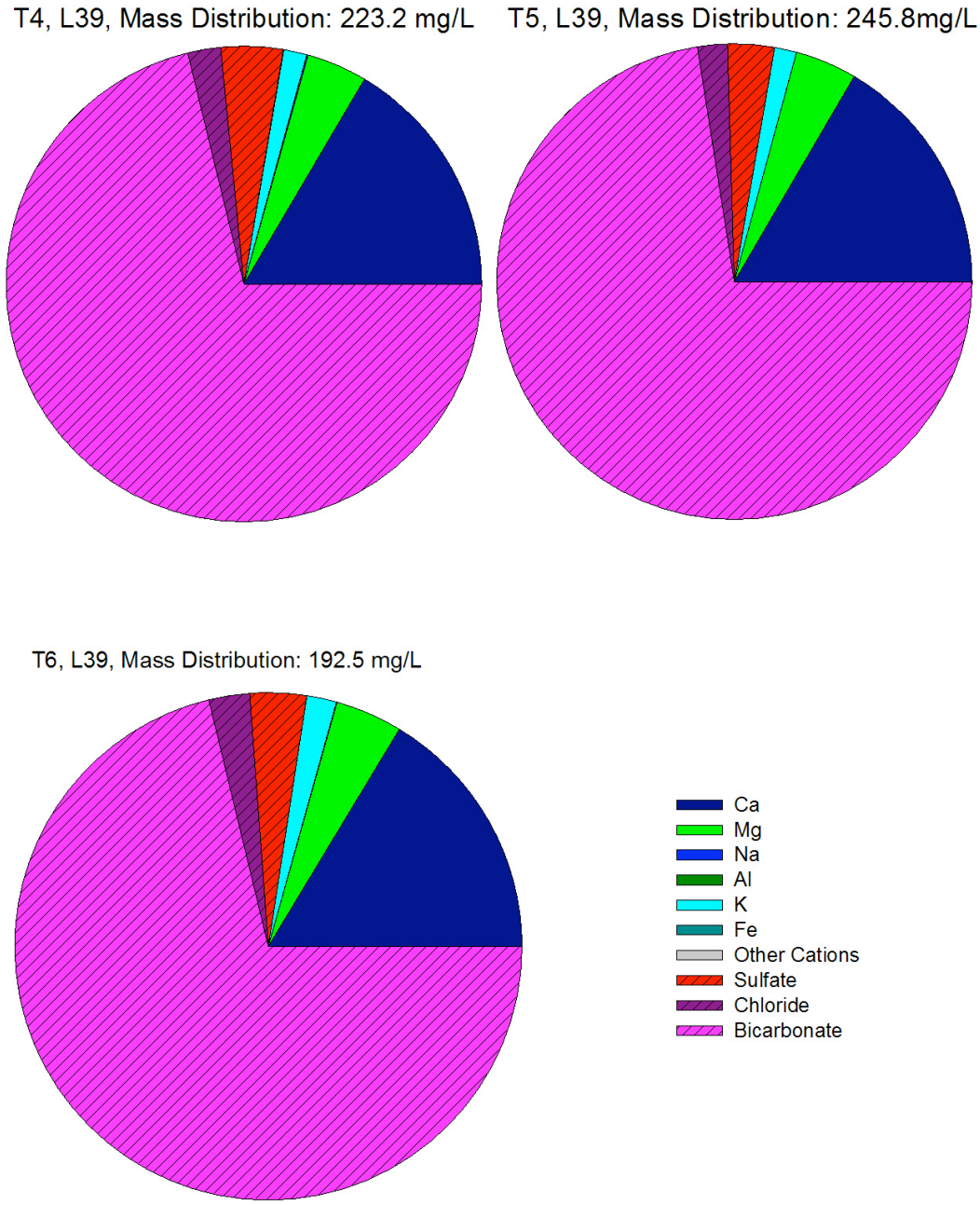

Figure 40. Mass distribution of dominant cations and anions at leach thirty-nine from columns leached with simulated acid rain (T4, pH 4.6), DI (T5, pH 6), and $CaCO_3$ (T6, pH 8.0). L = Leach #.

CHAPTER 5. EFFECTS OF LEACHING CYCLE

Overall treatment effects and summary statistics are presented in Table 9.

Table 9. Summary of repeated measures statistical analysis on various leaching cycles.

Source	pH	EC	HCO_3	SO_4	Al	As	Ca	Cd	Cl	Cu	Fe	K	Mg	Mn	Na	Ni	Pb	Se	Zn
TRT	**	*	**	NS	NS	NS	NS	NS	*	NS	NS	NS	NS	NS	NS	NS	NS	NS	NS
Leach#	***	***	***	***	***	***	***	***	***	***	***	***	***	***	***	***	***	***	***
TRT * Leach#	***	NS	**	NS	***	***	NS	***	NS	NS	***	*	NS	NS	NS	NS	***	NS	NS

TRT, Treatment; NS, Not significant; * $P < 0.05$, ** $P < 0.01$, and *** $P < 0.001$

Electrical Conductivity

Leaching cycle (frequency) had a strong overall effect ($p = 0.0348$; via repeated measures analysis) on EC values from the mine spoil over the first ten leaching cycles. Leachate EC from columns dosed once per week was significantly greater than the EC from the columns dosed daily. Significant differences across these leaching cycles can be seen in Figure 41. Initial leachate EC varied considerably, ranging from 1500 μS cm^{-1} - 2100 μS cm^{-1}. Electrical conductivity levels dropped rapidly in all treatments over the first three leaching cycles, declining below 500 μS cm^{-1} after leach four. Interestingly, dosing cycle appeared to influence the number of leaching cycles it took for leachate EC to fall below the threshold of 500 μS cm^{-1}. Columns dosed daily and twice per week fell below the threshold after leach three, while columns leached once per week and twice per month dropped below it after leach four. Treatments eight (1x $week^{-1}$) and nine (2x $month^{-1}$) leveled off around 300 μS cm^{-1}, while treatment seven (2x $week^{-1}$) reached steady state around 260 μS cm^{-1}. Treatment ten (1x day^{-1}) yielded the lowest overall EC levels, steadily decreasing to 125 μS cm^{-1}. As previously described rapid and trace oxidation of pyrite and other sulfides, coupled with the flushing of salts and other hydrated reaction products from the edges of mineral grains via exchange and

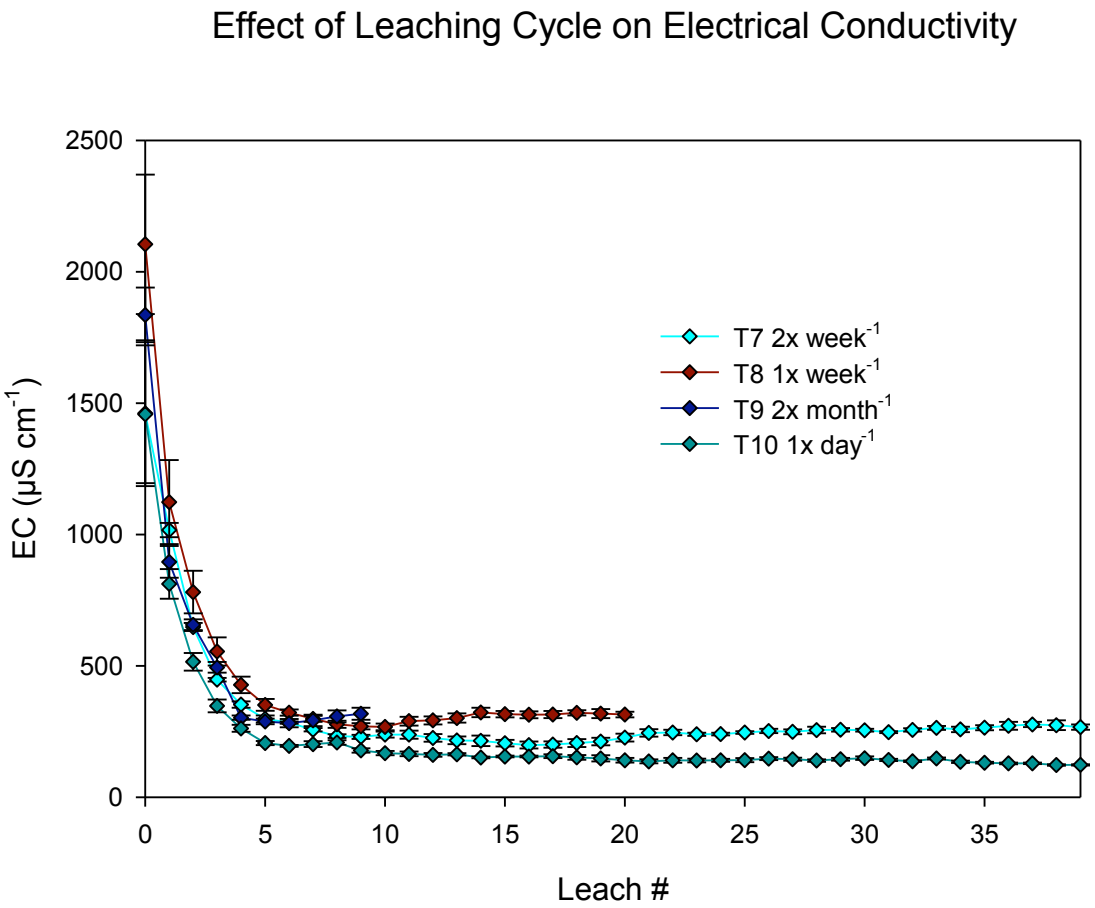

Figure 41. Leachate electrical conductivity (EC) from columns dosed 2x week^{-1}, 1x week^{-1}, 2x month^{-1}, and 1x day^{-1}. The 40 leaching cycles for columns leached 1x day^{-1} occurred over 40 days. The 40 leaching events for columns dosed 2x week^{-1}, 20 leaching events for columns leached 1x week^{-1}, and 10 events for columns leached 2x month^{-1} occurred over a period of twenty weeks. Three leaching cycles correspond to one pore volume. Error bars represent one standard error above and below the mean. Due to spatial limitations, the level of significance associated with treatment differences is not given, but in general, the values shown by leach # can be considered significantly different when greater than two standard errors apart.

rapid hydrolysis likely drove the EC release over the first ten leaching cycles (Orndorff et al., 2010).

Even though overall treatment effects (via repeated measures analysis) could only be analyzed over the first ten leaching cycles, dosing cycle continued to significantly affect leachate EC over more extended periods. As seen in Figure 41, leachate EC from treatment eight (1x week^{-1}) for leaches eleven through twenty was significantly greater than the EC from both treatments seven (2x week^{-1}) and ten (1x day^{-1}) ($p < 0.01$). In addition, treatment seven (2x per week) eluted higher EC values than treatment ten (1x day^{-1}) over this period ($p < 0.01$) as well. These differences were also observed over leaches twenty-one through forty, where columns leached twice per week eluted higher EC values than columns leached daily ($p < 0.01$). This suggests that longer time intervals between leaching cycles corresponded to higher EC levels due to accumulation of hydrated reaction products on weathering surfaces between events. Electrical conductivity release over the later leaching cycles likely reflected carbonate dissolution and weathering of associated minerals, predominantly feldspars.

Leachate pH

Dosing cycle had a strong overall treatment effect on leachate pH ($p < 0.0001$) over the first ten leaching cycles, as shown in Figure 42. Leachate from columns leached twice per month and once per week eluted significantly higher pH values than either columns leached 2x week^{-1} or 1x day^{-1}. In addition, leachate from columns leached 2x week^{-1} was higher in pH than that of columns leached daily. Therefore, longer dosing cycles corresponded to higher leachate

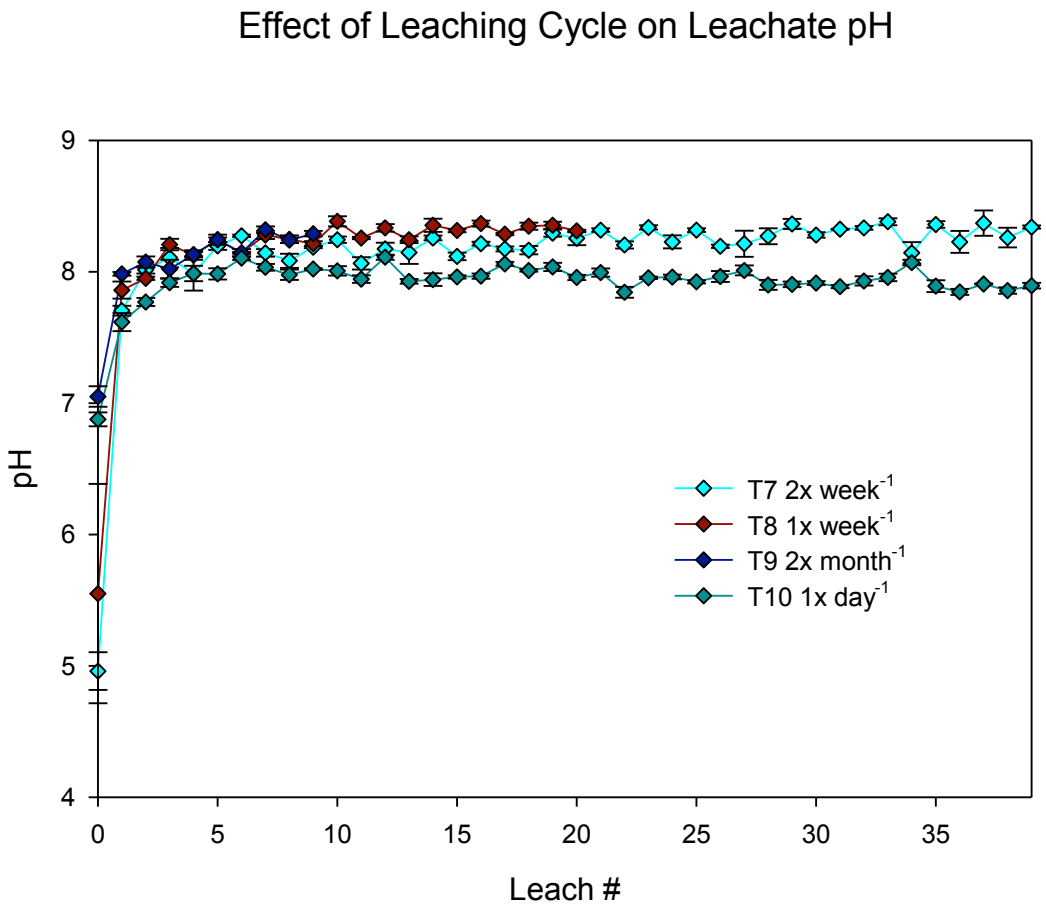

Figure 42. Leachate pH from columns dosed 2x week^{-1}, 1x week^{-1}, 2x month^{-1}, and 1x day^{-1}. The 40 leaching cycles for columns leached 1x day^{-1} occurred over 40 days. The 40 leaching events for columns dosed 2x week^{-1}, 20 leaching events for columns leached 1x week^{-1}, and 10 events for columns leached 2x month^{-1} occurred over a period of twenty weeks. Three leaching cycles correspond to one pore volume. Error bars represent one standard error above and below the mean. Due to spatial limitations, the level of significance associated with treatment differences is not given, but in general, the values shown by leach # can be considered significantly different when greater than two standard errors apart.

pH values over this span. Initial leachate pH values ranged from 5.0 to 7.0, and reflected the acid base neutralization reactions associated with rapid trace pyrite oxidation and associated carbonate dissolution. Leach zero was excluded from the statistical analysis due to the considerable variability in initial values and because initial dosing occurred at the same time and thus the values do not reflect differences due to dosing cycles. Treatments eight (1x $week^{-1}$) and nine (2x $month^{-1}$) equilibrated around pH 8.3, while treatments seven (2x $week^{-1}$) and ten (1x day^{-1}) leveled off around pH 8.2 and 7.9 respectively.

Over longer periods, dosing cycle also significantly affected the leachate pH. As shown in Figure 42, columns with longer times between leaching events maintained higher pH values compared to columns with shorter leaching cycles. While CO_2 partial pressures were not measured, as the time between leaching events increased the partial pressure of CO_2 would likely increase as well. The higher pH values associated with longer leaching cycles presumably reflected the longer duration effects of elevated CO_2 partial pressures within the column pore voids on carbonate mineral dissolution. In addition, longer contact time between the simulated acid rain held at field capacity and the mine spoil allowed for greater carbonate mineral dissolution. Previous work by Berg and Banwart (2000) and Karberg et al. (2005) suggests that in soils elevated CO_2 partial pressures may increase the rate of mineral weathering (carbonates and feldspars). The elevated CO_2 partial pressures (greater CO_2 partial pressures with longer time between leaching events) and increased contact time between the spoil and the acidic leaching solution possibly caused a brief decrease in internal column pH, which in turn may have increased carbonate mineral dissolution, ultimately yielding higher leachate pH values.

Sulfate

Interestingly, release of sulfate from the mine spoil over the first ten leaching cycles was not affected by dosing cycle. Initial sulfate concentrations varied substantially, 600 mg L^{-1} – 1000 mg L^{-1}, as shown in Figure 43. However, this likely reflected the natural variability of sulfur in the spoil, not actual treatment effects since all columns were initially dosed at the same time. Concentrations quickly declined over the first five leaching cycles and leveled off between 10 mg L^{-1} and 20 mg L^{-1}. However, over more extended periods (cycles), it appeared that dosing cycle did affect the release of sulfate. As seen in Figure 43, over leaches twenty-two through thirty-nine, sulfate concentrations in leachate from the columns leached twice per week were significantly higher than the columns leached once per day ($p < 0.01$). Rapid and trace pyrite oxidation during the initial leaching cycles likely drove the bulk of the early sulfate release from the columns. The accelerated leaching cycle used with treatment ten likely yielded higher levels of saturation in the columns compared to treatment seven. This may also indicate that the increased saturation in the columns leached 1x day^{-1} suppressed pyrite oxidation.

Bicarbonate

Dosing cycle had a strong overall effect on bicarbonate leaching ($p = 0.0021$) over the first ten leaching cycles. Columns dosed twice per month eluted the highest levels of bicarbonate. Specific treatment effects across all leaching cycles can be seen in Figure 44. Bicarbonate concentrations from the columns leached once per week were significantly higher than the columns leached daily. The bicarbonate from treatments seven and eight as well

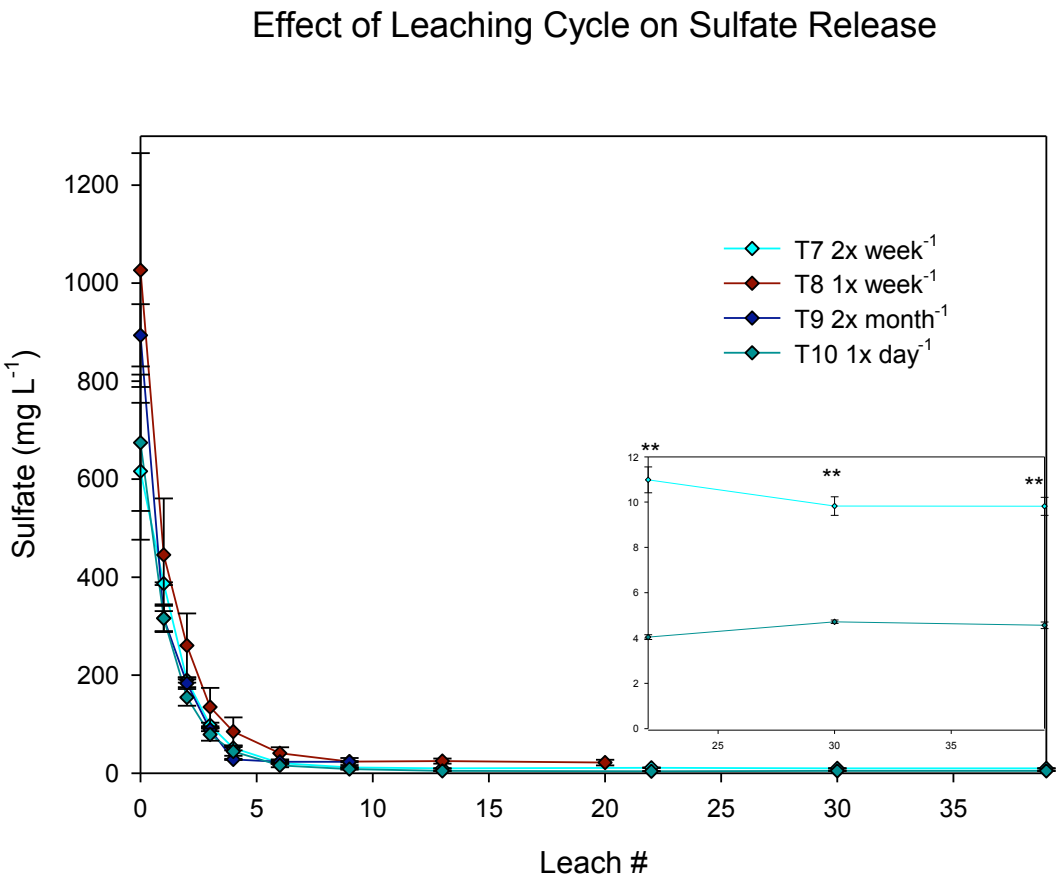

Figure 43. Leachate sulfate (SO_4) from columns dosed 2x week^{-1}, 1x week^{-1}, 2x month^{-1}, and 1x day^{-1}. The 40 leaching cycles for columns leached 1x day^{-1} occurred over 40 days. The 40 leaching events for columns dosed 2x week^{-1}, 20 leaching events for columns leached 1x week^{-1}, and 10 events for columns leached 2x month^{-1} occurred over a period of twenty weeks. Three leaching cycles correspond to one pore volume. Error bars represent one standard error above and below the mean. Where indicated, treatment means by date were significantly different * $P < 0.05$, ** $P < 0.01$, and *** $P < 0.001$. Detection limit = 0.12 mg L^{-1} and values below the detection limit were reported as 0.12 mg L^{-1}.

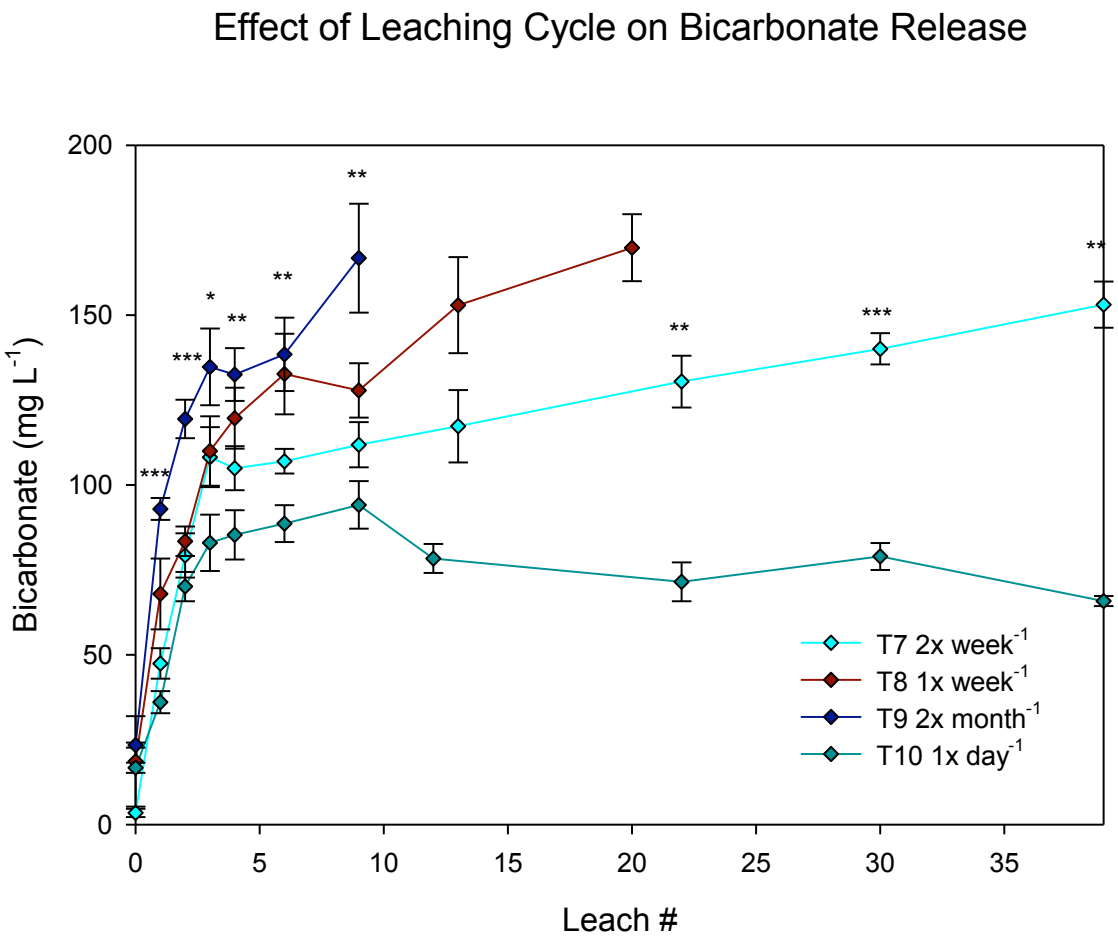

Figure 44. Leachate sulfate (SO_4) from columns dosed 2x week^{-1}, 1x week^{-1}, 2x month^{-1}, and 1x day^{-1}. The 40 leaching cycles for columns leached 1x day^{-1} occurred over 40 days. The 40 leaching events for columns dosed 2x week^{-1}, 20 leaching events for columns leached 1x week^{-1}, and 10 events for columns leached 2x month^{-1} occurred over a period of twenty weeks. Three leaching cycles correspond to one pore volume. Error bars represent one standard error above and below the mean. Where indicated, treatment means by date were significantly different * $P < 0.05$, ** $P < 0.01$, and *** $P < 0.001$.

as seven and ten were not significantly different over the first ten leaching cycles. However, over leaches twenty-two through thirty-nine, bicarbonate from columns dosed twice per week was significantly higher than that of columns dosed once per day ($p < 0.01$). Bicarbonate levels from treatments eight (1x $week^{-1}$) and nine (2x $month^{-1}$) sharply increased over all leaching cycles, peaking around 170 mg L^{-1}. The amount of bicarbonate leached from treatment seven (2x $week^{-1}$) also increased through the first five leaching cycles, then gradually increased over remaining leaching cycles, ending around 150 mg L^{-1}. Bicarbonate levels from treatment ten (1x day^{-1}) rapidly increased to 94 mg L^{-1} through leach nine before slowly decreasing for the remainder of the study, ending around 65 mg L^{-1}.

The low concentrations of bicarbonate seen over the first leaching cycles possibly reflected acid base neutralization reactions associated with rapid pyrite oxidation vs. more limited carbonate dissolution rates. Increasing bicarbonate concentrations seen over time reflect continued carbonate mineral dissolution vs. decreased pyrite oxidation. Longer dosing cycles potentially allowed for greater bicarbonate dissolution due to the effects of CO_2 partial pressure in the columns described above. As described above, greater CO_2 partial pressures associated with longer times between leaching events and elevated contact time between the spoil and leaching solution may have increased carbonate mineral dissolution. The accelerated leaching cycle applied to treatment ten (1x day^{-1}) likely increased the water saturation level in the spoil causing a decrease in CO_2 partial pressure and decreased the contact time between leaching solution and the spoil, ultimately resulting in less carbonate mineral dissolution.

Arsenic (As) and Selenium (Se)

Overall, Arsenic and Se levels were unaffected by dosing cycle. However, treatment eight eluted significantly higher levels of both As and Se than the other three treatments on leaches six and nine as shown in Figures 45 and 46. Arsenic was eluted in very low concentrations across all treatments and rapidly fell below the detection limit of 0.30 μg L^{-1} between leaches six and thirteen. Although Se was largely unaffected by dosing cycle, it exceeded the CMC of 20 μg L^{-1} over the first three leaching cycles, but eventually dropped below the CCC of 5 μg L^{-1} after leach four. Concentrations of As and Se fell below the detection limits between leaches nine and thirteen. The release patterns of these trace metals were very similar to sulfate, albeit at much lower concentrations. Arsenic was likely present in pyrite and subsequently released during the initial and rapid trace pyrite oxidation reactions mentioned above. Selenium was likely present in the spoil as a metal sulfide, possibly PbSe (J. Unrine, personal communication) or in reduced sulfide forms and subsequently released via rapid trace sulfide oxidation.

Calcium (Ca), Iron (Fe), Magnesium (Mg), and Manganese (Mn)

The release of Ca from the mine spoil was not significantly affected by dosing cycle over the first ten leaching cycles. However, treatments eight and nine appeared to leach higher amounts of Ca over leaches three through nine (Figure 47). Initial Ca release ranged from 200 mg L^{-1} to 320 mg L^{-1} and rapidly declined over the first four leaching cycles. Treatments seven (2x $week^{-1}$) and eight (1x day^{-1}) leveled off at approximately 35 mg L^{-1} and 40 mg L^{-1}, respectively, while treatments nine ($2x^{-1}$ month) and ten (1x day^{-1}) fluctuated around 40 mg L^{-1} and 15 mg L^{-1}. While the overall treatment effect for the first ten leaching cycles was not

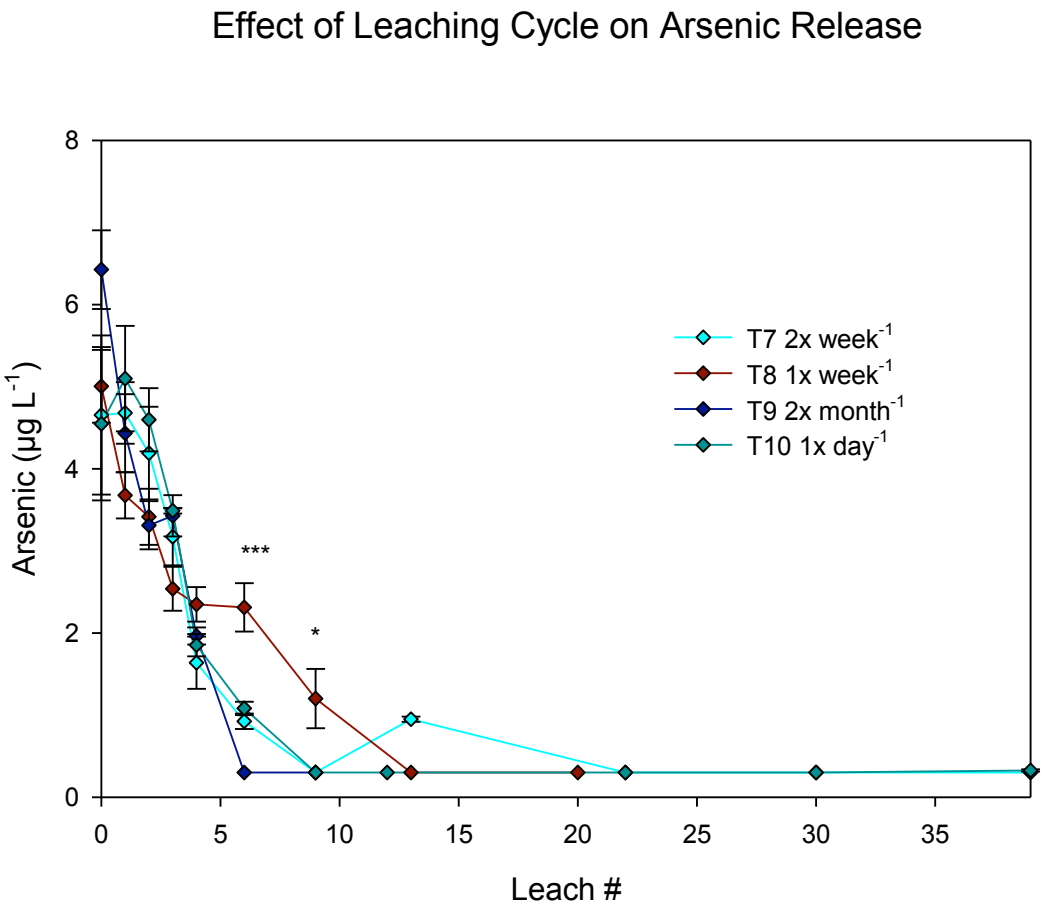

Figure 45. Leachate As from columns dosed 2x week^{-1}, 1x week^{-1}, 2x month^{-1}, and 1x day^{-1}. The 40 leaching cycles for columns leached 1x day^{-1} occurred over 40 days. The 40 leaching events for columns dosed 2x week^{-1}, 20 leaching events for columns leached 1x week^{-1}, and 10 events for columns leached 2x month^{-1} occurred over a period of twenty weeks. Three leaching cycles correspond to one pore volume. Error bars represent one standard error above and below the mean. Where indicated, treatment means by date were significantly different * $P < 0.05$, ** $P < 0.01$, and *** $P < 0.001$. Detection limit = 0.3 µg L^{-1}and values below the detection limit were reported as 0.3 µg L^{-1}.

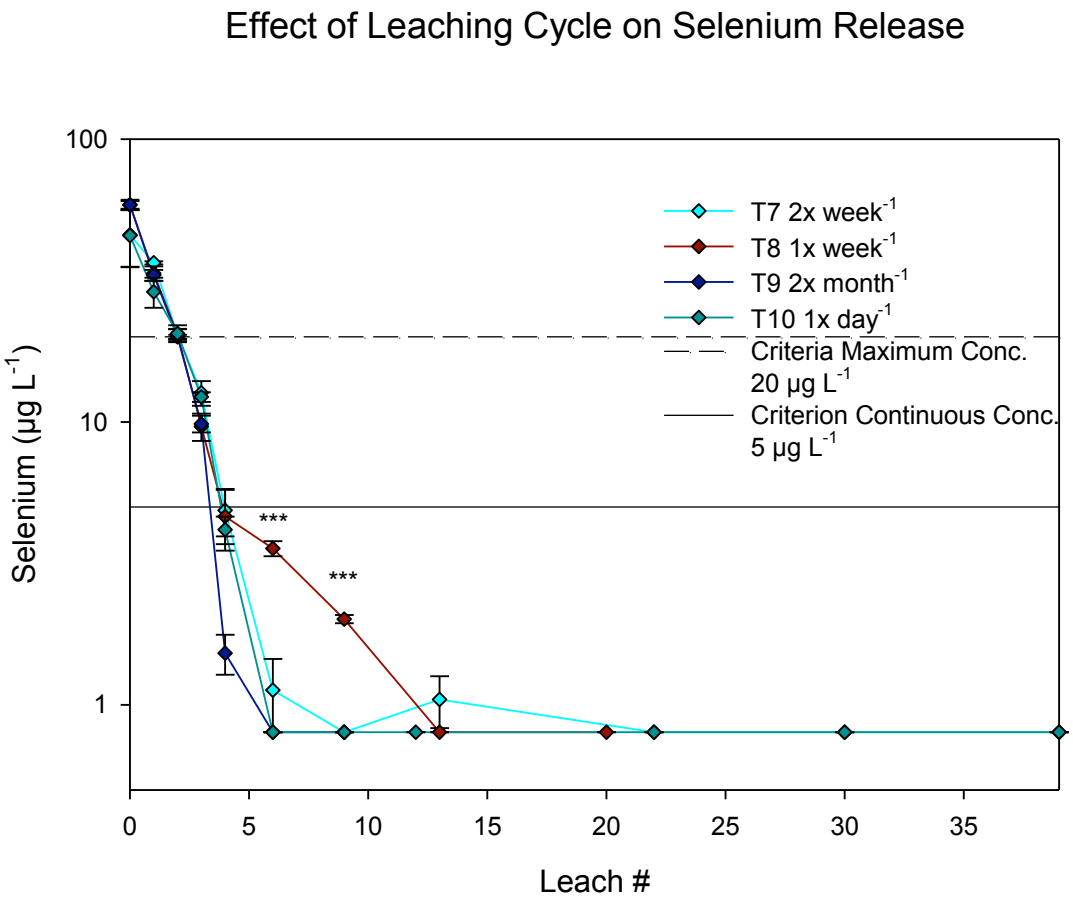

Figure 46. Leachate Se from columns dosed 2x week^{-1}, 1x week^{-1}, 2x month^{-1}, and 1x day^{-1}. The 40 leaching cycles for columns leached 1x day^{-1} occurred over 40 days. The 40 leaching events for columns dosed 2x week^{-1}, 20 leaching events for columns leached 1x week^{-1}, and 10 events for columns leached 2x month^{-1} occurred over a period of twenty weeks. Three leaching cycles correspond to one pore volume. Error bars represent one standard error above and below the mean. Where indicated, treatment means by date were significantly different * $P < 0.05$, ** $P < 0.01$, and *** $P < 0.001$. Detection limit = 0.8 µg L^{-1} and values below the detection limit were reported as 0.8 µg L^{-1}.

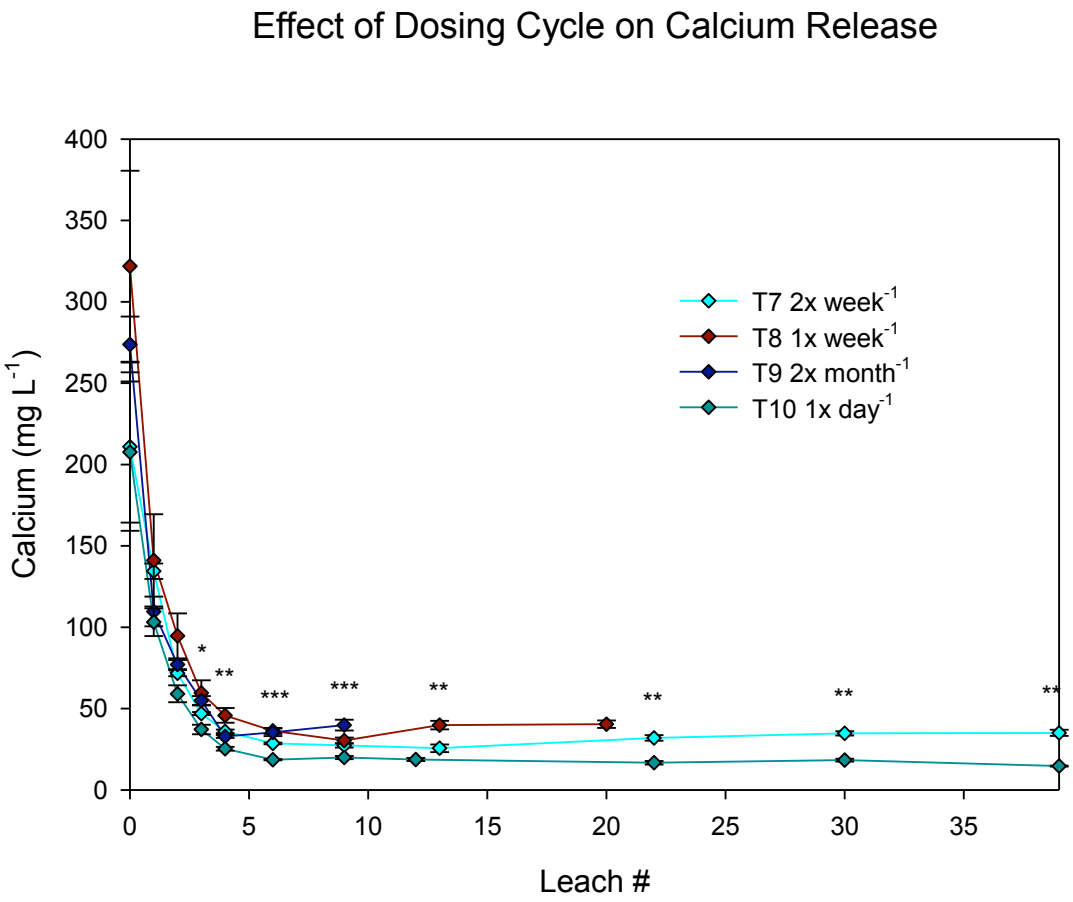

Figure 47. Leachate Ca from columns dosed 2x week^{-1}, 1x week^{-1}, 2x month^{-1}, and 1x day^{-1}. The 40 leaching cycles for columns leached 1x day^{-1} occurred over 40 days. The 40 leaching events for columns dosed 2x week^{-1}, 20 leaching events for columns leached 1x week^{-1}, and 10 events for columns leached 2x month^{-1} occurred over a period of twenty weeks. Three leaching cycles correspond to one pore volume. Error bars represent one standard error above and below the mean. Where indicated, treatment means by date were significantly different * $P < 0.05$, ** $P < 0.01$, and *** $P < 0.001$. Detection limit = 0.01 mg L^{-1} and values below the detection limit were reported as 0.01 mg L^{-1}.

significant, over longer periods of time, the dosing cycle strongly affected leaching of Ca from the spoil. As shown in Figure 47, over leaches thirteen, twenty-two, thirty, and thirty-nine, treatments with longer dosing cycles were significantly higher in Ca than treatments with shorter dosing cycles ($p < 0.01$). The release pattern of Ca over the first ten leaching cycles closely followed that of sulfate, which suggested that the initial Ca release was likely associated with carbonates interacting with pyrite oxidation. In addition, proton exchange reactions (hydrolysis) occurring at the surfaces of fractured feldspars were likely adding to the Ca release. Calcium leaching over time was most likely driven by carbonate dissolution since increases in bicarbonate were observed over similar leaching cycles. The observed treatment effects likely reflect the effects of CO_2 partial pressure on carbonate dissolution described above. Thus, longer dosing cycles allowed for greater weathering of the spoil and greater release of Ca.

Iron leaching from the mine spoil was not significantly affected by dosing cycle over the first ten leaching cycles. Initial Fe release varied considerably, presumably the result of dispersed colloids passing through the filter materials in the bottom of the columns. As shown in Table 10, on leach one, the unfiltered leachate from the columns leached daily was considerably higher in Fe than the leachate filtered through a 0.45 μm filter. After the initial spike, treatments seven, eight, and nine fluctuated close to the detection limit of 5.0 μg L^{-1} for all subsequent leaching events. However, Fe concentrations from treatment ten (1x day^{-1}) varied greatly, but generally seemed to increase over time. While the overall treatment effect was not significant over the first ten leaching cycles, over the final ten leaching cycles, it appeared that Fe was influenced by dosing cycle, as shown in Appendix E, Figure E-1. On leach thirty, Fe levels from columns leached daily were significantly higher than that of columns leached twice per week. Iron release from all treatments did not follow the release patterns of other pyrite oxidation

products, Presumably because Fe likely precipitated in the columns as insoluble oxy-hydroxides. The rapid leaching cycle for treatment ten potentially increased the saturation level in the columns. Iron oxy-hydroxide formation would be less favorable in this environment as well as partial reduction of Fe^{3+} to water soluble Fe^{2+} causing the slightly higher levels observed over time.

Table 10. Filtered vs. unfiltered leachate for selected elements at leach one from columns leached 2x $week^{-1}$ (T7), 1x $week^{-1}$ (T8), 2x $month^{-1}$ (T9), and 1x day^{-1} (T10).

Leach 1		Al	As	Cd	Cu	Fe	Mn	Na	Ni	Pb	Se
		μg L^{-1}									
T7	Filtered	39 (10)	5 (1)	0.1 (0)	2 (0)	5 (0)	529 (71)	3500 (520)	0.3 (0)	0.5 (0)	38 (2)
	Unfiltered	49 (9)	5 (1)	0.1 (0)	2 (0)	5 (0)	528 (74)	3472	2 (2)	0.5 (0)	37 (1)
T8	Filtered	37 (33)	4 (1)	0.1 (0)	2 (0)	5 (0)	713 (528)	3393 (297)	3 (3)	0.5 (0)	34 (7)
	Unfiltered	41 (4)	4 (1)	0.1 (0)	2 (0)	5 (0)	713 (528)	3393	3 (3)	0.5 (0)	34 (7)
T9	Filtered	11 (4)	4 (1)	0.1 (0)	2 (0)	5 (0)	307 (21)	2992 (493)	0.4 (0)	0.5 (0)	31 (4)
	Unfiltered	8 (43)	4 (1)	0.1 (0)	2 (0)	5 (0)	307 (21)	2992	0.4 (0)	0.5 (0)	31 (4)
T10	Filtered	12 (8)	5 (1)	0.1 (0)	1 (0)	5 (0)	236 (56)	2516 (389)	3 (2)	0.5 (0)	31 (4)
	Unfiltered	46 (42)	5 (1)	0.1 (0)	1 (0)	45 (69)	237 (55)	2519	3 (2)	0.5 (0)	29 (6)

Detection limit for Cd = 0.1 μg L^{-1}, Fe = 5 μg L^{-1}, Ni = 0.3 μg L^{-1}, and Pb = 0.5 μg L^{-1}. Values expressed as mean and (standard deviation)

Dosing cycle had a slight treatment effect ($p = 0.0666$) on the release of Mg from the spoil over the first ten leaching cycles. Columns leached once per week eluted significantly higher concentrations of Mg than the columns leached daily and twice per week. As shown in Figure 48, the strongest overall treatment effects were observed over leaches three through nine ($p < 0.05$), where higher levels of Mg were released from columns with longer times between leaching events. Initial Mg release from columns dosed twice per week and daily was

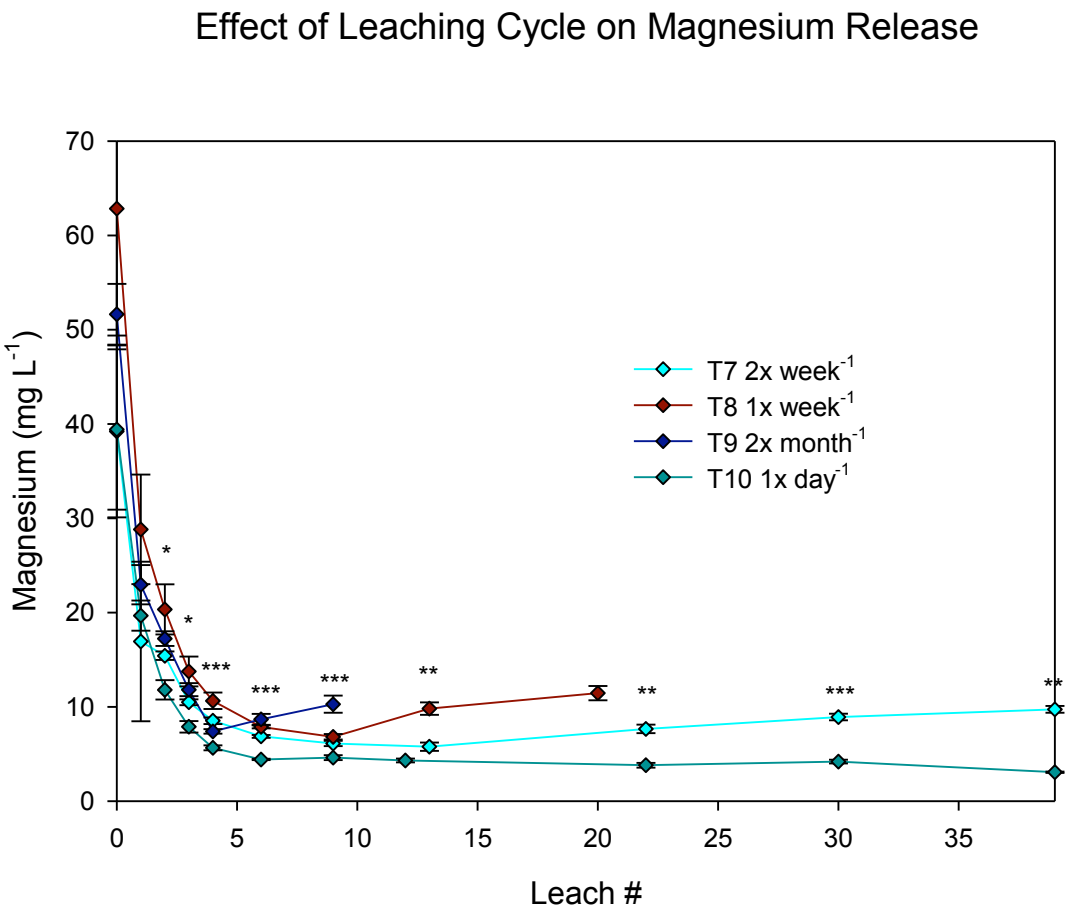

Figure 48. Leachate Mg from columns dosed 2x week^{-1}, 1x week^{-1}, 2x month^{-1}, and 1x day^{-1}. The 40 leaching cycles for columns leached 1x day^{-1} occurred over 40 days. The 40 leaching events for columns dosed 2x week^{-1}, 20 leaching events for columns leached 1x week^{-1}, and 10 events for columns leached 2x month^{-1} occurred over a period of twenty weeks. Three leaching cycles correspond to one pore volume. Error bars represent one standard error above and below the mean. Where indicated, treatment means by date were significantly different * $P < 0.05$, ** $P < 0.01$, and *** $P < 0.001$. Detection limit = 0.005 mg L^{-1} and values below the detection limit were reported as 0.005 mg L^{-1}.

approximately 40 mg L^{-1}, while the columns dosed once per week and twice per month ranged from 50 mg $L^{-1}$to 63 mg L^{-1}. Concentrations of Mg rapidly declined below 10 mg L^{-1}over the first five leaching cycles before leveling off between 5 mg L^{-1}– 10 mg $L^{-1}$and slowly increasing over time. This pattern of release was observed for all treatments. However, Mg from columns leached daily slowly declined over the rest of the experiment.

While dosing cycle had a modest overall treatment effect on Mg release over the first ten leaching cycles, dosing cycle showed the strongest treatment effects over longer periods of time. As shown in Figure 48, over leaches thirteen, twenty-two, thirty, and thirty-nine, treatments with longer dosing cycles were significantly higher in Mg than treatments with shorter dosing cycles ($p < 0.01$). The release pattern of Mg over the first ten leaching cycles closely followed that of sulfate and Ca, which suggests that the initial Mg release was likely associated with carbonates interacting with the products of pyrite oxidation. Magnesium release over time also follows the release pattern of bicarbonate and Ca, suggesting that longer-term carbonate mineral dissolution was driving Mg elution over time as previously described.

The release of Mn over the first ten leaching cycles was not affected by dosing cycle. In contrast, treatments seven and eight were significantly greater than treatment nine by leach cycle nine (Figure 49), and the treatments continued to separate over additional cycles. Initial Mn elution varied substantially across treatments, probably due to initial flux of dispersed colloids, and ranged from approximately 850 μg L^{-1} to 3600 μg L^{-1}. Like Ca and Mg, the release of Mn over the first ten leaching cycles likely reflected the interaction between pyrite oxidation and carbonate dissolution. Over the first ten leaching cycles Mn concentrations steadily declined for treatments seven, eight, and nine. However, as shown in Figure 49, sharp drops in

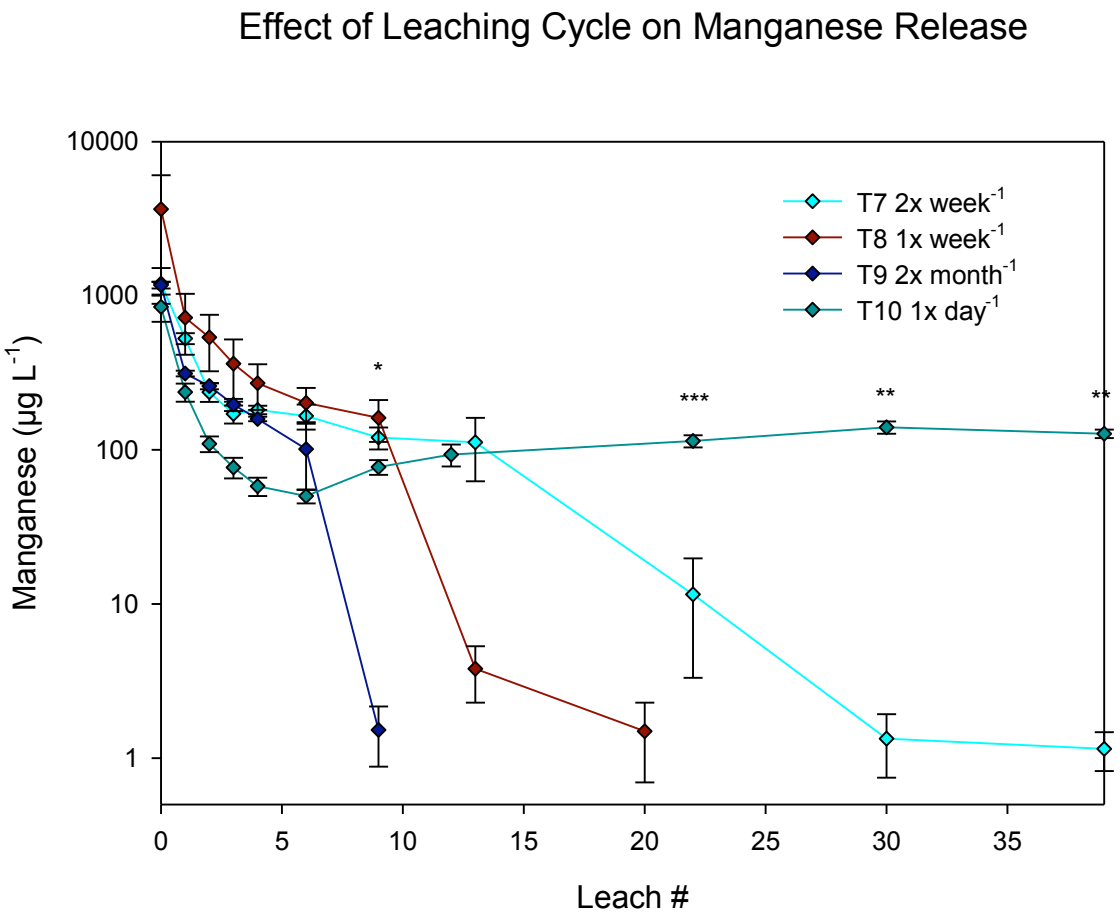

Figure 49. Leachate Mn from columns dosed 2x week^{-1}, 1x week^{-1}, 2x month^{-1}, and 1x day^{-1}. The 40 leaching cycles for columns leached 1x day^{-1} occurred over 40 days. The 40 leaching events for columns dosed 2x week^{-1}, 20 leaching events for columns leached 1x week^{-1}, and 10 events for columns leached 2x month^{-1} occurred over a period of twenty weeks. Three leaching cycles correspond to one pore volume. Error bars represent one standard error above and below the mean. Where indicated, treatment means by date were significantly different * $P < 0.05$, ** $P < 0.01$, and *** $P < 0.001$. Detection limit = 0.5 µg L^{-1} and values below the detection limit were reported as 0.5 µg L^{-1}.

concentration, possibly due to changes in redox chemistry in the columns, were seen for certain treatments after leaches one, six, nine, and thirteen. Manganese concentrations for treatment ten (1x per day) followed the same initial pattern, but then leveled off around 100 μg L^{-1} after seven leaching cycles and actually increased slightly over more extended cycles.

Even though dosing cycle did not affect Mn release from mine spoil over the first ten leaching cycles, the time between leaching cycles did affect Mn elution over time. Over leaches twenty-two through thirty-nine, columns leached daily released significantly more Mn than the columns leached twice per week ($p < 0.001$), as shown in Figure 49. The pattern of Mn release for all treatments closely followed that of sulfate, Ca, and Mg, although Mn did not increase over time. It should be noted that the sharp decrease in Mn concentrations near the end of the experiment coincided with the slight increases seen with EC, bicarbonate, Ca, and Mg.

Cadmium (Cd), Copper (Cu), Nickel (Ni), Lead (Pb), and Zinc (Zn)

Dosing cycle did not affect the release of Cd, Cu, Ni, Pb, and Zn from the mine spoil. These trace metals were present in low concentrations and exhibited similar patterns of release. However, Ni exceeded the CCC over the initial leaching cycle. As seen in Figures E-2 to E-6 presented in Appendix E, the release of these metals is characterized by an initial spike and subsequent rapid decrease in concentration near or below the detection limit of each parameter. Although present in low concentrations, the patterns of release were similar to sulfate. The presumed chalcophilic nature of the trace metals suggested that their release was driven by rapid and trace pyrite oxidation. However, siderite dissolution may have contributed to the relatively high Zn concentrations in the leachate.

Aluminum (Al), Chloride (Cl), Potassium (K), and Sodium (Na)

Overall, Al release from the mine spoil was not affected by dosing cycle. Although initial Al release varied considerably (100 μg L^{-1} – 2200 μg L^{-1}), all columns were leached at the same time so this is variability was likely due to dispersed colloids passing through the filter materials, as shown in Table 10. After this initial spike, Al concentrations leveled off between 15 μg L^{-1} - 30 μg L^{-1}. However, the columns leached daily eluted greater concentrations of Al than all other treatments at leach three and were greater than treatment seven over leaches twenty-two and thirty ($p < 0.05$), seen in Appendix E, Figure E-7. Aluminum leaching over the first few leaching cycles was likely due to rapid hydrolysis of Al on the edges of mineral grains, which caused instability in the structure and subsequent release. As the pH of the leachate increased, Al concentrations rapidly declined due to low Al solubility in moderately alkaline solutions. The slightly higher levels of Al seen in leachates from the daily columns could have been the result of increased hydrolysis since their level of saturation was higher.

Dosing cycle had a significant overall treatment effect on Cl release ($p = 0.0253$). Columns leached once and twice per week eluted significantly higher levels of Cl compared to columns leached daily and twice per month. As shown in Figure 50, the overall treatment effect was strongest over leaches one and two ($p = 0.0272$, $p = 0.0202$). Initial Cl release ranged between 20 mg L^{-1}, for treatments nine and ten, and up to 60 mg L^{-1} for treatments seven and eight, after which it quickly declined. After the fifth leaching cycle, concentrations remained at

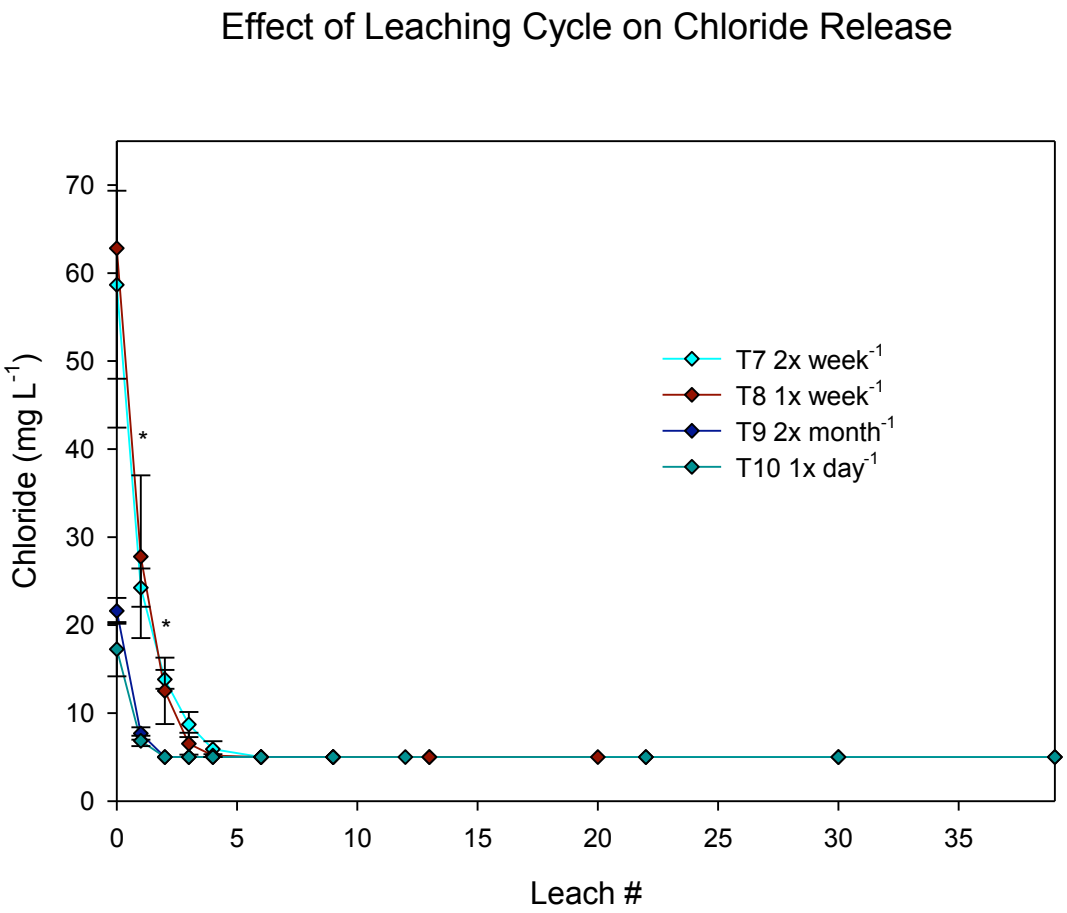

Figure 50. Leachate Cl from columns dosed 2x week^{-1}, 1x week^{-1}, 2x month^{-1}, and 1x day^{-1}. The 40 leaching cycles for columns leached 1x day^{-1} occurred over 40 days. The 40 leaching events for columns dosed 2x week^{-1}, 20 leaching events for columns leached 1x week^{-1}, and 10 events for columns leached 2x month^{-1} occurred over a period of twenty weeks. Three leaching cycles correspond to one pore volume. Error bars represent one standard error above and below the mean. Where indicated, treatment means by date were significantly different * $P < 0.05$, ** $P < 0.01$, and *** $P < 0.001$. Detection limit = 5.0 mg L^{-1} and values below the detection limit were reported as 5.0 mg L^{-1}.

or below detection limit of 5 mg L^{-1} for all subsequent leaching cycles. This pattern of release was very similar to that of sulfate, but at much lower overall levels. It was expected that Cl release would simply be a function of water movement in the columns coupled with simple dissolution of trace Cl in the mine spoils, however it is unclear as to what caused the observed treatment effects.

Overall, potassium leaching was unaffected by dosing cycle over the first ten leaching cycles. Initial K release across all treatments ranged from 30 mg $L^{-1}$to 40 mg L^{-1}. Potassium levels dropped below 10 μg L^{-1} over the first six leaching cycles and slowly declined for the remainder of the experiment. The initial release of K from the mine spoil was probably driven by rapid exchange reactions at the surfaces of feldspars and the edges of micas. However, over time, dosing cycle seems to have a minor treatment effect on K release. As shown in Figure 51, on leaches twenty-two, thirty, and thirty-nine, columns leached twice a week eluted higher levels of K than the columns leached daily ($p < 0.01$). In addition, at leach thirteen, columns leached once per week eluted K concentrations significantly higher than columns leached twice per week ($p = 0.0270$). This suggested that K release over time was potentially accelerated due to longer times between leaching cycles. Longer times between dosing cycles would allow for more oxidation and weathering of the feldspars and micas present in the spoil, leading to higher K in the leachates.

Dosing cycle did not affect the release of Na from the mine spoil. Initial concentrations ranged between 5000 μg L^{-1} - 7000 μg L^{-1} and dropped rapidly over the first six leaching cycles. Concentrations leveled off between 175 μg L^{-1}- 300 μg L^{-1} around leach nine, as shown in Figure D-8 in Appendix D. The release of Na was very similar to K, as the weathering of feldspars in the spoil likely drove Na release.

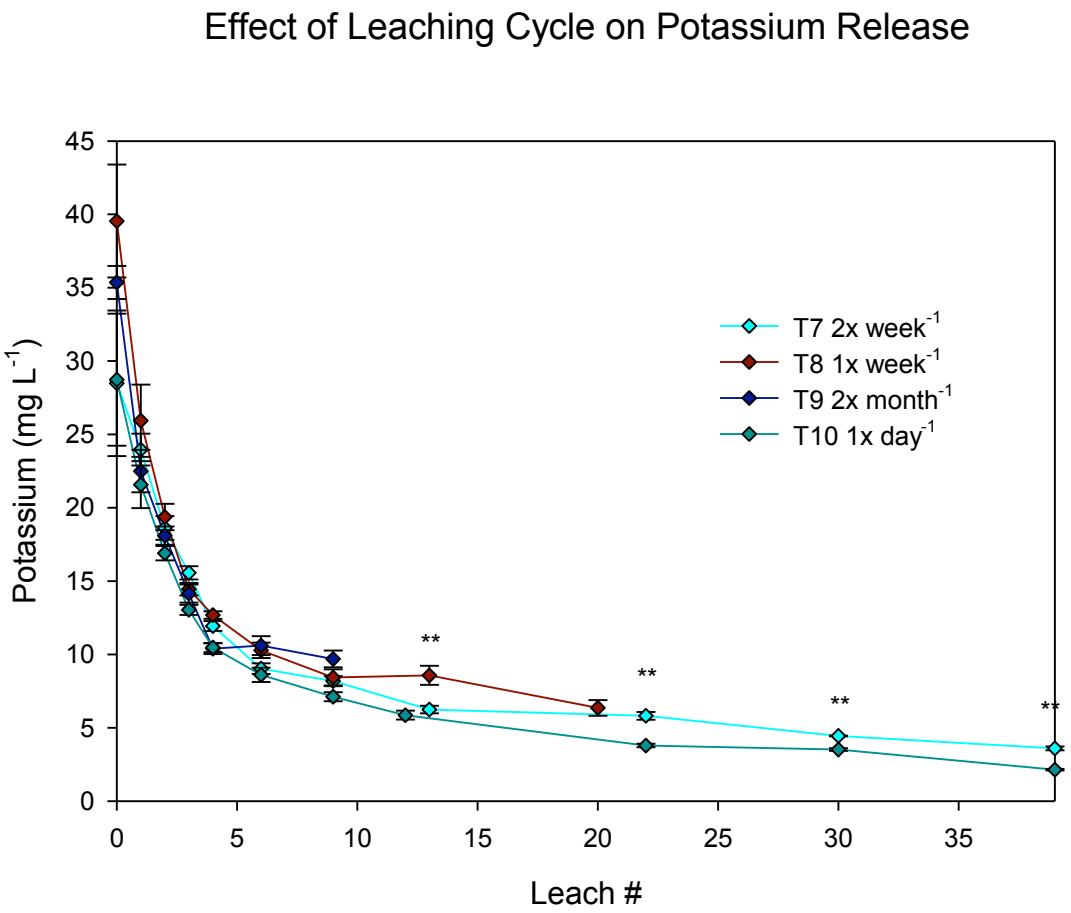

Figure 51. Leachate K from columns dosed 2x week^{-1}, 1x week^{-1}, 2x month^{-1}, and 1x day^{-1}. The 40 leaching cycles for columns leached 1x day^{-1} occurred over 40 days. The 40 leaching events for columns dosed 2x week^{-1}, 20 leaching events for columns leached 1x week^{-1}, and 10 events for columns leached 2x month^{-1} occurred over a period of twenty weeks. Three leaching cycles correspond to one pore volume. Error bars represent one standard error above and below the mean. Where indicated, treatment means by date were significantly different * $P < 0.05$, ** $P < 0.01$, and *** $P < 0.001$. Detection limit = 0.005 mg L^{-1} and values below the detection limit were reported as 0.005 mg L^{-1}.

Charge and Mass Distribution

The distribution of cations and anions did not appear to be affected by varied dosing cycles. As shown in Figures 52 and 53 all treatments showed an approximate 50:50 split between cations and anions in both leach one and leach nine. This suggests that the balance of cations and anions does not change over time. However, the distribution of $mmol_c$ from anions changes from leach one to leach nine. Sulfate dominates during the peak elution (L1), while bicarbonate is the main contributor over time (L9). In contrast, the relative contributions toward the total $mmol_c$ from the major cations (Ca and Mg) did not change over time. The change from a sulfate to bicarbonate system was likely a function of increased carbonate dissolution over time coupled with decreasing pyrite oxidation due to low total S in the spoil (< 0.02%).

Similar to the charge distribution, dosing cycle did not seem to drastically alter the mass distribution of the primary TDS constituents, as shown in Figures 54 and 55. Sulfate was the greatest contributor of TDS during leach one due to rapid and trace pyrite oxidation occurring in the columns. However, just like with the charge distribution over time bicarbonate became the greatest contributor of TDS (approximately 60 %).

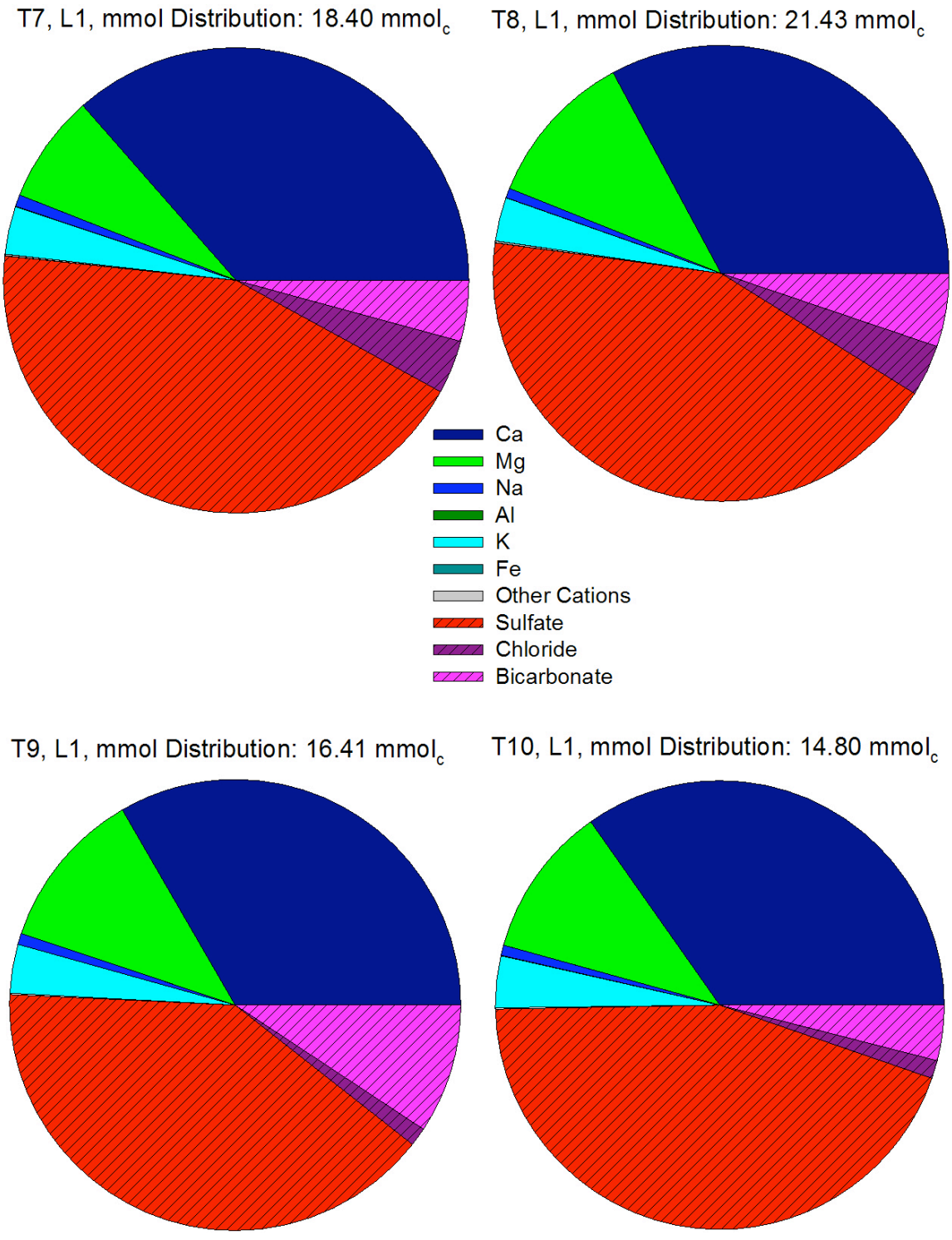

Figure 52. Charge distribution of dominant cations and anions at leach one from columns leached 2x week^{-1} (T7), 1x week^{-1} (T8), 2x month^{-1} (T9), and 1x day^{-1} (T10). L = Leach #.

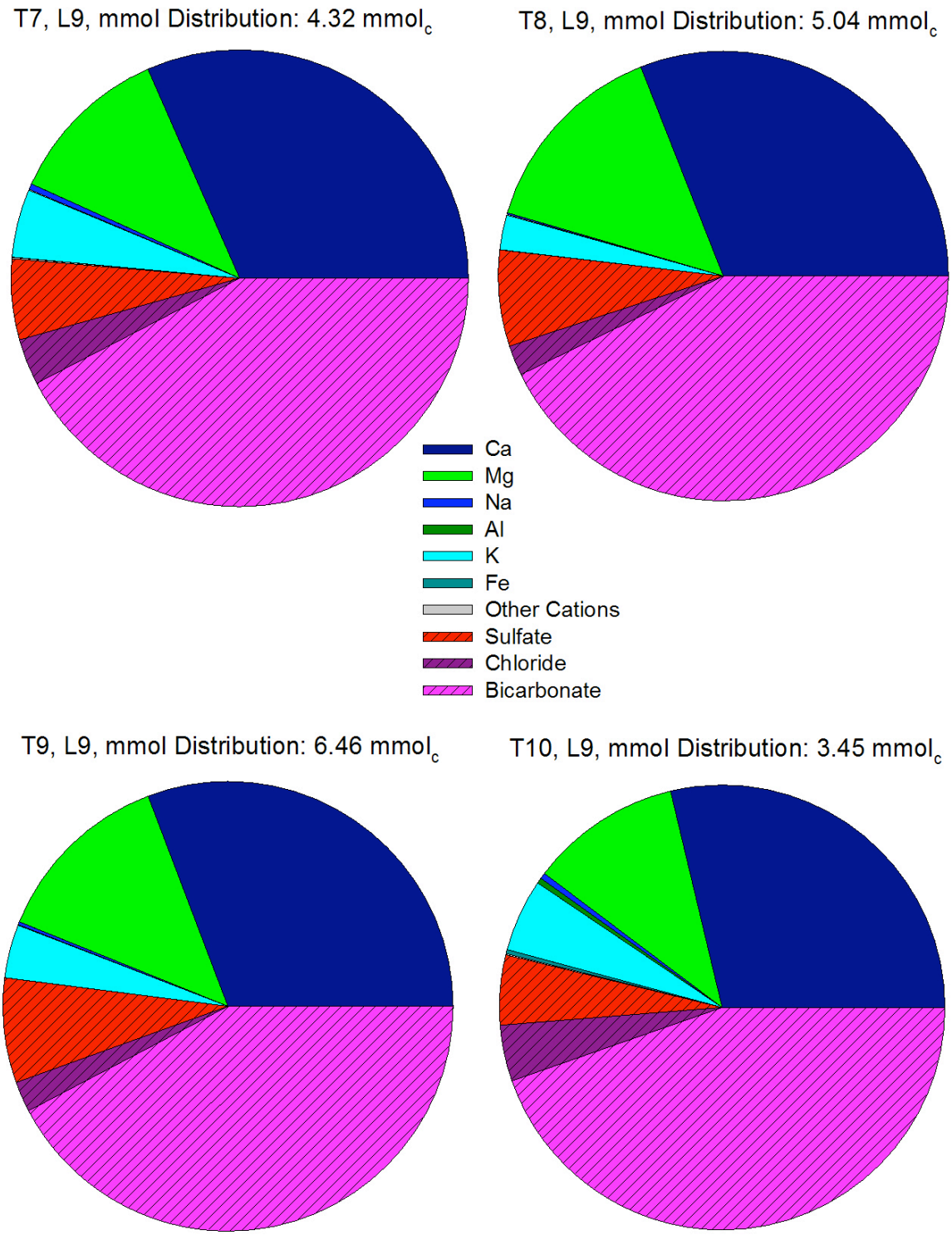

Figure 53. Charge distribution of dominant cations and anions at leach nine from columns leached 2x week^{-1} (T7), 1x week^{-1} (T8), 2x month^{-1} (T9), and 1x day^{-1} (T10). L = Leach #.

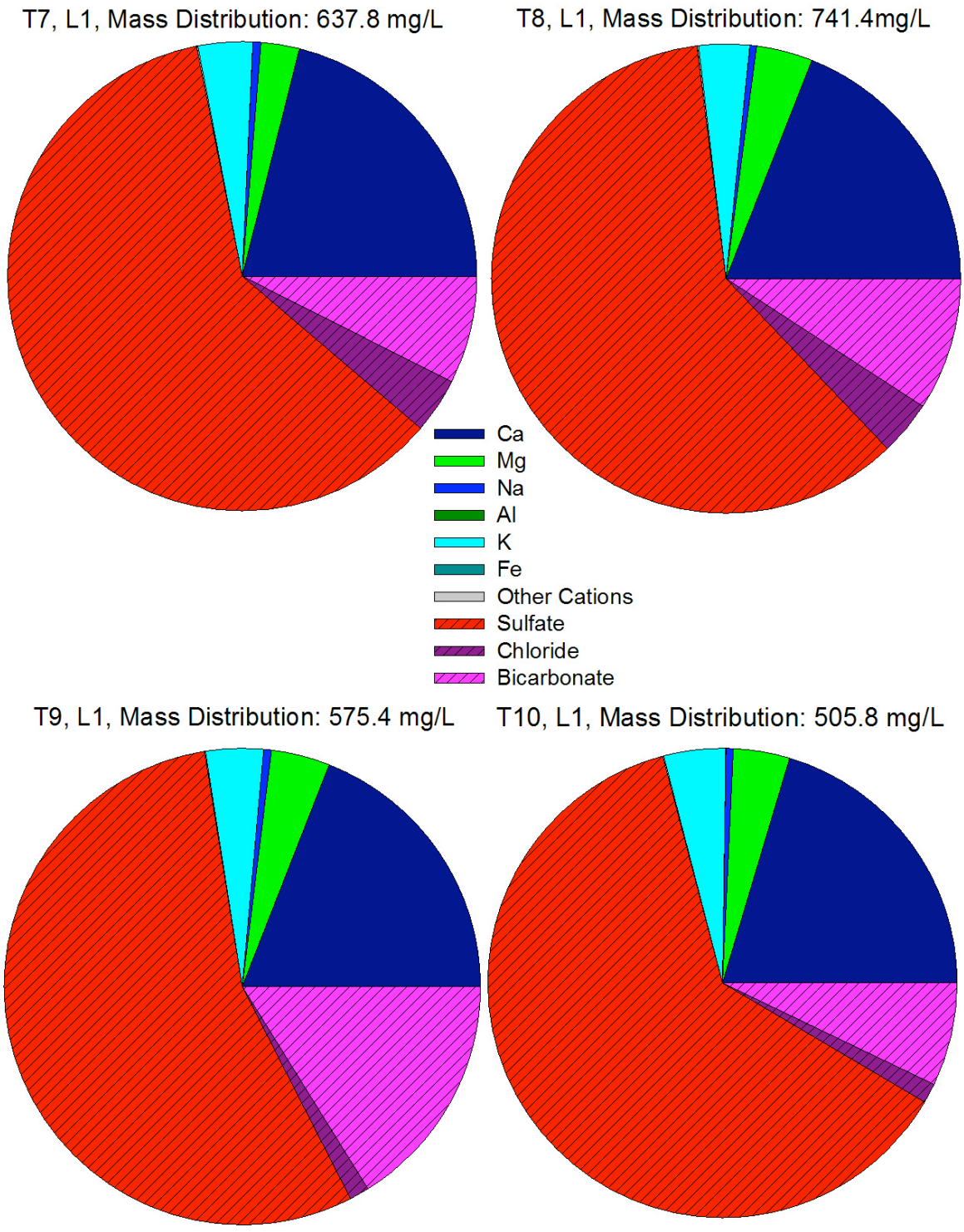

Figure 54. Mass distribution of dominant cations and anions at leach one from columns leached 2x week^{-1} (T7), 1x week^{-1} (T8), 2x month^{-1} (T9), and 1x day^{-1} (T10). L = Leach #.

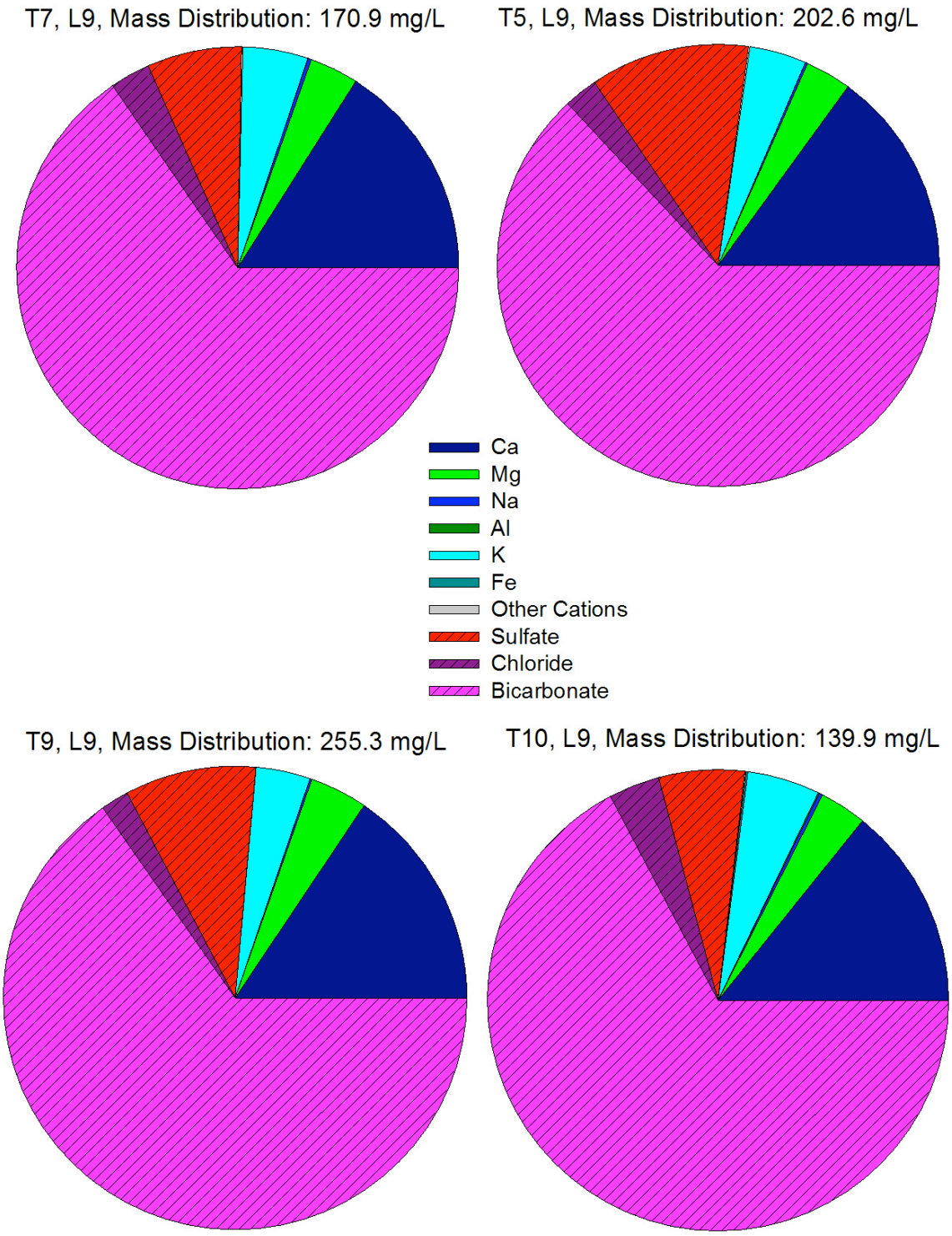

Figure 55. Mass distribution of dominant cations and anions at leach nine from columns leached 2x week^{-1} (T7), 1x week^{-1} (T8), 2x month^{-1} (T9), and 1x day^{-1} (T10). L = Leach #.

CHAPTER 6. PEAK ELUTION TOTAL MASS LOSSES

Effect of Saturation and Vacuum

With the exception of Se, all of the observed treatment effects and possible explanations closely followed those with the concentration data and will not be discussed again. Various saturation levels significantly impacted the total mass of sulfate, bicarbonate, As, Cd, Cu, K, Mn, Na, Pb, Se, and Zn released during the peak elution phase (first five leaching cycles). Total original mass of each parameter of interest is presented in Tables 11 and 12. Total mass losses for each element/compound and associated statistical analyses of treatment effects are presented in Tables 13 and 14. Mass loss expressed as a percent of the original mass is shown in Tables 15 and 16.

Table 11. Total original mass (mg) of sulfate, Ca, K, Mg, and Na per leaching column (1.5 kg spoil).

Sample ID	Sulfate	Al	Ca	Fe	K	Mg	Mn	Na
Harlan VA-16	900 (35)	39,178 (3196)	4861 (641)	29,828 (958)	10,673 (732)	5655 (32)	757 (23)	1554 (109)

Note: acid digestion used HCl so Cl in the spoil could not be effectively quantified. Sulfur values were numerically converted to sulfate. Values expressed as mean and (standard deviation).

Table 12. Total mass (μg) of As, Cd, Cu, Ni, Pb, Se, and Zn per leaching column (1.5 kg spoil).

Sample ID	As	Cd	Cu	Ni	Pb	Se	Zn
Harlan VA-16	4717 (150)	60 (14)	20,851 (652)	23,789 (569)	13,188 (349)	1489 (0)	60,233 (6842)

Note: Se in the spoil was below detection and calculated using the detection limit of 0.8 μg L^{-1}. Values expressed as mean and (standard deviation).

Table 13. Total mass (mg) of sulfate, bicarbonate, Ca, Cl, K, Mg, and Na leached from the standpipe (T1), saturated (T2), vacuum (T3), and standard columns (T4) during the first five leaching cycles.

Treatment	SO_4	HCO_3	Ca	Cl	K	Mg	Na
1	156 (2) a	54 (2) b	56 (1) a	4 (1) a	12 (0.2) a	11 (0.1) a	2 (0.1) ab
2	128 (8) b	74 (3) a	52 (2) a	9 (1) a	11 (0.5) b	11 (0.4) a	1 (0.1) c
3	160 (17) a	36 (3) c	57 (5) a	9 (4) a	12 (0.7) a	11 (1) a	2 (0.1) a
4	154 (4) a	48 (3) b	54 (3) a	9 (3) a	12 (0.2) a	11 (0.4) a	1 (0) b

Values within columns followed by different letters are significantly different at P = 0.05. Values expressed as mean and (standard deviation).

Table 14. Total mass (μg) of Al, As, Cd, Cu, Fe, Mn, Ni, Pb, Se, and Zn leached from the standpipe (T1), saturated (T2), vacuum (T3), and standard columns (T4) during the first five leaching cycles.

Treatment	Al	As	Cd	Cu	Fe	Mn	Ni	Pb	Se	Zn
1	28 (13) a	2.7 (0.1) b	0.1 (0) b*	2 (0.4) a	4 (1) a	212 (16) b	6 (2) a	0.3 (0) b	14 (1) ab	41 (16) b
2	82 (35) a	2.0 (0.2) c	0.1 (0) b*	1 (0.3) b	73 (40) a	307 (30) a	4 (1) a	0.4 (0.1) b	10 (1) c	22 (7) b
3	148 (80) a	3.1 (0.2) a	5 (4) a*	3 (0.4) a	240 (213) a	195 (38) b	9 (3) a	1 (0.3) a	15 (1) a	148 (88) a
4	167 (113) a	2.3 (0.3) c	0.1 (0) b*	1 (0.2) b	22 (12) a	206 (33) b	4 (2) a	0.5 (0.2) b	113 (1) b	18 (19) b

Values within columns followed by different letters are significantly different at P = 0.05. * Indicates slight treatment effect (p = 0.0562). Values expressed as mean and (standard deviation).

Table 15. Percent release of sulfate, Ca, K, Mg, and Na from the standpipe (T1), saturated (T2), vacuum (T3), and standard columns (T4) during the first five leaching cycles.

Treatment	Sulfate	Ca	K	Mg	Na
1	17.3	1.2	0.11	0.20	0.10
2	14.2	1.1	0.10	0.19	0.08
3	17.7	1.2	0.11	0.20	0.10
4	17.1	1.1	0.11	0.20	0.09

Table 16. Percent release of Al, As, Cd, Cu, Fe, Mn, Ni, Pb, Se, and Zn from the standpipe (T1), saturated (T2), vacuum (T3), and standard columns (T4) during the first five leaching cycles.

Treatment	Al	As	Cd	Cu	Fe	Mn	Ni	Pb	Se	Zn
1	7.0E-05	0.06	1E-05	0.01	1E-05	0.03	0.02	3E-03	9.4	0.07
2	2.1E-04	0.04	1E-05	0.01	2E-04	0.04	0.01	3E-03	6.8	0.04
3	3.8E-04	0.07	8E-04	0.01	8E-04	0.03	0.04	8E-03	9.9	0.25
4	4.3E-04	0.05	1E-05	5E-03	7E-05	0.03	0.02	4E-03	8.4	0.03

As shown in Table 15, approximately 14% (saturated columns) and 17% (standard method and vacuum) of the total sulfate-S in the spoil leached from the columns during the first five leaching cycles. This further supports my assumption that the bulk of S release was likely due to rapid oxidation of trace pyrite and other sulfides and the total amount of sulfate released was so low compared to the carbonates that it did not affect bulk pH of the leachate.

As shown in Table 16, the relative mobility of As, Cu, and Cd was relatively low, with < 0.07% As, < 0.0001% Cd, and < 0.01% Cu of original spoil mass leached during peak elution. This suggests that the majority of As, Cd, and Cu were bound in a sulfide form resistant to the leaching conditions in the columns. As shown in Table 16, < 0.01% of Zn leached from the saturated or standard method columns, while 0.25% was released from the columns leached under vacuum. Similar to the other trace metals, excluding Se, Zn apparently was present in a non-readily weatherable phase. Less than 0.01% of the Pb in the overburden was released during the first five leaching cycles, suggesting that the majority of the Pb was in a non-readily weatherable phase like many of the other trace metals. The amounts seen in the leachate were likely due to rapid pyrite oxidation releasing trace amounts of Pb.

The total mass of Se that leached from the mine spoil strongly responded to the level of relative oxygenation in the columns ($p = 0.0039$). Columns leached under vacuum eluted the greatest amount of Se (14.7 μg), followed by the standard method (12.5 μg), and lastly the saturated columns with 10.2 μg. Interestingly, Se was considerably more mobile than the other sulfide bound trace metals. As shown in Table 16, Se release ranged from 7% (saturated) to 10% (unsaturated). However, the true total release of Se is likely greater than 7 – 10% because the total Se in the spoil may be less than the reported value (limited by detection), yielding a greater percent release. The detection limit of 0.8 μg L^{-1} was used to calculate a theoretical maximum

amount of Se that could have been present since the true amount is unknown. In general, Se is associated with sulfides. The increased oxygen in vacuum and unsaturated standard method possibly allowed for greater trace pyrite and other sulfide oxidation compared to the saturated conditions and overall Se release, while saturated conditions could have suppressed this mechanism. A higher fraction of Se may have been pyrite (or other reactive sulfide) bound compared to As and the other trace metals.

As shown in Table 15, approximately 0.10% of the K and Na in the spoil leached from the mine spoil during the first five leaching cycles. Feldspars (tectosilicates) have higher silica to oxygen ratios than other aluminosilicates, which makes them more resistant to weathering and less likely to leach under the experimental conditions used. As shown in Table 16, 0.03% (unsaturated) and 0.04% (saturated) of the original mass Mn present in the spoil was released during peak elution.

The total mass of Al, Ca, Cl, Mg, Al, Fe, and Ni leached from the mine spoil during the first five leaching cycles was not affected by the various saturation levels. Details can be found in Table 16. However, it should be noted that approximately 1% of the Ca present in the spoil at the beginning of the study leached from the columns. This is considerably more than any of the other cations (Fe, K, Mg, Na), suggesting that the majority of Ca was in a carbonate phase mineral, which was readily dissolved throughout the experiment.

Leaching Solution pH

The observed treatment effects and possible explanations closely match those observed with the concentration data and will not be discussed in detail again. Total mass release for each parameter of interest and associated treatment effects are presented in Tables 17 and 18 and mass losses expressed as a percentage of the original mass are found in Tables 19 and 20.

The total amount of Al and Fe released during the first five leaching cycles was < 0.001% of the total Al and Fe in the mine spoil, as shown in Table 20. This further supports the fact that the majority of Al and Fe was retained in the columns as previously discussed. As shown in Table 20, the majority of Pb remained in the columns, as <0.005% of Pb leached from the spoil during the first five leaching cycles, suggesting that the Pb is not easily released.

The total mass of sulfate, As, Ca, Cd, Cl, Cu, K, Mg, Mn, Na, Ni, Se, and Zn released from the mine spoil during peak elution was not affected by the different leaching solution pH values, Tables 17 and 18. With the exception of sulfate (17 – 20%), Ca (1%), and Se (9%), the release of the trace metals and other cations was less than 0.25% of the original total mass in the samples, Tables 19 and 20. The mechanisms behind the percent release are described in detail in the effects of saturation section.

Table 17. Total mass (mg) of sulfate, bicarbonate, Ca, Cl, K, Mg, and Na released from the columns leached with simulated acid rain (T4), DI water (T5), and $CaCO_3$ (T6) during the first five leaching cycles.

Treatment	Sulfate	Bicarbonate	Ca	Cl	K	Mg	Na
4	154 (4) a	48 (3) a	54 (3) a	9 (3) a	12 (0.2) a	11 (0.4) a	1 (0) a
5	177 (41) a	52 (12) a	62 (12) a	9 (3) a	12 (1) a	13 (3) a	1 (0) a
6	149 (9) a	33 (4) b	55 (3) a	14 (2) a	11 (0.6) a	11 (0.3) a	1 (0.1) a

Values within columns followed by different letters are significantly different at P = 0.05. Values expressed as mean and (standard deviation).

Table 18. Total mass (µg) of Al, As, Cd, Cu, Fe, Mn, Ni, Pb, Se, and Zn released from columns leached with the simulated acid rain (T4), DI water (T5), and $CaCO_3$ (T6) leaching during the first five leaching cycles.

Treatment	Al	As	Cd	Cu	Fe	Mn	Ni	Pb	Se	Zn
4	167 (113) b	2 (0.3) a	0.1 (0) a	1 (0.2) a	22 (12) b	206 (33) a	4 (2) a	0.5 (0.2) ab	13 (1) a	18 (19) a
5	77 (43) b	2 (0.3) a	0.1 (0) a	1 (0.1) a	15 (9) b	304 (101) a	4 (2) a	0.3 (0.1) b	14 (1) a	6 (4) a
6	387 (98) a	2 (0.1) a	0.1 (0) a	1 (0.2) a	48 (11) a	232 (25) a	4 (0) a	0.6 (0.1) a	14 (1) a	29 (25) a

Values within columns followed by different letters are significantly different at P = 0.05. Values expressed as mean and (standard deviation).

Table 19. Percent release of sulfate, Ca, K, Mg, and Na from the columns leached with simulated acid rain (T4), DI water (T5), and $CaCO_3$ (T6) during the first five leaching cycles.

Treatment	Sulfate	Ca	K	Mg	Na
4	17.1	1.1	0.1	0.2	0.1
5	19.7	1.3	0.1	0.2	0.1
6	16.6	1.1	0.1	0.2	0.1

Table 20. Percent release of Al, As, Cd, Cu, Fe, Mn, Ni, Pb, Se, and Zn released from columns leached with simulated acid rain (T4), DI water (T5), and $CaCO_3$ (T6) during the first five leaching cycles.

Treatment	Al	As	Cd	Cu	Fe	Mn	Ni	Pb	Se	Zn
4	4E-04	0.05	1E-05	0.01	7E-05	0.03	0.02	0.004	8.4	0.03
5	2E-04	0.05	1E-05	0.004	5E-05	0.04	0.02	0.003	9.4	0.01
6	10E-04	0.04	2E-05	0.01	2E-04	0.03	0.02	0.005	9.1	0.05

Dosing Cycle

Dosing cycle had a strong effect on the total mass of bicarbonate, Cd, Cl, Fe, and Pb leached during peak elution. Total mass losses of each element and associated treatment effects are shown in Tables 21 and 22 and the percent release of each parameter of interest is presented in Tables 23 and 24. The total amount of bicarbonate leached from the columns dosed twice per week (42 mg) was significantly greater than the columns dosed daily (36 mg), but considerably less than columns leached twice per month (56 mg; $p = 0.0153$). Columns leached once per week were not significantly different from the standard method (2x $week^{-1}$).

Table 21. Total mass (mg) of sulfate, bicarbonate, Ca, Cl, K, Mg, and Na released from the columns leached 2x $week^{-1}$ (T7), 1x $week^{-1}$ (T8), 2x $month^{-1}$ (T9), and 1x day^{-1} (T10) during the first five leaching cycles.

Treatment	Sulfate	HCO_3	Ca	Cl	K	Mg	Na
7	151 (5) a	42 (5) b	57 (1) a	13 (1) a	12 (0.2) a	10 (2) a	2 (0.1) a
8	211 (86) a	46 (6) ab	72 (20) a	13 (6) a	12 (1.3) a	15 (4) a	2 (0.1) a
9	159 (3) a	56 (7) a	58 (1) a	5 (0) b	11 (0.2) a	12 (0.3) a	1 (0.1) a
10	157 (1) a	36 (5) b	54 (1) a	5 (0) b	11 (0.5) a	10 (0.3) a	1 (0.1) a

Values within columns followed by different letters are significantly different at $P = 0.05$. Values expressed as mean and (standard deviation).

Table 22. Total mass (µg) of Al, As, Cd, Cu, Fe, Mn, Ni, Pb, Se, and Zn released from columns leached 2x week^{-1} (T7), 1x week^{-1} (T8), 2x month^{-1} (T9), and 1x day^{-1} (T10) during the first five leaching cycles.

Treatment	Al	As	Cd	Cu	Fe	Mn	Ni	Pb	Se	Zn
7	234 (157) a	2 (0.3) a	0.1 (0) a	1 (0.3) a	59 (18) a*	258 (18) a	4 (1) a	0.6 (0.1) a	14 (1) a	17 (8) a
8	309 (251) a	2 (0.2) a	0.1 (0) a	1 (0.2) a	39 (24) ab*	570 (536) a	6 (3) a	0.6 (0.3) a	14 (0) a	12 (3) a
9	21 (3) a	2 (0.2) a	0.1 (0) a	1 (0.1) a	6 (2) b*	222 (5) a	4 (2) a	0.3 (0) b	13 (1) a	10 (8) a
10	49 (13) a	2 (0.3) a	0.1 (0) a	1 (0.2) a	36 (24) ab*	167 (13) a	7 (2) a	0.3 (0) b	14 (1) a	8 (5) a

Values within columns followed by different letters are significantly different at P = 0.05. * Indicates slight treatment effect (Fe p =0.0557). Values expressed as mean and (standard deviation).

Table 23. Percent release of sulfate, Ca, K, Mg, and Na from the columns leached 2x week^{-1} (T7), 1x week^{-1} (T8), 2x month^{-1} (T9), and 1x day^{-1} (T10) during the first five leaching cycles.

Treatment	Sulfate	Ca	K	Mg	Na
7	16.8	1.2	0.1	0.2	.09
8	23.5	1.5	0.1	0.3	.1
9	17.6	1.2	0.1	0.2	.09
10	17.5	1.1	0.1	0.2	.09

Table 24. Percent release of Al, As, Cd, Cu, Fe, Mn, Ni, Pb, Se, and Zn released from columns leached 2x week^{-1} (T7), 1x week^{-1} (T8), 2x month^{-1} (T9), and 1x day^{-1} (T10) during the first five leaching cycles.

Treatment	Al	As	Cd	Cu	Fe	Mn	Ni	Pb	Se	Zn
7	6E-04	0.05	2E-05	6E-03	2E-04	0.03	2E-02	5E-03	9.2	0.03
8	8E-04	0.04	2E-05	5E-03	1E-04	0.08	2E-02	4E-03	9.3	0.02
9	5E-05	0.04	1E-05	5E-03	2E-05	0.03	2E-02	2E-03	8.9	0.02
10	1E-04	0.05	1E-05	5E-03	1E-04	0.02	3E-02	2E-03	9.3	0.01

The total amount of Cd released during the first five dosing cycles was < 0.0002% of the total Cd present in the spoil sample (Table 24). As previously stated, the Cd was present in a fraction of the spoil resistant to leaching under the experimental conditions. Similar to Cd, < 0.0002% percent of the total original mass Fe and < 0.004% of Pb leached from the columns as shown in Table 24. Percent release of Cl could not be determined as HCl was used in the acid digestion process.

The total mass of sulfate, Al, As, Ca, Cu, K, Mg, Mn, Na, Ni, Se, and Zn released from the mine spoil was not affected by the various dosing cycles. The percent release of sulfate, Ca and Se (18-23%, 1%, and 9%), Tables 23 and 24, indicates that the elements were relatively mobile as previously described.

CHAPTER 7. SUMMARY AND CONCLUSIONS

SUMMARY

The mine spoil used for the project was an unweathered gray sandstone from the Harlan formation located at the Powell River Project site in Southwestern Virginia. The samples were typical of overburden from that region as they were non-sulfidic (< 0.02% total S), showed a relatively uniform TDS elution curve (relative to other spoils recently studied by our group), and a moderately alkaline pH (Orndorff et al., 2010; Schatzel and Stewart, 2012). Particle size analysis showed that the soil-sized fraction derived from the spoil was approximately 84% sand, 10% silt and 6 % clay. Based on the results from column leaching trials, leachate pH and EC across all treatments including the standard method, both peak and long term, were markedly different than the saturated paste extracts. The moderate CCE of the spoil (3.53%) is reflected in both the slightly alkaline saturated paste extract and moderately alkaline leachates. Total elemental analysis showed that the original spoil had levels of Al, Ca, Fe, K, Mg, and Na characteristic of feldspars, carbonates and micas that are common in the central Appalachian region (Schatzel and Stewart, 2012). Trace metal content was low (< 30 mg kg^{-1}) and Se levels in the overburden were below detection.

The highest levels of TDS (estimated via EC) occurred during the first three leaching cycles and was possibly due to the acid-base reactions associated with trace sulfide oxidation, carbonate dissolution, and hydrolysis of freshly abraded mineral grains (primarily feldspars). This possible explanation for the leaching behavior was based on the high levels of sulfate, Ca, K, and other reaction products observed in the leachate. Based on the increasing levels of bicarbonate seen in the leachate over time the long-term EC levels were likely controlled by carbonate mineral dissolution. The moderately acidic initial leachate pH values were potentially

caused acid-base neutralization reactions associated with sulfide oxidation coupled with carbonate dissolution. Carbonate mineral dissolution may have accounted for the moderately alkaline leachate pH values seen over extended periods of time as bicarbonate concentrations increased throughout the study. Rapid oxidation of trace pyrite and other metal sulfides during the first three leaching cycles accounted for the majority sulfate release as the sulfate release patterns across all treatments were similar to patterns in previous research by Orndorff et al. (2010).

The release patterns of As, Cd, Cu, Ni, Pb, Se, and Zn closely matched that of sulfate as the leaching of these elements was driven by rapid and trace oxidation of pyrite and metal sulfides in the spoil. It should be noted that Se exceeded the current surface water quality standard during the beginning leaching cycles. Most of the Al and Fe leaching occurred during the first leaching cycle due to rapid hydrolysis and possibly via dispersed colloids passing through the filter media. The majority of Al and Fe released by initial weathering reactions likely precipitated in the columns as insoluble oxy-hydroxides as the pH of the leachate was moderately alkaline. The release of Ca, Cl, K, Mg, Mn, and Na followed the release pattern of sulfate during peak elution. This reinforced the assumption that acid base neutralization reactions associated with pyrite oxidation and carbonate dissolution were driving the bulk of the leaching behavior observed. Slight increases in Ca and Mg concentrations over time corresponded to increasing bicarbonate levels, suggesting that carbonate dissolution drove the release of Ca and Mg. Rapid hydrolysis and chemical dissolution of feldspars drove the release of K and Na from the spoil, while Cl leaching was simply the weathering of trace Cl in the spoil.

Effect of Saturation and Vacuum

The perching of leachate at the sand spoil interface in the bottom of the treatment zone, as suggested by Orndorff et al. (2010), was only visually confirmed on one occasion, while faint staining of the tubing and precipitates were observed in all standpipes. This suggested that perching, or other reducing conditions in the columns, might have occurred infrequently throughout the experiment. However, the perching events were neither numerous nor frequent enough to significantly alter the leachate chemistry as demonstrated by the lack of statistical significance. In addition, the increased aeration from the standpipe did not appear to affect the leachate, as the standard method and standpipe treatments were not statistically different for any parameters of interest except Cu. However, Cu concentrations for both the standpipe and standard method were well below the water quality standards and from a regulatory perspective presented little importance

Overall, leachate pH and the release of EC, sulfate, bicarbonate, As, Cu, Cd, Fe, K, Mg, Mn, Pb, and Zn were strongly affected by the level of saturation (oxygen supply) in the columns. Leachate pH was significantly higher under unsaturated conditions (standard method and vacuum) than under saturated conditions. This appeared to be due to the effects of assumed higher CO_2 partial pressure in the unsaturated columns potentially increasing dissolution of carbonate minerals. The overall treatment effect analysis (via repeated measures) showed that EC release from the standard leaching method was higher than that of the vacuum columns, with the effect being especially pronounced over time. Even though the repeated measures analysis did not show any overall significant difference between the leachate EC values from saturated and unsaturated columns, the specific leach contrasts showed lower short-term and lower long-term EC release under saturated conditions compared to the standard method. As expected, the

unsaturated conditions for the standard method may have allowed for greater pyrite oxidation due to increased aeration while saturated conditions likely suppressed this process resulting in lower sulfate release. Interestingly, greater aeration from the vacuum did not reflect this trend, and sulfate concentrations were not significantly different than the saturated treatment or standard method. However, the increased airflow from the vacuum may have accelerated pyrite oxidation, but the formation of secondary sulfate precipitates in the columns would have masked this effect. This is reflected in the high concentration of sulfide-bound trace metals found in the vacuum leachate compared to leachates from the other treatment methods without increased airflow.

Overall, bicarbonate concentrations increased for the duration of the experiment. The levels of saturation affected short-term bicarbonate release as the treatment effects of saturation were most pronounced over the first ten dosing cycles. Initially, bicarbonate release was related to saturation level of the columns with the saturated, standard, and vacuum columns yielding successively lower levels of bicarbonate. Acid-base neutralization reactions likely consumed the bicarbonate in unsaturated columns yielding higher leachate pH, but lower concentrations compared to saturated columns. Over time, however, complete saturation, vacuum, and standard leaching practices did not seem to influence the release of bicarbonate.

The release of As, Cd, Cu, Pb, and Zn were significantly higher under vacuum compared to both the standard method and saturated columns. The increased concentration of trace metals seen under vacuum is likely due to greater amounts of rapid and trace oxidation of pyrite and other metal sulfides due to the increased airflow. All of the trace metals followed a release pattern similar to sulfate (rapid initial release) further reinforcing that pyrite oxidation controlled the release of these elements.

The release of Fe was strongly affected by the level of saturation in the columns. The vacuum columns eluted considerably more iron than both the standard and saturated columns. This was possibly driven by increased pyrite oxidation in addition to fine colloids being pulled through the filter media considering that increased aeration should have oxidized the iron to insoluble hydroxide precipitates as seen with the standard method. However, the potential for siderite dissolution was noted as an additional source of Fe leaching. Potassium release was most likely due to the weathering of feldspars and perhaps micas present in the spoil, and concentrations were significantly higher in columns leached with the standard method than under saturated conditions. The increased airflow from the vacuum did not seem to affect the release of K since it is not redox sensitive.

Manganese concentrations were much greater under saturated conditions than under both standard and vacuum conditions, with vacuum columns yielding the lowest levels of Mn. Previous research by Evangelou (1995) found that amorphous Mn can form a redox couple with Fe, leading to enhanced Mn solubility. This suggests that the oxygen level in the columns affected Mn leaching, which controlled the formation of the redox couple by altering the amount of reduced Fe. This suggests that as the level of oxygen in the columns increased, Mn concentrations in the leachate decreased. Magnesium concentrations were greater in the columns treated with the standard leaching method than those run under vacuum. Levels of Mg released from saturated and vacuum columns did not differ significantly. As a whole, the standard method leached higher concentrations of Mg than the saturated columns. However, the spike in Mg levels in the saturated columns during the beginning leaching cycles masked this overall effect from a statistical perspective. Interestingly, the increased aeration from the vacuum did not elevate the release of Mg. The level of saturation in the columns did not significantly affect the

release of Al, Ca, Cl, Na, Ni, and Se. However, specific leach contrasts showed that differences in oxygen supply might have affected the release of some of these parameters during peak elution and over time.

Effect of Leaching Solution pH

The leaching of Al, Fe, K, and Pb from the mine spoil was affected by leaching solution pH. However, for bicarbonate, Al, and Pb, the observed treatment effects were most pronounced between the DI water (pH 6) and the $CaCO_3$ leaching solutions while the standard method (acid rain) was not significantly different. The $CaCO_3$ leaching solution eluted significantly more Fe and Pb than both the DI and the simulated acid rain. In contrast, the DI treatment yielded higher levels of K than both the $CaCO_3$ and acid rain treatments. Leachate pH and EC were moderately affected by the pH of the leaching solutions. Once again, leachate from the DI treatment was higher in EC and pH than leachate from the $CaCO_3$ columns, while the standard method (e.g. simulated acid rain) was not significantly different. However, EC from all treatments fell below 500 $\mu S\ cm^{-1}$ after four leaching cycles where they remained for all subsequent leaching events.

Higher leachate pH and EC, bicarbonate, Al, and K observed with the DI leaching solution compared to the $CaCO_3$ were likely due to the effects of decreased internal column pH resulting in increased carbonate mineral dissolution. Previous research by Bruno et al. (1992) suggested that bicarbonate can accelerate the dissolution of hematite, which may account for the greater Fe levels seen with the $CaCO_3$ solution. Considerable variability in the initial leaching event may have contributed to $CaCO_3$ leaching solution yielded significantly higher levels of Pb, but the concentrations were well below regulatory standards. The release of sulfate, As, Ca, Cd,

Cl, Cu, Mg, Mn, Na, Ni, Se, and Zn were not affected by the pH of the leaching solution. These elements were all characterized by an initial peak and subsequent rapid decrease and then remained at low concentrations for the duration of the study. Leaching solution pH did not appear to significantly alter pyrite oxidation or the leaching of associated metal sulfides.

Effect of Leaching Cycle

Leaching cycle significantly impacted leachate pH, as well as EC and the release of bicarbonate and Cl from the mine spoil. During peak elution and over time, longer dosing cycles relative to the standard method correspond to higher leachate pH values while columns with more rapid dosing cycles eluted significantly lower pH values. Although the longer dosing cycles (2x per month, 1x per week) were significantly ($p < 0.0001$) higher in pH than the standard method, the values were moderately alkaline (pH 8.1-8.3) after the initial leaching, which suggests little ecological importance. Longer times between dosing cycles allowed for greater contact time between the leaching solution and the spoil, which accounted for the increased carbonate mineral dissolution and higher pH values.

The repeated measures analysis on short-term EC release did not reveal any significant differences between the standard method and other treatments. However, the results of specific leach contrasts indicated that over time the length of the dosing cycle did affect EC values. Longer and shorter dosing cycles, relative to the standard method, yielded higher and lower leachate EC, respectively. Similar to pH and EC, longer dosing cycles corresponded to higher bicarbonate concentrations compared to the standard method while shorter times between leaching events (relative to the standard method) yielded lower amounts. This was true during peak elution and for long-term bicarbonate leaching. As mentioned above, longer times between

leaching events allowed for longer contact time between the simulated acid rain and the spoil, which accelerated the dissolution of carbonates, releasing bicarbonate.

Although the overall treatment effects on chloride release suggests that the standard method yields higher Cl levels compared to columns leached 2x $month^{-1}$ and 1x day^{-1}, the Cl levels were low and an insignificant TDS contributor Chloride release was a function of water movement through the column and weathering (presumably via simple dissolution) of trace amounts present in the soil, however, the treatment effects did not reflect this.

During the first ten leaching cycles, Mg release was slightly higher for columns leached 1x $week^{-1}$ when compared to the standard method. However, no difference was seen in Mg release between the standard method and columns leached 1x day^{-1} or 2x $month^{-1}$. In contrast, Mg release over time was strongly influenced by dosing cycle as longer dosing cycles corresponded to higher Mg levels. While Ca and K were not affected by dosing cycle during peak elution, long-term Ca, Mg, and K showed longer dosing cycles corresponded to higher concentrations. The standard method yielded higher Ca and K levels than columns leached daily, suggesting that longer dosing cycles correspond to greater amounts of Ca and K release. The release of sulfate, Al, As, Cd, Cu, Fe, Mn, Na, Ni, Pb, Se, and Zn was not significantly affected by leaching cycle.

The longer dosing cycles allowed for greater hydration of mineral surfaces and enhanced dissolution between leaching events. In addition, longer times between leachings likely allowed for greater CO_2 partial pressures and contact time between the leaching solution held at field capacity and the spoil, which accelerated the weathering of carbonate minerals over time. This likely resulted in the higher concentrations of Ca, and Mg over time.

Charge and Mass Distribution

Varying saturation levels did affect charge and mass distributions of the leachate. Under saturated conditions, bicarbonate and sulfate were both major contributors to TDS during peak elution, but over time, bicarbonate became the dominant contributor. Sulfate dominated TDS during peak elution, but bicarbonate became the major long-term contributor of TDS under unsaturated conditions. Leaching solution pH and dosing cycle did not appear to affect either the charge or mass distributions of the leachate as the cations and anions were balanced. Sulfate was the dominant anion contributing to the charge and the overall greatest contributor to TDS during peak elution. However, over time, bicarbonate emerged as the dominant anion contributing to total charge and the major contributor to TDS. The relative distribution of cations did not change over time; Ca was the greatest cation contributor to both charge and TDS.

Peak Elution Mass Losses

Total mass losses during the peak elution cycle (first five leaching events) was summed and discussed here. Total mass loss for the duration of the experiment cannot be reported since not all elements were analyzed for all leaching cycles after leach five. With the exception of Se, all of the observed treatment effects, results, and possible mechanisms of release closely followed those with the concentration data and will not be discussed in detail here.

Sulfate

The total mass of sulfate leached from the columns during the first five leaching cycles was strongly affected by the level of saturation in the columns. Leaching solution pH and leaching cycle did not affect the mass of sulfate released during peak elution. The percent release

across all treatments (T1-T10) ranged from 14-23%. This supports the assumption that bulk sulfate release was potentially due to the rapid oxidation of trace pyrites and sulfides present in the spoil and saturation likely suppressed the weathering of the sulfides and pyrite.

Bicarbonate

Leaching solution pH, level of saturation in the columns, and leaching cycle strongly affected the total mass of bicarbonate released during peak elution. Columns leached under saturated conditions released significantly more bicarbonate than those leached using the standard method and vacuum. Columns leached with simulated acid rain and DI water eluted considerably more bicarbonate than columns leached with the $CaCO_3$ solution. In addition, longer times between dosing cycles corresponded to a greater total mass of bicarbonate in the leachate.

Arsenic (As) and Selenium (Se)

The total masses of As and Se released during peak elution were strongly affected by the level of saturation in the column. The masses of As and Se released were not affected by dosing cycle or leaching solution pH. The percent release of As was extremely low (< 0.1%). This was characteristic of the leaching behavior of many other sulfide bound trace metals. Conversely, the percent release of Se was at least an order of magnitude higher than all other trace metals (7-10%). The Se may have been bound as a more reactive sulfide form ,considering it was more mobile than all other trace metals. However, this is a conservative estimate as the detection limit was used to calculate a theoretical maximum; the true percent release has the potential to be significantly higher, which is alarming from an environmental standpoint as Se is extremely

toxic to aquatic life (Lindberg et al., 2011). Previous work by Ziemkiewicz et al. (2011) showed Se release up to 30% and suggested that the dominant form was selenite.

Calcium (Ca), Iron (Fe), Magnesium (Mg), and Manganese (Mn)

The level of saturation in the columns, leaching solution pH, and leaching cycle, did not affect the total mass of Ca released during peak elution. The percent release of Ca (1%) compared to other base cations was fairly high, suggesting that the Ca was present in an easily dissolved carbonate phase mineral. Leaching solution pH and dosing cycle affected the total mass of Fe released during the first five leaching cycles. Various levels of saturation did not affect the mass of Fe released. The percent release of Fe is extremely low and likely because the majority of Fe was retained in the columns.

Various levels of saturation, leaching solution pH, and leaching cycles did not affect the total mass of Mg leached during peak elution. The percent release (< 0.25%) was greater than many other base cations, again reinforcing that Mg, like Ca, was lost from a carbonate phase mineral. The total mass of Mn was strongly affected by the level of saturation present in the columns; however, leaching solution pH and leaching cycle did not alter the total mass loss. Manganese exhibited low percent release, similar to many of the other sulfide oxidation products.

Cadmium (Cd), Copper (Cu), Nickel (Ni), Lead (Pb), and Zinc (Zn)

The saturation level in the columns and leaching cycle slightly affected the total mass of Cd released during peak elution. Leaching solution pH did not affect the mass of Cd leached. The total mass of Cu released from the mine spoil was significantly affected by the saturation

level in the column; however, leaching solution pH and dosing cycle did not have any noticeable effects. Saturation, leaching solution pH, and leaching cycle did not affect the mass of Ni released during peak elution. However, the total mass of Pb leached was strongly affected by the level of saturation, leaching solution pH, and leaching cycle. The effects due to dosing cycle were largely inconsistent and likely reflect variability in the initial leaching event. The level of saturation in the columns significantly affected the total mass of Zn released from the mine spoil, while leaching solution pH and leaching cycle had no discernable effects.

Cadmium, Cu, Ni, Pb, and Zn all exhibited extremely low mass losses (< 0.07%) as these trace metals are generally found as metal sulfides in pyrite and other S phases as previously described. However, under vacuum the percent release of Zn was an order of magnitude higher than the other trace metals and as previously described, increased siderite weathering may have been the source.

Aluminum (Al), Chloride (Cl), Potassium (K), and Sodium (Na)

The total mass of Al released was strongly affected by leaching solution pH, while level of saturation and dosing cycle had no significant effects. Aluminum exhibited a low percent release as much of the Al was retained in the columns similar to Fe. Chloride mass losses were affected by leaching cycle; however, the treatment effects were inconsistent and due to the complexity of the internal column chemistry it is unclear what led to the observed effects. Both the total masses of K and Na leached from the columns were strongly affected by the level of saturation in the columns. The percent release of K and Na was less than many other base cations as feldspars (tectosilicates) are more resistant to weathering than the carbonate phases controlling the release of Ca and Mg.

CONCLUSIONS

Overall, perching at the bottom of the treatment zone was confirmed, however, it was very infrequent (observed only once) and brief (< 15 min) and likely did not affect the leachate chemistry. Therefore the standard leaching method can be considered to be "unsaturated" without a need to account for a saturated zone and confounding redox effects at the lower column spoil/sand interface. However, the level of water saturation in the columns strongly influenced the EC level, release of major TDS contributors (sulfate, bicarbonate, K, and Mg), and leaching of trace metals. Leaching solution pH did not significantly alter leachate chemistry (major contributors to TDS) as the simulated acid rain leachate results did not differ from the higher pH DI and $CaCO_3$ leaching solutions. However, several differences between the higher pH leaching solutions were noted.

Dosing cycle significantly altered the leachate chemistry of the mine spoil. Longer times between dosing cycles corresponded to higher levels of TDS (estimated via EC), bicarbonate, Ca, Mg, and K, with the effects most pronounced over time. In general, total mass losses during peak elution closely matched the treatment effects of the concentration data as expected. However, unsaturated conditions led to greater mass losses of Se compared to saturated conditions. Based on total mass losses, sulfate, Se, and Ca exhibit the greatest mobility and the increased mobility of Se is particularly alarming due to its high aquatic toxicity.

Overall, the method of oxygen supply and level of saturation in the columns greatly affected the leaching of TDS (proxy via EC), leachate pH, and major TDS contributors (sulfate, bicarbonate, Ca, K, and Mg) during peak elution as well as extended periods of time. The standard column leaching method is sufficient in obtaining a general idea of the release patterns for many parameters of interest, but care should be taken when values are close to regulatory

limits, as column leaching procedures can affect both short and long-term release of TDS, its major constituents, and elements of concern (Se). The results from the column leach trials suggest that weather patterns (time between precipitation events) and saturation level could potentially have an impact on the leaching of TDS from valley fills.

REFERENCES

Abdalla, Charles. 2009. SHAPING PROPOSED CHANGES TO PENNSYLVANIA'S TOTAL DISSOLVED SOLIDS STANDARD. Ed. Joy Drohan. Penn State Extension, Web. 14 Nov. 2011. http://extension.psu.edu/water/resources/publications/consumption-and-usage/TDS-highres-updateDec09.pdf/view (accessed 5 December 2012).

Agouridis, C., P. Angel, T. Taylor, C. Barton, R. Warner, X. Yu, and C. Wood. 2012. Water quality characteristics of discharge from reforested loose-dumped mine spoil in eastern Kentucky. J. Environ. Qual. 41:454-468.

Anthony, J.W., R.A. Bideaux, K.W. Bladh, and M.C. Nichols, Eds., Handbook of Mineralogy 2005, Mineralogical Society of America, Chantilly, VA 20151-1110, USA. http://www.handbookofmineralogy.org/.

AOAC International. 2002. Official Methods of Analysis of AOAC, International 17th Ed. AOAC International, Gaithersburg, MD, USA, Official Method 955.01.

Beck, M., W.L. Daniels, and M.J. Eick. 2007. Leachate chemistry of mixtures of fly ash and alkaline coal refuse. In: Proc. World of Coal Ash, Covington, KY. 7-10 May 2007. Center for Applied Energy Research, Lexington, KY, and American Coal Ash Association, Aurora, CO. Available on-line at: http://www.flyash.info/2007/157beck.pdf (accessed 4 December 2012)

Berg, A., and S.A. Banwart. 2000. Carbon dioxide mediated dissolution of Ca-feldspar: implications for silicate weathering. Chem. Geol. 163(1-4):25-42.

Berner, R.A, and J.W. Morse. 1974. Dissolution kinetics of calcium carbonate in seawater; IV, Theory of calcite dissolution. American Journal of Science 274(2): 108-134.

Bernhardt, E.S., B.D. Lutz, R.S. King, J.P. Fay, C.E. Carter, A.M. Helton, D. Campagna, and J. Amos. 2012. How many mountains can we mine? Assessing the regional degradation of central Appalachian rivers by surface coal mining. Environ. Sci. and Technology. 46(15): 8112-8115.

Bodkin, R., J. Kern, P. McClellan, A.J. Butt, and C. Martin. 2007. Limiting total dissolved solids to protect aquatic life. Jour. of Soil and Water Cons. 62(3): 57-61.

Bogner, J.E., and A.A. Sobek. Distribution of selected transition and heavy metals in clastic overburden units of the Appalachian and Interior Coal Basins: water quality implications. Illinois: Argonne National Lab. (US); 1979 Jan. 1 p. Report No.: CONF-7905124-1.

Bradham, W.S., and F.T. Caruccio. 1990. A comparative study of tailings analysis using acid/base accounting, cells, columns, and soxhlets. P. 19-25. In J. Skousen et al. (ed.) Proc., 1990 Mining and Reclamation Conf. and Exhibition, Charleston, WV. 23-26 Apr. 1990. Am. Soc. For Surface Mining and Reclamation, Lexington, KY. http://www.asmr.us/Publications (accessed 5 December 2012).

Bruno, J., W. Stumm, P. Wersin, F. Brandberg. 1992. On the influence of carbonate in mineral dissolution: I. The thermodynamics and kinetics of hematite dissolution in bicarbonate solutions at T = 25°C. Geochimica et Cosmochimica Acta 56(3): 1139-1147.

Bryant, G., S. McPhilliamy, and H. Childers. 2002. . A Survey of the Condition of Streams in the Primary Region of Mountaintop Mining/Valley Fill Programmatic Environmental Impact Statement. Region 3, U.S. Environmental Protection Agency, Philadelphia, Pennsylvania. Available on-line at: http://www.cet.edu/pdf/mtmvfchemistry.pdf (accessed 5 December 2012).

Burt, R. (ed.) 2004. Soil Survey Laboratory Methods Manual. Soil Survey Investigations Report No. 42, Version 4.0. U.S. Department of Agriculture, Natural Resources Conservation Service, National Soil Survey Center, Lincoln, NE.

Caruccio F., W. Bradham, and G. Geidel. 1993. Overburden analyses; some important factors. WV Surface Mine Drainage Task Force Symposium, April 1993, Morgantown, WV. p 27-28 In; 14th Annu. Symp. West Virginia Surf. Mine Drain. Task Force, Morgantown, WV.

Chapman, P.M., H.B. Bailey, and E. Canaria. 2000. Toxicity of total dissolved solids associated with two mine effluents to chironomid larvae and early life stages of rainbow trout. Environ. Tox. and Chem. 19(1): 210-214.

Cormier, S.M., G.W. Suter II, and L. Zheng. 2013. Derivation of a benchmark for freshwater ionic strength. Environ. Toxicol. Chem. 32(2):263-271.

Daniels, W.L., L.W. Zelazny, and B.R. Stewart. 1999. Characterization of acid leaching reactions in coal refuse/coal fly ash bulk blends. p. 460-466. In: Proc. 1999 Int. Ash Util. Symp., Lexington, KY. 18-20 Oct. 1999. University. of Kentucky Center for Applied Energy Research, Lexington. KY. Available on-line at: http://www.flyash.info/1999/environ/daniel2.pdf (accessed 5 December 2012).

Daniels, W.L., M. Beck, and M.J. Eick. 2006. Development of Rapid Assessment Protocols for Beneficial Use of Post-2000 Coal Combustion Products in Virginia Coal Mines. 57 p. Final Report to USDI OSM for 2005-2006 Applied Science Program. USDI OSM, Parkway Center, Pittsburgh. http://www.mcrcc.osmre.gov/MCR/Resources/ccb/PDF/VT%20Final%20Applied%20Science%20Report%209-8-06%20Daniels%20CCB.pdf (accessed 7 May 2013)

Daniels, W. L., M. Beck, M.J. Eick and Z.W. Orndorff. 2009. Predicting Contaminant Leaching Potentials for Central Appalachian Overburden and Coal Refuse Materials. Final Report to OSM Applied Science Research Program, December 2009. http://www.techtransfer.osmre.gov/nttmainsite/appliedscience/2007/Projects/VTLeachingPotentialNPointon07FR.pdf

Doepker, R. and D., and W.K. O'Connor. 1991. Column leach study II: Heavy metal dissolution characteristics from selected lead-zinc mine tailings. Mine Water and the Environment 10: 73-92.

Doye, I., and J. Duchesne. 2005. Column leaching test to evaluate the use of alkaline industrial wastes to neutralize acid mine tailings. Jour. of Environ. Eng. 131(8): 1221–1229.

Evangelou, V. P. 1995. Pyrite Oxidation and its Control. CRC Press, Boca Raton, FL.

Forsberg, L.S., J.P. Gustafsson, D.B. Kleja, and S. Ledin. 2008. Leaching of metals from oxidizing sulphide mine tailings with and without sewage sludge application. Water Air Soil Pollut. 2008. 194: 331-341.

Goodfellow, W.L., L.W. Ausley, D.T. Burton, D.L. Denton, P.B. Dorn, D.R. Grothe, M.A. Heber, T.J. Norberg-King and J.H. and J.R. Rodgers. 2000. Major ion toxicity in effluents: a review with permitting recommendations. Environ. Toxicol. Chem. 19: 175-182.

Green, J., M. Passmore, and H. Childers. 2000. A Survey of the Condition of Streams in the Primary Region of Mountaintop Mining/Valley Fill Programmatic Environmental Impact Statement. U.S. Environmental Protection Agency, Region III, Wheeling, WV. http://www.cet.edu/pdf/mtmvfbenthics.pdf (accessed 6 June 2013)

Halvorson, H.G. and C.E. Gentry. 1990. Long-term leaching of mine spoil with simulated precipitation. p 27-32 In Skousen, J., J. Sencindiver, and D. Samuel ed. Proceedings of the 1990 mining and reclamation conference and exhibition, Charleston, WV. 23-26 Apr. 1990. ASMR, Lexington, KY. http://www.asmr.us/Publications/Conference%20Proceedings/1990%20Meetings%20Vol%201/Halverson%2027-32.pdf

Hartman, K.J., M.D. Kaller, J. W. Howell, and J. A. Sweka. 2005. How much do valley fills influence headwater streams? Hydrobiologia 532: 91-102.

Hood, W.C., and A.O. Oertel. 1984. A leaching column method for predicting effluent quality from surface mines. P. 271-277. In D. Graves (ed.) 1984 National Symp. on Surface Mining, Hydrology, Sedimentology, and Reclamation, Lexington Ky. 2-7 Dec. 1984. Univ. of Kentucky College of Eng., Lexington, KY.

Howard, J.L., D.F. Amos, and W.L. Daniels. 1988. Phosphorus and potassium relationships in southwestern Virginia mine spoils. J. Environ. Qual.17 (4) 695-671.

Huffman, G.P., F.E. Huggins, N. Shah, and J. Zhao. 1994. Speciation of arsenic and chromium in coal and combustion ash by XAFS spectroscopy. Fuel Process. Technol. 39(1-3):47-62.

Jackson, M.L., B.R. Stewart, and W.L. Daniels. 1993. Influence of fly ash, topsoil, lime and rock P on acid mine drainage from coal refuse. p. 266-275. In: Proc. 10th Annual Meeting, Am. Soc. for Surf. Min. Rec., Spokane, WA. 14-18 Jun. 1993. ASMR, Princeton, WV. http://wvmdtaskforce.com/proceedings/93/94JAC/94JAC.HTM (accessed 12 June 2012)

Karberg, N.J., K.S. Pregitzer, J.S. King, A.L. Friend, and J.R. Wood. 2005. Soil carbon dioxide partial pressure and dissolved inorganic carbonate chemistry under elevated carbon dioxide and ozone. Oecologia. 142(2):296-306.

Kleinmann, R.L. P., D.A. Crerar, and R.R. Pacelli. 1981. Biogeochemistry of acid mine drainage and a method to control acidity formation. Mining Engineering 33: 300-305.

Li, W.C., and M.H. Wong 2010. Effects of bacteria on metal bioavailability, speciation, and mobility in different metal mine soils: a column study. Jour. of Soils and Sediments 10: 313-325

Lindberg T.T., E.S. Bernhardt, R. Bier, A.M. Helton, R.B. Merola, A. Vengosh, and R. T. Di Giulio. 2011. Cumulative impacts of mountaintop mining on an Appalachian watershed. Proceedings of the National Academy of Science 108: 20929–20934.

McBride, M. B. (1994). ENVIRONMENTAL CHEMISTRY OF SOILS. USA. Oxford University Press.

Móricz, F., F. Mádai, and I.F. Walder. 2012. Pyrite oxidation under circumneutral pH conditions. Geosci. Engineering. 1(2):111-116.

Mount, D.R., J.M. Gulley, J.R. Hockett, T. D. Garrison, and J. M. Evans. 1997. Statistical models to predict the toxicity of major ions to *Ceriodaphnia dubia, Daphnia magna,* and fathead minnows (*Pimephales promelas*). Environ. Toxic. and Chem. 16:2009–2019.

National Mining Association v. Jackson. 42 ELR 20165. (2011). Retrieved from The Environmental Law Reporter.

Orndorff, Z.W. 2001. Evaluation of Sulfidic Materials in Virginia Highway Corridors. PhD Dissertation, Virginia Poly. Inst. and State Univ. Blacksburg, VA, p 175.

Orndorff, Z.W., W.L. Daniels, M. Beck, and M.J. Eick. 2010. Leaching potentials of coal spoil and refuse: Acid-base interactions and electrical conductivity. p. 736-766. In: R.I. Barnhisel (ed.) Proc. Am. Soc. Min. Reclam., Pittsburgh, PA. 5-11 Jun. 2010. ASMR, Lexington, KY. http://www.asmr.us/Publications/Conference%20Proceedings/2010/0053-Orndoff-VA-abs.pdf

Palmer, M.A., E.S. Bernhardt, W.H. Schesinger, K.N. Eshleman, E. Foufoula-Georgiou, M.S. Hendryx, A.D. Lemly, G.E. Likens, O.L. Loucks, M.E. Power, P.S. White, and P.R. Wilcock. 2010. Mountaintop mining consequences. Science 327: 148-149.

Pond, G.J., M.E. Passmore, F.A. Borsuk, L. Reynolds, and C.J. Rose. 2008. Downstream effects of mountaintop coal mining: comparing biological conditions using family- and genus-level macroinvertebrate bioassessment tools. J. N. Am. Benthol. Soc. 2008 27(3):717–737.

Pond, G.J. 2010. Patterns of Ephemeroptera taxa loss in Appalachian headwater streams (Kentucky, USA). Hydrobiologia, 641:185–201. DOI 10.1007/s10750-009-0081-6.

Rhoades, J.D. 1996. Salinity: Electrical conductivity and total dissolved solids. p. 417-435. *In* D.L. Sparks (ed.) Methods of Soil Analysis. Part 3. Chemical Methods. Soil Science Society of America Book Series 5. SSSA and ASA, Madison, WI.

Roberts, J.A., W.L. Daniels, J.C. Bell, and J.A. Burger. 1988. Early stages of mine soil genesis in a Southwest Virginia spoil lithosequence. Soil Sci. Soc. Am. J. 52:716-723.

Schatzel, S.J., and B.W. Stewart. 2012. A provenance study of mineral matter in coal from Appalachian Basin coal mining regions and implications regarding the respirable health of underground coal workers: a geochemical and Nd isotope investigation. Int. J. Coal Geol. 94:123-136.

Shikazono, N. 1977. Composition of siderite and the environments of formation of vein-type deposits in Japan. Econ. Geol. 72:632-641.

Silva, P.S., and C. Giles. 2010. Improving EPA Review of Appalachian Surface Coal Mining Operations under the Clean Water Act, National Environmental Policy Act, and the Environmental Executive Order. United States Environemntal Protection Agency. http://www.epa.gov/owow/wetlands/guidance/pdf/appalachian_mtntop_mining_detailed.pdf. (accessed 5 May 2013)

Singer, P.C. and W. Stumm. 1970. Acid mine drainage: the rate-determining step. Science. 167, 1121–1123.

Stewart, B.R., W.L. Daniels, and M.L. Jackson. 1997. Evaluation of leachate quality for codisposed coal fly ash and coal refuse. Jour. Environ. Qual. 26:1417-1424.

Stewart, B R., W.L. Daniels, L.W. Zelazny, and M. L. Jackson. 2001. Evaluation of leachates from coal refuse blended with fly ash at different rates. Jour. Environ. Qual. 30:1382-1391.

Swaine, D. J. (1990) TRACE ELEMENTS IN COAL. London. Butterworths. pp. 278

U.S. EPA. 2001. Inductively coupled plasma mass spectrometry, method 6010B, rev.2. *In* SW-846: Test Methods for Evaluating Solid Waste, Physical/Chemical Methods. USEPA, Office of Solid Waste, Washington, DC.

U.S. EPA. 2007. Inductively coupled plasma mass spectrometry, method 6020A, rev.1. *In* SW-846: Test Methods for Evaluating Solid Waste, Physical/Chemical Methods. USEPA, Office of Solid Waste, Washington, DC.

U.S. EPA. 2007. Microwave assisted acid digestion of sediments, sludges, soils and oils, method 3051A, rev.1. *In* SW-846: Test Methods for Evaluating Solid Waste, Physical/Chemical Methods. UESPA, Office of Solid Waste, Washington, DC.

U.S. EPA. 2009. Drinking Water Contaminants 2009. US EPA. Office of Water Programs. http://water.epa.gov/drink/contaminants/index.cfm (accessed 5 December 2012).

U.S. EPA. 2011. The Effects of Mountaintop Mines and Valley Fills on Aquatic Ecosystems of the Central Appalachian Coalfields (2011 Final). U.S. Environmental Protection Agency, Washington, DC, EPA/600/R-09/138F.

U.S. Geological Survey. Harlan Sandstone. Mineral Resources On-line Spatial Data. http://mrdata.usgs.gov/geology/state/sgmc-unit.php?unit=VAPAh%3B0 (accessed 6 June 2013

Weber-Scannel, P.K. and L.K. Duffy. 2007. Effects of total dissolved solids on aquatic organisms: A review of literature and recommendation for salmonid species. Amer. Jour. of Environ. Sci. 3: 1-6.

Ziemkiewicz, P.F., M. O'Neal, and R. J. Lovett. 2011. Selenium leaching kinetics and in situ control. Mine Water Environ. 30(2):141-150.

Zysset, M., and D. Beggren. 2001. Retention and release of dissolved organic matter in Podzol B horizons. Eur. Jour. of Soil Science 52: 409-421.

APPENDICES

Appendix A: Leaching and analysis schedules

Table A-1. Leaching and analysis schedule for treatments 1-7.

LEACH	WEEK	Date	Mass	pH	EC	METALS	S	IC	AP
0	1	**11/2/12**							
1		**11/6/12**							
2	2	**11/9/12**							
3		**11/13/12**							
4	3	**11/16/12**							
5		**11/20/12**							
6	4	**11/23/12**							
7		**11/27/12**							
8	5	**11/30/12**							
9		**12/4/12**							
10	6	**12/7/12**							
11		**12/11/12**							
12	7	**12/14/12**							
13		**12/18/12**							
14	8	**12/21/12**							
15		**12/25/12**							
16	9	**12/28/12**							
17		**1/1/13**							
18	10	**1/4/13**							
19		**1/8/13**							
20	11	**1/11/13**							
21		**1/15/13**							
22	12	**1/18/13**							
23		**1/22/13**							
24	13	**1/25/13**							
25		**1/29/13**							
26	14	**2/1/13**							
27		**2/5/13**							
28	15	**2/8/13**							
29		**2/12/13**							
30	16	**2/15/13**							
31		**2/19/13**							
32	17	**2/22/13**							
33		**2/25/13**							
34	18	**3/1/13**							
35		**3/5/13**							
36	19	**3/8/13**							
37		**3/12/13**							
38	20	**3/15/13**							
39		**3/19/13**							

Table A-2. Leaching and analysis schedule for treatment 8.

LEACH	WEEK	Date	Mass	pH	EC	METALS	S	IC	AP
0	1	**11/2/12**							
1		**11/9/12**							
2	2	**11/16/12**							
3		**11/23/12**							
4	3	**11/30/12**							
5		**12/7/12**							
6	4	**12/14/12**							
7		**12/21/12**							
8	5	**12/28/12**							
9		**1/4/13**							
10	6	**1/11/13**							
11		**1/18/13**							
12	7	**1/25/13**							
13		**2/1/13**							
14	8	**2/8/13**							
15		**2/15/13**							
16	9	**2/22/13**							
17		**3/1/13**							
18	10	**3/8/13**							
19		**3/15/13**							
20	11	**3/22/13**							

Table A-3. Leaching and analysis schedule for treatment 9.

LEACH	WEEK	Date	Mass	pH	EC	METALS	S	IC	AP
0	1	**11/2/12**							
1		**11/16/12**							
2	2	**12/4/12**							
3		**12/18/12**							
4	3	**1/1/13**							
5		**1/15/13**							
6	4	**1/29/13**							
7		**2/12/13**							
8	5	**2/26/13**							
9		**3/12/13**							

Table A-4. Leaching and analysis schedule for treatment 10.

LEACH	WEEK	Date	Mass	pH	EC	METALS	S	IC	AP
0	1	**11/2**							
1		**11/3**							
2	2	**11/5**							
3		**11/6**							
4	3	**11/7**							
5		**11/8**							
6	4	**11/9**							
7		**11/12**							
8	5	**11/13**							
9		**11/14**							
10	6	**11/15**							
11		**11/16**							
12	7	**11/17**							
13		**11/18**							
14	8	**11/19**							
15		**11/20**							
16	9	**11/21**							
17		**11/22**							
18	10	**11/23**							
19		**11/24**							
20	11	**11/25**							
21		**11/26**							
22	12	**11/27**							
23		**11/28**							
24	13	**11/29**							
25		**11/30**							
26	14	**12/1**							
27		**12/2**							
28	15	**12/3**							
29		**12/4**							
30	16	**12/5**							
31		**12/6**							
32	17	**12/7**							
33		**12/8**							
34	18	**12/9**							
35		**12/10**							
36	19	**12/11**							
37		**12/12**							
38	20	**12/13**							
39		**12/14**							

Appendix B. Correlation matrices

Table B-1. Treatment four correlation matrix over leaches zero to nine.

		pH	EC	Al	As	Ca	Cd	Cl	Cu	Fe	K	Mg	Mn	Na	Ni	Pb	Se	Zn	HCO_3	SO_4
pH	**Pearson Correlation Coefficient**	1.																		
	R Standard Error																			
	t																			
	p-value																			
	H0 (5%)																			
EC	**Pearson Correlation Coefficient**	-0.97137	1.																	
	R Standard Error	0.01129																		
	t	-9.14354																		
	p-value	0.00026																		
	H0 (5%)	rejected																		
Al	**Pearson Correlation Coefficient**	-0.93273	0.98695	1.																
	R Standard Error	0.026	0.00519																	
	t	-5.78428	13.70253																	
	p-value	0.00217	0.00004																	
	H0 (5%)	rejected	rejected																	
As	**Pearson Correlation Coefficient**	-0.90425	0.85513	0.80629	1.															
	R Standard Error	0.03647	0.05375	0.06998																

	t	-4.7352	3.68844	3.04789																
	p-value	0.00517	0.01417	0.02849																
	H0 (5%)	rejected	rejected	rejected																
Ca	**Pearson Correlation Coefficient**	-0.96046	0.99831	0.99441	0.84056	1.														
	R Standard Error	0.01555	0.00067	0.00223	0.05869															
	t	-7.71352	38.45441	21.06546	3.46966															
	p-value	0.00058	0.	0.	0.01786															
	H0 (5%)	rejected	rejected	rejected	rejected															
Cd	**Pearson Correlation Coefficient**	-0.92998	0.98645	0.99966	0.79866	0.99384	1.													
	R Standard Error	0.02703	0.00538	0.00014	0.07243	0.00246														
	t	-5.65698	13.44556	85.66099	2.96764	20.04903														
	p-value	0.0024	0.00004	0.	0.03124	0.00001														
	H0 (5%)	rejected	rejected	rejected	rejected	rejected														
Cl	**Pearson Correlation Coefficient**	-0.93367	0.98857	0.99978	0.81041	0.99546	0.99959	1.												
	R Standard Error	0.02565	0.00455	0.00009	0.06865	0.00181	0.00016													
	t	-5.82939	14.65999	105.99053	3.09307	23.37651	78.36105													
	p-value	0.0021	0.00003	0.	0.02707	0.	0.													
	H0 (5%)	rejected	rejected	rejected	rejected	rejected	rejected													
Cu	**Pearson Correlation**	-0.9201	0.95006	0.93279	0.75613	0.94905	0.93561	0.93649	1.											

	Coefficient	7																		
	R Standard Error	0.03066	0.01948	0.02598	0.08565	0.01986	0.02493	0.0246												
	t	-5.2552	6.80779	5.78732	2.5836	6.73455	5.92616	5.97108												
	p-value	0.00331	0.00104	0.00217	0.04922	0.00109	0.00195	0.00189												
	H0 (5%)	rejected	rejected	rejected	rejected	rejected	rejected	rejected												
Fe	**Pearson Correlation Coefficient**	-0.91511	0.97609	0.99611	0.77112	0.9862	0.99494	0.99478	0.91716	1.										
	R Standard Error	0.03251	0.00945	0.00155	0.08107	0.00548	0.00202	0.00208	0.03176											
	t	-5.07504	10.04087	25.28473	2.70819	13.31775	22.13433	21.80267	5.14606											
	p-value	0.00385	0.00017	0.	0.04237	0.00004	0.	0.	0.00363											
	H0 (5%)	rejected	rejected	rejected	rejected	rejected	rejected	rejected	rejected											
K	**Pearson Correlation Coefficient**	-0.99163	0.98106	0.94697	0.93193	0.97196	0.94388	0.94934	0.91784	0.92737	1.									
	R Standard Error	0.00333	0.00751	0.02065	0.0263	0.01106	0.02182	0.01975	0.03151	0.028										
	t	-17.17485	11.32417	6.58998	5.74634	9.24319	6.39031	6.7552	5.17046	5.54247										
	p-value	0.00001	0.00009	0.00121	0.00224	0.00025	0.00139	0.00108	0.00355	0.00262										
	H0 (5%)	rejected	rejected	rejected	rejected	rejected	rejected	rejected	rejected	rejected										
Mg	**Pearson Correlation Coefficient**	-0.96469	0.99921	0.99052	0.83481	0.99905	0.9905	0.99178	0.95309	0.98173	0.97302	1.								
	R Standard Error	0.01387	0.00032	0.00377	0.06062	0.00038	0.00378	0.00328	0.01833	0.00724	0.01065									
	t	-8.19022	56.12811	16.12296	3.3907	51.20513	16.10268	17.32864	7.04046	11.53813	9.43022									
	p-value	0.00044	0.	0.00002	0.01945	0.	0.00002	0.00001	0.00089	0.00009	0.00023									

	H0 (5%)	rejected	rejected	rejected	rejected	rejected	rejected	rejected	rejected	rejected	rejected									
Mn	**Pearson Correlation Coefficient**	-0.91467	0.96789	0.9637	0.70224	0.96892	0.96728	0.96444	0.95073	0.96295	0.91017	0.97565	1.							
	R Standard Error	0.03268	0.01264	0.01426	0.10137	0.01224	0.01287	0.01397	0.01922	0.01455	0.03432	0.00962								
	t	-5.05993	8.6097	8.07096	2.20559	8.75893	8.5257	8.16002	6.8573	7.98435	4.91305	9.94753								
	p-value	0.0039	0.00035	0.00047	0.07854	0.00032	0.00037	0.00045	0.00101	0.0005	0.00442	0.00018								
	H0 (5%)	rejected	rejected	rejected	accepted	rejected	rejected	rejected	rejected	rejected	rejected	rejected								
Na	**Pearson Correlation Coefficient**	-0.97556	0.99614	0.98294	0.89217	0.99457	0.98095	0.98453	0.93701	0.96948	0.98941	0.99286	0.94276	1.						
	R Standard Error	0.00966	0.00154	0.00677	0.04081	0.00217	0.00755	0.00614	0.0244	0.01202	0.00422	0.00285	0.02224							
	t	-9.92661	25.38169	11.94982	4.41643	21.37074	11.29063	12.56361	5.99851	8.84239	15.23905	18.61158	6.32164							
	p-value	0.00018	0.	0.00007	0.00691	0.	0.0001	0.00006	0.00185	0.00031	0.00002	0.00001	0.00146							
	H0 (5%)	rejected	rejected	rejected	rejected	rejected	rejected	rejected	rejected	rejected	rejected	rejected	rejected							
Ni	**Pearson Correlation Coefficient**	-0.9349	0.98686	0.99936	0.79693	0.9939	0.99951	0.99881	0.93436	0.99569	0.94525	0.99107	0.96939	0.9809	1.					
	R Standard Error	0.02519	0.00522	0.00025	0.07298	0.00243	0.0002	0.00048	0.02539	0.00172	0.0213	0.00356	0.01206	0.00757						
	t	-5.89044	13.65527	62.66056	2.95	20.14838	71.27826	45.77484	5.86334	24.00916	6.47678	16.61801	8.82879	11.27506						
	p-value	0.002	0.00004	0.	0.03189	0.00001	0.	0.	0.00205	0.	0.00131	0.00001	0.00031	0.0001						
	H0 (5%)	rejected	rejected	rejected	rejected	rejected	rejected	rejected	rejected	rejected	rejected	rejected	rejected	rejected						
Pb	**Pearson Correlation Coefficient**	-0.92998	0.98645	0.99966	0.79866	0.99384	1.	0.99959	0.93561	0.99494	0.94388	0.9905	0.96728	0.98095	0.99951	1.				
	R Standard Error	0.02703	0.00538	0.00014	0.07243	0.00246	1.73472E-19	0.00016	0.02493	0.00202	0.02182	0.00378	0.01287	0.00755	0.0002					

	t	-5.65698	13.44556	85.66099	2.96764	20.04903	2,400,959,708.74862	78.36105	5.92616	22.13433	6.39031	16.10268	8.5257	11.29063	71.27826					
	p-value	0.0024	0.00004	0.	0.03124	0.00001	0.E+0	0.	0.00195	0.	0.00139	0.00002	0.00037	0.0001	0.					
	H0 (5%)	rejected	rejected	rejected	rejected	rejected	rejected	rejected	rejected	rejected	rejected	rejected	rejected	rejected	rejected					
Se	**Pearson Correlation Coefficient**	-0.97183	0.98265	0.96167	0.92246	0.97924	0.95741	0.96423	0.92309	0.94725	0.99104	0.976	0.90914	0.99308	0.95645	0.95741	1.			
	R Standard Error	0.01111	0.00688	0.01504	0.02981	0.00822	0.01667	0.01405	0.02958	0.02054	0.00357	0.00948	0.03469	0.00276	0.01704	0.01667				
	t	-9.22048	11.84711	7.84217	5.3425	10.80187	7.41471	8.13427	5.36695	6.6091	16.59395	10.02258	4.881	18.90966	7.32711	7.41471				
	p-value	0.00025	0.00008	0.00054	0.00308	0.00012	0.0007	0.00046	0.00302	0.00119	0.00001	0.00017	0.00455	0.00001	0.00074	0.0007				
	H0 (5%)	rejected	rejected	rejected	rejected	rejected	rejected	rejected	rejected	rejected	rejected	rejected	rejected	rejected	rejected	rejected				
Zn	**Pearson Correlation Coefficient**	-0.94506	0.99005	0.99907	0.81378	0.99608	0.99848	0.99857	0.93727	0.99485	0.95459	0.99316	0.9663	0.98612	0.9993	0.99848	0.96521	1.		
	R Standard Error	0.02137	0.00396	0.00037	0.06755	0.00156	0.00061	0.00057	0.02431	0.00206	0.01775	0.00273	0.01325	0.00551	0.00028	0.00061	0.01367			
	t	-6.46464	15.73307	51.79379	3.13107	25.18202	40.54234	41.73712	6.01183	21.94009	7.16492	19.01903	8.3941	13.28251	59.67134	40.54234	8.25411			
	p-value	0.00132	0.00002	0.	0.02593	0.	0.	0.	0.00183	0.	0.00082	0.00001	0.00039	0.00004	0.	0.	0.00043			
	H0 (5%)	rejected	rejected	rejected	rejected	rejected	rejected	rejected	rejected	rejected	rejected	rejected	rejected	rejected	rejected	rejected	rejected			
HCO_3	**Pearson Correlation Coefficient**	0.6944	-0.75159	-0.78154	-0.8233	-0.76755	-0.77355	-0.78504	-0.68772	-0.76307	-0.76426	-0.74209	-0.60826	-0.79439	-0.76105	-0.77355	-0.8255	-0.76874	1.	
	R Standard Error	0.10356	0.08702	0.07784	0.06443	0.08217	0.08032	0.07674	0.10541	0.08354	0.08318	0.08986	0.126	0.07379	0.08416	0.08032	0.06371	0.08181		
	t	2.15779	-2.54783	-2.80128	-3.24341	-2.6776	-2.72943	-2.83379	-2.11826	-2.64001	-2.64993	-2.47558	-1.71355	-2.92436	-2.62337	-2.72943	-3.27052	-2.68768		
	p-value	0.08342	0.0514	0.03794	0.02286	0.04395	0.04131	0.03651	0.0877	0.04598	0.04543	0.05614	0.14728	0.03285	0.04691	0.04131	0.02219	0.04342		
	H0 (5%)	accepted	accepted	rejected	rejected	rejected	rejected	rejected	accepted	rejected	rejected	accepted	accepted	rejected	rejected	rejected	rejected	rejected		

SO_4	**Pearson Correlation Coefficient**	-0.96339	0.99723	0.99236	0.86404	0.9987	0.99094	0.99359	0.94244	0.9824	0.97819	0.99635	0.95518	0.99787	0.99052	0.99094	0.9869	0.9939	-0.7938	1.
	R Standard Error	0.01437	0.0011	0.00304	0.05069	0.00052	0.00361	0.00256	0.02236	0.00698	0.00863	0.00146	0.01753	0.00085	0.00377	0.00361	0.00521	0.00243	0.07398	
	t	-8.03529	30.00276	17.98861	3.83779	43.77257	16.49683	19.64862	6.30218	11.75951	10.52978	26.09854	7.21497	34.21203	16.12317	16.49683	13.67718	20.14368	-2.91853	
	p-value	0.00048	0.	0.00001	0.01215	0.	0.00001	0.00001	0.00148	0.00008	0.00013	0.	0.0008	0.	0.00002	0.00001	0.00004	0.00001	0.03307	
	H0 (5%)	rejected	rejected	rejected	rejected	rejected	rejected	rejected	rejected	rejected	rejected	rejected	rejected	rejected	rejected	rejected	rejected	rejected	rejected	

Table B-2. Treatment four correlation matrix over leaches thirteen to thirty-nine.

		pH	EC	Al	As	Ca	Cd	Cl	Cu	Fe	K	Mg	Mn	Na	Ni	Pb	Se	Zn	HCO_3	SO_4
pH	**Pearson Correlation Coefficient**	1.																		
	R Standard Error																			
	t																			
	p-value																			
	H0 (5%)																			
EC	**Pearson Correlation Coefficient**	0.39896	1.																	
	R Standard Error	0.42042																		
	t	0.61531																		
	p-value	0.60104																		
	H0 (5%)	accepted																		
Al	**Pearson Correlation Coefficient**	-0.8457	0.01884	1.																
	R Standard Error	0.1424	0.49982																	
	t	-2.24113	0.02664																	
	p-value	0.1543	0.98116																	
	H0 (5%)	accepted	accepted																	
As	**Pearson Correlation Coefficient**	0.40336	-0.65494	-0.76497	1.															
	R Standard Error	0.41865	0.28553	0.20741																
	t	0.6234	-1.22567	-1.67968																
	p-value	0.59664	0.34506	0.23503																

	H0 (5%)	accepted	accepted	accepted																
Ca	**Pearson Correlation Coefficient**	0.31419	0.98759	0.14743	-0.73784	1.														
	R Standard Error	0.45064	0.01234	0.48913	0.2278															
	t	0.46804	8.89158	0.2108	-1.54592															
	p-value	0.68581	0.01241	0.85257	0.26216															
	H0 (5%)	accepted	rejected	accepted	accepted															
Cd	**Pearson Correlation Coefficient**	1.	1.	1.	1.	1.	1.													
	R Standard Error	0.E+0	0.E+0	0.E+0	0.E+0	0.E+0														
	t	#N/A	#N/A	#N/A	#N/A	#N/A														
	p-value	#N/A	#N/A	#N/A	#N/A	#N/A														
	H0 (5%)																			
Cl	**Pearson Correlation Coefficient**	1.	1.	1.	1.	1.	1.	1.												
	R Standard Error	0.E+0	0.E+0	0.E+0	0.E+0	0.E+0	0.E+0													
	t	#N/A	#N/A	#N/A	#N/A	#N/A	#N/A													
	p-value	#N/A	#N/A	#N/A	#N/A	#N/A	#N/A													
	H0 (5%)																			
Cu	**Pearson Correlation Coefficient**	0.40336	-0.65494	-0.76497	1.	-0.73784	1.	1.	1.											
	R Standard Error	0.41865	0.28553	0.20741	9.59519E-18	0.2278	0.E+0	0.E+0												
	t	0.6234	-1.22567	-1.67968	322,829,510.84405	-1.54592	#N/A	#N/A												
	p-value	0.59664	0.34506	0.23503	0.E+0	0.26216	#N/A	#N/A												
	H0 (5%)	accep	accept	accep	reject	accept														

		ted	ed	ted	ed	ed														
Fe	**Pearson Correlation Coefficient**	0.58383	-0.22647	-0.92212	0.81778	-0.37119	1.	1.	0.81778	1.										
	R Standard Error	0.32957	0.47435	0.07484	0.16562	0.43111	0.E+0	0.E+0	0.16562											
	t	1.01698	-0.32883	-3.37062	2.00946	-0.56534	#N/A	#N/A	2.00946											
	p-value	0.41617	0.77353	0.07788	0.18222	0.62881	#N/A	#N/A	0.18222											
	H0 (5%)	accepted	accepted	accepted	accepted	accepted			accepted											
K	**Pearson Correlation Coefficient**	-0.20318	-0.96876	-0.15058	0.74803	-0.95495	1.	1.	0.74803	0.27264	1.									
	R Standard Error	0.47936	0.03075	0.48866	0.22023	0.04404	0.E+0	0.E+0	0.22023	0.46283										
	t	-0.29345	-5.52434	-0.21541	1.59397	-4.55061	#N/A	#N/A	1.59397	0.40075										
	p-value	0.79682	0.03124	0.84942	0.25197	0.04505	#N/A	#N/A	0.25197	0.72736										
	H0 (5%)	accepted	rejected	accepted	accepted	rejected			accepted	accepted										
Mg	**Pearson Correlation Coefficient**	0.28563	0.99252	0.13821	-0.74167	0.99337	1.	1.	-0.74167	-0.32643	-0.98254	1.								
	R Standard Error	0.45921	0.00745	0.49045	0.22496	0.00661	0.E+0	0.E+0	0.22496	0.44672	0.0173									
	t	0.4215	11.49667	0.19735	-1.56369	12.21915	#N/A	#N/A	-1.56369	-0.4884	-7.46945									
	p-value	0.71437	0.00748	0.86179	0.25833	0.00663	#N/A	#N/A	0.25833	0.67357	0.01746									
	H0 (5%)	accepted	rejected	accepted	accepted	rejected			accepted	accepted	rejected									
Mn	**Pearson Correlation Coefficient**	-0.60462	-0.95553	0.1479	0.48473	-0.94419	1.	1.	0.48473	0.14343	0.85259	-0.92249	1.							
	R Standard Error	0.31722	0.04348	0.48906	0.38252	0.05425	0.E+0	0.E+0	0.38252	0.48971	0.13655	0.0745								
	t	-1.073	-4.582	0.21148	0.78374	-4.053	#N/A	#N/A	0.78374	0.20496	2.30729	-3.379								

		49	42			64						64								
	p-value	0.39538	0.04447	0.8521	0.51527	0.05581	#N/A	#N/A	0.51527	0.85657	0.14741	0.07751								
	H0 (5%)	accepted	rejected	accepted	accepted	accepted			accepted	accepted	accepted	accepted								
Na	**Pearson Correlation Coefficient**	-0.16489	-0.94485	-0.14815	0.7369	-0.92293	1.	1.	0.7369	0.23588	0.9956	-0.96083	0.80796	1.						
	R Standard Error	0.48641	0.05363	0.48903	0.22849	0.0741	0.E+0	0.E+0	0.22849	0.47218	0.00439	0.0384	0.1736							
	t	-0.23643	-4.0801	-0.21185	1.5416	-3.39055	#N/A	#N/A	1.5416	0.34328	15.02411	-4.90315	1.93918							
	p-value	0.83511	0.05515	0.85185	0.2631	0.07707	#N/A	#N/A	0.2631	0.76412	0.0044	0.03917	0.19204							
	H0 (5%)	accepted	accepted	accepted	accepted	accepted			accepted	accepted	rejected	rejected	accepted							
Ni	**Pearson Correlation Coefficient**	-0.94904	-0.6662	0.66932	-0.09709	-0.59716	1.	1.	-0.09709	-0.37697	0.49183	-0.57219	0.8233	0.44988	1.					
	R Standard Error	0.04966	0.27809	0.27601	0.49529	0.3217	0.E+0	0.E+0	0.49529	0.42895	0.37905	0.3363	0.16109	0.3988						
	t	-4.25853	-1.26331	1.27401	-0.13796	-1.05285	#N/A	#N/A	-0.13796	-0.57558	0.79885	-0.98669	2.05129	0.71239						
	p-value	0.05096	0.3338	0.33068	0.90291	0.40284	#N/A	#N/A	0.90291	0.62303	0.50817	0.42781	0.1767	0.55012						
	H0 (5%)	accepted	accepted	accepted	accepted	accepted			accepted	accepted	accepted	accepted	accepted	accepted						
Pb	**Pearson Correlation Coefficient**	1.	1.	1.	1.	1.	1.	1.	1.	1.	1.	1.	1.	1.	1.	1.				
	R Standard Error	0.E+0	0.E+0	0.E+0	0.E+0	0.E+0	0.E+0	0.E+0	0.E+0	0.E+0	0.E+0	0.E+0	0.E+0	0.E+0	0.E+0					
	t	#N/A	#N/A	#N/A	#N/A	#N/A	#N/A	#N/A	#N/A	#N/A	#N/A	#N/A	#N/A	#N/A	#N/A					
	p-value	#N/A	#N/A	#N/A	#N/A	#N/A	#N/A	#N/A	#N/A	#N/A	#N/A	#N/A	#N/A	#N/A	#N/A					
	H0 (5%)																			
Se	**Pearson Correlation Coefficient**	0.40336	-0.65494	-0.76497	1.	-0.73784	1.	1.	1.	0.81778	0.74803	-0.74167	0.48473	0.7369	-0.09709	1.	1.			
	R Standard Error	0.41865	0.28553	0.20741	-2.52619E-17	0.2278	0.E+0	0.E+0	-2.74303E-17	0.16562	0.22023	0.22496	0.38252	0.22849	0.49529	0.E+0				

					17															
	t	0.6234	-1.22567	-1.67968	#N/A	-1.54592	#N/A	#N/A	#N/A	2.00946	1.59397	-1.56369	0.78374	1.5416	-0.13796	#N/A				
	p-value	0.59664	0.34506	0.23503	#N/A	0.26216	#N/A	#N/A	#N/A	0.18222	0.25197	0.25833	0.51527	0.2631	0.90291	#N/A				
	H0 (5%)	accepted	accepted	accepted		accepted				accepted	accepted	accepted	accepted	accepted	accepted					
Zn	**Pearson Correlation Coefficient**	-0.14026	-0.95017	-0.32292	0.84769	-0.98344	1.	1.	0.84769	0.51613	0.94741	-0.97793	0.87293	0.91827	0.4443	1.	0.84769	1.		
	R Standard Error	0.49016	0.04859	0.44786	0.14071	0.01642	0.E+0	0.E+0	0.14071	0.36681	0.05121	0.02182	0.119	0.07839	0.4013	0.E+0	0.14071			
	t	-0.20034	-4.31043	-0.48252	2.2598	-7.67481	#N/A	#N/A	2.2598	0.8522	4.18666	-6.6197	2.53055	3.27975	0.70136	#N/A	2.2598			
	p-value	0.85974	0.04983	0.67708	0.15231	0.01656	#N/A	#N/A	0.15231	0.48387	0.05259	0.02207	0.12707	0.08173	0.5557	#N/A	0.15231			
	H0 (5%)	accepted	rejected	accepted	accepted	rejected			accepted	accepted	accepted	rejected	accepted	accepted	accepted		accepted			
HCO_3	**Pearson Correlation Coefficient**	0.48572	0.98991	-0.11057	-0.5549	0.95575	1.	1.	-0.5549	-0.08663	-0.95407	0.9685	-0.95316	-0.93593	-0.73007	1.	-0.5549	-0.89742	1.	
	R Standard Error	0.38204	0.01004	0.49389	0.34604	0.04327	0.E+0	0.E+0	0.34604	0.49625	0.04488	0.03101	0.04574	0.06202	0.2335	0.E+0	0.34604	0.09732		
	t	-0.78583	-9.87913	-0.15733	-0.94329	-4.59437	#N/A	#N/A	-0.94329	-0.12297	-4.50372	-5.50023	-4.45668	-3.75825	-1.51086	#N/A	-0.94329	-2.87678		
	p-value	0.51428	0.01009	0.88943	0.4451	0.04425	#N/A	#N/A	0.4451	0.91337	0.04593	0.0315	0.04684	0.06407	0.26993	#N/A	0.4451	0.10258		
	H0 (5%)	accepted	rejected	accepted	accepted	rejected			accepted	accepted	rejected	rejected	rejected	accepted	accepted		accepted	accepted		
SO_4	**Pearson Correlation Coefficient**	-0.91828	-0.01065	0.95627	-0.73247	0.0866	1.	1.	-0.73247	-0.78107	-0.17735	0.11102	0.23986	-0.20211	0.74735	1.	-0.73247	-0.26306	-0.11726	1.
	R Standard Error	0.07838	0.49994	0.04277	0.23174	0.49625	0.E+0	0.E+0	0.23174	0.19497	0.48427	0.49384	0.47123	0.47958	0.22073	0.E+0	0.23174	0.4654	0.49313	
	t	-3.28004	-0.01506	4.62391	-1.52156	0.12294	#N/A	#N/A	-1.52156	-1.76891	-0.25485	0.15798	0.34941	-0.29185	1.59071	#N/A	-1.52156	-0.3856	-0.16698	
	p-value	0.08172	0.98935	0.04373	0.26753	0.9134	#N/A	#N/A	0.26753	0.21893	0.82265	0.88898	0.76014	0.79789	0.25265	#N/A	0.26753	0.73694	0.88274	
	H0 (5%)	accepted	accepted	rejected	accepted	accepted			accepted	accepted	accepted	accepted	accepted	accepted	accepted		accepted	accepted	accepted	

Appendix C. Effects of saturation figures

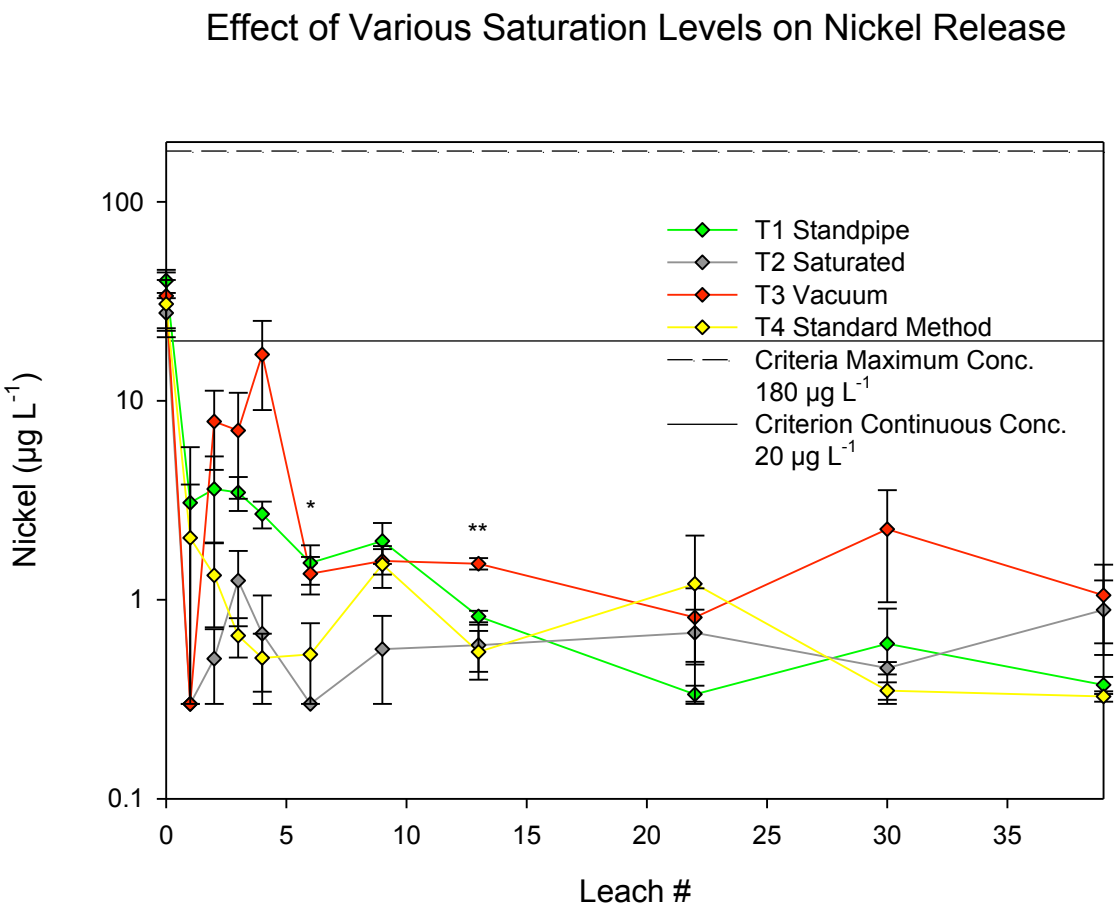

Figure C-1. Leachate Ni from standpipe, saturated, vacuum and standard method columns. The 40 leaching cycles occurred over 20 weeks. Three leaching cycles correspond to one pore volume. Error bars represent one standard error above and below the mean. Where indicated, treatment means by date were significantly different * $P < 0.05$, ** $P < 0.01$, and *** $P < 0.001$. Detection limit = 0.3 µg L^{-1} and values below the detection limit were reported as 0.3 µg L^{-1}.

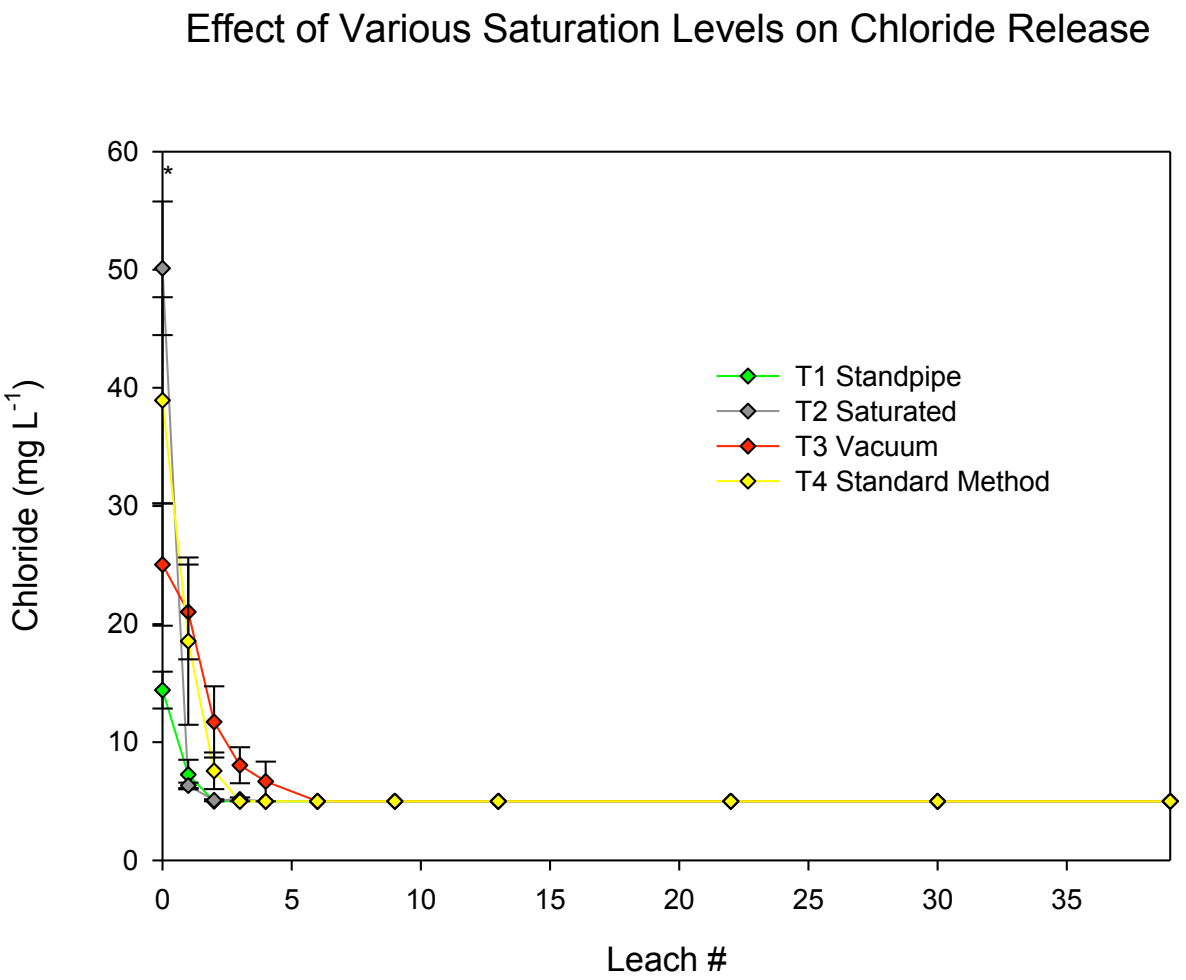

Figure C-2. Leachate Cl from standpipe, saturated, vacuum and standard method columns. The 40 leaching cycles occurred over 20 weeks. Three leaching cycles correspond to one pore volume. Error bars represent one standard error above and below the mean. Where indicated, treatment means by date were significantly different * $P < 0.05$, ** $P < 0.01$, and *** $P < 0.001$. Detection limit = 5.0 mg L^{-1} and values below the detection limit were reported as 5.0 mg L^{-1}

Appendix D. Leaching solution pH figures

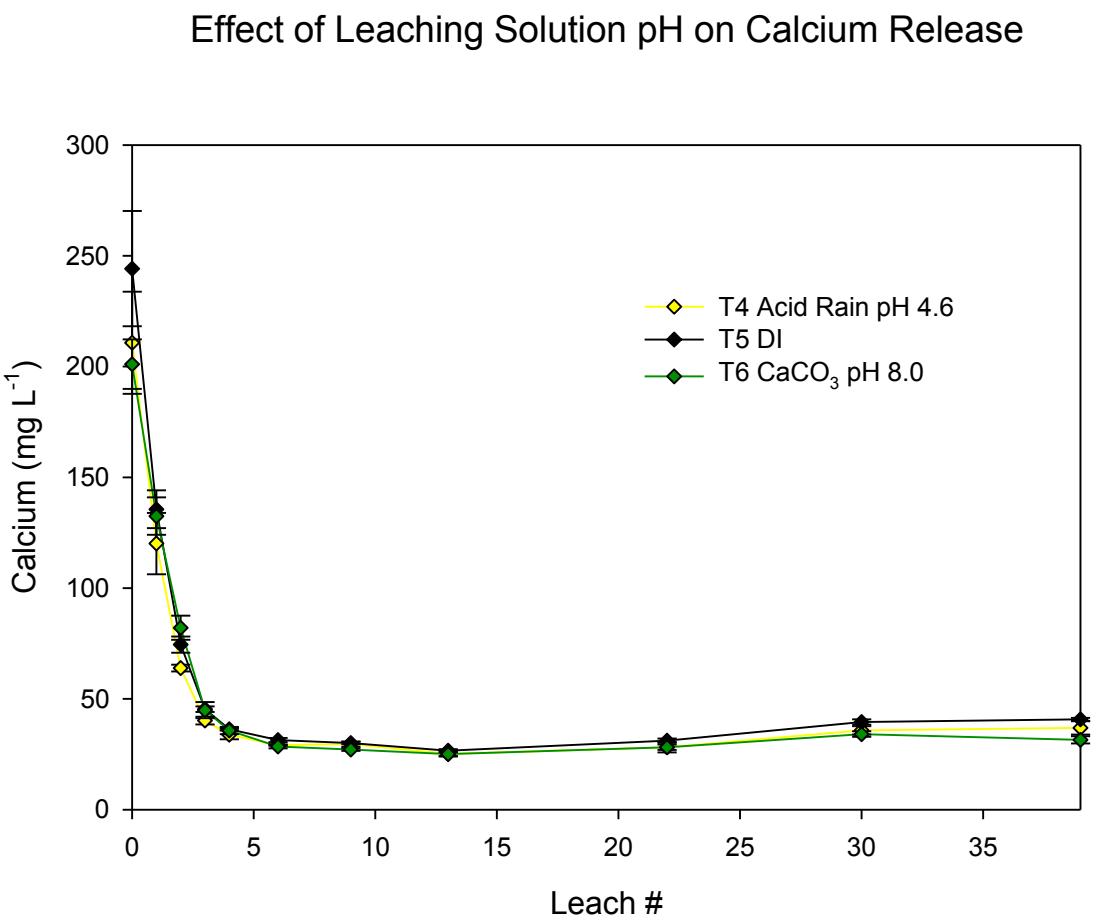

Figure D-1. Leachate Ca from columns leached with simulated acid rain, DI water and CaCO3. The 40 leaching cycles occurred over 20 weeks. Three leaching cycles correspond to one pore volume. Error bars represent one standard error above and below the mean. Detection limit = 0.01 mg L^{-1} and values below the detection limit were reported as 0.01 mg L^{-1}.

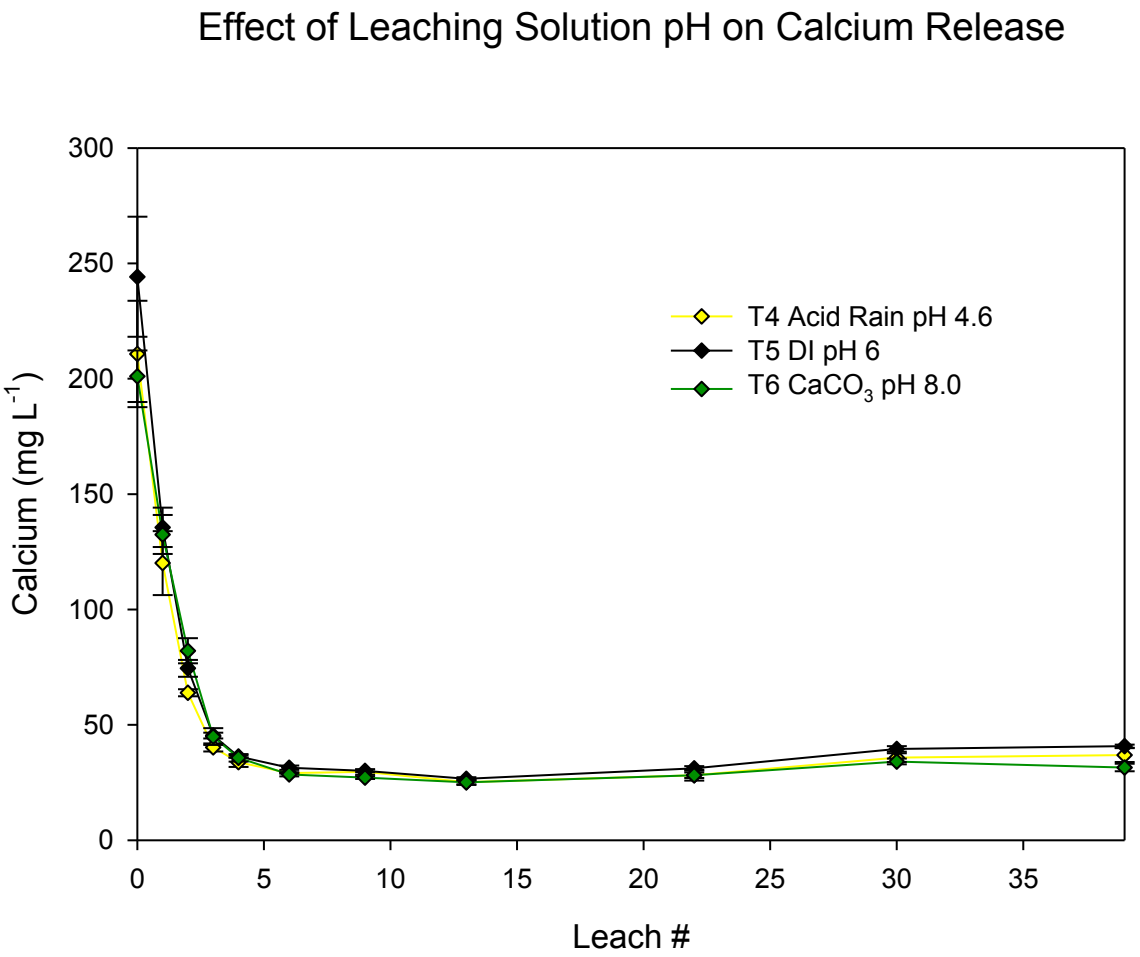

Figure D-2. Leachate Mg from columns leached with simulated acid rain, DI water and CaCO3. The 40 leaching cycles occurred over 20 weeks. Three leaching cycles correspond to one pore volume. Error bars represent one standard error above and below the mean. Detection limit = 0.005 mg L^{-1} and values below the detection limit were reported as 0.005 mg L^{-1}.

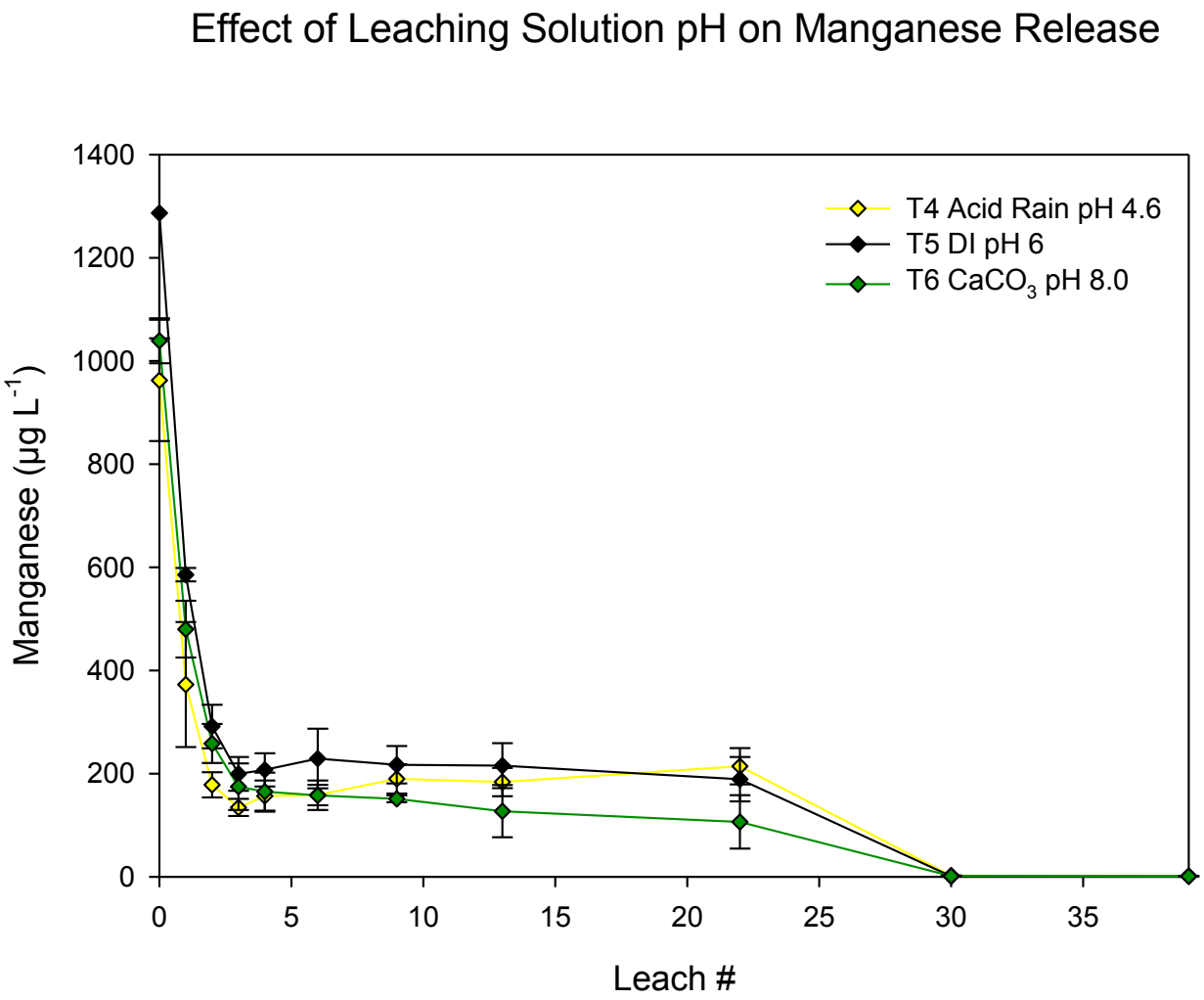

Figure D-3. Leachate Mn from columns leached with simulated acid rain, DI water and CaCO3. The 40 leaching cycles occurred over 20 weeks. Three leaching cycles correspond to one pore volume. Error bars represent one standard error above and below the mean. Detection limit = 0.5 µg L^{-1} and values below the detection limit were reported as 0.5 µg L^{-1}.

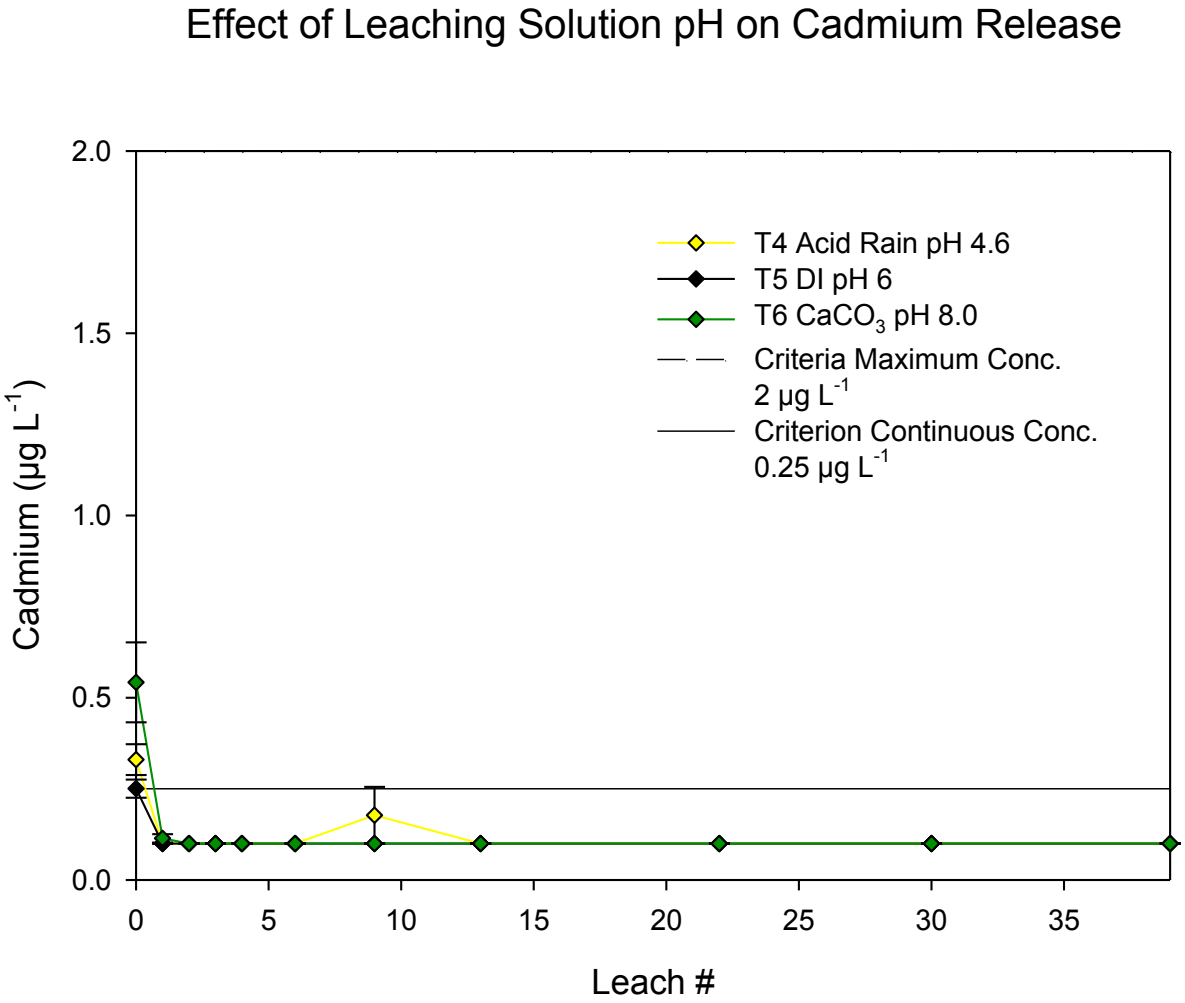

Figure D-4. Leachate Cd from columns leached with simulated acid rain, DI water and CaCO3. The 40 leaching cycles occurred over 20 weeks. Three leaching cycles correspond to one pore volume. Error bars represent one standard error above and below the mean. Detection limit = 0.1 µg L^{-1} and values below the detection limit were reported as 0.1 µg L^{-1}.

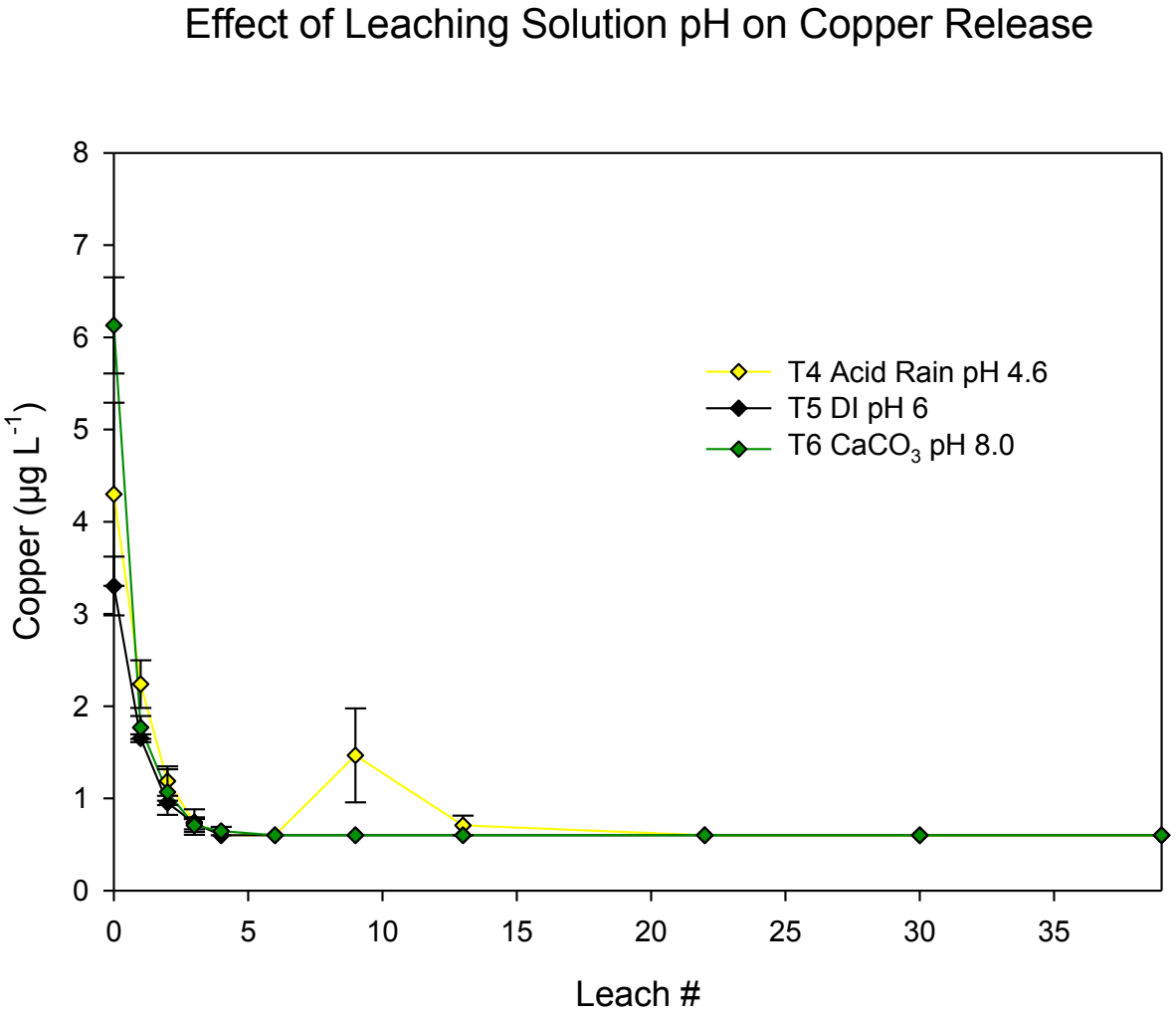

Figure D-5. Leachate Cu from columns leached with simulated acid rain, DI water and CaCO3. The 40 leaching cycles occurred over 20 weeks. Three leaching cycles correspond to one pore volume. Error bars represent one standard error above and below the mean. Detection limit = 0.6 µg L^{-1} and values below the detection limit were reported as 0.6 µg L^{-1}.

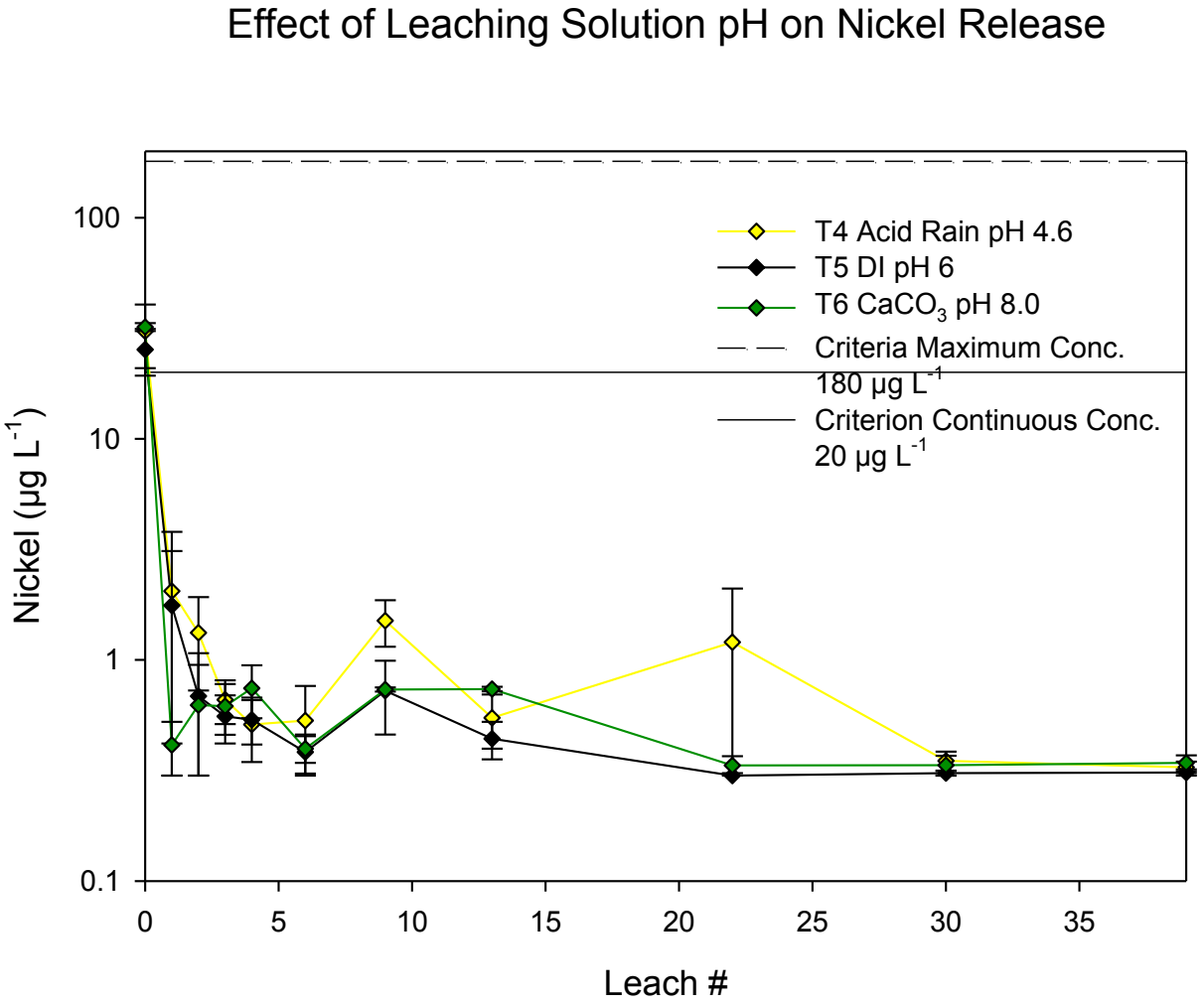

Figure D-6. Leachate Ni from columns leached with simulated acid rain, DI water and CaCO3. The 40 leaching cycles occurred over 20 weeks. Three leaching cycles correspond to one pore volume. Error bars represent one standard error above and below the mean. Detection limit = 0.3 µg L^{-1} and values below the detection limit were reported as 0.3 µg L^{-1}.

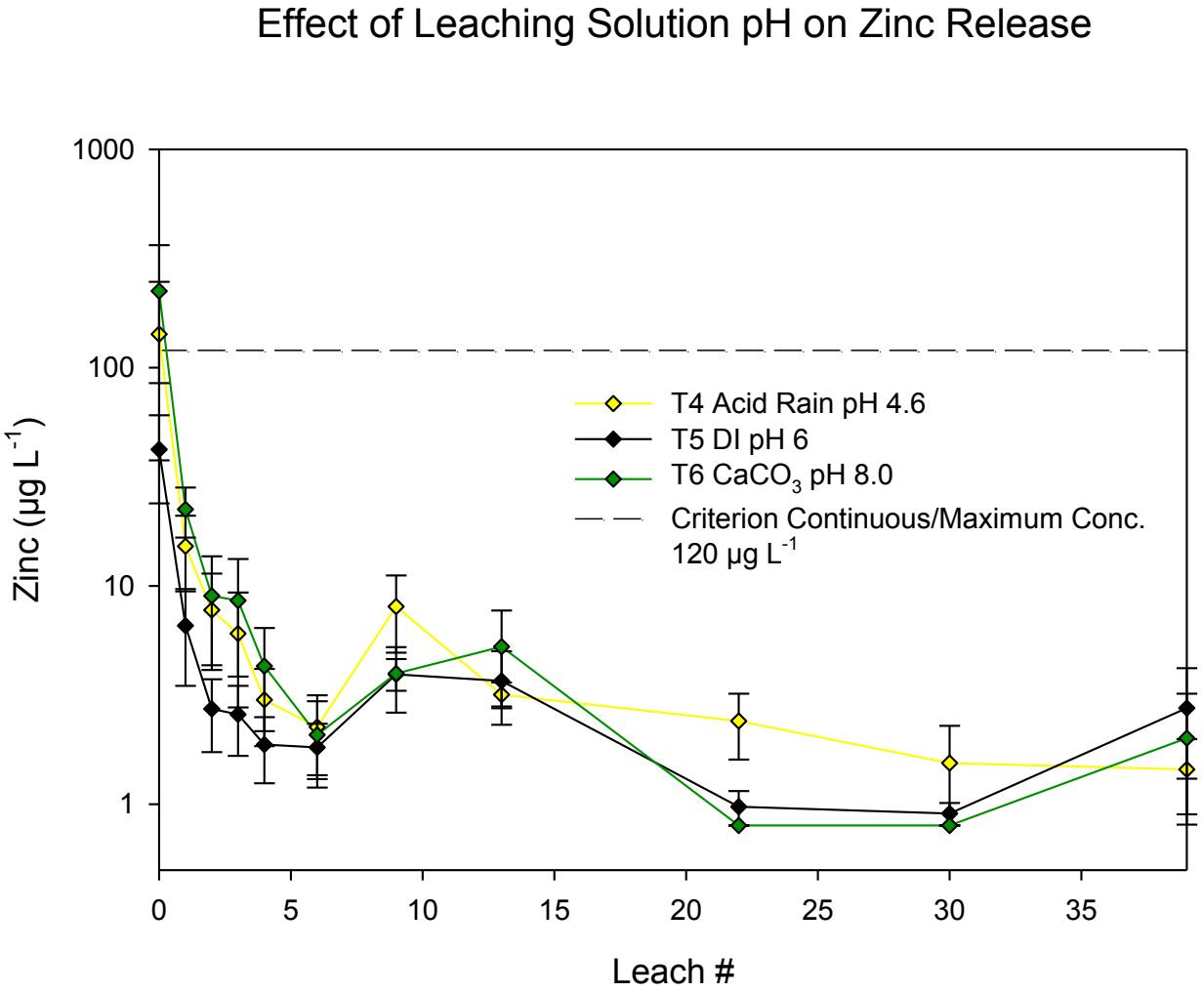

Figure D-7. Leachate Ni from columns leached with simulated acid rain, DI water and CaCO3. The 40 leaching cycles occurred over 20 weeks. Three leaching cycles correspond to one pore volume. Error bars represent one standard error above and below the mean. Detection limit = 0.8 µg L^{-1} and values below the detection limit were reported as 0.8 µg L^{-1}.

Appendix E. Effect of leaching cycle figures

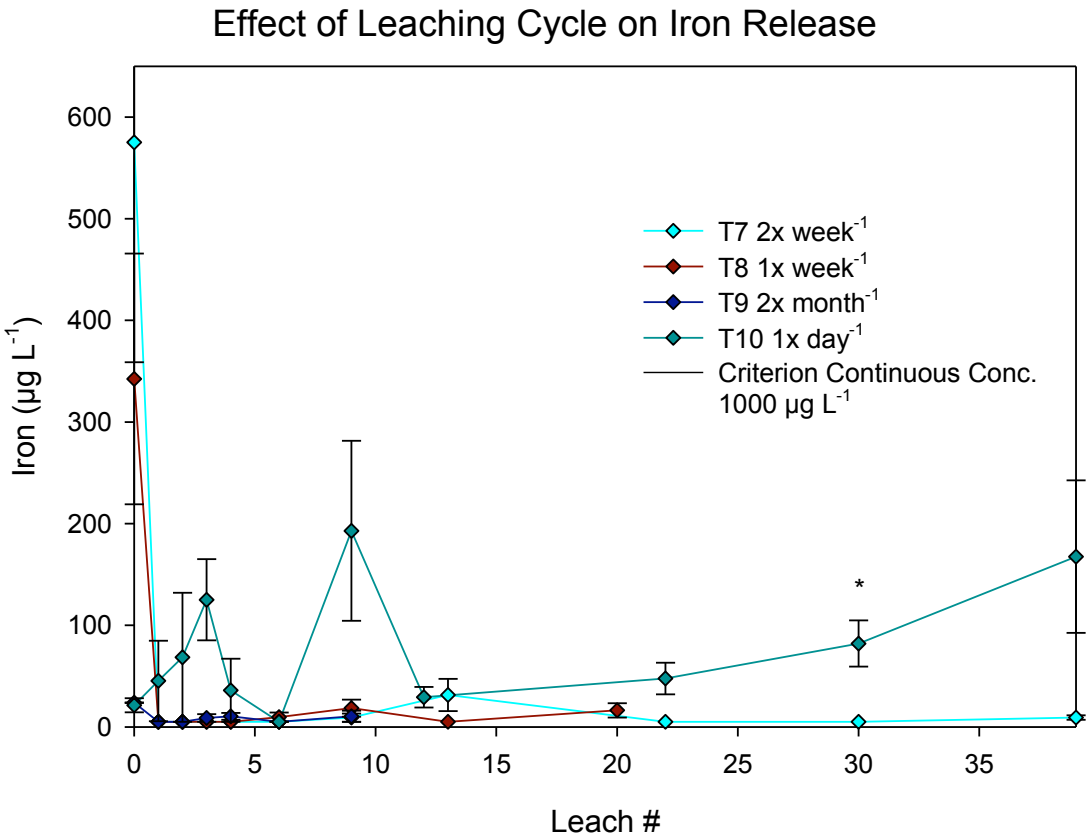

Figure E-1. Leachate Fe from columns dosed 2x week^{-1}, 1x week^{-1}, 2x month^{-1}, and 1x day^{-1}. The 40 leaching cycles for columns leached 1x day^{-1} occurred over 40 days. The 40 leaching events for columns dosed 2x week^{-1}, 20 leaching events for columns leached 1x week^{-1}, and 10 events for columns leached 2x month^{-1} occurred over a period of twenty weeks. Three leaching cycles correspond to one pore volume. Error bars represent one standard error above and below the mean. Where indicated, treatment means by date were significantly different * $P < 0.05$, ** $P < 0.01$, and *** $P < 0.001$. Detection limit = 5.0 µg L^{-1} and values below the detection limit were reported as 5.0 µg L^{-1}.

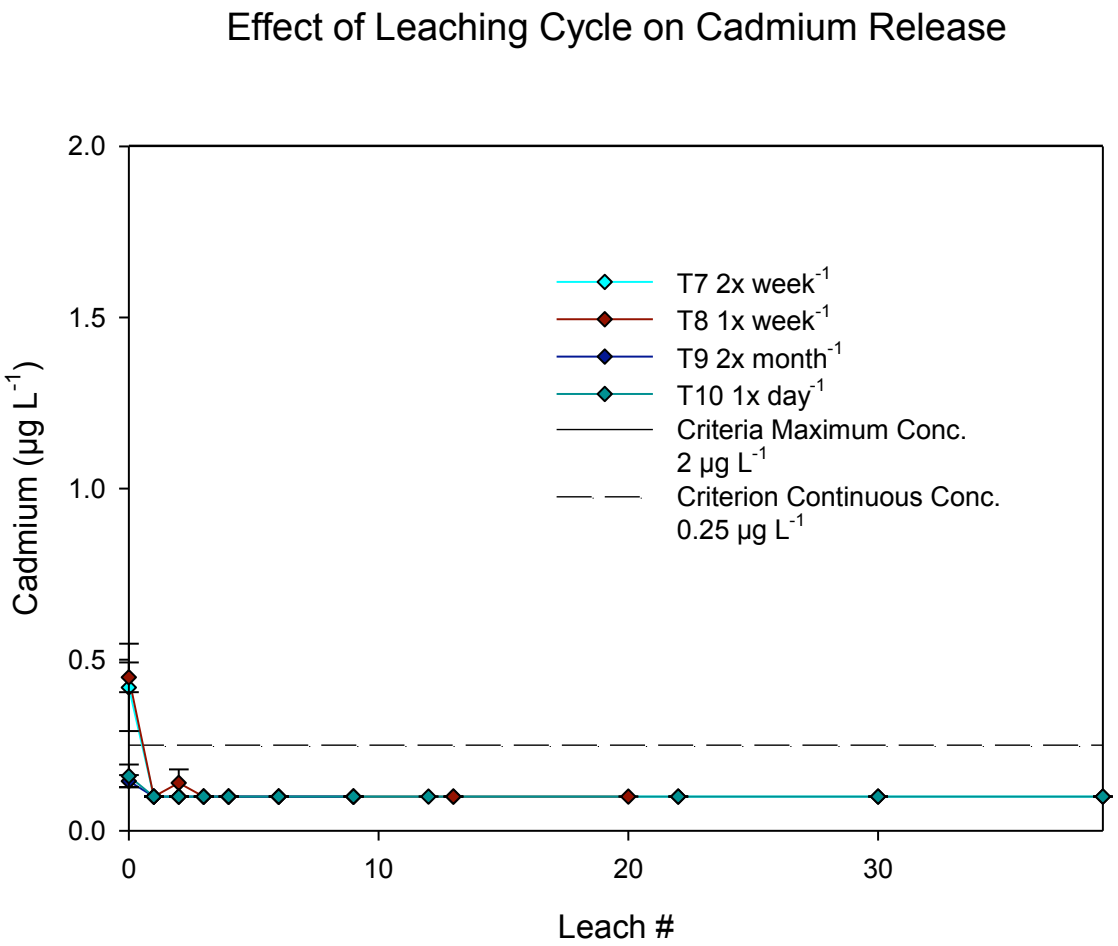

Figure E-2. Leachate Cd from columns dosed 2x week^{-1}, 1x week^{-1}, 2x month^{-1}, and 1x day^{-1}. The 40 leaching cycles for columns leached 1x day^{-1} occurred over 40 days. The 40 leaching events for columns dosed 2x week^{-1}, 20 leaching events for columns leached 1x week^{-1}, and 10 events for columns leached 2x month^{-1} occurred over a period of twenty weeks. Three leaching cycles correspond to one pore volume. Error bars represent one standard error above and below the mean. Detection limit = 0.1 µg L^{-1} and values below the detection limit were reported as 0.1 µg L^{-1}.

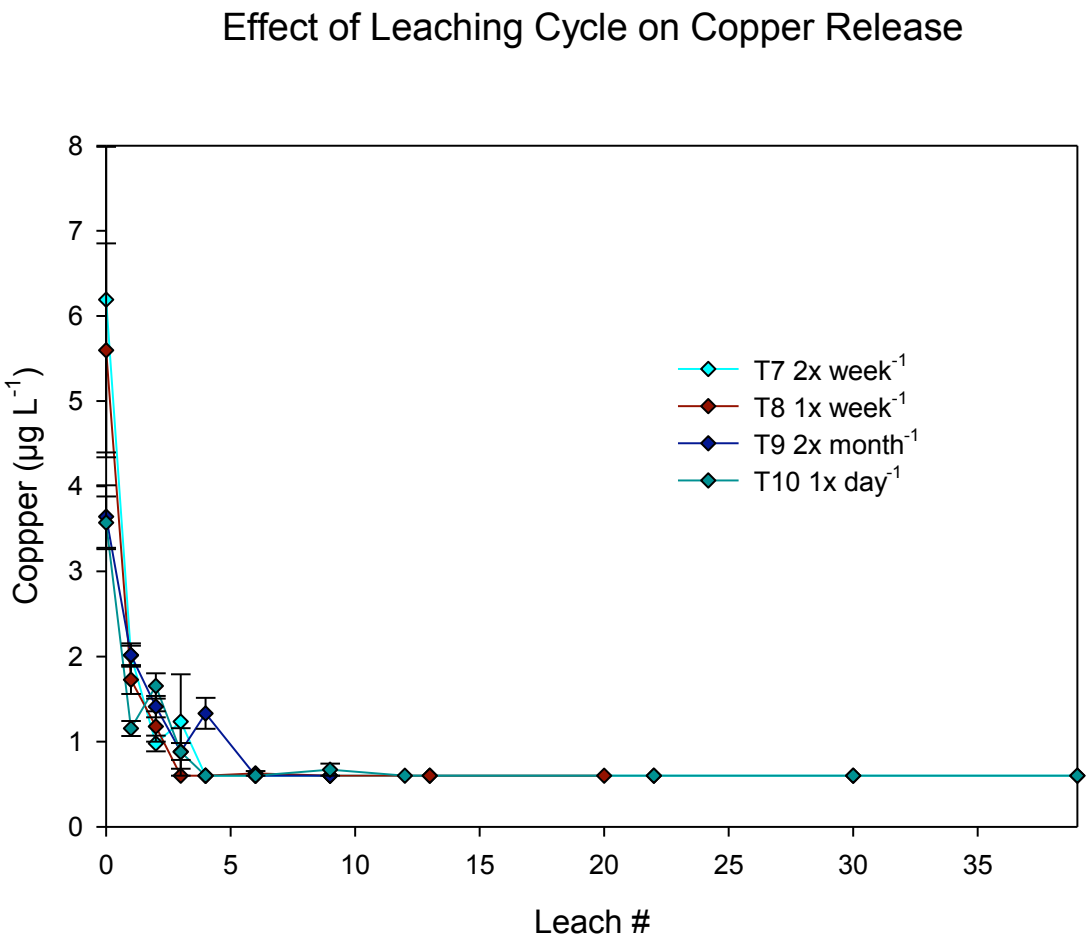

Figure E-3. Leachate Cu from columns dosed 2x week^{-1}, 1x week^{-1}, 2x month^{-1}, and 1x day^{-1}. The 40 leaching cycles for columns leached 1x day^{-1} occurred over 40 days. The 40 leaching events for columns dosed 2x week^{-1}, 20 leaching events for columns leached 1x week^{-1}, and 10 events for columns leached 2x month^{-1} occurred over a period of twenty weeks. Three leaching cycles correspond to one pore volume. Error bars represent one standard error above and below the mean. Detection limit = 0.6 µg L^{-1} and values below the detection limit were reported as 0.6 µg L^{-1}.

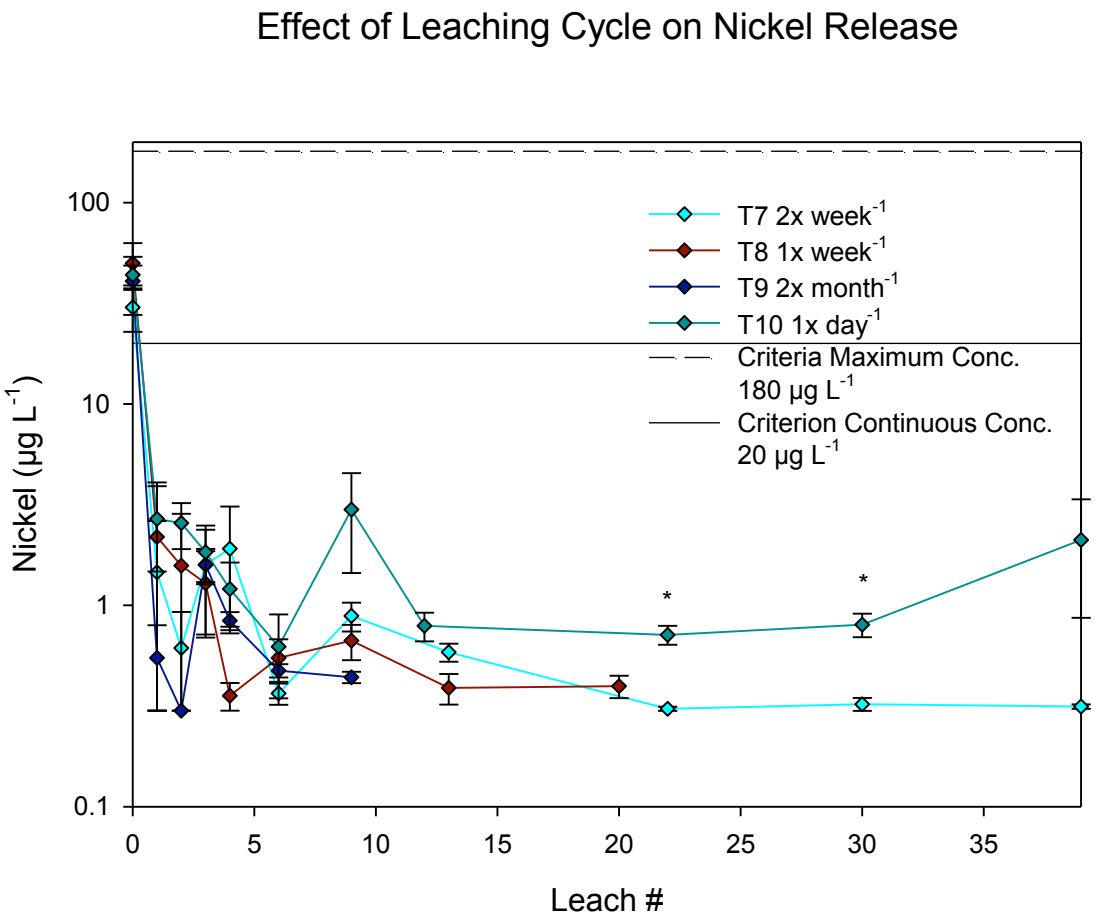

Figure E-4. Leachate Ni from columns dosed 2x week^{-1}, 1x week^{-1}, 2x month^{-1}, and 1x day^{-1}. The 40 leaching cycles for columns leached 1x day^{-1} occurred over 40 days. The 40 leaching events for columns dosed 2x week^{-1}, 20 leaching events for columns leached 1x week^{-1}, and 10 events for columns leached 2x month^{-1} occurred over a period of twenty weeks. Three leaching cycles correspond to one pore volume. Error bars represent one standard error above and below the mean. Where indicated, treatment means by date were significantly different * $P < 0.05$, ** $P < 0.01$, and *** $P < 0.001$. Detection limit = 0.3 µg L^{-1} and values below the detection limit were reported as 0.3 µg L^{-1}.

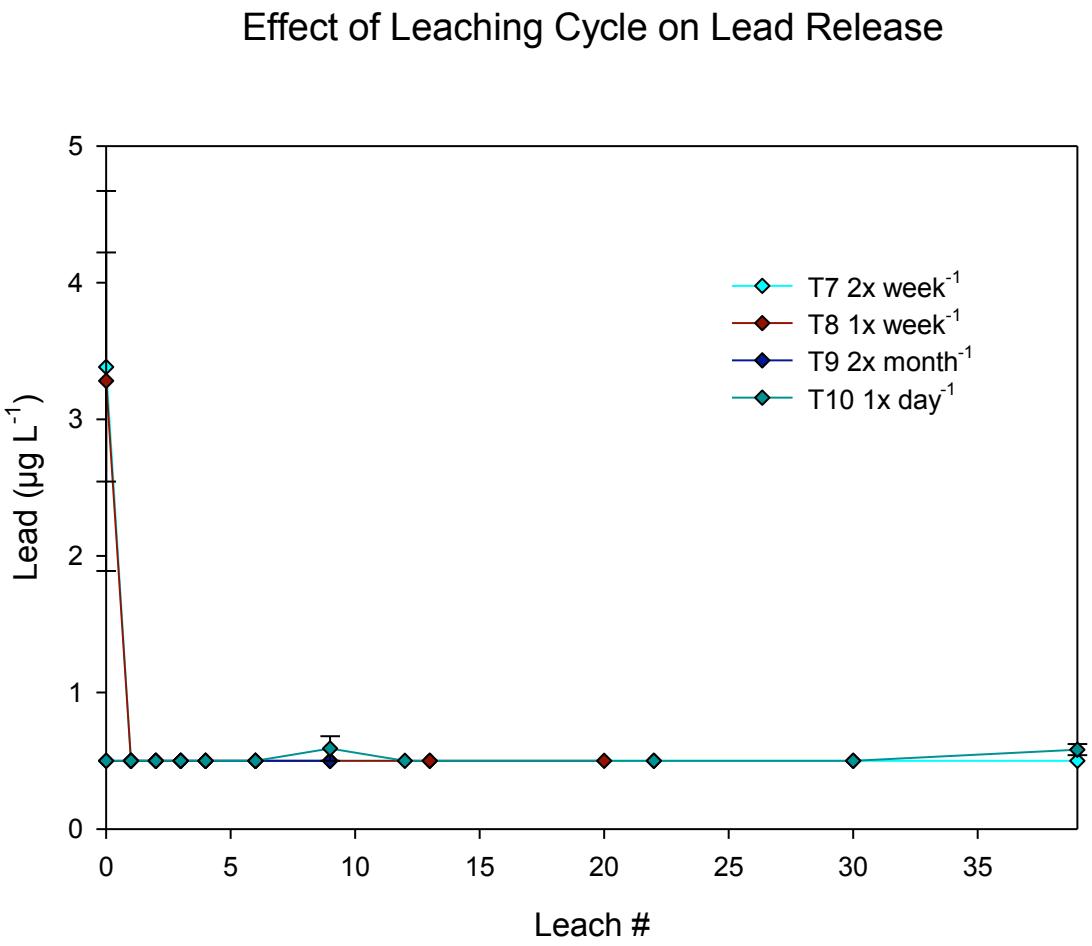

Figure E-5. Leachate Pb from columns dosed 2x week^{-1}, 1x week^{-1}, 2x month^{-1}, and 1x day^{-1}. The 40 leaching cycles for columns leached 1x day^{-1} occurred over 40 days. The 40 leaching events for columns dosed 2x week^{-1}, 20 leaching events for columns leached 1x week^{-1}, and 10 events for columns leached 2x month^{-1} occurred over a period of twenty weeks. Three leaching cycles correspond to one pore volume. Error bars represent one standard error above and below the mean. Detection limit = 0.5 µg L^{-1} and values below the detection limit were reported as 0.5 µg L^{-1}.

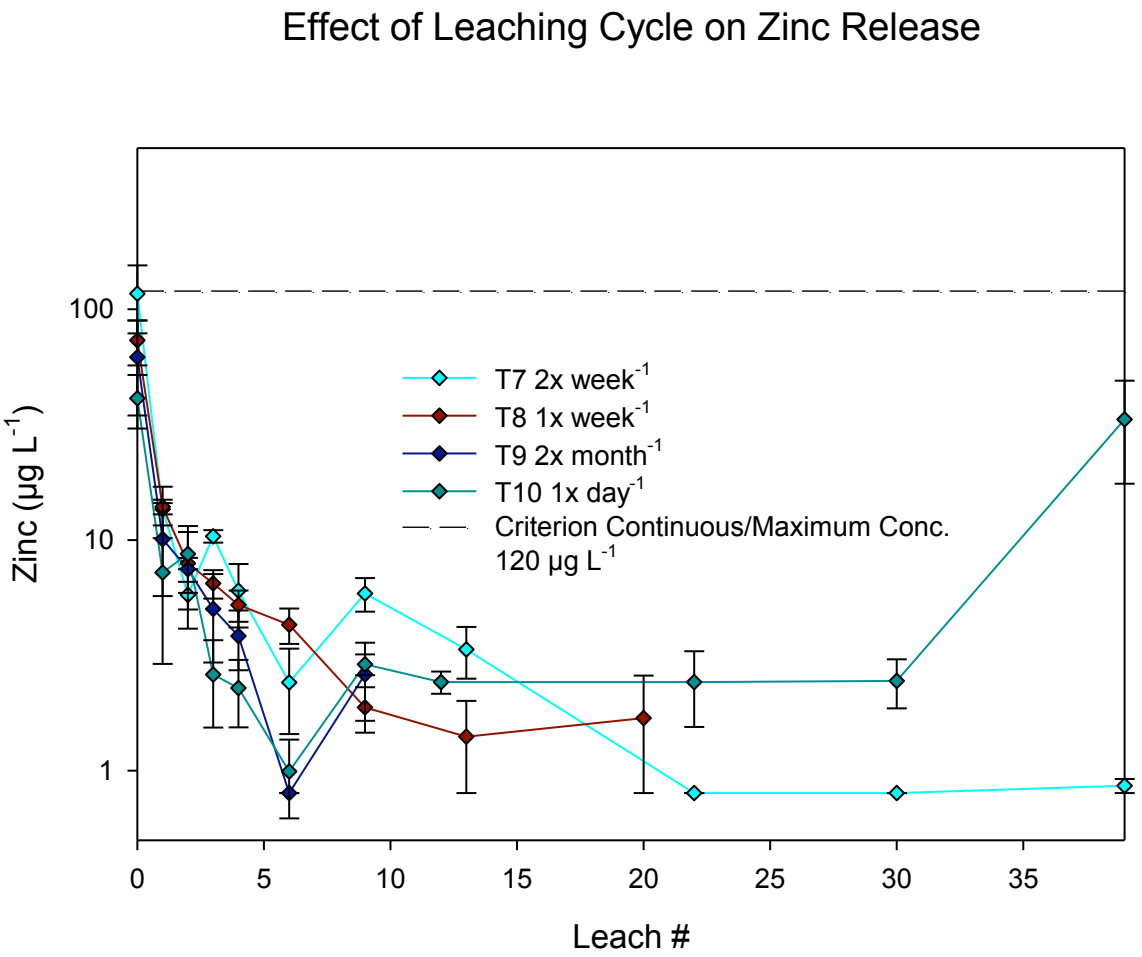

Figure E-6. Leachate Pb from columns dosed 2x week^{-1}, 1x week^{-1}, 2x month^{-1}, and 1x day^{-1}. The 40 leaching cycles for columns leached 1x day^{-1} occurred over 40 days. The 40 leaching events for columns dosed 2x week^{-1}, 20 leaching events for columns leached 1x week^{-1}, and 10 events for columns leached 2x month^{-1} occurred over a period of twenty weeks. Three leaching cycles correspond to one pore volume. Error bars represent one standard error above and below the mean.. Detection limit = 0.8 µg L^{-1} and values below the detection limit were reported as 0.8 µg L^{-1}.

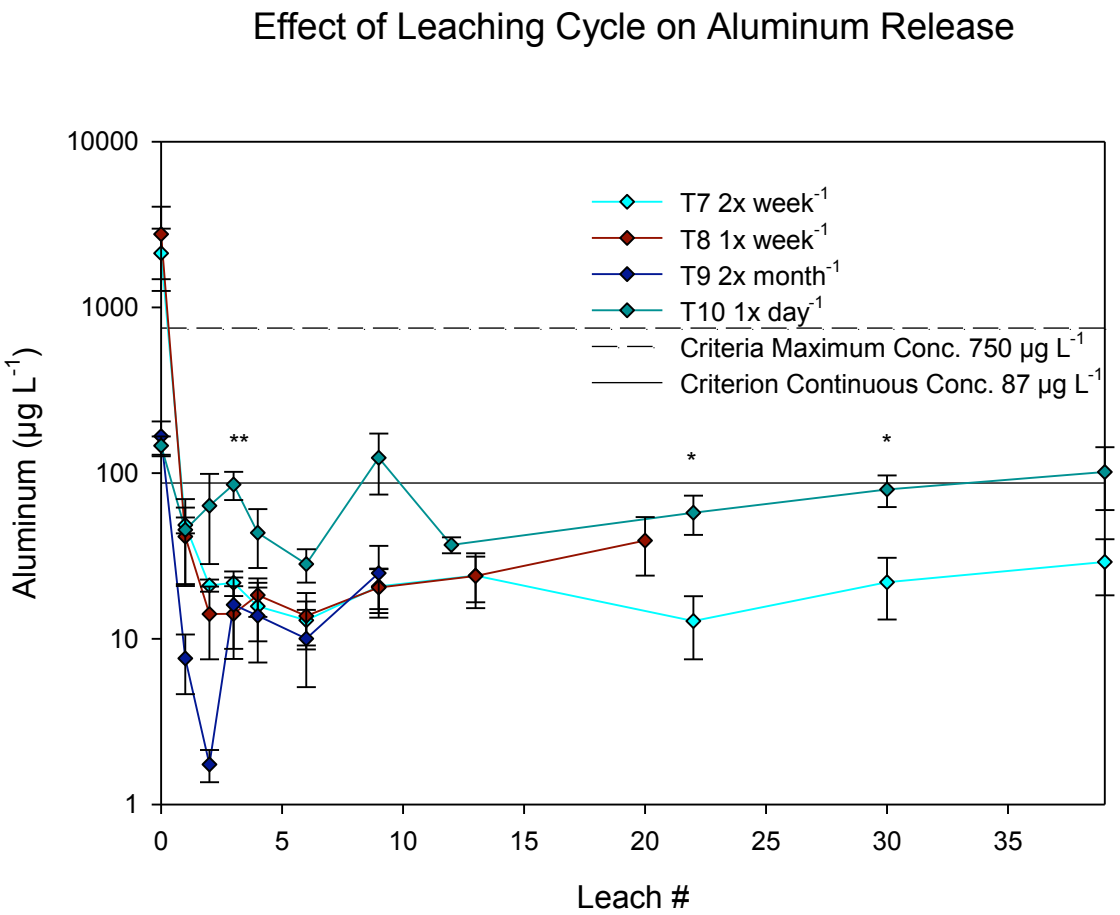

Figure E-7. Leachate Al from columns dosed 2x week^{-1}, 1x week^{-1}, 2x month^{-1}, and 1x day^{-1}. The 40 leaching cycles for columns leached 1x day^{-1} occurred over 40 days. The 40 leaching events for columns dosed 2x week^{-1}, 20 leaching events for columns leached 1x week^{-1}, and 10 events for columns leached 2x month^{-1} occurred over a period of twenty weeks. Three leaching cycles correspond to one pore volume. Error bars represent one standard error above and below the mean. Where indicated, treatment means by date were significantly different * $P < 0.05$, ** $P < 0.01$, and *** $P < 0.001$. Detection limit = 1.0 µg L^{-1} and values below the detection limit were reported as 1.0 µg L^{-1}.

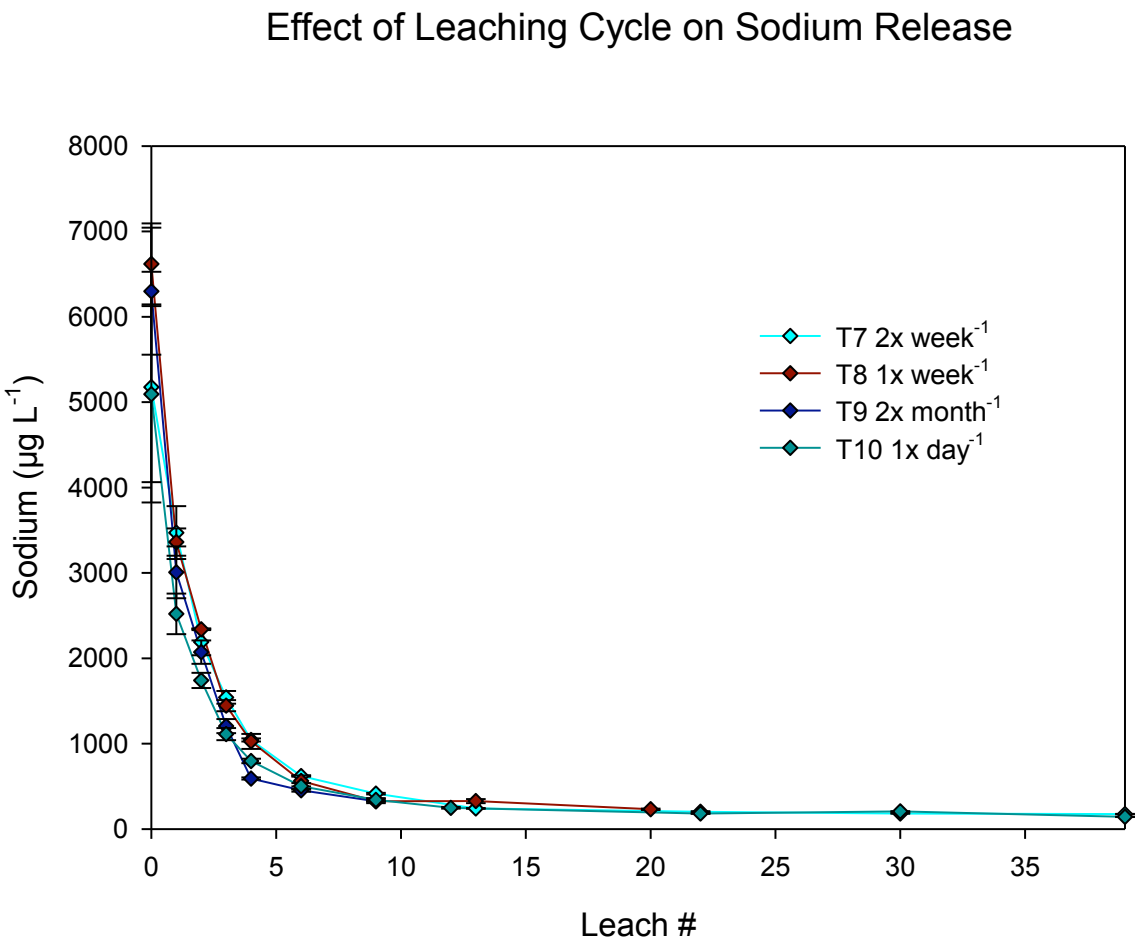

Figure E-8. Leachate Na from columns dosed 2x week^{-1}, 1x week^{-1}, 2x month^{-1}, and 1x day^{-1}. The 40 leaching cycles for columns leached 1x day^{-1} occurred over 40 days. The 40 leaching events for columns dosed 2x week^{-1}, 20 leaching events for columns leached 1x week^{-1}, and 10 events for columns leached 2x month^{-1} occurred over a period of twenty weeks. Three leaching cycles correspond to one pore volume. Error bars represent one standard error above and below the mean. Detection limit = 5.0 µg L^{-1} and values below the detection limit were reported as 5.0 µg L^{-1}.